University of Plymouth

PEARL **https://pearl.plymouth.ac.uk**

04 University of Plymouth Research Theses 01 Research Theses Main Collection

2017

Modulation of innate immune cells by the NAD+ pathway

Al-Shabany, Abbas Jawad

http://hdl.handle.net/10026.1/8304

http://dx.doi.org/10.24382/545
University of Plymouth

All content in PEARL is protected by copyright law. Author manuscripts are made available in accordance with publisher policies. Please cite only the published version using the details provided on the item record or document. In the absence of an open licence (e.g. Creative Commons), permissions for further reuse of content should be sought from the publisher or author.

Modulation of innate immune cells by the NAD^+ pathway

by

Abbas Jawad Al-Shabany

A thesis submitted to Plymouth University in partial fulfilment for the degree of

DOCTOR OF PHILOSOPHY

School of Biological Sciences

Faculty of Science and Engineering

April 2016

Copyright Statement

This copy of the thesis has been supplied on the condition that anyone who consults it is understood to recognise that its copyright rests with its author and that no quotation from the thesis and no information derived from it may be published without the author's prior consent.

Dedication

I dedicate this thesis to my beloved mother, father and to my beloved family:

My wife

My lovely daughter, Ayiat

My sons, Haider and Abdu-Allah

Modulation of innate immune cells by the NAD^+ pathway

Abbas Jawad Al-Shabany

Abstract

NAD^+ has previously been shown to regulate TNF-α synthesis and TNF-α has been shown to regulate NAD^+ homeostasis, thus providing a link between a pro-inflammatory response and redox status. Despite the well-established link between TNF-α and NAD^+, the mechanism as to how NAD^+ modulates TNF-α release is not fully understood. To achieve this, this link was investigated using THP-1 cell line-derived M1-like (pro-inflammatory) and M2-like (anti-inflammatory) macrophages using PMA and vitamin D_3, respectively. NAD^+ levels differed markedly between M1-like and M2-like macrophages, with M1-like having much higher basal levels. LPS increases NAD^+ levels and TNF-α secretion in M1-like but not M2-like cells. In an effort to investigate the source of the NAD^+ levels and the association with TNF-α release, three inhibitors (FK866, DPI and 1D-MT) were used. Following stimulation, NAD^+ is produced partially via NADH oxidation and partially through NAD^+ synthesis. Both DPI and FK866 reduced TNF-α secretion with DPI showing the largest effect. The two phenotypes showed differential profiles of NAD^+ homeostasis gene expression compared with each other and with the progenitor THP-1 in both resting and activated states. While IDO expression was induced in both phenotypes, CD38 and NAMPT were upregulated in M1-like cells whereas CD157 was upregulated in M2-like cells. LPS induced M1-like cells to up-regulate CD38 and CD157 and down-regulate NAMPT unlike M2-like cells which up-regulated NAMPT and CD38 and down-regulated CD157. M1s increased glycolysis activity whereas conversely, decreased oxidative metabolism during LPS stimulation confirming previous findings showing that classical M1s are predominantly glycolytic. Collectively, these data suggest that the relationship between NAD^+ levels and pro-/anti-inflammatory responses is complex and may be regulated via a combination of pathways. These findings open the possibility of pharmacological manipulation of NAD^+ synthesis as a way of selectively modulating macrophage responses which may be beneficial for the development of therapeutics targeting inflammatory diseases.

Table of Contents

Copyright Statement ii

Dedication iii

Abstract iv

Table of Contents v

List of Figures ix

List of Tables xix

Abbreviations xx

Author's Declaration xxvi

Publications & Conferences xxvii

Acknowledgements xxviii

CHAPTER 1 1

GENERAL INTRODUCTION 1

1. Introduction 2

1.1 Innate immune response and pathogen recognition 2

1.1.1. Macrophages 4

1.1.2. Macrophage polarisation 7

1.1.3. Macrophages and TNF-α signalling pathways 12

1.2 NAD^+ homoeostatic enzymes and the inflammatory response 15

1.2.1 NAD^+ recycling pathways and the inflammatory response 16

1.2.2 NAD^+-dependent pathways and the inflammatory response 23

1.3 Metabolic pathways and immune responses 29

1.3.1 Classical activation (M1 macrophages) and glycolysis 30

1.3.2 Alternative activation (M2s) and oxidative metabolism 35

1.4 NAD^+ Homeostasis and metabolic pathways 37

1.5 The THP-1 cell line as model of macrophage differentiation 39

1.6 Aims of the current study 43

CHAPTER 2 44

GENERAL MATERIALS & METHODS 44

2. General materials and methods 45

2.1 Materials 45

2.2. Methods 48

2.2.1 Cell line maintenance and culture 48

2.2.2 Cell differentiation with PMA or vitamin D3 (VD3) and stimulation with LPS-K12 48

2.2.3 Assessment of cell viability 49

2.2.4 Vitality assay 49

2.2.5 Preparation of cell extracts and protein quantification assay 50

2.2.6 NAD(H) Micro-cycling assay for the measurement of intracellular NAD^+ and NADH levels 52

2.2.7 Determination of IDO-kynurenine activity in M1-like and M2-like macrophages 53

2.2.8 Measurement of Lactate production 54

2.2.9 Quantitative analysis of cytokines levels 55

2.2.10 RNA extraction, reverse transcription and real time qPCR 56

2. 2.11 Agarose gel electrophoresis for RNA analysis 59

2. 2.12 Characterisation of the bioenergetic flux in differentiated macrophages 60

2.2.13 Scanning electron microscopy 61

2.2.14 Statistical analysis 62

CHAPTER 3 64

NAD^+ HOMEOSTASIS PROFILE IN PRO-INFLAMMATORY (M1-LIKE) AND ANTI-INFLAMMATORY (M2-LIKE) MACROPHAGES 64

3.1 Introduction 65

3.2 Results 67

3.2.1 M1-like and M2-like macrophage subsets differ in their morphology and the ability to secrete cytokines in response to LPS stimulation 67

3.2.2 The association between LPS stimulation and NAD^+ levels in differentiated macrophages 72

3.2.3 Differential profiles of NAD^+ homeostasis in resting macrophages 74

3.2.4 Macrophage differentiation induces gene expression of selected NAD^+ homeostatic enzymes 78

3.2.5 LPS-induces differential gene expression profile of human M1-like versus M2-like differentiation 80

3.3 Discussion 82

CHAPTER 4 93

PHARMACOLOGICAL MODULATION OF NAD^+ LEVELS CONTROLS TNF-α SECRETION IN DIFFERENTIATED MACROPHAGES 93

4.1 Introduction 94

4.2 Results 97

4.2.1 Toxicity assessment of inhibitors 97

4.2.2 Elevated NAD^+ levels are associated with TNF-α secretion in response to LPS stimulation 100

4.2.3 DPI treatment decreases both NAD^+ and TNF-α levels in M1-like MΦs but only TNF-α in M2-like MΦs during LPS stimulation 103

4.2.4 FK866 stops the increase of both NAD^+ and TNF-α release in M1-like but not in M2-like macrophages in response to LPS challenge 106

4.2.5 Inhibition of IDO with 1-MT attenuates NAD^+ levels but does not affect TNF-α release in differentiated macrophages during stimulation 109

4.2.6 Determination of IDO-kynurenine pathway (IDO-KP) activity in differentiated macrophage-like subsets 111

4.3 Discussion 113

CHAPTER 5 126

MODULATION OF NAD^+ LEVELS MODULATES GLYCOLYTIC FLUX IN PRO-INFLAMMATORY M1-LIKE MACROPHAGES 126

5.1 Introduction 127

5.2. Results 131

5.2.1 LPS-induced NAD^+ affect the NAD^+/NADH ratio in M1 but not in M2 MΦs 131

5.2.2 LPS enhances ECAR but not OCR in M1-like macrophages 133

5.2.3 LPS stimulation increases glycolytic flux and glycolysis capacity in M1-like macrophages..... 136

5.2.4 LPS-induced lactate production increases in M1-like but not in M2-like macrophages 138

5.2.5 FK866 and DPI treatment block LPS-induced increases in the NAD^+/NADH ratio in differentiated macrophages 140

5.2.6 DPI inhibits LPS-induced glycolysis activity increase in M1-like macrophages 142

5.2.7 FK866 inhibits LPS-induced glycolytic activity increase but not OXPHOS activity following LPS stimulation in M1-like macrophages..... 144

5.2.8 1D-MT treatment does not affect LPS-induced glycolytic activity in M1-like macrophages 146

5.3 Discussion 148

GENERAL DISCUSSION 157

6.1 Discussion 158

6.2 Future work 165

REFERENCES 171

Appendices 203

List of Figures

Chapter 1

Figure 1.1 Differentiated macrophages exhibit differential profiles of cytokine gene expression, receptor markers and immune function. Proposed model of differentiation macrophages in which a range of functional phenotypes effector subsets exist. M1s are induced by LPS and IFN-γ or TNF-α and differentiated by M-CSF, whereas regulatory or anti-inflammatory M2 phenotypes are subdivided to accommodate similarities and differences between interleukin-4 (IL-4/1L-13): (M2a), immune complex/TLR ligands (M2b), and IL-10/glucocorticoids (M2c). This diagram is adapted and modified as required from Liu and Yang (2013) and Foey (2015)..... 11

Figure 1.2 The TNF-α signalling pathway. This diagram shows the recognition process of the bacterial component LPS and the subsequent release of TNF-α that follows LPS stimulation. LPS sensing occurrs via LPS-binding protein (LBP) and the monocytic receptor, CD14. This binding, in turn, triggers signalling pathways for induction of the gene encoding TNF-α (nuclear factor-kappaB, NF-κB) and protein kinases, resulting in regulation of TNF-α synthesis. IKBα is phosphorylated and ubiquitinated by IKB kinase. IKBα is then degraded to release NF-kB that is finally translocated into the nucleus. TLR4, toll-like receptor; IKK, Ikappa B kinase, LPS, lipopolysaccharide; MAPK, mitogen-activated protein kinase; ERK 1 and 2, extracellular signal-regulated kinases; JNKs, c-Jun N-terminal kinase, AP-1; activator protein-1. This diagram was adapted and modified as required from Beutler and Rietschel (2003)..... 14

Figure 1.3 The NAD^+ homeostasis pathways. Tryptophan (TRP), nicotinamide (NAM), nicotinic acid (NA), nucleosides NAM riboside (NR) and NA riboside (NAR), quinolinic acid (QA), NA mononucleotide (NAMN), nicotinamide mononucleotide (NMN), QA phospho ribosyl transferase (QAPRT), nicotinamide phospho ribosyl transferase (NAMPT), nicotinic acid phospho ribosyl transferase (NAPRT), extracellular NAMPT (eNAMPT), nicotinamide riboside kinases (NRK), NMN adenylyl transferases (NMNAT), NAD^+ synthetase (NADs), NAD kinase (NADK), O-acetyl-ADP ribose (OAcADPR), ploy ADP ribose polymerase (PARP). The diagram is adapted from Nikiforov *et al*. (2015). 22

Figure 1.4 The NAD^+ consuming enzymes share one common step that uses NAD^+ as a substrate for protein deacetylation, ribosylation and cyclic ADP ribose production, yielding de-acetylated protein and liberating nicotinamide (NAM) as the end product. The latter is converted back into NAD^+ through the activity of the salvage enzyme pathways including NAMPT, NMNAT and NR (Agnieszka, 2009; Chiarugi *et al.,* 2012). 24

Figure 1.5 Sirtuin enzymatic reactions. Sirtuin members exhibit deacetylase activity in which NAD^+ is used as substrate to cleave acetyl groups from target proteins in a reaction that generates 2-O-acetyl-ADP-ribose and NAM as an end product. Sirtuin also display ADP-ribosyl transferase (ARTs) activity in which the ADP-ribosyl moiety of NAD^+ is transferred to a substrate protein. This figure is adapted from Houtkooper *et al*. (2010). 26

Figure 1.6 The enzymatic activity of CD38. CD38 is involved in the generation of range of secondary messengers including nicotinic acid adenine dinucleotide phosphate (NAADP), cyclic ADP-ribose (cADPR), ADP-ribose (ADPR) and ADP-ribose-2'-phosphate (ADPRP), which are known to mediate intracellular calcium mobilization. The diagram is adapted from Lee (2006). 27

Figure 1.7 Metabolic profile of an M1 macrophage. Glycolytic metabolism is induced in classical activation (M1s) resulting in increased lactate production. HIF-1α is also induced in M1s allowing induction of pro-inflammatory cytokines. Meanwhile, the activity of PPP is initiated, allowing an increase in ROS production supporting the bacterial killing mechanism used in M1s. G6P, glucose-6-phosphate; F6P, fructose-6-phosphate; R5P, ribose-5-phosphate; HIF-1α, Hypoxia inducible factor-1α; G3P, glyceraldehyde-3-phosphate; ROS, reactive-oxygen species. This diagram is adapted from Galvan-Pena and O'Neill (2014). 33

Figure 1.8 Metabolic profiles of an M2 macrophage. Alternative activation is via induced oxidative metabolism and β-oxidation activity. STAT6 and PGC-1β drive mitochondrial activity as well as the production of anti-inflammatory cytokines. This can also occur via the accompanying activity of AMPK, adenosine monophosphate activated protein kinase, and SIRT1. G6P, glucose-6-phosphate; G3P, glyceraldehyde-3-phosphate.This diagram is adapted from Galvan-Pena and O'Neill (2014). 36

Chapter 2

Figure 2.1 The BSA protein standard curve. BSA was diluted in assay buffer to create standards of known concentrations and was quantified for protein estimation with BCA assay reagents. Absorbance was measured at 562 nm and plotted as a function of BSA concentration. 51

Figure 2.2 The NAD(H) standard curve, generated using the NAD(H) cycling assay. NADH was dissolved in PBS and diluted to known standard concentrations. The absorbance was measured spectrophotometrically at 565 nm and plotted as function of NAD(H) concentration. 53

Figure 2.3 Example standard curve generated using the lactate assay. Lactate was diluted in assay buffer to create standards of known concentrations and absorbance was measured at 340 nm and plotted as a function of concentration. 55

Figure 2.4 Determination of RNA integrity, using gel electrophoresis. Total RNA from each samples were run on 1% agarose gel and stained with Syber® Safe nucleic acid gel stain to evaluate the RNA integrity. The intact RNA (high quality RNA) shows two ribosomal RNA (rRNA) bands- 28S and 18S- with one approximately double the size of the other. 57

Figure 2.5 Schematic diagram depicting the basic steps of the gene transcription process using real time quantitative PCR (RT qPCR) analysis. The mRNA was extracted from the sample, the integrity of the sample was confirmed using gel electrophoresis, before reverse transcription and finally qPCR were performed. The product was tested for purity using melting curve analysis. 59

Figure 2.6 General schematic diagrams summarizing the experimental design and the assays carried out during this study. THP-1 cells were differentiated into M1-like and M2-like macrophages using 25 ng/ml PMA and 10 nM vitamin D_3 respectively. The morphological changes were determined using SEM technique as mentioned in section 2.2.13. After stimulation with LPS, the cells were lysed and assayed for NAD^+, protein and kynurenine. The cells free supernatant was used for ELISA, lactate and extracellular kynurenine. Finally, bioenergetics flux was determined in viable cells free medium. 63

Chapter 3

Figure 3.1 Scanning electron micrographs showing the morphological changes of differentiated macrophages compared to non-differentiated THP-1 cells. THP-1 cells were differentiated with either 25 ng/ml PMA or 10 nM vitamin D_3. Scale bars=1 and 10 µm. 70

Figure 3.2 LPS stimulation induces differential cytokine secretion profiles in M1-like and M2-like MΦs. THP-1 cells were differentiated into M1-like and M2-like macrophages using either PMA (25 ng/ml) or vitamin D_3 (10nM), respectively. Differentiated cells were then stimulated with LPS-K12 (100 ng/ml). Cytokine production is expressed in pg/10^6 cells for (A) TNFα and (B) IL-6. Data are the mean ± SE of three biological experiments, n=3-4. The data were analysed by two-way ANOVA with Bonferroni test. Significant differences in cytokine production between activated M1 and M2 MΦs are indicated as *P < 0.05, **P< 0.01, ***P < 0.001..... 71

Figure 3.3 LPS stimulation increases NAD^+ levels in pro-inflammatory M1-like macrophages. Differentiated macrophages were induced by incubation with PMA and vitamin D_3 prior to stimulation with LPS. Pellets were harvested at intervals for NAD^+ analysis using NAD^+ cycling assay (A) Differential profile of basal NAD^+ levels in differentiated and non-differentiated (control) cells. NAD^+ levels increased in M1-like cells (B), while it was not affected in M2-like macrophages under LPS challenge (C). Data shown are mean ± SE of three biological experiments (n = 3). Results are significantly different (*P < 0.05, **P < 0.01, ***P < 0.001) when analysed by two-way and one way ANOVA followed by *post hoc* multiple pairwise Bonferroni comparisons compared to the control. 73

Figure 3.4 The effect of FK866, nicotinamide (NAM) and giunolate (QUN) on NAD^+ levels in undifferentiated THP-1 cells over time. THP-1 cells were incubated with (A) FK866 (0.1-1000 nM), (B) nicotinamide (10-1000) µM for 1-3 days and finally with (C) quinolate (10-300) µM for 1-3 days. Data shown are mean ± SE of three replicate samples (n = 3). Results are significantly different (*P< 0.05, **P < 0.01, ***P < 0.001) analysed by one way ANOVA followed by Bonferroni *post hoc* test compared to the control. 76

Figure 3.5 Resting macrophages exhibit differential profiles of NAD^+ levels. Differentiated MΦs were incubated with 100 nM FK866 and then the NAD^+ content was measured in unit of pmol/10^6 cells in (A) M1-like MΦs and (B) M2-like MΦs over 24 h. Differentiated MΦs were incubated with 300 µM

nicotinamide for 1-3 days and NAD^+ levels were measured in (C) M1- and M2-like MΦs. Similarly, 300 μM was chosen and differentiated MΦs were incubated for the same time and NAD^+ levels were measured in (D) M1- and M2-like cells. Data shown are mean ± SE of three separate experiments (n = 3). Results are significantly different (*P < 0.05, **P < 0.01, ***P < 0.001) when data were analysed by one way and two way ANOVA followed by Bonferroni *post hoc* test compared to the control..... 77

Figure 3.6 The expression of NAD^+ homeostasis enzyme genes in both macrophage subsets in the resting state. The expression of genes relating to the activity of selected enzymes of NAD metabolism were analysed in (A) M1-like (B) M2-like and (C) M1/M2-like MΦs. Data shown are mean ± SE of three separate experiments (n = 3-4). The data were analysed by one way ANOVA followed by Bonferroni test, *P < 0.05. 79

Figure 3.7 The kinetic expression profiles of NAD^+ homeostasis enzymes in (A) M1-like MΦs and (B) M2-like MΦs during LPS stimulation. Differentiated cells were stimulated with LPS (100ng/ml) and the gene expression levels measured using RT-qPCR. . Data shown are mean ± SE of three separate experiments (n = 3-4). The data were analysed by one way ANOVA plus Bonferroni *post hoc* test *P < 0.05. 81

Figure 3.8 Schematic diagram depicting the differences in NAD^+ homeostasis and cytokine production between M1-like and M2-like MΦs during LPS stimulation. M1-like cells displayed higher levels of NAD^+ and TNF-α compared to M2-like cells which displayed high levels of IL-6 in response to LPS. These are also observed by others (Daigneault *et al*., 2010; Foey and Crean, 2013). M1-like MΦs increase the expression of CD38, CD157, NAMPT and NMNAT which might reflect the unusual changes in NAD^+ levels. On the other hand, M2-like cells increase the expression of NAMPT, CD38 but not CD157 and NMNAT in response to LPS challenge compared to M1-like cells. 92

Chapter 4

Figure 4.1 Cell vitality was determined using the MTT assay. Differentiated cells were pre-incubated with 100 μM DPI, (0.5 h) or 25 μM sirtinol, (24 h) or 200 μM 1-MT, (2 h) or FK886 100 nM, (1 h) prior to stimulation with LPS. Results were analysed by two way ANOVA followed by the Bonferroni test. Significantly different results are indicated as follows: *P<0.05, **P<0.01, ***P<0.001. 99

Figure 4.2 NAD^+ levels are associated with TNF-α release in differentiated macrophages during LPS stimulation. LPS increases TNF-α release in M1-like cells (A) but not in M2-like macrophages (B). Pro-inflammatory M1-like macrophages were pre-incubated with sirtinol prior LPS stimulation (C) Sirtinol (25 μM, 24 h) treatment caused decrease in TNF-α release in response to LPS stimulation. However, incubation M1-like with 25 μM sirtinol for 1 h prior to LPS stimulation led to increase in both (D) TNF-α and (E) NAD^+ levels over the experiment. Data shown are means ± SE of three separate experiments (n = 3). Results were analysed by two way ANOVA followed by the Bonferroni *post hoc* test. Significantly different results are indicated as follows: *P<0.05, **P<0.01, ***P<0.001. 102

Figure 4.3 DPI treatment blocks LPS-induced NAD^+ levels and TNF-α release in differentiated macrophages. The cells were incubated in the presence or absence of 100 μM, 0.5 h DPI prior LPS challenge. Incubation of M1-like MΦs with DPI led to inhibited NAD^+ levels (B) and TNF-α (C) while in M2-like cells it did not affect NAD^+ levels (C) but did affect TNF-α levels (D) during LPS stimulation. Data shown are mean ± SE of separate experiments in triplicate (n = 3-4). Results were analysed by two way ANOVA followed by the Bonferroni *post hoc* test, and significant results are indicated as follows:*P < 0.05, **P < 0.01, ***P < 0.001. 105

Figure 4.4 FK866 inhibits LPS-induces NAD^+ levels and TNF-α release in pro-inflammatory differentiated (M1-like) macrophages and not in anti-inflammatory (M2-like) macrophages. Differentiated macrophages pre-incubated with and without 100nM FK866 (1h) prior LPS stimulation for the indicated time points. Cells were then harvested for NAD determination and supernatant were collected, from the same sample, for TNF-α measurement. FK866 treatment reduced in time dependent manner (A) NAD^+ levels and (B) TNF-α in M1-like while it did not affect (C) NAD^+ levels and (D) TNF-α in M2-like under LPS challenge. Data shown are means ± SE of three separate experiments (n = 3). Results were analysed by two way ANOVA followed by the Bonferroni *post hoc* test. Significantly different results are indicated as follows:*P < 0.05, **P < 0.01, *** P < 0.001). 108

Figure 4.5 1-MT (1-methyl tryptophan) pre-treatment for LPS stimulated pro-inflammatory (M1-like) differentiated macrophages reduced NAD^+ levels but not TNF-α release while anti-inflammatory (M2-like) macrophages were not affected. After differentiation, macrophages were stimulated with LPS post-incubation with and without 200 μM 1-MT (2 h). 1-MT treatment reduced in time-dependent manner (A) NAD^+ levels but not TNF-α (B) in M1-like cells while it did not affect (C) NAD^+ levels and (D) TNF-α in M2-like MΦs. Data shown are means ± SE of three separate experiments (n = 3). Results were analysed

by two way ANOVA followed by the Bonferroni *post hoc* test. Significantly different results are indicated as follows:*P < 0.05, **P < 0.01, *** P < 0.001). 110

Figure 4.6 The 1-MT treatment does not affect kynurenine formation during LPS stimulation in differentiated macrophages. (A) The linearity of kynurenine standards using the Ehrlich assay. The kynurenine was dissolved in 0.5 M HCl and serial dilutions were prepared. The effect of 1-MT treatment on extracellular kynurenine levels in (B) M1-like and (C) M2-like cells during LPS stimulation is also shown. After differentiation, macrophages were incubated with kynurenine and the rate of kynurenine consumption was measured. (D) The kynurenine consumption in resting macrophages. Data shown are means ± SE of four separate experiments (n = 3-4). Results were analysed by two way ANOVA followed by the Bonferroni test. Significantly different results are indicated as follows:*P < 0.05, **P < 0.01, *** P < 0.001). 112

Figure 4.7 The stimulation of macrophages with LPS promotes NAD^+ level-mediated TNF-α release which in turns activates macrophages for its secretion. FK866 inhibits NAMPT activation resulted in inhibition of NAD^+ levels and TNF-α release. NAD kinase uses NAD^+ to produce NADP. NADP serves as substrate for NADPH oxidase activity that activates TNF-α release in an NF-κB dependent manner. The inhibition of NADPH oxidase by DPI (an NADPH oxidase inhibitor) blocks TNF-α release. The secretion of TNF-α is regulated by NAD-dependent sirtuin activity. Sirtuin activation is inhibited by sirtinol causing a reduction in TNF-α release. 125

Chapter 5

Figure 5.1 Schematic diagrams depicting the bioenergetics of the metabolism in classical (M1) macrophages versus alternative activation (M2) macrophages. Classical M1s utilize anaerobic glycolysis for rapid response and to generate new nucleotides as well as pentose phosphate pathway (PPP)-mediated NADPH production, while alternative M2s use oxidative phosphorylation to build up reserves of ATP for longer-term function. 130

Figure 5.2 LPS stimulation regulates NAD^+, NADH and NAD^+/NADH ratio differentially in M1- and M2-like macrophages. Differentiated macrophages were stimulated with 100 ng ml^{-1} LPS-K12 for the indicated time periods and intracellular NAD^+/NADH was measured. (A) LPS increases NAD^+ levels in

M1-like MΦs in a time-dependent manner. (B) LPS does not affect NAD^+ levels in M2-like MΦs. (C) LPS stimulation increases NAD^+/NADH ratio in M1-like but not in M2-like MΦs. Data are means ± SE from three independent experiments performed in triplicate. 132

Figure 5.3 LPS stimulation of macrophages promotes ECAR induction but not OCR in M1-like MΦs. Differentiated MΦs were checked for OCR and ECAR with or without 100 ng/ml LPS (the later representing the control). OCR is expressed as the absolute rate in pmol/min, while ECAR is expressed in mpH/ min. Both ECAR and OCR were measured after sequential interferences with specific inhibitors, using Seahorse XF-24 extracellular flux technology, for glycolysis and respiration, respectively. (A) and (B) provide an overview of ECAR and OCR measurement, respectively. The baseline refers to ECAR and OCR in the saturation state prior to inhibitor injection. The glycolysis and respiration activity was obtained after glucose injection whereas 100 mM 2-DG, an inhibitor of glycolysis, was added to correct for non-glycolytic acidification. After inhibition with oligomycin (Oligo, 1 µM), an inhibitor of mitochondrial ATP production, maximum glycolysis and coupling efficiency (CE) were obtained. LPS stimulation increases ECAR (C) while it decreases OCR (D) in M1-like MΦs. LPS increases ECAR (E) but not OCR parameters (F). The data are averaged means ± SE from 3-4 wells of a single XF24 microplate. Each set of data was measured in triplicates. The data were analysed by one way ANOVA followed by the Bonferroni *post hoc* test and significant differences are indicated as *P < 0.05, **P < 0.01, ***P < 0.001. 135

Figure 5.4 LPS stimulation of macrophages induces glycolytic metabolism. (A) Glycolysis rate and (B) maximum glycolytic activity were induced by LPS exposure whereas coupling efficiency and respiration activity was not affected. Inhibition with rotenone/antimycin A (R/A, 1 µM/ 2 µM), inhibitors of complex II and III, respectively, were used to calculate reserve capacity. (C) LPS stimulation increases glycolytic reserve and do not affect respiratory reserve in M1-like macrophages. Each data point represent mean value ± SE, n = 3-4 independent experiments performed in 3-4 wells/ treatment. The data were analysed by one way ANOVA followed by the Bonferroni *post hoc* test and significant differences are indicated as *P < 0.05, **P< 0.01, ***P < 0.001. 137

Figure5.5 LPS stimulation of macrophages promotes lactate production in M1-like macrophages during LPS stimulation. In response to LPS stimulation, lactate production was increased in M1-like macrophages (A) while it was not affected in M2-like macrophages (B). Each data point represents mean ± SE, n = 3-4 independent experiments performed in 3-4 wells/ treatment. The data were analysed by one

way ANOVA followed by the Bonferroni *post hoc* test and significant differences are indicated as *P < 0.05, **P < 0.01, ***P < 0.001..... 139

Figure 5.6 Pharmacological modulation with DPI (A) and FK866 (B) decreases the NAD^+/NADH ratio in response to LPS stimulation in pro-inflammatory M1-like MΦs. Differentiated M1s were pre-incubated with DPI (100 µM) or FK866 (100 nM) for 0.5 h and 1 h, respectively, prior to LPS stimulation. LPS-induced NAD^+/ NADH ratio increase is inhibited with (A) DPI and (B) FK866. Each data point represents mean ± SE, (n = 3) independents experiments performed in triplicate. The data were analysed by one way ANOVA followed by Bonferroni *post-hoc* test and significant differences are indicated as *P < 0.05, **P < 0.01, ***P < 0.001..... 141

Figure 5. 7 DPI treatment decreased glycolytic activity in M1-like macrophages. Differentiated cells were pre-incubated with DPI (100 µM) or with culture medium for 0 h and 0.5 h prior to stimulation with LPS. Both OCR and ECAR were measured in seeded cells after sequential addition of glucose (11 µM), oligomycin 1 µM), 2-DG (100 mM) and finally (rotenone/antimycin (1 µM/ 2 µM, respectively). The effect of DPI on LPS induced (A) max glycolytic and coupling efficiency, (B) glycolysis and respiration rate, (C) glycolytic and respiration reserve. In each case, +/- indicates addition/non-addition of DPI/LPS. Data shown are the means ± SE of (n = 3-4) independent experiments performed in triplicate. The data were analysed by one way ANOVA followed by the Bonferroni test and significant differences are indicated as *P < 0.05, **P < 0.01, ***P < 0.001. 143

Figure 5.8 FK866 treatment decreased LPS-induced glycolysis, but had no effect on mitochondrial respiration. Differentiated cells were incubated with the presence of FK866(100 nM) or with culture medium for 1 h prior to stimulation with LPS for 0 h and 4 h. ECAR and OCR were calculated as previously described in Materials and Methods (chapter 2, section 2.2.12). FK866 treatment decreases LPS-induced maximum glycolysis activity but not coupling efficiency (A), glycolysis and not respiratory rate (B) and glycolytic reserve while it does not affect respiratory reserve in macrophages (C). In each case, +/- indicates addition/non-addition of FK866/LPS. Data shown are the means ± SE, (n = 3) independent experiments performed in triplicate. The data were analysed by one way ANOVA followed by the Bonferroni test and significant differences are indicated as *P < 0.05, **P < 0.01, ***P < 0.001. 145

Figure 5.9 1D-MT treatment causes no effect on anaerobic glycolytic and mitochondrial respiration during LPS stimulation in differentiated macrophages. Cells were seeded in a Seahorse V7 plate and allowed to differentiate for 72 h prior to ECAR/ OCR measurement. Prior to stimulation with LPS, for 0 h and 4 h, differentiated cells were pre-incubated with 1D-MT (200 μM) for 2 h. The effect of 1D-MT treatment on LPS induce max glycolytic actvity and coupling efficiency (A), glycolysis rate and respiration rate (B) and finally glycolytic reserve and respiratory reserve in macrophages (C). In each case, +/- indicates addition/ non-addition of 1D-MT/LPS Data shown are the means ± SE, (n = 3) independent experiments performed in triplicate..... 147

Figure 5.10 Pharmacological modulation of NAD metabolism controls glycolysis metabolism in pro-inflammatory macrophages. FK866 and DPI (but not 1-MT) inhibits LPS-induced glycolytic capacity by controlling the availability of NAD^+ that is required for deriving glycolysis pathway. FK866= inhibitor of nicotinamide phosphoribosyl transferase (NAMPT); DPI = diphenylene iodonium, an inhibitor of NADPH oxidase. 1-MT= 1-methyl tryptophan, an inhibitor of IDO pathway; G6P= glucose-6-phosphate, G3P= glyceryl aldehyde-3-phosphate; PPP = pentose phosphate pathway. 156

Chapter 6

Figure 6.1 Metabolic profiles differ between M1-like (classical) and M2-like (alternative) macrophages during LPS stimulation. In M1-like macrophages, PMA induces TLR 4, 2 expression and NAMPT activity resulting in TNF-α release induction being supported. TNF-α release is regulated by MMP and SIRT 1, 6 activities which are sensitive to NAD^+/NADH ratio. LPS also increase PPP (pentose phosphate pathway) mediated NADPH generation that is required for NADPH oxidase activity. This enzyme regulates glycolysis via providing additional NAD^+. Moreover, HIF-1α increases glucose uptake to support glycolysis activity in classical M1s. In M2-like macrophages, TLRs are down-regulated by vitamin D_3 resulting in decrease TNF-α release. Similarly, MMP expression is downregulated in vitamin D_3-treated cells. In addition, treatment with vitamin D_3 leads to upregulated AMPK which is required to drive mitochondrial activity in M2s (alternative) via up-regulation of PPAR-γ..... 164

List of Tables

Table 1.1 Tissue resident macrophages (MΦs). MΦs are found in different tissues whereby they can participate in a broad range of specialised functions according to tissue localisation. Adapted and modified from Pollard (2009). 6

Table 2.1 Cytokines, stimulants and antibodies used during this study and their suppliers 45

Table 2.2 Chemicals and buffers used in the current study, and their suppliers 46

Table 2.3 Inhibitors, reagent kits, plus other materials used, and their suppliers 47

Table 2.4 The primer sequences of selective genes in NAD^+ metabolism pathway 58

Table 4.1 The chemical structure and solvents used for the inhibitors used in this study 98

Abbreviations

Abbreviation	*meaning*
1D-MT	1dextro-methyl tryptophan
2-DG	2-deoxyglucose
ADAMs	A disintegrins and metalloproteinases
ADH	Alcohol dehydrogenase
ADPR	Adenosine diphosphate ribose
ADPRP	ADP-ribose 2'- phosphate
AML	Acute myeloblastic leukaemia
ANOVA	Analysis of variance
AP-1	Activated protein-1
ARTs	ADP-ribose transferases
ATP	Adenosine triphosphate
BSA	Bovine serum albumin
cADPR	Cyclic adenosine diphosphate ribose
CARKL	Carbohydrate kinase-like protein
cDNA	Complementary DNA
DCs	Dendritic cells

DMSO	Dimethyl sulfoxide
DPBS	Dulbecco's PBS
DPI	Diphenylene iodonium
ECAR	Extracellular acidification rate
EDTA	Ethylenediaminetetracetic acid
ELISA	Enzyme-linked immunosorbent assay
eNAMPT	Extracellular NAMPT
ERK	Extracellular signal-regulated kinases
FBS	Fetal bovine serum
MG-CSF	Macrophage colony stimulation factor
GLUT-1	Glucose transporter -1
hIDO2	Human IDO2
HIF1-α	Hypoxia inducible factor alpha
HL60	Human leukaemia cells
HRP	Horseradish peroxidise
IDO	Indoleamine 2, 3-dioxygenase
IFN-γ	Interferons-γ
iNOS	Inducible nitric oxide synthase

IRAK	Interleukin-1 receptor-associated kinase 1
KRH	Krebs-Ringer buffer
KYN	Kynurenine
LDH	Lactate dehydrogenase
LPS	Lipopolysaccharide
M1-like	Macrophage -like
MAPK	Mitogen-activated protein kinase
MIF	Migration inhibitory factor
MMPs	Matrix metalloproteinases
mTOR	Mechanistic target of rapamycin
MTT	3-(4, 5-dimethylthiazole-2-yl)-2, 5-diphenyl tetrazolium bromide
MyD88	Myeloid differentiation 88
NA	Nicotinic acid
NAADP	Nicotinic acid adenine dinucleotide phosphate
NAD^+	Nicotinamide adenine dinucleotide
NADase	NAD glycohydrolase
NADK	NAD kinase
NADP	Nicotinamide adenine dinucleotide phosphate

NADs	NAD synthetase
Nam	Nicotinamide
NaMN	Nicotinic acid mononucleotide
NAMPT	Nicotinamide phosphoribosyl transferase
NAPRT	Nicotinic acid phosphoribosyl transferase
NAR	NA riboside
NBT	Nitroblue tetrazolium
NMN	Nicotinamide mono nucleotide
NMNAT	Nicotinamide mononucleotide adenylyltransferase
NODs	Nucleotide-binding oligomerization domain receptors
NOS	Nitric oxide synthase
NR	Nicotinamide riboside
NRK	Nicotinamide riboside kinase
OAcADPR	O-acetyl-ADP-ribose
OCR	Oxygen consumption rate
OXPHOS	Oxidative phosphorylation
PARP	Poly-ADP-ribose-polymerase
PBS	Phosphate buffered saline

PES	Phenazine ethosulfate
PKC	Protein kinase C
PMA	Phorbol 12-myristate 13-acetate
PPP	Pentose phosphate pathway
PRRs	Pattern recognition receptors
QA	Quinolinic acid
QPCR	Quantitative polymerase chain reaction
QUIN	Quinolinic acid
ROS	Reactive oxygen species
SEM	Scanning electron microscope
SiRNA	Small interfering RNA
SIRT	Sirtuin
STAT1	Signal transducer and activator of transcription 1
TACE	TNF-alpha-converting enzyme
TAMs	Tumor associated macrophages
TCA	Trichloro acetic acid
TDO	TRP dioxygenase
Th	T helper

TLR	Toll-like receptors
TMB	3,3,5,5-Tetramethyl benzidine
TNF-α	Tumour necrosis factor-α
TRP	Tryptophan
VD_3	1,25-(OH)2-Vitamin D_3

Author's Declaration

At no time during the registration for the degree of Doctor of Philosophy has the author been registered for any other University award without prior agreement of the Graduate Committee.

Work submitted for this research degree at the Plymouth University has not formed part of any other degree either at Plymouth University or at another establishment. This study was financed with the aid of Ministry of the Higher Education and Scientific Research/Iraq.

Relevant scientific seminars and conferences were regularly attended at which work was often presented. One paper has been accepted for publication in refereed journal.

Signed ----------

Date ----------

Word count of main body of this thesis: (45.131 words)

Publications & Conferences

Publications:

Alshabany, A. J., Moody, A. J., Foey, A. D. & Billington, R. A. 2016. Intracellular NAD^+ levels are associated with LPS-induced TNF-α release in pro-inflammatory macrophages. *Biosci. Rep*.13;36 (1). pii: e00301. doi: 10.1042/BSR20150247

Alshabany, A. J., Moody, A. J., Foey, A. D. & Billington, R. A. 2014. Pharmacological modulation of NAD alters TNF-alpha responses in macrophage subsets. *Immunology*, 143**,** 180-180 (conference paper).

Alshabany, A. J., Moody, A. J., Foey, A. D. & Billington, R. A. 2013. NAD levels modulate macrophage subset responses. *Immunology*, 140, 92-92. (conference paper).

Alshabany, A. J., Moody, A. J., Foey, A. D. & Billington, R. A. 2015. Modulation of NAD synthesis controls TNF-α responses in macrophage phenotypes. (https://www.biochemistry.org/Portals/0/ conference paper).

Conferences

Platform presentation:

Modulation of NAD synthesis controls TNF-α responses in macrophage phenotypes, Joint Biochemical Society/British Society for Immunology, Birmingham, UK, 2015.

Poster presentation:

NAD^+ levels in anti- and pro-inflammatory macrophages. Centre for research in translational biomedicine (CRTB), Plymouth, UK, July (2013).

Pharmacological Modulation of NAD^+ alters TNF-α responses in macrophage subsets. British Society for Immunology Congress (BSI), Liverpool, UK, December (2013).

Modulation of NAD^+ homeostasis controls TNF-α responses in macrophage phenotype. British Society for Immunology Congress (BSI), Brighton, UK, December (2014).

Modulation of NAD synthesis controls TNF-α responses in macrophage phenotypes, Joint Biochemical Society/British Society for Immunology, Birmingham, UK, March (2015).

Differential expression of NAD^+ homeostasis enzymes and immune response in pro- and anti-inflammatory macrophages. NAD metabolism and signaling, FASEB, Timmendorfer Strand, Germany August (2015)

Modulation of NAD^+ homeostasis controls TNF-α secretion in differentiated macrophages, 4th European Congress of Immunology, Vienna, Austria, September (2015).

Acknowledgements

I would like to express my special appreciation and thanks to my supervisor, Dr. Richard Billington for the continuous support of my PhD study and research, for his patience, motivation, enthusiasm, and immense knowledge. His guidance helped me in all the time of research and writing of this thesis. My sincere thanks also go to Dr. Andy Foey and Dr. John Moody for their continued support throughout my project.

Besides my supervisors, I would also like to extend my thanks to all my colleagues, especially Dr. Wondwossen Abate who always answered my request for help. In addition, I would like to thank the following people (in no particular order) for providing chemicals, advice throughout my project, Lynne Cooper, Dr. William Vevers, Dr. Paul Waines, Andy Atfield, Matt Emery and Sarah Jamieson. I am also grateful for Dr. Charles Affourtit who kindly allowed me to work in his lab and use the equipment and reagents. Also, I want to thank Charlie's team Verena Hirschberg and Jonathan Barlow. In addition, I would like to thank Mr Alexander Strachan and the EM technicians, Peter Bond and Glenn Harper for assistance. I must also express my very profound gratitude to my country, the Ministry of the Higher Education and Scientific Research, Republic of Iraq, for providing necessary funding, and the School of Biological Sciences of Plymouth University for giving me the opportunity to study for this Ph.D.

Finally, lots of love and many thanks to my family especially my wife who continues to be so supportive for me all time, throughout my years of study and through the process of researching and writing this thesis.

CHAPTER 1

GENERAL INTRODUCTION

1. Introduction

1.1 Innate immune response and pathogen recognition

The innate immune response constitutes the first line of the host defence and therefore it is responsible for triggering the pro-inflammatory response in the early phase of infection against an invading pathogen (Medzhitov and Janeway, 2000; Warrington *et al*., 2011). The innate response is comprised of several defensive barriers including mechanical, chemical, physiological and cellular barriers, against invading pathogens (Medzhitov and Janeway, 2000; Basset *et al*., 2003). The chemical defence elements include cytokines, chemokines, anti-microbial peptides and pattern recognition receptors that could be soluble or cell-associated (Medzhitov and Janeway, 2000; Basset *et al*., 2003). The mechanical elements represent the physical barriers including skin and mucosal secretions (by mucosal surfaces) along with physiological elements including cilia action (by ciliated respiratory cells), low pH and fever (Basset *et al*., 2003). The cellular defence mechanism is represented by epithelial cells, mast cells, antigen presenting cells (APCs) including dendritic cells (DCs), phagocytic granulocytes and macrophages (MΦs**;** Matzinger, 2002; Basset *et al*., 2003; Iwasaki and Medzhitov, 2004). These cells play an important function in the innate immune response via (i) pathogen recognition (ii) recruiting effector cells to the site of inflammation via production of chemokines and finally (iii) phagocytosis to digest and engulf pathogens (Si-Tahar *et al*., 2009; Jounai *et al*., 2012). Indeed, the innate responses, are multi-cellular in all organisms, facilitating immune defence via recognition of a variety of microbial components known as pathogen associated molecular patterns (PAMPs), via a set of a specific pattern recognition receptors (PRRs) including Toll-like (TLRs) and NOD (nucleotide-binding oligomerization domain)-like receptors (NLRs; Iwasaki and Medzhitov,

2010; Jounai *et al*., 2012). PRRs play important functions in autophagy, phagocytosis and immune complements to limit and eliminate microbes early on during infection (Basset *et al*., 2003). Examples of PRRs include TLRs and NLRs (Medzhitov, 2001; Gordon, 2003; Van Ginderachter *et al*., 2006; Kabelitz and Medzhitov, 2007; Iwasaki and Medzhitov, 2010; Jounai *et al*., 2012). TLRs consist of a group of 10 members (TLR 1 to 10) in humans (O'Neill *et al*., 2006), while the other family is composed of NODs, leucine-rich-repeat-containing proteins, IL-1β-converting enzyme (ICE)-protease activating factor (IPAF) and neuronal apoptosis inhibitor factors (NAIPs) (Ting *et al*., 2006). Each of these family receptors is triggered by specific microbial structures initiating a series of complex signalling reactions that lead to activation of a range of immune cells that help in orchestrating specific and non-specific responses. One of these cell types is the macrophage (Forman and Torres, 2001). Activated macrophages are able to produce pro-inflammatory cytokines, chemokines, and reactive oxygen and nitrogen species (ROS/RNS; Si-Tahar *et al*., 2009). While the immune response is essential for host protection, an improper response can cause damage to the host itself (Joos and Tamm, 2005). Given that macrophages play a key role in developing optimal response, it is crucial to control the inflammatory responses of macrophages.

1.1.1. Macrophages

Macrophages are heterogeneous populations of APCs that exist in most tissues and are involved in the recognition and elimination of invading pathogens and toxic molecules. MΦs first were described by Elie Metchnikoff in 1882, and may be described as mononuclear phagocytic immune cells that represent a crucial component of initial and adaptive immune responses (Cavaillon, 2011). MΦs originate mainly from the circulating monocyte precursors which migrate from the blood vessels and through the endothelium; once they arrive in the tissue they differentiate into macrophages in response to infection and/ or inflammatory stimuli (Hume, 2006). Indeed, it is considered that the main role of monocyte precursors is to renew tissue macrophage. Tissue MΦs represent a subpopulation of specialised-tissue resident macrophages that are distributed throughout the body, involved in homeostatic function, such as Kupfer cells in the liver, alveolar MΦs in the lung, microglial MΦs in the brain and osteoclasts in bone (Table 1.1; Gordon and Taylor, 2005; Lambrecht, 2006; Strauss-Ayali *et al.*, 2007; Mosser and Edwards, 2008). Given that macrophages exist almost in every tissue and organ in the body, it is perhaps not surprising that they are involved in combatting a variety of chronic diseases. An example of macrophage influence in pathology is cancer, where MΦs are recruited to the tumour microenvironment. Here they are referred to tumour associated macrophages (TAMs). It has been shown that TAMs play key roles in promoting tumour progression and malignancy, for instance, in promoting angiogenesis (Bingle *et al*., 2006; Mantovani *et al*., 2006). Indeed, there is a correlation between TAMs and poor prognosis in almost 80% of cancer cases in humans (Bingle *et al*, 2002). Other examples of their involvement in autoimmune diseases include (i) Crohn's disease, an infectious inflammatory autoimmune disease, which is associated with the upregulation of pro-inflammatory cytokines, IL (interleukin)-12 and IFN (interferons) -γ, which is linked to

the pro-inflammatory M1-like environment (Bouma and Strober, 2003; Foey, 2015) and (ii) MΦs are also correlated with progression of acute and chronic rheumatoid arthritis (RA), sterile inflammatory autoimmune disease, where MΦs are activated in numerous inflamed synovial membranes (Mulherin *et al*., 1996; Kinne *et al*., 2000). Indeed, pro-inflammatory M1s have been shown to play a pivotal role in the pathology of RA via TNF-α regulated ROS production (Miesel *et al*., 1996). Therefore, pharmacological modulation of MΦ immune function might be a useful strategy for targeting disease-associated inflammation, for instance, rheumatoid arthritis. Thus, the diversity of macrophage specialization and distribution reflects the heterogeneity of macrophage subsets allowing a wide variety of relevant homeostatic functions (Gordon and Taylor, 2005). Indeed, MΦs are involved in a range of protective and pathogenic mechanisms from microbial killing, inflammatory (anti-tumoral responses), anti-inflammatory process (pro-tumoral responses), and wound healing to tissue repair, as well as antigen processing and presentation (Vega and Corbí, 2006). The variety in these functions is defined by a range of distinct macrophage subpopulations which has been suggested to be determined by the impact of several factors including heterogeneity, reprogramming, differentiation and microenvironment (Foey, 2015). In general, macrophages are categorized by two distinct forms, that reflect the activation and differentiation state, known as M1 (classical) and M2 (alternative) macrophages which are paradigm of Th_1/Th_2 (T helper 1/2) polarization (Mills *et al*., 2000). Given macrophage heterogeneity, it is not surprising that macrophages show plasticity and fluidity, and hence, give rise to a sliding scale of functionally polarized subsets in response to environmental stimuli (Mantovani *et al*., 2004).

Tissue	Macrophage	Function
Bone	Osteoclast	Bone remodelling and providing a stem cell niche
	Bone marrow	Erythropoiesis
Intestine	Crypt macrophage	Immune surveillance
Ovary	Macrophage	Steroid hormone production and ovulation
Pancreas	Macrophage	Islet development
Eye	Macrophage	Vascular remodelling
Epidermis	Langerhans cell	Immune surveillance
Lung	Alveolar	Immune surveillance
Brain	Microglial	Neuronal survival and repair after injury
Uterus	Uterine DC	Angiogenesis and decasualization
	macrophage	Cervical ripening

Table 1.1 Tissue resident macrophages (MΦs). MΦs are found in different tissues whereby they can participate in a broad range of specialised functions according to tissue localisation. Adapted and modified from Pollard (2009).

1.1.2. Macrophage polarisation

Macrophages belong to a heterogeneous myelomonocytic lineage that can be polarised in response to a variety of local environmental signals (Mantovani *et al*., 2004). These include cytokines, bacterial components and chemokines that have been recognised to play a major role in the orchestration of the activation of functional effector phenotypes. Based on this, M1s, referred to as classical activation, are induced by IFN-γ alone or in combination with classical stimuli, such as lipopolysaccharide (LPS), a component of Gram-negative bacteria, or with TNF-α. In addition, classical M1s can also be induced when interaction occurs with phorbol myristate acetate, PMA (Kielian and Cohn, 1981; Green and Phillips, 1994). Granulocyte macrophage colony stimulation factor (GM-CSF) is another factor which was also shown to enhance the differentiation of M1s in a model of human monocytes (Finnin *et al*., 1999). On the other hand, M2s are induced by IL-4 in concert with IL-13 signal that is collectively known to derive M2-like mediated tumour growth and progression (Anderson and Mosser, 2002; Mantovani *et al*., 2002; Gordon, 2003; Mosser and Edwards, 2008).

M1s reveal enhanced anti-microbial capacity and secrete large quantities of pro-inflammatory cytokines (TNF-α, IL-1β, IL-6, IL-18 and IL-23), and express chemokines (CXCL 1, 2, 3, 5, 8, 10, CCL3, 4, 5, 11, 17 and 22; Figure 1.1). M1s are also characterized by the expression of inducible nitric oxide synthase (iNOS) which is involved in L-arginine catabolism resulting in nitric oxide (NO) production that is known as a major mediator of macrophage cytotoxicity (Nathan and Hibbs, 1991). Indeed, iNOS expression was shown to be correlated with the antimicrobial activity effects of NO (Granger *et al*., 1988). Interestingly, iNOS mRNA translation was inhibited by the induction of arginase-mediated arginine depletion (Lee *et al*., 2003). In addition, macrophages are known to enhance production of ROS such as

superoxide anions and hydroxyl radicals (Sindrilaru *et al*., 2011). Toxic intermediates and ROS are considered to be important markers of classical activation and M1s use them to increase their killing activity during the early response against an invading pathogen. It has been suggested that TLRs, in particular TLR 2, 4 and 5, which directly link to NF-κB (nuclear factor-kappa B) activation and pro-inflammatory cytokine secretion, represent a distinct features in LPS-induced M1s (Bosisio *et al*., 2002; Van Ginderachter *et al*., 2006; Foey, 2015) On the other hand, IL-13 and IL-4 mediation of M2 activation was shown to counteract these receptors (Bosisio *et al*., 2002; Nau *et al*., 2002; Gordon, 2003; Van Ginderachter *et al*., 2006). Both of the family receptors (TLRs/NLRs) constitute a key role in the recruitment of immune cells such as neutrophils and macrophages (Fukata *et al*., 2009). M1 activation is also characterised by upregulation of the expression of MHC II (HLA-DR, surface molecule), co-stimulatory B-7.2 (CD 86; cluster differentiation 86) and IL-12 enhanced the ability to activate Th1-mediated responses to resident pathogens and to develop anti-tumour protection (Louis *et al*., 1998; Holscher *et al*., 2001; Mosser, 2003). This upregulation in expression accompanied by IL-23, which is produced by M1s, supports the differentiation and function of Th17 cells (Stockinger and Veldhoen, 2007). In general, M1s can be identified by the expression of matrix metalloproteinases (MMP-1,-2,-7,-9 and -12) under inflammatory conditions (Gibbs *et al*., 1999; Van Ginderachter *et al*., 2006). Finally, M1 polarisation can also be defined by transcription factors such as STAT1 and NF-κB involved in the induction of pro-inflammatory cytokine expression (Liu *et al*., 2008). Functionally, classically activated macrophages participate in micro pathogen killing, tissue damage and pro-inflammatory responses via deriving Th1 response (Mills *et al*., 1992&2000; Krausgruber *et al*., 2011).

Conversely, M2s (alternative activation), are characterised by their immune regulatory, anti-inflammatory and tissue repair abilities as well as tumour promotion and angiogenesis via inhibition of Th1 inflammatory responses and stimulation of the Th2-mediated anti-inflammatory response (Anderson and Mosser, 2002; Lopez-Castejon *et al*., 2011; Takeuch and Akira, 2011). It has been shown that M2s exhibit a distinct activation profile with abundant expression (Mantovani *et al*., 2002; Gordon, 2003) of mannose receptor (MR, CD206) as a distinct marker of the anti-inflammatory phenotype (Figurer 1.1). Upon activation with IL-4, other important markers (arginase I, Arg^+ I) have been shown to be upregulated in M2s (Gordon, 2003; Gordon and Taylor, 2005) resulting in L-arginine degradation into ornithine and urea which is further catabolised into polyamines and proline (Gordon, 2003; Gordon and Taylor, 2005; Classen *et al*., 2009). Arginase has been shown to be involved in tumour invasion via producing myeloid immune suppressor cells in cancer patients (Zea *et al*., 2005). These play a key role in protection against diseases allowing immune inhibitory mechanism (Highfill *et al*., 2010). Additionally, the cytokine profile has also been recognised as a marker of macrophage polarization. As such, M1s are characterised by IL-12^{high} and IL-10^{low} whereas M2 macrophages, dampen pro-inflammatory cytokines and thus they are characterised by IL-10^{high} and IL-12^{low} (Mantovani *et al*., 2004). In similar way to 1L-4 and 1L-13, alternative activation is shaped by exposure to IL-10, M-CSF, glucocorticoids or other steroid (vitamin D_3) signals (Goerdt and Orfanos, 1999; Mantovani *et al*., 2004). Finally, considering the plasticity of M2 macrophages which have been described to be polarised by activator stimuli and differentiation factors, alternative M2s can be subdivided into three forms: M2a are induced by exposure to IL-4 or IL-13 and secretes TGF-β (tumour growth factor- β), IL-1R and IL-1ra, while expressing CCL-17, 18, 22 and 24 (in Figure 1.1). In contrast, M2b macrophages are induced by immune complexes (IC) and

agonists of TLRs or IL-1β receptors, secrete cytokines such as TNF-α, IL-8 and IL-1β and express CCL-1 (Figure 1.1). Finally immunosuppressive M2c are induced by IL-10 and TGF-β or glucocorticoids, secrete TGF-β and IL-23^{lo} and express CCL-16 and 18, as well as CXC-18. In addition, M2b and M2c have been described as regulatory macrophages as in figure 1.1 (Gordon, 2003; Martinez *et al*., 2009).

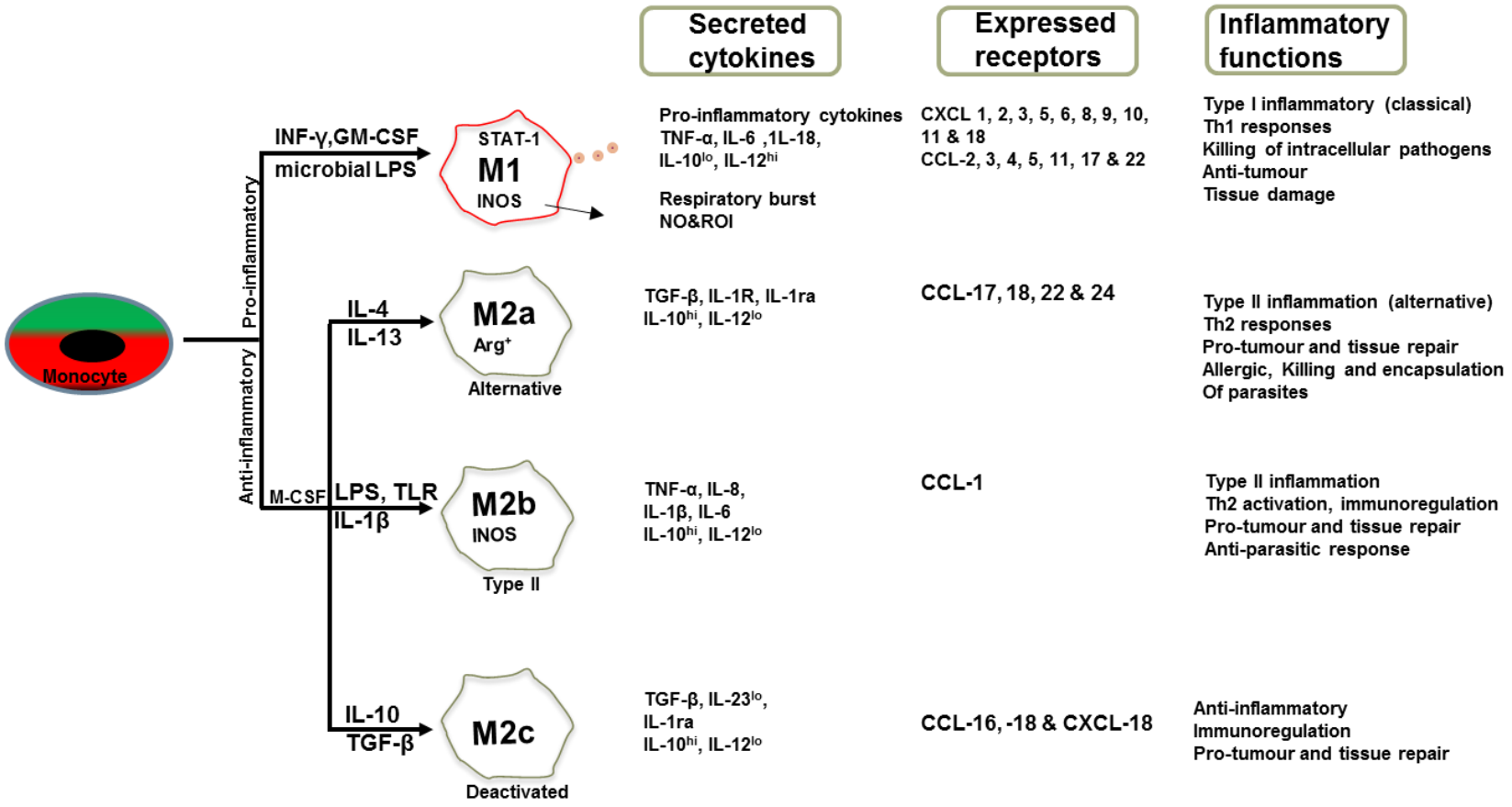

Figure 1.1 Differentiated macrophages exhibit differential profiles of cytokine gene expression, receptor markers and immune function. Proposed model of differentiation macrophages in which a range of functional phenotypes effector subsets exist. M1s are induced by LPS and IFN-γ or TNF-α and differentiated by M-CSF, whereas regulatory or anti-inflammatory M2 phenotypes are subdivided to accommodate similarities and differences between interleukin-4 (IL-4/1L-13): (M2a), immune complex/TLR ligands (M2b), and IL-10/glucocorticoids (M2c). This diagram is adapted and modified as required from Liu and Yang (2013) and Foey (2015).

1.1.3. Macrophages and TNF-α signalling pathways

Macrophages are considered to be the major producer of a potent pleiotropic pro-inflammatory cytokine, TNF-α and, somewhat conversely, they are themselves highly sensitive to it (Vassalli *et al*., 1992; Parameswaran and Patial, 2010). Indeed, TNF-α has been shown to play a central role in regulating the inflammatory responses of macrophages (Parameswaran and Patial, 2010). In general, activation of macrophages and TNF-α production occur via a range of activatory signals one of which is the LPS-mediated signalling pathway (Sweet and Hume, 1996; van der Bruggen *et al.,* 1999). LPS signalling occurs via LPS-binding protein (LBP) in plasma (Ulevitch and Tobias, 1995), thus, the LBP/LPS complex binds the surface bound receptor of 14 (CD14) on monocyte/macrophage, as shown in figure 1.2 (Tobias *et al*., 1993; Delude *et al*., 1994). LPS is then delivered to a signalling transmembrane molecule, TLR4 (Beutler and Rietschel, 2003). The TLR4/LPS binding leads to the activation of various intracellular pathways such as the NF-κB pathway that is activated via MyD88 and IRAK, which mediates the phosphorylation and ubiquitination of IκBα. As a consequence, IκBα is degraded and the NFκB is released (Chen, 2005; Kawai and Akira, 2007; Karin, 2009). The active NF-κB (p50/p65) is finally translocated into the nucleus (Sun and Ley, 2008; Vallabhapurapu and Karin, 2009). Consequently, LPS-induced NF-κB activation enhances TNF-α gene expression in macrophages (Shakhov *et al*., 1990). After these signalling events, a pro forma type II transmembrane TNF-α with a molecular mass of 26 KDa is produced (Beutler and Cerami, 1989). This form exists as a membrane bound precursor that can be proteolyticaly cleaved by TACE (TNF-alpha-converting enzyme), a disintegrins and metalloproteinases (ADAMs), to yield a secreted 17 KDa mature TNF-α (Beutler and Cerami, 1989; Black *et al*., 1997; Moss *et al*., 1997; Peschon *et al*., 1998). In addition, the induction of TNF-α expression is also

triggered via networks of signalling pathways such mitogen-activated protein kinase (MAPK) pathways involving extracellular signal-regulated kinases (ERK 1, 2), p38 and c-Jun N-terminal kinase (JNKs) as well as other transcription factor such as activated protein-1 (AP-1; Tsushima and Mori, 2001; Beutler and Rietschel, 2003; Sun and Ley, 2008). Activation of JNKs (Swantek *et al*., 1997), P38 and ERK1, 2 (Geppert *et al*., 1994; Lee and Young, 1996) in RAW 264.7 is required for LPS-induced TNF-α production. Additionally, the NF-κB can also be activated independently of the MyD88 activation pathway via protein kinases C (PKC α and β) in response to LPS and PMA stimulation (Martin *et al*., 2003; Foey and Brennan, 2004). Despite this, TNF-α is crucial for macrophage immune function and host defence, with uncontrolled TNF-α production sometimes leading to damaging to host tissue (Parameswaran and Patial, 2010). For instance, excessive production for TNF-α was shown to have a negative impact on the pathology of inflammatory conditions as in autoimmune disease as prolonged TNF-α secretion lead to tissue damage in rheumatoid arthritis (Drexler *et al*., 2008) or excessive response to infectious agents in sepsis (Conte *et al*., 2006; Smith *et al*., 2006). Therefore, a regulatory mechanism must evolve to dampen the excessive production of pro-inflammatory TNF-α which may help in creating therapeutic options for the disease-associated inflammation.

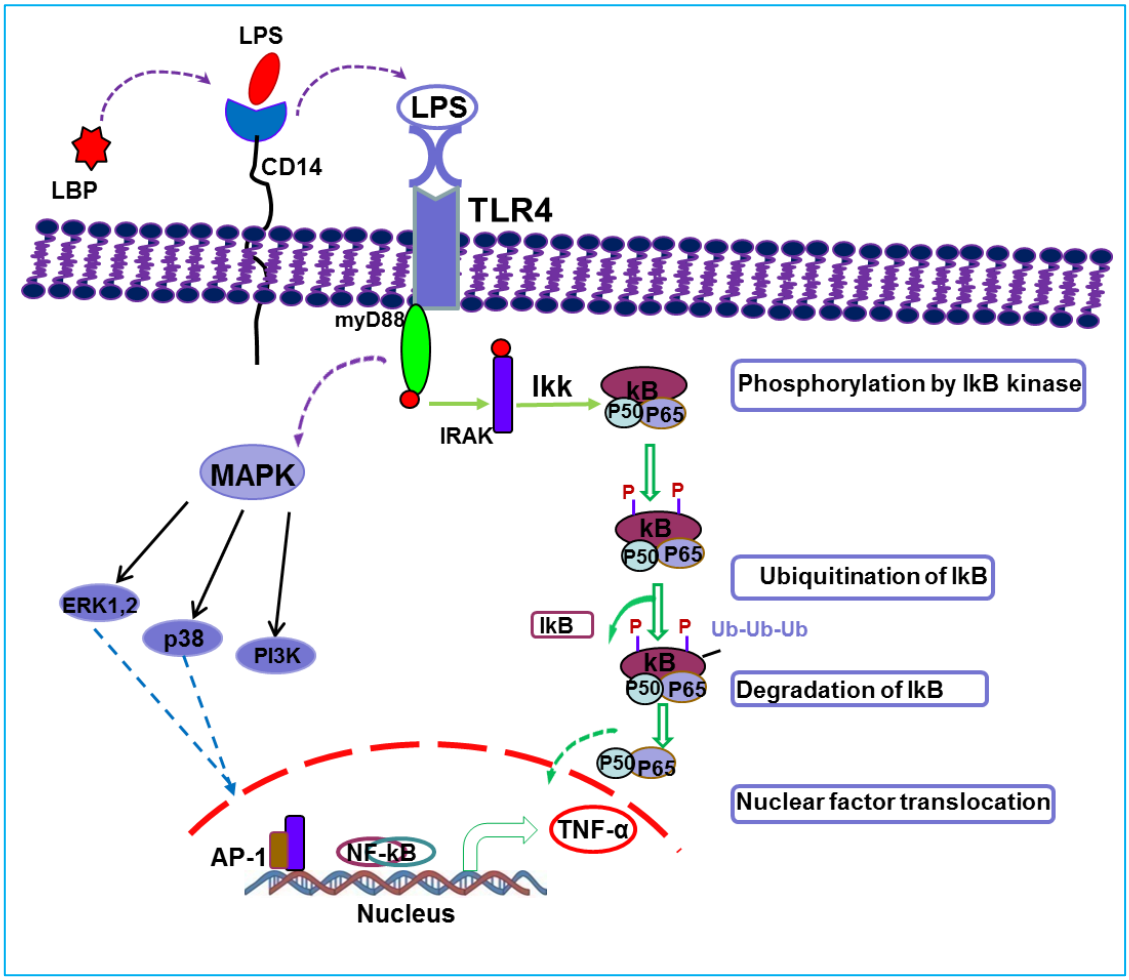

Figure 1.2 The TNF-α signalling pathway. This diagram shows the recognition process of the bacterial component LPS and the subsequent release of TNF-α that follows LPS stimulation. LPS sensing occurrs via LPS-binding protein (LBP) and the monocytic receptor, CD14. This binding, in turn, triggers signalling pathways for induction of the gene encoding TNF-α (nuclear factor-kappaB, NF-κB) and protein kinases, resulting in regulation of TNF-α synthesis. IKBα is phosphorylated and ubiquitinated by IKB kinase. IKBα is then degraded to release NF-kB that is finally translocated into the nucleus. TLR4, toll-like receptor; IKK, Ikappa B kinase, LPS, lipopolysaccharide; MAPK, mitogen-activated protein kinase; ERK 1 and 2, extracellular signal-regulated kinases; JNKs, c-Jun N-terminal kinase, AP-1; activator protein-1. This diagram was adapted and modified as required from Beutler and Rietschel (2003).

1.2 NAD^+ homoeostatic enzymes and the inflammatory response

It is well known that inflammatory responses are tightly linked to NAD^+ homeostasis pathways. NAD^+ homeostasis is a complex system including many proteins mediating the biosynthesis and consumption of NAD^+ (nicotinamide adeninedinucleotide; Houtkooper *et al*., 2010). In fact, NAD^+ and its related proteins are considered as key elements of a variety of signalling pathways (Berger *et al*., 2004; Belenky *et al*., 2007; Magni *et al*., 2008; Houtkooper *et al*., 2010). Although NAD^+ has long been known to play an important role as redox cofactor in oxidation-reduction reactions (Ziegler, 2000), it is also involved in immune transcriptional and translational regulation due to its co-enzymatic activity (Chiarugi *et al*., 2012). In innate immune cells, for example, NAD^+ mediates control of TNF-α production via NAD^+-dependent sirtuin (SIRT) deacetylase activity (van Gool *et al*., 2009). Furthermore, it has been shown that the phosphorylation of NAD^+ via NAD kinase (NADK) activity results in the generation of $NADP^+$ (nicotinamide adeninedinucleotide phosphate) which is important for the production of ROS and oxidative burst for immune defence (Chiarugi *et al*., 2012). In addition, NAD^+ is vital not only for signalling-mediated immune function, but also for energy production. Thus, NAD^+ serves as a cofactor for redox reactions involved in glycolysis, the trichloroacetic acid cycle (TCA), OXPHOS (oxidative phosphorylation) and the catabolism of carbohydrates and fat (Bogan and Brenner 2008; Garten *et al*., 2009). Therefore, NAD^+ has emerged as an important link between regulatory processes and cellular bioenergetics redox metabolism (Chiarugi *et al*., 2012). Since NAD^+ is required for metabolic pathways, it is perhaps not surprising that NAD^+ levels have also been linked to immune function in macrophages. Also, NAD^+ can serve as a metabolic factor for other cellular processes, including protein transcription, DNA repair, G-protein coupled and intracellular calcium signalling (Bogan and Brenner 2008; Garten *et al*., 2009). It is now accepted that

there is a link between NAD^+ homeostasis, metabolism and immune response. Given this link, an interest in the pharmacological modulation of NAD^+ has grown as a method for regulating the NAD^+ levels. In particular, focus has grown on the modulation of NAD^+ homeostasis as a way of decreasing intracellular NAD^+ levels, thus reducing the activity of NAD^+-dependent immune function, particularly, in MΦs. In general, intracellular NAD^+ can be produced and consumed via networks of different pathways. For NAD^+ generation, three different pathways and precursors are involved: nicotinamide (Nam) and nicotinic acid (NA) via NAMPT (nicotinamide phosphoribosyl transferase) the salvage pathway (Jacobson *et al*., 1995; Rongvaux *et al*., 2003; Magni *et al*., 2008), nicotinamide riboside (NR) via nicotinamide riboside kinase pathway (NRK; Bieganowski and Brenner, 2004) and finally tryptophan (TRP) via the indole amine 2,3-dioxygenase (IDO) pathway (*de novo* pathway; Yamazaki *et al*., 1985; Kudo and Boyd, 2000). These are shown in figure 1.3.

1.2.1 NAD^+ recycling pathways and the inflammatory response

Replenishment of NAD^+ is essential to maintain appropriate immune responses with NAD^+ generation enzymes playing key roles in immune regulatory processes, in particular, in the regulation of TNF-α synthesis (van Gool *et al*, 2009). Indeed, the depletion of NAD^+ pool, via suppression NAMPT-mediated NAD^+ biosynthesis by FK866, a well-known inhibitor of the NAD^+ recycling pathway, decreased TNF-α levels in THP-1 cells, human monocyte and macrophages (Nau *et al*., 2002; Hasmann and Schemainda, 2003; Iqbal and Zaidi, 2006; Li *et al*., 2008; Friebe *et al*., 2011; Schilling *et al*., 2012) during LPS stimulation. Since adequate NAD^+ levels are required for optimal TNF-α production (van Gool *et al*., 2009), the immune cells need to maintain the NAD^+ pool in order to support immune signalling pathways as well as other NAD^+-dependent signalling pathways. To achieve this, NAD^+ can be synthesised, via the salvage pathway, using a range of dietary precursors including NA, NAM and/ or

nucleosides, NR and NAR (NA riboside). Also, NAD^+ can be synthesised *de novo* from tryptophan via the IDO-kynurenine pathway (Braidy *et al*., 2011). The dietary deficiency of these precursors is associated with human diseases like pellagra; patients with pellagra ultimately die as a result of diarrhoea, dermatitis, and dementia (Hegyi *et al*., 2004), although the dietary supplementation of these precursors however can easily treat this disease, thus confirming their dietary importance (Houtkooper *et al*., 2010). It is worth noting that the conversion of tryptophan in NAD^+ *de novo* biosynthesis is limited to the liver under conditions of stress and thus tryptophan alone is insufficient to maintain NAD^+ levels (Magni *et al*., 2004). This could indicate that the salvage pathway from the two precursors (NAM and NA) is the main source of NAD^+ generation in mammals. Unlike NAM, NA content is low (Kirkland, 2009) in mammals, due to its rapid excretion, therefore the utilization of NA in NAD^+ salvage pathway is limited compared to that of NAM. Indeed, in humans, NAM is the preferable metabolite in NAD^+ synthesis (Olesen *et al*., 2008 & 2010; Watson *et al*., 2009). Intriguingly, NAM was found to act as anti-inflammatory agent via, *in vitro*, inhibiting the pro-inflammatory mediators such as TNF-α, IL-6 and IL-1β synthesis (Ungerstedt *et al*., 2003). Also, NAM has been shown to inhibit intercellular adhesion molecule-1 (ICAM-1) expression in a model of cultured human thyroid cells (Hiromatsu *et al*., 1993) and also prevent IL-1β effect mediated nitric oxide (NO) production in rat islets of Langerhans (Andersen *et al*., 1994). The pathway starts with NAM, allowing NAD^+ synthesis, which is catalysed by NAMPT, the rate limiting enzyme of NAD^+ salvage pathway (Figure 1.3). NAMPT was first identified as pre-B cell colony-enhancing factor (PBEF), and it has this name due to its role in maturation of B-cell precursors (Nau *et al*., 2002). It has been documented that expression of NAMPT is induced in primary macrophages (Iqbal and Zaidi, 2006). The induction of NAMPT expression was also shown during stimulation with

inflammatory stimuli in various immune cells including monocytes, neutrophils and dendritic cell that is reported to rely mainly on the NAMPT salvage pathway for NAD^+ generation (Van Beijnum *et al*., 2002; Revollo *et al*., 2004; Busso, 2008; Luk *et al*., 2008; Rongvaux *et al*., 2003&2008).

The elevated levels of NAMPT expression might reflect a critical role for this enzyme in immune regulatory mechanisms, in activated immune cells, via the provision of a sufficient intracellular NAD^+ pool required for NAD^+-dependent enzyme-mediated immune signalling (van Gool *et al*., 2009). Thus, NAMPT has been suggested to induce myeloid differentiation (Skokowa *et al*., 2009), via up-regulation of the differentiation factor GM-CSF in a sirtuin-dependent pathway. Similarly, NAMPT was also found to increase specific pro-inflammatory production of cytokines such as TNF-α. Decreasing NAD^+ levels, through inhibition of NAMPT attenuates LPS-stimulated TNF-α levels in THP-1 cells and human monocytes (Busso *et al*., 2008; van Gool *et al*., 2009; Schilling *et al*., 2012). Furthermore, it has been reported that NAMPT inhibition led to a decrease in other inflammatory mediators such as TNF-α, IL-6 and IL-1β levels in different inflammatory settings (Busso *et al*., 2008; van Gool *et al*., 2009; Schilling *et al*., 2012). Together, these observations suggest that a link exists between NAD^+ biosynthesis, intracellular NAD^+ levels, and pro-inflammatory responses in macrophages, offering a potential therapeutic target for modulation of immune inflammatory effector functions. In addition to intracellular localization (iNAMPT), NAMPT has been found to reside extracellularly (eNAMPT) but with no enzymatic activity (Li *et al*., 2008; Hara *et al*., 2011). Also known as visfatin, eNAMPT is secreted into the extracellular environment by visceral fat tissues (Figure 1.3; Fukuhara *et al*., 2005). Interestingly, eNAMPT was shown to be highly expressed in diabetes and obesity with a role mimicking the hormonal insulin effect, as this protein is able to bind to the insulin receptor at a different

site to that of insulin (Arner, 2006; Stephens and Vidal-Puig, 2006). It seems that eNAMPT exhibits its immune regulatory functions as a cytokine, but not as an enzyme, as mentioned earlier for iNAMPT, by inducing pro-inflammatory responses in macrophages and neutrophils

The other two niacin precursors are converted by two distinct salvage pathways. The first pathway of NAD^+ biosynthesis, known as the Preiss-Handler pathway (Preiss and Handler, 1958), is comprised of the conversion of NA into NAMN (NA mononucleotide) by nicotinic acid phosphoribosyl transferase (NAPRT). This pathway was shown to be well conserved and also highly active in bacteria (Preiss and Handler, 1958; Houtkooper *et al*., 2010). Recently, a second pathway, derived from nicotinamide riboside has also been described; it starts with the phosphorylation of NR to NMN (Figure 1.3), a process which is catalysed by NRK. This enzyme exists in two isoforms: the ubiquitously expressed NRK1 and the localized NRK2 (Bieganowski and Brenner, 2004). It has been suggested recently that this pathway appears to be highly conserved and active in both yeasts and humans (Bieganowski and Brenner, 2004). Beyond the salvage pathway, NAD^+ can also be generated *de novo* from tryptophan via the IDO pathway (Figure 1.3). In this pathway, IDO is the rate-limiting enzyme that catalyses the oxidative catabolism of the essential amino acid tryptophan along the kynurenine (KYN) pathway, through a series of enzymatic reactions, into quinolinic acid (QA) which, in turn, is converted to NAD^+ (Orabona *et al*., 2006; Pallotta *et al*., 2011). Similarly, the oxidative catabolism of TRP is also catalysed by the TRP dioxygenase (TDO) enzyme (Figure 1.3; Opitz *et al*., 2011b; Pilotte *et al*., 2012). While TDO is expressed in the liver, IDO is expressed in most body tissues (Revollo *et al*., 2004). IDO expression is induced by classical inflammatory stimuli molecules such as LPS in an autocrine dependent or a manner independent of IFN-γ regulated by NF-κB (Grohmann *et al*., 2003; Mellor and Munn,

2004). This enzyme was shown to be highly upregulated by certain professional APCs, often macrophages and DCs, in response to pro-inflammatory stimuli, for which two related but distinct enzymes have been described, namely IDO1 and IDO2 (Ball *et al*., 2007; Metz *et al*., 2007). IDO activity has been shown to modify both the innate and the adaptive immune system (Taylor and Feng, 1991) via two main mechanisms. The first proposed mechanism is centred around the fact that IDO-mediated tryptophan depletion results in starvation of the cell microenvironment (Orabona *et al*., 2006) via the action of IDO that might directly inhibit T-cell proliferation in different inflammatory settings (Mellor and Munn, 1999; Frumento *et al*., 2002). Several studies on DCs have revealed that IDO expression is required as a co-stimulatory signal with B7 ligation leading to enhanced T regulatory cells (T_{reg}) cells that is known to mediate immune modulatory effects (Grohmann *et al*., 2003). This might suggest an important role for IDO expression in regulating the ability of DCs to regulate T-cell associated immune responses (Mellor, 2005). Also, it is documented that IDO upregulation in DCs inhibits Th1 cell responses (Grohmann *et al*., 2003). Thus, others have reported that Th1 cells are activated by inhibiting IDO function via the use of 1-methyl tryptophan as a potent inhibitor for IDO enzymatic activity (Kwidzinski *et al*., 2005). This might suggest that innate immune cells expressing IDO might have an impact on the balance of Th1/Th2 responses. The second proposed mechanism is the ability of IDO to produce downstream immune regulatory and cytotoxic intermediates (Stone and Darlington, 2002), such as kynurenine metabolites, which exert their effects on tissue microenvironments, suppressing cell activation and proliferation (Opitz *et al*., 2011b). IDO is highly expressed by a large range of tumour cells such as acute myeloid leukaemia (AML) cells and therefore tryptophan-degradation mediates kynurenine production resulting in regulating T-cell responses in a way to enable effective tumour evasion of host immune defences (Watanabe *et al*., 1980).

Additionally, IDO plays a key role in mediating the flux between pathways that lead to pro-/anti-inflammatory cytokine production (Pilotte *et al*., 2012). In general, the NAD^+ biosynthesis pathways, from all known precursors, share one major step which is common to all pathways, that is the formation of the mononucleotides, NMN or NAMN (Chiarugi *et al*., 2012). This step is facilitated by nicotinamide mononucleotide adenylyl transferases (NMNAT), which mediate the reaction between AMP (adenosine monophosphate, the adenylate moiety of ATP, adenosine triphosphate) and pyridine mononucleotide (Figure 1.3) allowing NAD^+ generation from NMN or NA adenine dinucleotide (NAAD) from NAMN (Chiarugi *et al*., 2012). Interestingly, three mammalian NMNAT isoforms have been described, each having a distinct tissue distribution and cellular location (Berger *et al*., 2005; Lau and Ziegler, 2009). Of the three isoforms, only one resides in the mitochondria while the other two isoforms are exclusively located in the nucleus (NMNAT1) or cytosol (NMNAT2), respectively (Nikiforov *et al*., 2015). It has been reported that the distribution of these isoforms are pronounced in wide range of tissue including brain, heart, pancreasand skeletal muscle as well as, although to a lesser degree, the thymus and tumour tissues (Emanuelli *et al*, 2001; Lau and Ziegler, 2009). Given the key role of NMNAT in NAD^+ formation, their pharmacological targeting could be relevant to NAD^+-depleting therapeutic strategies (Chiarugi *et al*., 2012). Finally, the formation of NAD^+ is carried out by NAD^+ synthetase (NADs) via the amidation of the nicotinic acid moiety of NAAD using glutamine as a donor of NH_2 groups (Nikiforov *et al*., 2015). It is now accepted that the involvement of NAD^+ biosynthesis in modulation of multiple immune regulatory responses might account for NAD^+ availability. Indeed, NAD^+ can act a substrate for a series of NAD^+-consuming enzymes such as sirtuin and CD38 (ADP-ribosyl cyclase; Figure 1.3) which have important role in inflammatory response regulation in immune cells.

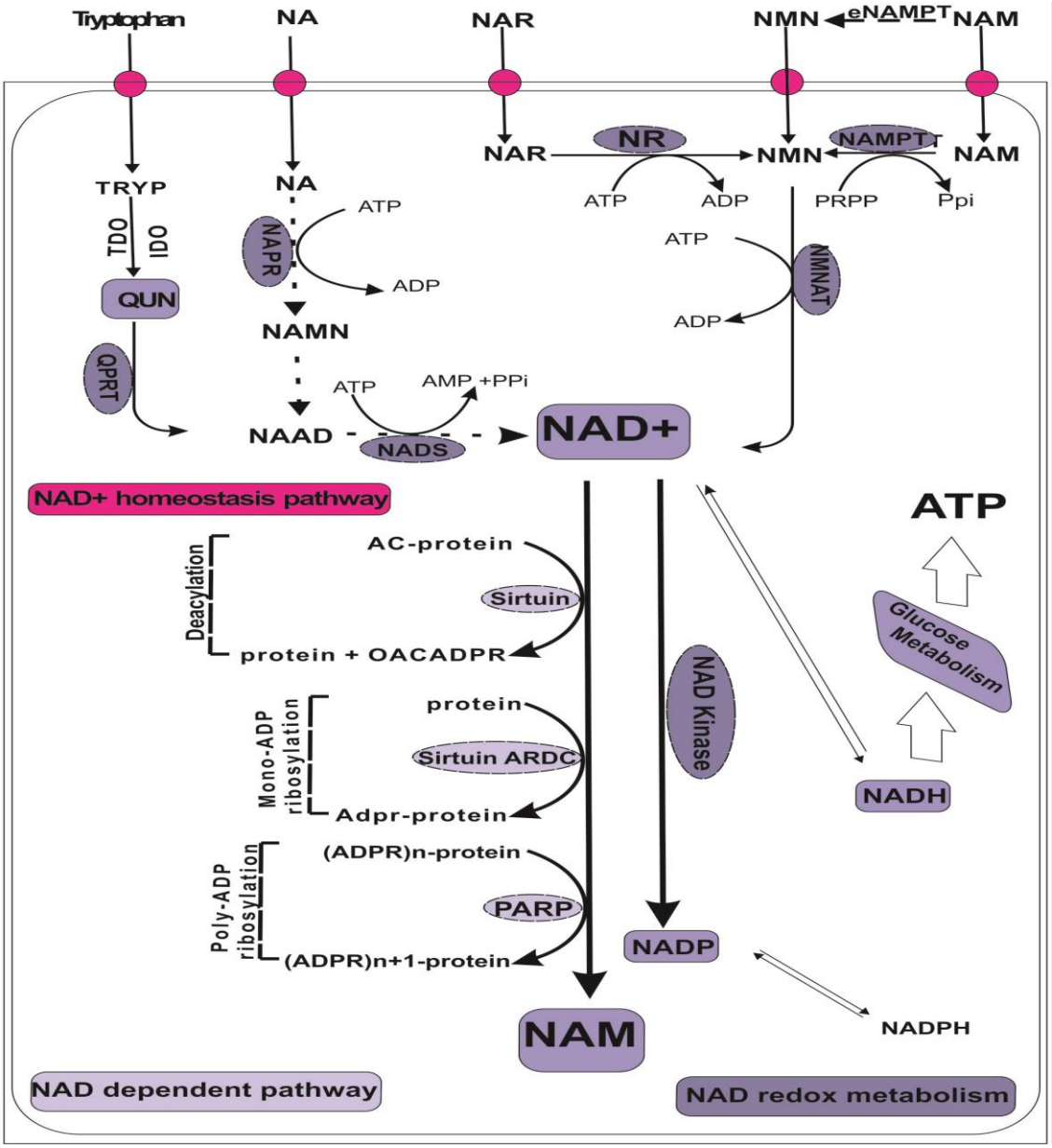

Figure 1.3 The NAD^+ homeostasis pathways. Tryptophan (TRP), nicotinamide (NAM), nicotinic acid (NA), nucleosides NAM riboside (NR) and NA riboside (NAR), quinolinic acid (QA), NA mononucleotide (NAMN), nicotinamide mononucleotide (NMN), QA phospho ribosyl transferase (QAPRT), nicotinamide phospho ribosyl transferase (NAMPT), nicotinic acid phospho ribosyl transferase (NAPRT), extracellular NAMPT (eNAMPT), nicotinamide riboside kinases (NRK), NMN adenylyl transferases (NMNAT), NAD^+ synthetase (NADs), NAD kinase (NADK), O-acetyl-ADP ribose (OAcADPR), ploy ADP ribose polymerase (PARP). The diagram is adapted from Nikiforov *et al*. (2015).

1.2.2 NAD^+-dependent pathways and the inflammatory response

Recent evidence has demonstrated that immune function is tightly regulated by a number of NAD^+-dependent enzymes including ADP-ribose transferases (ARTs), cyclic ADP-ribose (cADPR) synthases (ADP-ribose cyclase) and protein-deacytlases (sirtuins) (Legutko *et al*., 2009). Although these enzymes catalyse different types of reactions, the common feature for all these reactions is the transfer of the ADP-ribose (ADPR) moiety from NAD^+ into a protein acceptor target with the concomitant release of NAM, which has been shown to not only affect the activity of NAD^+-consuming enzymes but also to modulate inflammatory responses by acting as an end-product inhibitor (Sanders *et al*., 2007; van Gool *et al*., 2009; Chiarugi *et al*., 2012; Figure 1.4). Indeed, NAM was shown to non-competitively inhibit sirtuin activity with a subsequent impact on immune responses (Bitterman *et al*., 2002; Anderson *et al*., 2003; Ungerstedt *et al*., 2003). An increase in NAM was shown to inhibit sirtuin-mediated histone deacetylation activity, affecting NF-κB activation (Fulco *et al*., 2003; Yeung *et al*., 2004). These findings suggest a key role for NAD^+-consuming enzymes in immune regulatory responses, for example histone de-acetylation enzymes, or sirtuins. Sirtuin belongs to the NAD^+-dependent protein deacetylase family and it was originally described as homologous to the yeast silent information regulator 2 (Sir2; Landry *et al*., 2000b; Smith *et al*., 2000; Sauve *et al*., 2006). In general, sirtuin uses NAD^+ as substrate to catalyse the protein de-acylation reactions in which an acyl group, from the lysine residue on a target protein, is transferred onto an ADPR moiety on NAD^+ (Jackson and Denu, 2002). This is accompanied by NAM liberation resulting in 2′, 3′-O acetyl-ADP-ribose (OAADPR) generation as a by-product (Figure 1.5; Landry *et al*., 2000b). As a consequence, NAD^+-dependent de-acetylation leads to modulation of the stability and localization of target

proteins (Sauve *et al*., 2006; Haigis and Sinclair, 2010; Canto and Auwerx, 2012; Chalkiadaki and Guarente, 2012).

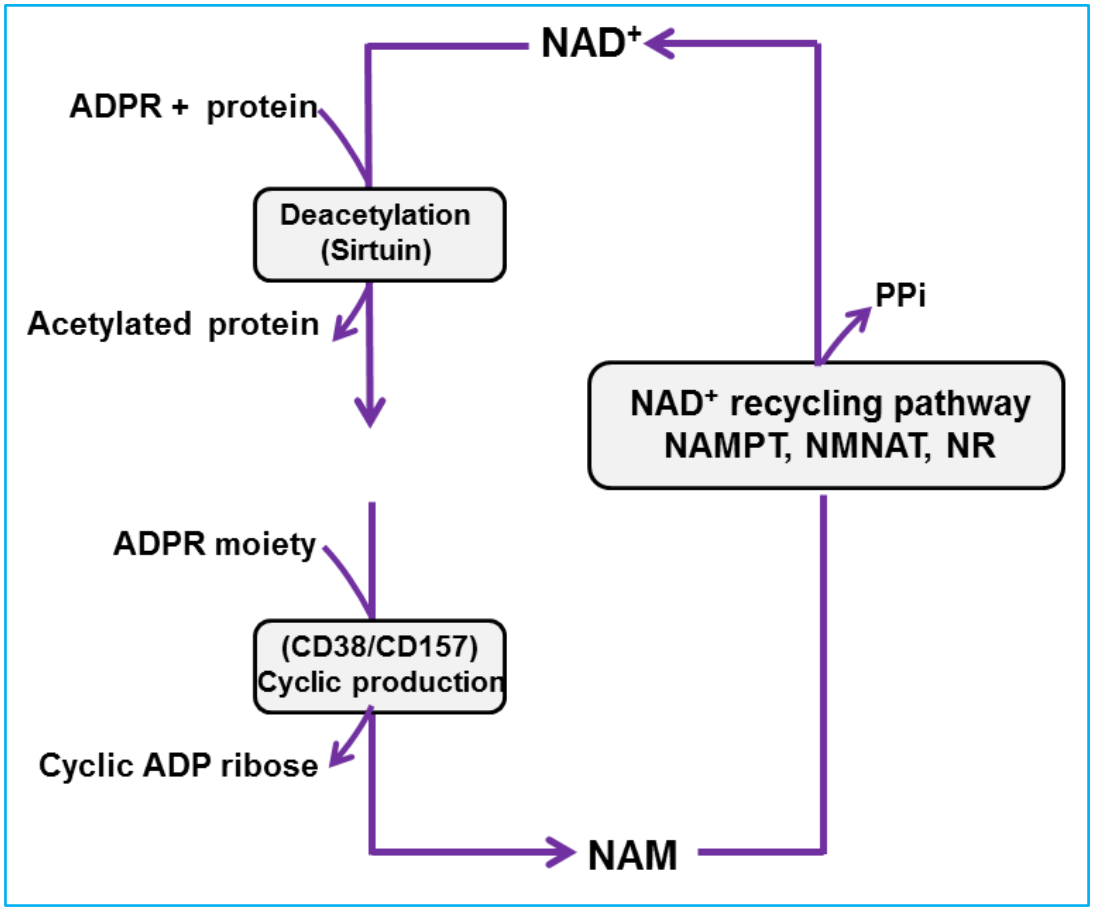

Figure 1.4 The NAD^+ consuming enzymes share one common step that uses NAD^+ as a substrate for protein deacetylation, ribosylation and cyclic ADP ribose production, yielding de-acetylated protein and liberating nicotinamide (NAM) as the end product. The latter is converted back into NAD^+ through the activity of the salvage enzyme pathways including NAMPT, NMNAT and NR (Agnieszka, 2009; Chiarugi *et al.*, 2012).

The mammalian sirtuin family consists of seven conserved homologs namely SIRT 1-7 (Michishita *et al*., 2005; Dali-Youcef *et al*, 2007; Michan and Sinclair, 2007) which are found in organisms ranging from bacteria to humans (Brachmann *et al*., 1995; Nikiforov *et al*., 2015) and share one NAD^+-catalytic domain comprised of 275 amino acids (Michan and Sinclair, 2007). SIRT1, 6 and 7 are found in the nucleolus, whereas SIRT 3-5 reside in

mitochondria. In contrast, SIRT 2 is mainly cytoplasmic, with an ability to shuttle from the cytoplasm to the nucleus to regulate gene expression by de-acetylating transcription factors (Michishita *et al*., 2005; Jing *et al*., 2007). The de-acetylation activity of sirtuins is highly sensitive to intracellular NAD^+ levels (Magni *et al*., 2004) or to the redox ratio (NAD^+/ NADH), thus sirtuins could act as sensors of the metabolic state of cells (Sauve *et al*., 2006; Chalkiadaki and Guarente, 2012) suggesting a direct link between metabolic bioenergetics, homeostasis and gene regulation (Chiarugi *et al*., 2012). Additionally, sirtuins can also control multiple cellular processes including gene silencing (Vaquero *et al*., 2004) and cell differentiation (Fulco *et al*., 2003). The best characterised mammalian sirtuin is SIRT1, and it has been shown to regulate the activity of a list of transcriptional regulators and co-regulators, by modulating their acetylation status; these include the peroxisome proliferator-activated receptor (PPAR), PPAR-coactivator-1 (PGC-1), p53 and NF-κB (Picard *et al*., 2004; Yeung *et al.*, 2004) illustrating an important role for SIRT1 in the immune response via regulation of pro-inflammatory transcription factors. Indeed, Yeung and his team (2004) were the first to suggest that SIRT can modulate the de-acylation of NF-κB via the de-acylation of the Rel A/p65 subunit of NF-κB; this occurs when SIRT1 physically interacts with NF-κB at lysine 310 resulting in inhibition of NF-κB activity (Salminen *et al*, 2008), thereby regulating the expression of genes associated with innate immunity (Chen *et al*., 2005). Accordingly, SIRT1 has been shown to regulate pro-inflammatory transcriptional activity via repression of the transcriptional activity of AP-1, another transcription factor (Huang *et al*., 2004). On the other hand, a key role has been shown for SIRT6, as a NAD-dependent enzyme, in regulating TNF-α production by acting at a post-transcriptional level, therefore decreasing NAD^+ levels and blocking the transcription of TNF-α (van Gool *et al.,* 2009; Galli *et al*., 2010). These observations suggest an exciting link between the redox and thus metabolic state of cell and

pro-inflammatory responses. It seems that sirtuin plays an important immunomodulatory role based on its ability to control TNF-α secretion. However, the inflammatory response is also regulated via other mechanisms through the crosstalk between sirtuin and other NAD^+ utilizing enzymes such as CD38 (Aksoy *et al*., 2006a; Iqbal and Zaidi, 2006) via its ability to modulate NAD^+ availability (Al-Abady *et al*., 2013).

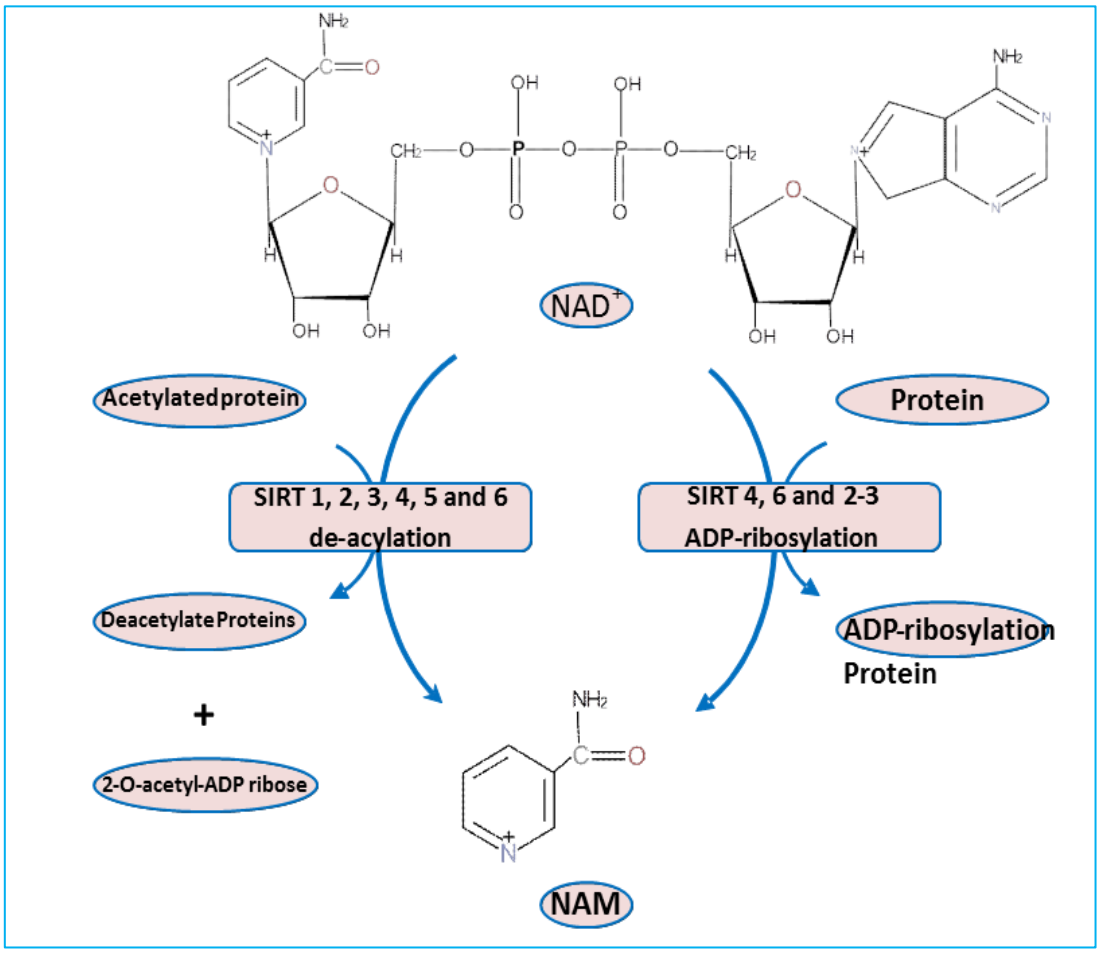

Figure 1.5 Sirtuin enzymatic reactions. Sirtuin members exhibit deacetylase activity in which NAD^+ is used as substrate to cleave acetyl groups from target proteins in a reaction that generates 2-O-acetyl-ADP-ribose and NAM as an end product. Sirtuin also display ADP-ribosyl transferase (ARTs) activity in which the ADP-ribosyl moiety of NAD^+ is transferred to a substrate protein. This figure is adapted from Houtkooper *et al*. (2010).

In mammals, two members of the ADP-ribose cyclase family, CD38 and CD157, are known as lymphocyte antigens with the latter being approximately 25% identical to CD157 (Lee, 2006). Both members are highly conserved ectoenzymes (Lee, 2006). They have been found in all organisms from sea slugs to mammals (Malavasi *et al*., 2006) and both proteins are ubiquitously expressed in most mammalian tissues (Lee, 2006). Importantly, the members of the ADP-ribose cyclase family use NAD^+ as a substrate (Figure 1.6) to catalyse the generation of secondary enzyme messengers such as cADPR, nicotinic acid adenine dinucleotide phosphate ($NAADP^+$) and ADP-ribose implicating ADP-ribose cyclase members in several complex processes (Lee, 2006) from calcium signalling (Fliegert *et al*., 2007), cell activation to proliferation, hormone secretion and immune responses (Malavasi *et al*., 2008). In addition, these proteins have been shown to serve as receptors with enzyme-dependent or independent signalling properties (Lund, 2006; Malavasi *et al*., 2006).

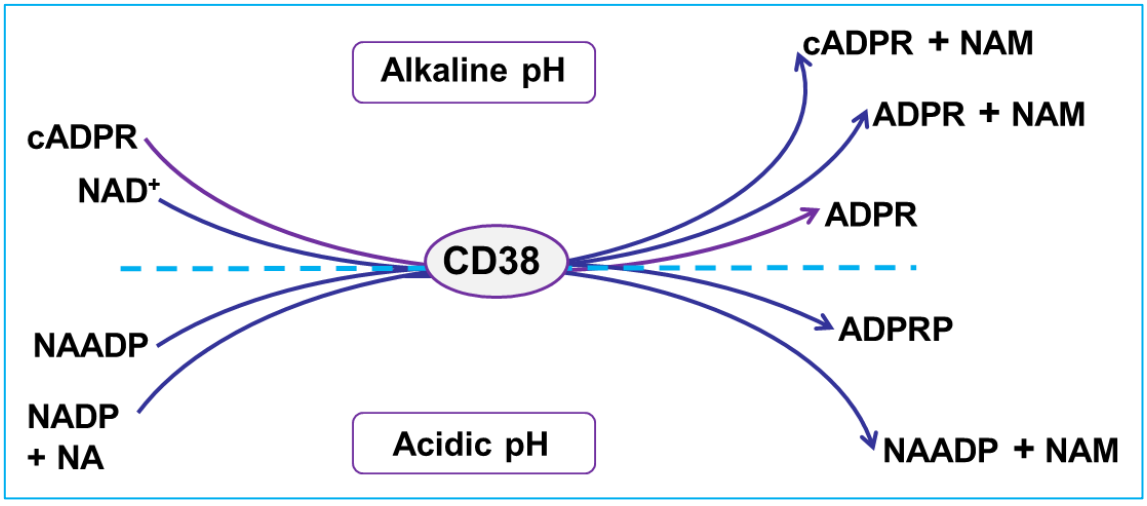

Figure 1.6 The enzymatic activity of CD38. CD38 is involved in the generation of range of secondary messengers including nicotinic acid adenine dinucleotide phosphate (NAADP), cyclic ADP-ribose (cADPR), ADP-ribose (ADPR) and ADP-ribose-2'-phosphate (ADPRP), which are known to mediate intracellular calcium mobilization. The diagram is adapted from Lee (2006).

The most studied ADP-ribose member is CD38 which has been suggested to play a key role in immunity (Lund, 2006; Malavasi *et al*., 2006; Malavasi, *et al*., 2008). CD38 was described as a type II glycosylated protein with a single transmembrane domain near its N terminus (Lee, 2006). CD38 plays critical roles in immune cell differentiation, as it was found to be highly upregulated on cells that are committed to differentiation. In a study conducted on different cell lines, CD38 was upregulated in response to IFN-γ on myelomonocytic such as U937, THP-1 and Mono-Mac-6. However, it was unaffected in promyelocytic cells like HL-60 (Drach *et al*., 1994). Similarly, CD38 was identified as marker for T and B lymphocyte activation and differentiation with activated lymphocytes and thymocytes mainly $CD38^{+}$ whereas resting T and B cells are $CD38^{-}$ (Shubinsky and Schlesinger, 1997).

In addition to these cells, CD38 is also constitutively expressed on other cells such as natural killer (NK) cells, monocytes and mature DCs (mDCs) (Mehta *et al*., 1996; Fedele *et al*., 2004). It has been reported that CD38 is merely a maturation marker as it was shown to display a peculiar pattern of distribution during the differentiation stage. For instance, immature DCs (iDCs) seem to lose surface CD38 which is induced again on mature DCs in response to LPS stimulation (Fedele *et al*., 2004; Malavasi *et al*, 2008). The immune regulatory role of CD38 is reflected by the unique pattern of CD38 expression which is important for immune cell function. The CD38 is important for macrophage and monocytic cell lines, mediating their antigen-presenting ability as well as the ability to secrete pro-inflammatory cytokines (Funaro *et al*., 1990; Lund *et al*., 1995). CD38 seems to critically regulate the expression of pro-inflammatory genes via an increase NF-κB activation and inhibition of ERK1/2 phosphorylation in response to TNF-α, indicating that CD38 is required for the TNF-α signalling pathway (Iqbal and Zaidi, 2007). Conversely, CD38 can also

regulate anti-inflammatory mediators since CD38 was involved in IL-4 secretion in chronic lymphocytic leukaemia, via regulation of cellular Histone de-acylation (HDAC) activity (activity). Decreasing the HDAC activity via TNFα-induced CD38 upregulation, enhanced IL-4 secretion in chronic lymphocytic leukaemia (Levesque *et al*., 2006), suggesting an immune regulatory role for CD38 via limitation of NAD^+ availability for sirtuin-mediated NAD^+ consumption. Similarly, it has also been suggested that CD157 plays a role in inflammation as it was shown to be involved in B cell development and antibody production, and also in immune function and polarization of human neutrophils (Legutko *et al*., 2009).

1.3 Metabolic pathways and immune responses

Cellular energy metabolism is required for sustaining efficient immune cell functions and therefore metabolic regulation. It may also be important for the control of metabolic reactions mediating immune cell responses. The degradation of nutrients via ATP-generating pathways leads to the production of chemically useful energy in the form of ATP (Delmastro-Greenwood and Piganelli, 2013). Overall, ATP can be synthesised through aerobic respiration (oxidative phosphorylation) and anaerobic metabolism (glycolysis) in innate immune cells. By using these pathways, cells are able to produce 28 ATP molecules per glucose molecule, via mitochondrial respiration, while only 2 molecules of ATP are generated via glycolysis metabolism (Delmastro-Greenwood and Piganelli, 2013). ATP can then be utilized for various functional events including housekeeping, migration, differentiation, proliferation, phagocytosis and antigen processing/presentation (Buttgereit *et al*., 2000; Krauss *et al*., 2001). The diversity in immune functions is reflected by the differences that exist in the various known macrophage metabolism profiles. For example, classically activated macrophages (M1s) are mainly glycolytic. Although glycolysis

metabolism is less efficient for energy generation, it is critical for immune cells function, especially in a hypoxic environment (Delmastro-Greenwood and Piganelli, 2013). It is known that glycolysis can operate under anaerobic conditions for short periods of time such as those that may be found at sites of infection but is unsustainable in the long term due to lactate production, reflecting the role of M1s. In contrast, alternatively-activated macrophages (M2s) mainly utilize mitochondrial respiration (Lacy-Hulbert and Moore, 2006; Vats *et al*., 2006) as it is more efficient for energy generation and can sustain for longer. This is why M2s are involved in much longer term anti-inflammatory response/activity. Thus M2s are much more suited to aerobic oxidative metabolism of glucose and fatty acids oxidation. While slower than glycolysis, it produces more ATP and can be sustained for longer. Importantly, the reliance of immune cells on metabolic pathways, for their immune function, makes them good targets for immunometabolism regulatory approaches.

1.3.1 Classical activation (M1 macrophages) and glycolysis

The tight link between metabolic pathways and innate immune function is well established. This link is bidirectional with examples including changes in metabolism being required in order to mount responses and with immune mediators being able to modulate metabolism (Schertzer and Steinberg, 2014). Indeed, the metabolic switch, from OXPHOS to glycolysis (Rodriguez-Prados *et al*., 2010; Pearce *et al*., 2013a) is induced by a range of stimuli such as LPS (Krawczyk *et al*., 2010) and type I interferon (Pantel *et al*., 2014). The activated macrophages among the cells that represent the first line of the immune defence, which takes place within hours, and thus it is perhaps not surprising that macrophages quickly increase glycolysis, allowing rapid increase in ATP generation (Vazquez *et al*., 2010), required for the rapid production of pro-inflammatory cytokines (McGettrick and O'Neill, 2013; Galvan-Pena

and O'Neill, 2014). Following classical activation, M1s increase their glycolytic activity, allowing for rapid ATP production to meet the high energy demand, whereas TCA activity is inhibited (Galvan-Pena and O'Neill, 2014). TCA, via its accumulated metabolites, has been found to be involved in immunometabolism in activated MΦs. Following MΦ activation with LPS, the TCA cycle is broken, resulting in mitochondrial accumulation of TCA intermediates including citrate and succinate (Tannahill *et al*., 2013; Jha *et al*., 2015). Both of those metabolites have been proven to possess signalling capacity and to the immune response (Tannahill *et al*., 2013; Jha *et al*., 2015). Tannahill and his team have shown that succinate is an inflammatory signal that can enhance IL-1β production through stabilisation of the expression of HIF-1α. This, in turn, enhances glycolytic activity via induction of lactate dehydrogenase (LDH) expression. This converts pyruvate (required for acetyl-CoA production that feeds into TCA) into lactate thereby limiting TCA activity (Kim *et al*., 2006). HIF-1α expression has been shown to be regulated by NAD^+-dependent sirtuin deacetylation which is also required for the regulation of TNF-α production (van Gool *et al*., 2009; Lim *et al*., 2010); these observations might strengthen the link between metabolism and immunity. Notably, HIF-1α has been shown to promote NAMPT-mediated NAD^+ production supporting glycolysis (Benita *et al*., 2009). Since NAD^+ is required for both glycolysis and TNF-α production, it seems that both NAD^+ and accumulated succinate, via HIF-1α, are needed to support glycolysis-mediated M1s immune responses. Citrate, another TCA intermediate that accumulates in M1s, is preferentially transported from mitochondria into the cytosol via the citrate transporter. Once in the cytosol, citrate is cleaved by citrate lyase into acetyl- CoA and oxaloacetate to then be fed into pathways that generate nitric oxide, ROS and arachidonic acid, which is required for prostaglandin production. These are inflammatory mediators required for macrophage immune functions suggesting that citrate is an important player in

inflammation (reviewed in O'Neill *et al*., 2016). Additionally, Citrate can also feed into *de novo* synthesis of fatty acids, which in turn degrades into glucose, thus supporting the metabolic switch into glycolysis in DCs and MΦs (reviewed in Kelly and O'Neill, 2015). Clearly, alteration of the TCA cycle plays an important role in the metabolic reprogramming in MΦs/DCs and thus in promoting their immune functions. Several studies have shown that macrophages were able to increase glycolysis via an increase in glucose uptake, with most glucose being converted into lactate, with little being used for OXPHOS (Figure 1.7; Newsholme *et al*., 1987). Moreover, it was shown that the expression of the glycolytic enzymes, such as hexokinase is also increased in activated macrophages, indicating an increase in glycolytic activity in these cells (Newsholme *et al*., 1986). Furthermore, the increase in glycolysis is accompanied by the increase in the flux through pentose phosphate pathway (PPP) (Figure 1.7; Haschemi *et al*., 2012; Freemerman *et al*, 2014; Galvan-Pena and O'Neill, 2014). The PPP branches off glycolysis and is considered to be an important source of nicotinamide adenine dinucleotide phosphate (NADPH) required for NOS and NADPH oxidase, which mediates ROS production (Borregaard and Herlin, 1982; Aktan, 2004; Bedard and Krause, 2007). Owing to its ability to disturb redox balance, ROS production can cause serious damage to immune cells. This can be prevented via the action of anti-oxidant enzyme, glutathione (GSH) that detoxify ROS, and which requires NADPH as co-factor (Grant, 2008). Indeed, GSH uses NADPH to regulate redox balance-mediated MΦ activation by LPS (Wang *et al*., 1999). It has been suggested that this switch in the metabolic state is correlated with immune cell responses (McGettrick and O'Neill, 2013). Therefore, the inhibition of glycolysis with 2-deoxyglucose (2DG, a glucose analogue) resulted in a decrease the LPS-induced production of inflammatory responses such as inhibition of the secretion of IL-1β (Tannahill *et al*., 2013). Also, 2-deoxy-glucose (2-DG) was able to block TNFα and IL-6

production via inhibition of NF-κB signalling in primary microglia as a result of blocking glycolysis by inhibiting hexokinase activity (Wang *et al*., 2014). In contrast, the inhibition of mitochondrial respiration, via mitochondrial inhibitors, showed no effect, indicating that oxidative metabolism is already shut down under such conditions (Kellett, 1966).

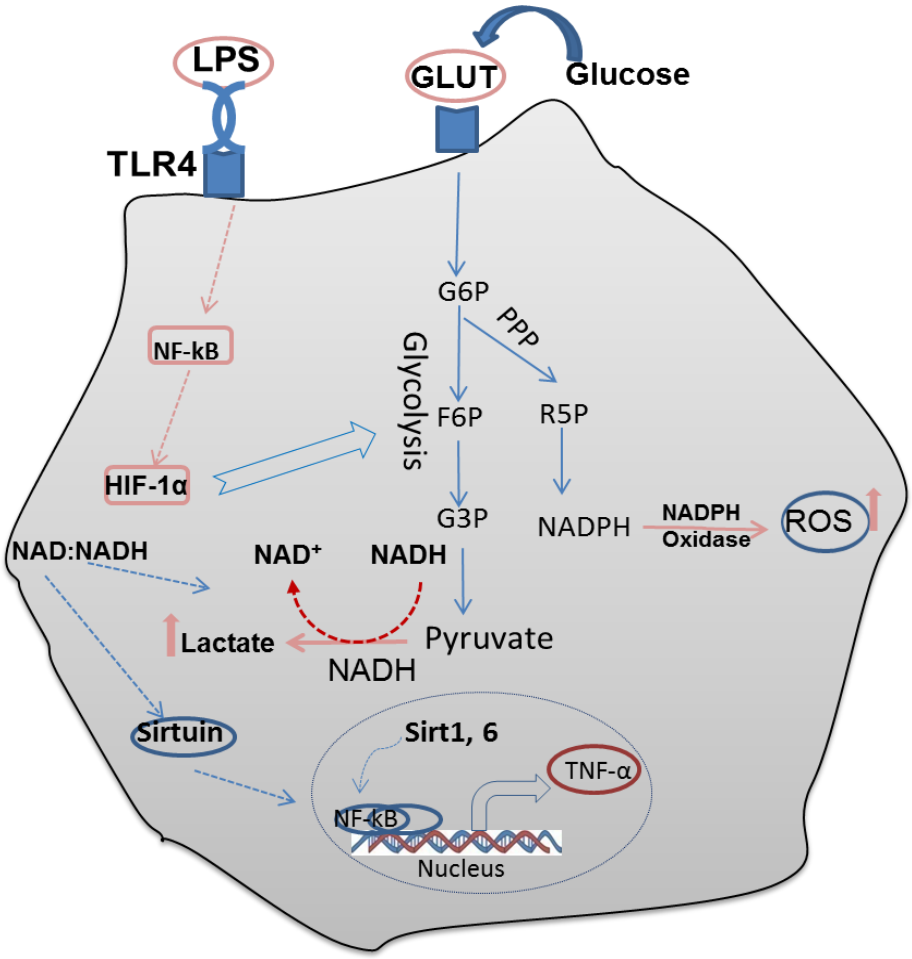

Figure 1.7 Metabolic profile of an M1 macrophage. Glycolytic metabolism is induced in classical activation (M1s) resulting in increased lactate production. HIF-1α is also induced in M1s allowing induction of pro-inflammatory cytokines. Meanwhile, the activity of PPP is initiated, allowing an increase in ROS production supporting the bacterial killing mechanism used in M1s. G6P, glucose-6-phosphate; F6P, fructose-6-phosphate; R5P, ribose-5-phosphate; HIF-1α, Hypoxia inducible factor-1α; G3P, glyceraldehyde-3-phosphate; ROS, reactive-oxygen species. This diagram is adapted from Galvan-Pena and O'Neill (2014).

Additionally, LPS increases glycolytic activity in macrophages through an increase in the expression of iNOS (inducible nitric oxide synthase) that generates NO (nitric oxide), which inhibits mitochondrial activity via ROS production. This occurs via NO-mediated nitrosylation of iron-sulfur proteins present in electron transport chain complexes such as complex I (Drapier and Hibbs, 1988; Clementi, *et al*., 1998) as well as cytochrome-*c* oxidase (Cleeter *et al*., 1994). These observations suggest that a metabolic switch in macrophages might be dependent on iNOS and NO-mediated inhibition of mitochondrial metabolism. Indeed, it was shown that inhibition of iNOS was able to restore mitochondrial respiration activity during LPS stimulation (Kelly and O'Neill, 2015). Finally, LPS was shown to induce glycolytic activity via another mechanism, this being the induction of the hypoxia inducible factor (HIF-1α; Denko, 2008). HIF-1α promotes the switch to glycolysis so that these cells can continue to produce ATP when oxygen is limited (as oxygen is not required for glycolysis). HIF-1α facilitates this metabolic switch by binding to hypoxia response elements in target genes (Semenza *et al*., 1991; Mole *et al*., 2009) such as the glucose transporter (GLUT1; Chen *et al*., 2001) and glycolytic enzymes. For example, HIF-1α is involved in the induction of lactate dehydrogenase (LDH) expression (Semenza *et al*., 1996) which catalyses lactate production from pyruvate, thereby limiting the production of acetyl-CoA for the TCA cycle. HIF-1α also increases the expression of pyruvate dehydrogenase kinase (Kim *et al*., 2006; Papandreou *et al*., 2006) which inhibits pyruvate dehydrogenase, an enzyme that catalyses the formation of acetyl-CoA from pyruvate (Cramer *et al*., 2003). Glycolysis seems to dominate in M1s during LPS stimulation, highlighting an important immune regulatory role for innate immune cells.

1.3.2 Alternative activation (M2s) and oxidative metabolism

Alternative activation (M2s), unlike classical (M1) activation, displays a different metabolic profile. In activated M2s, the metabolism is shifted toward oxidative metabolism, while glycolysis is attenuated (McGettrick and O'Neill, 2013). This switch increases fatty acid utilization and decreases the PPP. The shift towards fatty acid oxidation occurs because M2 stops ROS production and thus activates respiratory redox chain activity promoting fatty acids oxidation. Indeed, the oxidation of fatty acid has been shown to be anti-inflammatory (Steinberg and Schertzer, 2014), hence the metabolism unsurprisingly reflects the function of M2 macrophages. Indeed, the main functions of M2s are involved in wound healing and anti-parasitic defence which last for longer term. Thus M2s utilize fatty acid and oxidative metabolism to obtain energy. While oxidative metabolism is slow, it can lead to the interconversion of more energy than glycolysis, and can be sustained for longer (Steinberg and Schertzer, 2014). Following activation, M2s increase the expression of the genes governing the electron transport chain allowing fully functional oxidative phosphorylation in addition to directing the pyruvate into the TCA cycle instead of lactate production as in M1s (Figure 1.8). Forcing a switch from glycolysis to oxidative metabolism can lead to a transformation in phenotype. Thus, the inhibition of oxidative phosphorylation was found to not only inhibit the M2 phenotype but also to drive the macrophage into an M1 phenotype (Freemerman *et al*, 2014). In addition, forcing oxidative metabolism in an M1 macrophage potentiates the M2 phenotype (Tannahill *et al*., 2013; Freemerman *et al*, 2014). M2s are known to induce carbohydrate kinase-like protein (CARKL), a sedoheptulose kinase that catalyses the conversion of sedoheptulose into sedoheptulose-7-phosphate. The activity of CARLK leads to limitation of PPP activity and a consequent decrease in NADPH generation (Haschemi *et al*., 2012), while it activates the oxidative metabolism under activation

conditions. Interestingly, it has been observed that CARKL levels are increased during M2s while it decreased in M1s during LPS stimulation (Haschemi *et al*., 2012). The knockdown of CARLK enhances LPS-induced cytokine production as well as M1 macrophage polarization. However, overexpression of CARKL decreased LPS-induced IL-6 secretion (Haschemi *et al*., 2012), suggesting a switch in phenotype effector functions.

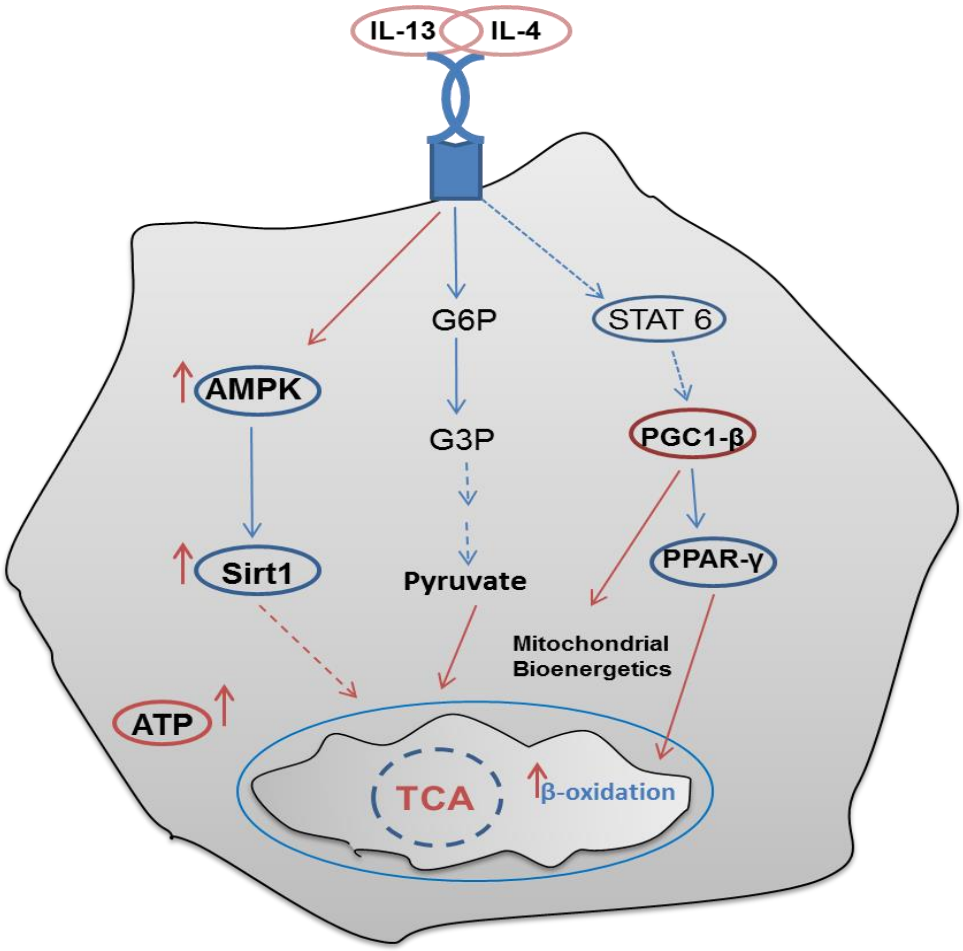

Figure 1.8 Metabolic profiles of an M2 macrophage. Alternative activation is via induced oxidative metabolism and β-oxidation activity. STAT6 and PGC-1β drive mitochondrial activity as well as the production of anti-inflammatory cytokines. This can also occur via the accompanying activity of AMPK, adenosine monophosphate activated protein kinase, and SIRT1. G6P, glucose-6-phosphate; G3P, glyceraldehyde-3-phosphate.This diagram is adapted from Galvan-Pena and O'Neill (2014).

In general, the oxidative metabolism of fatty acid in mitochondria is tightly controlled by, adenosine monophosphate activated protein kinase (AMPK) in M2s (Sag *et al*., 2008) via targeting the nuclear receptor, PPARs (Vats *et al*., 2006). The expression of PPARs has been found to be induced in response to the alternative stimulation signal (IL-4 and IL-13) resulting in increased expression of proteins involved in mitochondrial respiratory chain (Vats *et al*., 2006). In addition, the activity of fatty acid β-oxidation is also increased in macrophages via IL-4-mediated PPARs enzymatic activity (Odegaard *et al*., 2007). Additionally, AMPK is highly active in M2s and it is involved in the regulation the production of anti-inflammatory responses in M2s via the control of IL-10 production (Sag *et al*., 2008). These observations further confirm the link between the immune response and metabolism. Finally, activation of M2 with IL-4 resulted in an increase in oxidative metabolism via the activity of mechanistic target of rapamycin (mTOR), an atypical serine/threonine kinase which is the mechanistic target of rapamycin (Byles *et al*., 2013). Therefore, the inhibition of mTOR by rapamycin treatment (Land and Tee, 2007) can also lead to a decrease in HIF-1α levels and therefore could result in reduced HIF-1α-dependent glycolytic and inflammatory gene expression (Pawlus and Hu, 2013).

1.4 NAD^+ Homeostasis and metabolic pathways

It is now acknowledged that NAD^+-sensing energy bridges the metabolism shift with the reprogramming of effector phenotypes. By sensing NAD^+, SIRT-1, 3 and 6-mediated de-acetylation play important roles in regulating pro-inflammatory genes and metabolic enzymes used in glycolysis (Haigis and Sinclair, 2010; Wang *et al*., 2010). Thus, SIRT 6 can regulate glucose metabolism (Xiao *et al*., 2010) by reversing the trans-activating acetylation of genes involved in glycolysis, thus antagonising HIF1α-induced glycolysis (Wang *et al*., 2010;

Zhong *et al*., 2010). A recent study has shown that knockdown of SIRT6 causes mice to die due to hypoglycaemia (Xiao *et al*., 2010). Conversely, SIRT1, which is located in mitochondria, was found to regulate fatty acid oxidation via NAD^+-sensing de-acetylation of multiple mitochondrial proteins, including members of the electron transport complexes I and III as well as isocitrate dehydrogenase, which supports the citric acid cycle, linking metabolism and inflammation (Lombard *et al*., 2007; Bell and Guarente, 2011). Importantly, SIRT1 plays a key role in regulating downstream phosphorylation and activation of AMPK (Lan *et al*., 2008). Once AMPK is activated, oxidative metabolism, which is associated with the anti-inflammatory state, is induced, whereas glycolysis, which is associated with inflammatory state, is inhibited (Beckers *et al*., 2006; Hawley *et al*., 2012). The link between SIRT1 and AMPK is well documented (Price *et al*., 2012). It has been found that SIRT1 knockdown led to block AMPK activation indicating that the SIRT1 is required for AMPK activation (Price *et al*., 2012). Interestingly, the involvement of AMPK in modulating energy metabolism is well established, and AMPK is essential in order to maintain energy balance through promotion of catabolic and inhibiting energy consuming processes (Jones *et al*., 2005). Conversely, it has been found that AMPK itself can activate SIRT1, probably via some sort of positive feedback loop (Canto *et al*., 2009), by inducing the expression of NAMPT and the subsequent increase in NAD^+ (Canto *et al*., 2009). NAD^+ levels can promote SIRT1 and the shift from the pro-inflammatory, (glycolytic) state to the anti-inflammatory, (oxidative) state, limiting inflammation (Pearce, 2010; Yang *et al*., 2010; Liu *et al*., 2012). This occurs via mediation of the suppression of PPARγ (a transcription factor) expression by SIRT 1, resulting in the regulation of multiples genes involved in fat storage (Wellen and Thompson, 2010). It has been show that NAD^+ is essential for energy metabolism, and thus that a decrease in NAD^+ levels via FK866-mrdiated NAMPT leads to the attenuation of

glycolysis at the glyceraldehyde 3-phosphate dehydrogenase step, in addition to limiting the pentose phosphate pathway activities (Tan *et al*., 2013). It has thus become clear that NAD^+ homeostasis is involved in both metabolism and pro-inflammatory responses. Therefore, a pharmacological approach must apply to control metabolism and to fine-tune appropriate immune inflammatory responses.

1.5 The THP-1 cell line as model of macrophage differentiation

It has been previously shown that the THP-1 cell line represents an appropriate model for native monocyte-derived macrophages (Tsuchiya *et al*. 1982; Reyes *et al*., 1999). Indeed, investigators have recently shown that THP-1 can be used as an accurate model to study the differentiation or maturation as well as the immune response of monocytes and macrophages in different conditions such as that of cardiovascular system (Tsuchiya *et al*. 1982; Auwerx, 1991; Daigneault *et al*., 2010; Qin, 2012). THP-1 cells were first established by Tsuchiya *et al*. (1980), who isolated the cells from the peripheral blood of a one year old human male with acute monocytic leukaemia .Tsuchiya (1980) described THP-1 as single rounded cells that grow in suspension, and that do not adhere to a culture plate, with the ability to express monocytic markers such as Fc-γ receptors and C3b receptors (Tsuchiya *et al*. 1980; Fleit and Kobasiuk, 1991). Due to the difficulty in obtaining sufficient quantities of human primary monocytes/macrophages, as well as the inherent variation between subjects, it seems reasonable to use THP-1 as an *in vitro* substitute cell line. The main question being whether or not the cell line successfully mimics the primary cells derived from patient blood. Interestingly, THP-1s have become widely used to study monocyte-macrophages because of their similarity to the monocytes in peripheral blood mononuclear cells (PBMCs; Auwerx, 1991; Sharif *et al*., 2007; Qin, 2008). Researchers have shown that THP-1, in a similar way to

PBMCs, can synthesize and secrete macrophage colony stimulation factor (M-CSF; Gaffney *et al*., 1986), IL-8 (Wang *et al*., 1996) and apolipoprotein E (Menju *et al*., 1989). In addition, it has been observed that THP-1 responses to LPS-induced gene expression are very similar to that of primary macrophages, even though they are a transformed and immortalised cell line (Verreck *et al*, 2006; Sharif *et al*., 2007). Sharif *et al*. (2007) observed that THP-1-derived macrophage responses to LPS activation are comparable to that of PBMCs. Furthermore, it has been reported that THP-1 cells constitute a better model system for macrophage differentiation when compared to other monocytic cells line such as U937 cells, which have been reported to respond differently to LPS stimulation, with both cell types showed differential profiles of CD14 expression (Sharif *et al*., 2007). Therefore, it seems that THP-1 can be considered as a reliable and accurate *in vitro* model to study macrophage differentiation.

Traditionally, THP-1 cells can be differentiated or activated via a range of agents, most commonly by PMA or vitamin D_3 (1α, 25-dihydroxyvitamin D_3; Auwerx, 1991; Schwende *et al*., 1996; Daigneault *et al*., 2010; Foey and Crean, 2013). Previous studies have reported that the monocyte differentiation is reflected by several criteria: (i) loss of proliferation, (ii) an increase in phagocytic ability and adherence, and (iii) changes in the cell morphology associated with irregular cell shape with obvious pseudopodia (Verreck *et al*., 2006; Sharif, *et al*. 2007). However, it is not clear whether these agents can induce macrophages that are comparable to tissue macrophages. A growing body of literature has shown that PMA is capable of inducing complete differentiation of THP-1 cells into macrophage-like cells although THP-1 is a monocytic cell line that has minimal receptor expression prior to exposure to PMA (Tsuchiya *et al*. 1982; Auwerx, 1991; Daigneault *et al*., 2010). Indeed, PMA treatment was found to activate macrophage differentiation that occurs via PKC, an

integral part of cellular signalling machinery. PMA was shown to induce differentiation, resembling diacylglycerol, which naturally mediates the differentiation process (Nishizuka, 1995; Livneh and Fishman, 1997). Interestingly, the differentiation can be determined by observing (i) alterations in cell morphology as cells become adherent and adopt an irregular shape coupled with elongated pseudopodia, (ii) a loss of proliferation, and (iii) increased phagocytic markers. Additionally, macrophages induced by PMA are also associated with induced gene expression of adhesion molecules such as the Ig-related molecules CD54 (ICAM-1), ICAM-2 and upregulated expression of complement receptors CR3 (CD18-CD11b) and CR4 (CD18-CD11c) resembling a tissue macrophage like state (Prieto *et al*., 1994; Traore *et al*., 2005). Furthermore, Daigneault *et al*. (2010) observed that PMA-derived THP-1 differentiation did not exhibit expression of CD206, a monocytic marker, when compared to monocyte-derived macrophages, suggesting that PMA-THP1 cells are very close to classical macrophages.

Alternatively, THP-1 differentiation can be induced by vitamin D_3, with the immune-regulatory role of vitamin D_3 on macrophages/monocytes being well recognised (Abe *et al*., 1983). Phenotypically, macrophages induced by vitamin D_3 mimic mature monocyte cells in that they exhibit upregulated CD14 expression, a surface antigen characteristic of mature mononuclear phagocytes (Fleit and Kobasiuk, 1991; Schwende *et al*., 1996; Hmama *et al*., 1999; Daigneault *et al*., 2010). In fact, macrophages and monocytes express high levels of the vitamin D_3 receptor (VDR) that causes those cells to be highly sensitized to the differentiation effect of vitamin D_3 (Abe *et al*., 1983). In support of this, vitamin D_3 was shown to attenuate the expression of TLR2 and TLR4 in a time-dependent manner in monocytes triggering a state of hypo-responsivity towards bacterial cell wall components in a VDR-dependent mechanism (Scherberich *et al*., 2005; Sadeghi *et al*., 2006). Sadeghi (2000)

showed that TLR2, 4 inhibition was associated with impaired NF-kB/RelA translocation to the nucleus, alongside p38 and p42/44 (extracellular signal-regulated kinase 1/2) phosphorylation. Recent studies reported by Coussens *et al*. (2009) showed that vitamin D_3 treatment inhibits the expression of some matrix metalloproteinases (MMP-7, 10) and secretion of MMP-7, as well as the secretion and activity of MMP-9 by *M. tuberculosis*-infected PBMCs. In this study, the investigators also reported that the secretion of IL-10 and prostaglandin E2 were induced by vitamin D_3 treatment from PBMCs (Coussens *et al*, 2009). Furthermore, vitamin D_3 is known to induce the MAPK phosphatase-1 (MAPKP-1) expression which is highly controlled by AMPK (Wu *et al*., 2015), which plays a key role in supporting oxidative metabolism in M2s (Sag *et al*., 2008). Additionally, PMA and vitamin D_3 modulatory effects are also reflected by the prevention of anti-inflammatory and pro-inflammatory cytokine release, respectively (Alappat *et al*., 2010; Daigneault *et al*., 2010). Collectively, these observations suggest that PMA and vitamin D_3 treated THP-1 cells is probably a valuable model to study macrophage immune-regulatory functions (Auwerx, 1991).

1.6 Aims of the current study

This research study aimed to investigate the immune modulating effect of NAD^+ homeostasis on macrophage immune responses, particularly TNF-α by utilizing of the THP-1 cell line in generating macrophage-like subset as a model for the current study. Initially, the NAD^+ levels and NAD^+ homeostasis gene expression was investigated in resting and activated macrophages generated from THP-1 cells differentiated with either PMA, to generate M1-like macrophages, or vitamin D_3, to generate M2-like macrophages (reported in Chapter 3). To understand more about the link between NAD^+ and TNF-α, the intention was to (1) investigate the source of NAD^+ generation using a pharmacological approach, (2) to investigate whether NAD^+ modulation can control LPS-induced TNF-α release and (3) to explore the mechanism(s) that underline how NAD^+ levels are linked to TNF-α release in both subsets (Chapter 4). It is known that NAD^+ levels are required for glycolysis; therefore, the next aim was to investigate the metabolic profile in differentiated macrophages under LPS stimulation (Chapter 5). To understand whether NAD^+ manipulation can modulate metabolic flux, a pharmacological approach was taken and metallic flux was measured, as reported in chapter 5.

CHAPTER 2

GENERAL MATERIALS & METHODS

2. General materials and methods

2.1 Materials

The cytokines, stimulants and antibodies used throughout this study, and their sources, are listed in table 2.1. Similarly, chemicals and buffers are shown in table 2.2, whilst table 2.3 lists kits, inhibitors and other materials. In addition, a general overview of the experimental design employed during the course of this study is shown in Figure 2.8.

Table 2.1 Cytokines, stimulants and antibodies used during this study and their suppliers

Cytokines, stimulants, antibodies	Supplier
Recombinant human TNF-α Recombinant human IL-6	BD Pharmingen, Oxford, UK
Mouse anti-Hu TNF-α Mab1 IgG1 Biotinylated mouse anti-Hu TNF-α Mab11 Rat anti-human IL-6 Mab MQ2-13A5 IgG1 Biotinylated Rat anti-Hu IL-6	BD Pharmingen, Oxford, UK
phorbol-12-myristate-13-acetate (PMA) 1,25-(OH)2-Vitamin D_3 (VD_3) MTT(3-(4,5-Dimethylthiazol-2-yl)-2,5-Diphenyltetrazolium Bromide) PES (5-ethylphenazinethylsulfate) ADH (alcohol dehydrogenase) NAD(H) Kynurenine Lactic acid	Sigma-Aldrich, Poole, UK
Bacterial lipopolysaccharide, *Escherichia coli* strain K12 (*E.coli* K12)	Autogen-Bioclear Ltd., Wiltshire, UK

Table 2.2 Chemicals and buffers used in the current study, and their suppliers

Media and chemicals	Supplier
RPMI 1640	Lonza, Wokingham, UK
TMB (3,3,5,5-Tetramethyl benzidine)	Insight Biotechnology Ltd., Middlesex, UK
Fetal bovine serum (FBS)	Sera Laboratories International Ltd, Hull, UK
Phosphate buffered saline (PBS) tablets Dulbecco's PBS (DPBS)	Melford Laboratories Ltd., Ipswich, U.K.
Bovine serum albumin (BSA) Dimethyl sulfoxide (DMSO) Ethanol (general laboratory grade) Ethylenediaminetetracetic acid (EDTA) Trypan Blue (0.4%) Hydrochloric acid (HCl) (37%) Concentrated Sulphuric acid (H_2SO_4) Glacial acetic acid (100%) Sodium hydroxide (NaOH) Kynurenine (KYN) Ehrlich Reagent (p-dimethyl amino benzaldehyde) (DMAB) Trypsin Glutamine Penicillin-Streptomycin Protease inhibitor Cocktail	Sigma-Aldrich, Poole, UK
Streptavidin conjugate Horseradish peroxidise (HRP)	Fisher Scientific U.K. Ltd., Loughborough, U.K.

Table 2.3 Inhibitors, reagent kits, plus other materials used, and their suppliers

Inhibitors, reagent kits, Other materials	Supplier
Micro BCA™ protein assay kit	Thermo scientific, Waltham, USA
Oligonucleotide primers	Eurofins MWG Operon, Ebersberg, Germany
Moloney Murine Leukaemia Virus (M-MLV) enzyme and buffer for cDNA synthesis Deoxynucleotides Gene Elute Mammalian Total RNA Mini Kit Random nonamers Ribonuclease Inhibitor SYBR® Green Jump Start Taq Ready Mix	Sigma-Aldrich, Poole, UK
FK866 (E-N-[4-(1-benzoyl piperidine)-4-yl) butyl] acrylamide-3-pryridin-3-yl)) 1D-methyl tryptophan (1D-MT) Diphenylene iodonium chloride (DPI) 2-deoxyglucose (2-DG) (Glycolysis inhibitor) Rotenone Antimycin Oligomycin	Sigma-Aldrich, Poole, UK
Sirtinol (Sirtuin inhibitor)	Santa Cruz Biotechnology Inc., Texas, U.S.A.

2.2. Methods

2.2.1 Cell line maintenance and culture

The human monocytic leukaemia cell line THP-1 (ECACC, Salisbury, Wiltshire, UK), was grown in suspension, was split every 3-4 days and was used routinely between passages 8 and 24. The cells were maintained in RPMI 1640 complete growth medium supplemented with 10% (v/v) heat inactivated fetal bovine serum, 2 mM L-glutamine, 100 U/ ml penicillin and 100 µg/ ml streptomycin (P/S). The cells were kept at 37 ºC, under 5% CO_2 in a humidified incubator.

2.2.2 Cell differentiation with PMA or vitamin D3 (VD3) and stimulation with LPS-K12

For THP-1 differentiation into macrophage-like subsets, the cells were plated (at a density of 1 x 10^6 cells/ ml) in complete medium (as described in the previous section) in six well tissue culture plates and incubated with either PMA (25 ng/ ml, three days; for differentiation into M1-like macrophages) or with 1,25-$(OH)_2$-Vitamin D_3 (10 nM, seven days; for differentiation into M2-like macrophages). PMA-treated THP-1 cells were washed after the initial three day stimulus, by replacing the PMA-containing media with fresh pre-warmed growth medium, and then incubated for further five days while VD_3-THP1 enhanced (Daigneault *et al.*, 2010). Differentiated cells were stimulated with 100 ng/ml lipopolysaccharide (LPS) derived from *E.coli* K12. Dead cells were aspirated while the supernatant were harvested following centrifugation at 200 x g for 5 min, before storage at -20 ºC until the day of analysis. For cell counting, adherent cells (M1-like) were detached by trypsinization using 0.5% (v/v) of trypsin with 0.25% (v/v) EDTA and trypsinization stopped with fresh medium

2.2.3 Assessment of cell viability

Viability assessment of suspended and adhered cells was carried out after differentiation. Viability was determined for all samples before they were used in each experiment. Ten microliters of cell suspension were mixed with 90 µl of 0.1% (v/v) Trypan blue. To determine the number of viable cells, 10 µl of this was placed into a Neubauer hemocytometer chamber and cell viability was visually determined. The viable cells had clear cytoplasm while non-viable cells had dark blue cytoplasm.

2.2.4 Vitality assay

Cell vitality measured using the MTT assay shows the ability of viable cells to reduce the yellow tetrazolium salt, MTT. Briefly, MTT is reduced by dehydrogenase enzymes, produced by viable cells, allowing the generation of reducing equivalents such as NADH and NADPH, and resulting in production of an insoluble purple formazan dye. The precipitated formazan is solubilized and spectrophotometrically quantified at 550 nm. The absorbance of the produced formazan signal is proportional to the number of viable cells.

The cells were seeded at density 10^4 cells/well in a 96-well microplate. The seeded cells were incubated for 2h at 37 ºC with an equal volume of assay medium containing thiazoyl blue tetrazolium (5 mg MTT in PBS). The resulting formazan crystals were solubilized in 100µl DMSO. The absorbance was read at 550 nm using the Versa Max plate reader (Molecular Devices, Sunny Vale, CA, USA) and the software processes the data was Soft max Pro version 2.4.1.

2.2.5 Preparation of cell extracts and protein quantification assay

The differentiated macrophage cultures (six well plate) were washed twice with 5ml ice-cold Dulbecco's modified phosphate buffered saline (DPBS), and the cells were removed from the plate using 0.25% (v/v) trypsin (for adherent cells) and aspiration (for suspension cells). Cell suspensions were centrifuged at 200 x g (Eppendorf 5418R, Hamburg, Germany) for 5 minutes. The supernatant was aspirated and the pellets were re-suspended in 250 µl ice-cold lysis buffer that contained 100 mM Tris hydrochloride (pH 7.4), 50 mM NaCl and with freshly added a 1x protease inhibitor (AEBSF 104 mM, Aprotinin 80 µM, Bestatin 4 mM, E-64 1.4 mM, Leupeptin 2 mM, Pepstatin A 1.5 mM). To aid cell lysis, samples were sonicated three times on ice for 10 s each time (SONICS Vibra cell, Newtown, USA). Following sonication, the extracts were centrifuged at 9000 x g (Eppendorf 5418R, Hamburg, Germany) for 10 mins at 4 ºC. The supernatants were stored at -20 ºC prior to NAD^+, lactate and kynurenine analysis (see sections 2.6, 7 and 8). All steps were carried out at 4 ºC. All the measurements for total protein were performed using a commercially available bicinchoninic acid (BCA) protein assay micro^{TM} BCA kit, according to the manufacturer's instructions (Smith *et al*., 1985).

The BCA assay is a colorimetric assay which is linear with increasing protein concentrations over a range of 5 to 200 µg/ml. The standards were prepared from known BSA protein concentrations by 1/3 dilutions in assay buffer to create known standard concentrations (5-200 µg/ ml; Figure 2.1, overleaf).

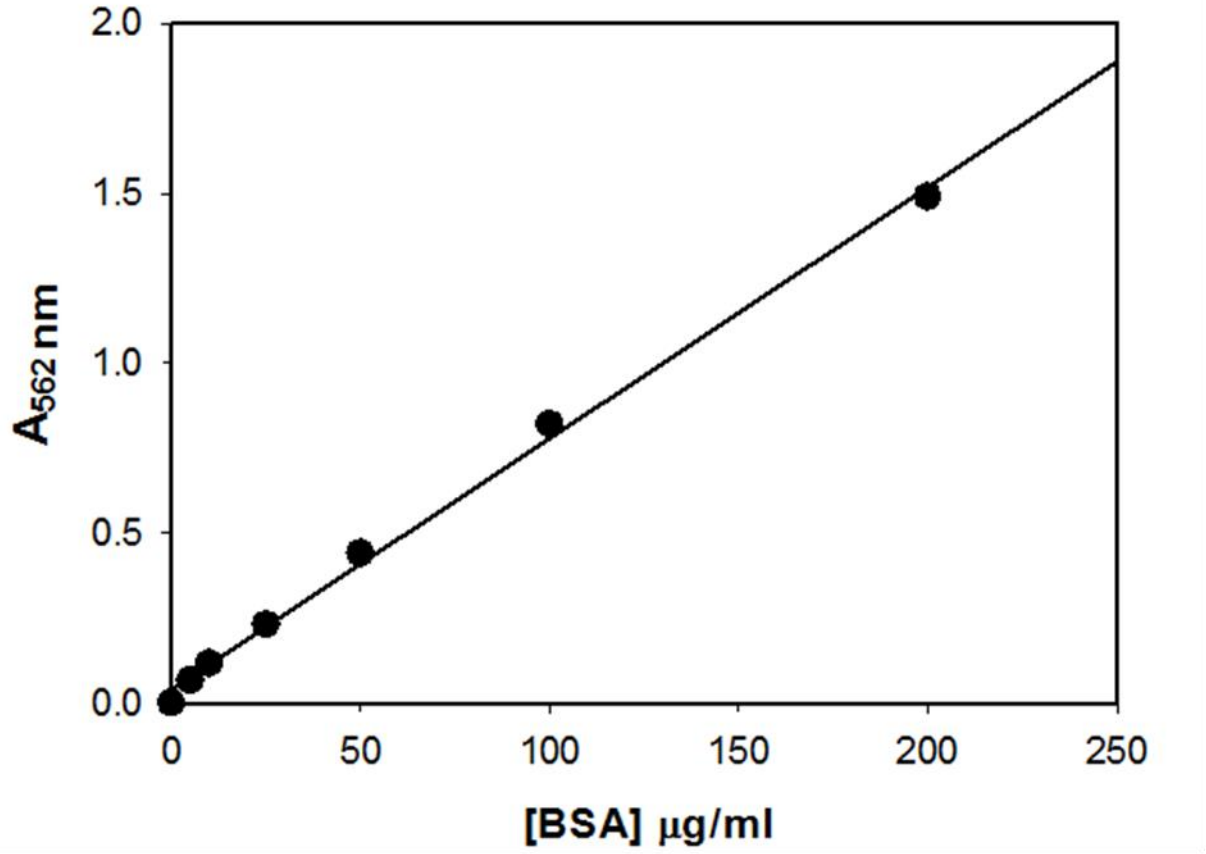

Figure 2.1 The BSA protein standard curve. BSA was diluted in assay buffer to create standards of known concentrations and was quantified for protein estimation with BCA assay reagents. Absorbance was measured at 562 nm and plotted as a function of BSA concentration.

Briefly, two microliters of sample were pipetted into a 96-well plate followed by 98µl assay buffer mixed with 10 x protease inhibitor. Next, an equal volume of BCA working reagent (Thermo Scientific # 23228) was added to each well. The reaction was performed at 37 ºC in a humidified incubator for 2 h. The absorbance was then read spectrophotometrically at 562 nm using a plate reader (Versa Max, Molecular Devices, Sunny Vale, CA, USA) and the unknown samples were determined from a standard curve created using BSA (Figure 2.1).

2.2.6 NAD(H) Micro-cycling assay for the measurement of intracellular NAD^+ and NADH levels

Intracellular NAD(H) concentrations were spectrophotometrically determined using a modified enzymatic cycling assay adapted for use in 96-well plates as previously described by Leonardo *et al*. (1996). The principle of this assay is based on the ADH cycling reaction. The reaction starts when ADH catalyzes the conversion of ethanol to acetaldehyde. This reduces all the available NAD^+ to NADH. This, in turn, reduces MTT to a blue formazan dye. The absorbance is proportional to the amount of NAD(H) present. Also, the absorbance is linear with increasing concentrations of NAD(H) content over range (5-60 µM), and can be measured at a wavelength of 565nm (see Figure 2.2 for an example standard curve). After harvesting, the cells were centrifuged for 5 mins at 200 x g and split in two fractions. One fraction was used for NAD^+ measurements while the other was used for measuring NADH. The cell pellets were then extracted with 250 µl 0.2 M HCl (or 250 µl 0.2M of NaOH for NADH measurement), and incubated at 100 ºC for 10 mins for NAD^+ quantification. Extracts were centrifuged at 9000 x g for 5 mins and kept on ice. Supernatant was removed and stored in -20 ºC until analysis.

The cycling assay was performed as follows. Forty nine microlitres of the acidic or alkaline extract was placed in each well, and 151 µl of cycling reagents, containing 98 mM sodium bicine buffer, pH 8.0, 1.626 mM of PES, 4.2 mM MTT, 9.8% (v/v) absolute ethanol, 3.92 mM of EDTA pH 8.0 (adjusted with 1M HCl), and 5 µl of yeast ADH (400 U/mg) in 0.1 M sodium bicine buffer, pH 8.0, were added to each well, followed by 30 mins incubation in the dark at room temperature. The absorbance was measured at 565 nm on a plate reader (Versa Max, Molecular Devices, Sunny Vale, CA, and USA). NAD^+ levels were expressed as pmol/10^6 cells. The NAD^+ and NAD(H) concentrations were measured using the NADH

standard curve (Figure 2.2). All samples were corrected for the blank (without NAD^+ and NADH) back ground activity and dilution factors before calculation.

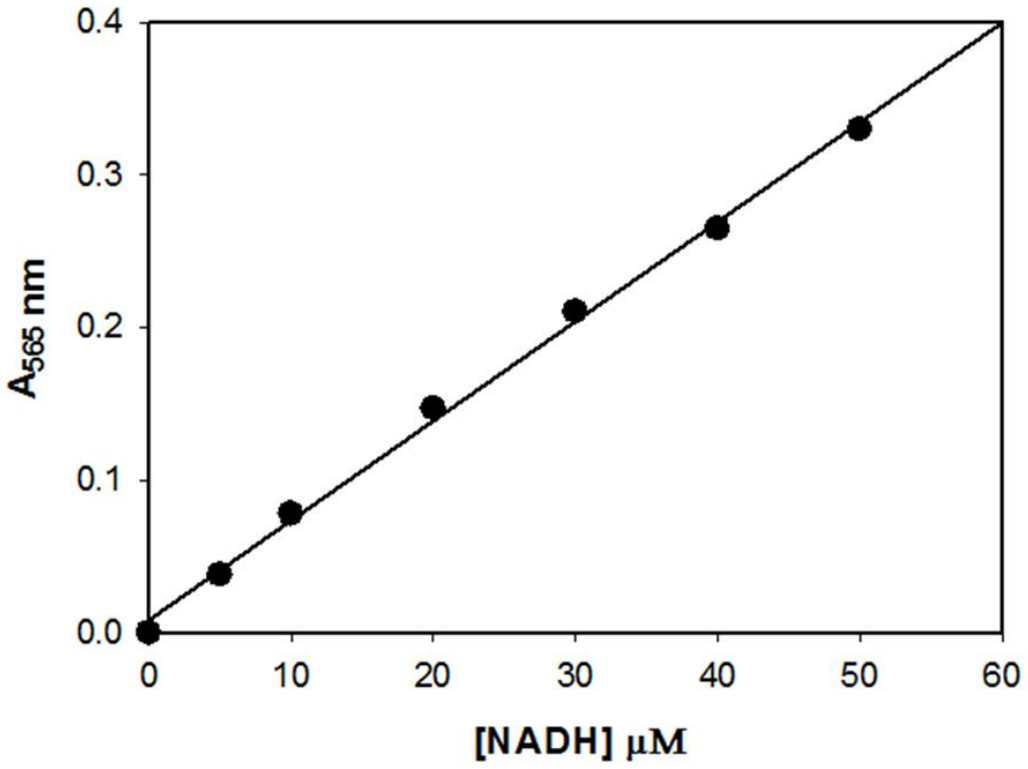

Figure 2.2 The NAD(H) standard curve, generated using the NAD(H) cycling assay. NADH was dissolved in PBS and diluted to known standard concentrations. The absorbance was measured spectrophotometrically at 565 nm and plotted as function of NAD(H) concentration.

2.2.7 Determination of IDO-kynurenine activity in M1-like and M2-like macrophages

Kynurenine was measured in culture supernatant for extracellular kynurenine while cells were lysed for intracellular kynurenine production. The Ehrlich colorimetric reaction assay was performed to determine the kynurenine concentration (Braun *et al*., 2005). Briefly, in order to precipitate protein, 60 µl samples were incubated with 30 µl 30% (w/v) TCA (trichloroacetic acid) at 50 ºC for 30 mins. Samples were then vortexed and centrifuged at

3000 x g for 10 minutes. A seventy five microliters volume of the upper phase was mixed with an equal volume of Ehrlich Reagent (2% (w/v) p-dimethyl amino benzaldehyde in 5 ml glacial acetic acid) in separate wells of a 96-well plate. Kynurenine was measured spectrophotometrically at 492 nm using a plate reader (Versa Max, Molecular Devices, Sunny Vale, CA, USA; Takikawa *et al*., 1986). The absorbance of a reagent blank was subtracted from sample absorbance values.

2.2.8 Measurement of Lactate production

Differentiated macrophages were either stimulated or not stimulated with *E.coli* k12-LPS (100 ng/ml). The supernatant from each sample was harvested and the lactate content was determined in a 96-well plate using an end-point colorimetric lactate assay. The lactate assay is based on the lactate dehydrogenase (LDH) reaction in which lactate is oxidized to pyruvate via the activity of LDH. Pyruvate is then decomposed by the action of hydrazine allowing the complete oxidation of all lactate molecules. To achieve this, NAD^+ is provided in excess and the concentration of lactate in the sample is proportional to the increase in absorbance as NAD^+ is reduced to NADH.

Briefly, 6 µl samples were incubated for 1 h at 37 ºC with 268 µl freshly prepared assay buffer containing 0.4 M hydrazine sulphate, 0.5 M glycine (adjusted to pH 9.0 with 3 M KOH), 80 mM NAD^+ and LDH (20 U/ml; Roche Diagnostics GmbH, Penzberg, Germany). Lactic acid was diluted in 50mM potassium phosphate buffer, pH 7.4, to create standards of known concentration (0-2000 µM; Figure 2.3) and absorbance was measured as function of lactate concentration. The absorbance was measured spectrophotometrically at 340 nm and lactate of unknown samples was quantified and normalised to proteins from each samples.

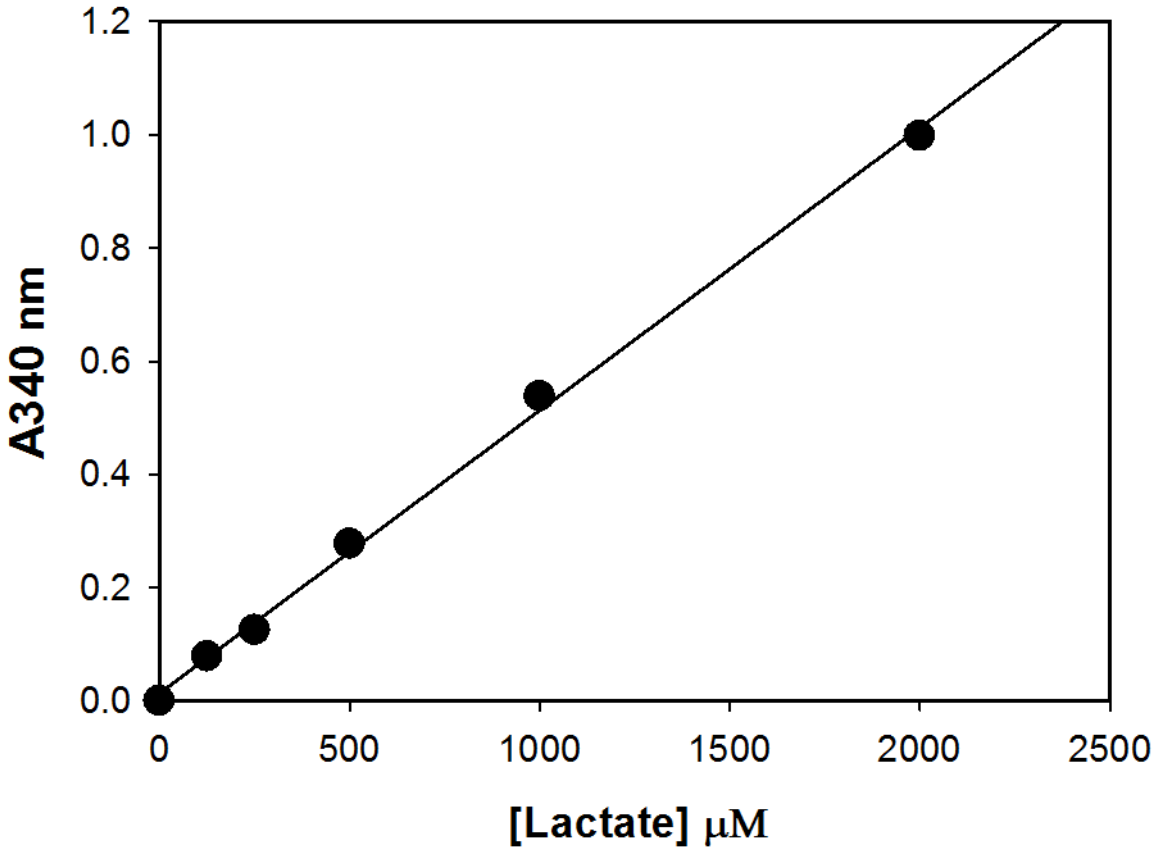

Figure 2.3 Example standard curve generated using the lactate assay. Lactate was diluted in assay buffer to create standards of known concentrations and absorbance was measured at 340 nm and plotted as a function of concentration.

2.2.9 Quantitative analysis of cytokines levels

To quantify TNF-α/IL-6 release, cell-free culture supernatants were collected and analyzed for cytokine secretion using sandwich enzyme-linked immunosorbent assay (ELISA) as previously described according to the manufacturer's instructions. The cells were centrifuged 3000 x g for 5 minutes and the supernatants were harvested, protocols were followed and the results compared to standard curves within the range 7 to 5,000 pg/ml. Briefly, 96-well ELISA plates (Nunc, Fisher Scientific, UK) were coated with either (4 µg/ml) of mouse anti-

human TNF-α or (1 µg/ml) of rat anti-human IL-6 in coating buffer (PBS) followed by overnight incubation at 4 ºC. After this step, the plate was blocked with 2% BSA (w/v in PBS). Fifty microliters samples and standard of TNF-α or IL-6 were added into the plate and incubated overnight at 4 ºC. For cytokines measurement, biotinylated mouse anti-TNF-α at 1 µg/ml or biotinylated rat anti-Human IL-6 at 0.5 µg/ml in 2% BSA (w/v in PBS) was applied to form a sandwich complex and incubated at room temperature for 3h. Additionally, (4x) horseradish peroxidase streptavidin conjugate (HRP) was added, followed by incubation with the substrate, TMB (3,3,5,5-tetramethyl benzidine). The reaction was stopped by addition of 1.17 mM sulphuric acid. Colour development was assayed spectrophotometrically using an OPTI Max tunable microplate reader set to 450 nm and the results analyzed by Soft max Pro version 2.4.1 software (Versa Max, Molecular Devices, Sunny Vale, CA, USA).

2.2.10 RNA extraction, reverse transcription and real time qPCR

Total RNA was extracted from 1 x 10^6 cultured cells, after twice washing with PBS, using a Gen Elute Mammalian Total RNA kit (Sigma-Aldrich, Poole, UK) with a DNase I digestion treatment for 15 mins according to the manufacturer's instructions. The quantity and purity of RNA samples were measured at 260 nm and 280 nm using a Nano-drop Plus spectrophotometer (Bioscience, Cambridge Bioscience Ltd, Cambridge, UK). For RNA purity, A 260/280 ratio, of equal to or less than 2, was considered as optimal. To test the quality of RNA, the extracted RNA was run on a 1% agarose gel (Figure 2.4) as mentioned in section 2.2.11. Total RNA (at a concentration of 25 ng/ ml) was subsequently was reversing transcribed in a total reaction volume of 20 µl containing: 2.5 µM random nonamers, 10 U/µl reverse transcriptase (RT) and 500 µM deoxynucleotide mix. The mixture was then incubated

for 1h at 42 ºC, followed by an inactivation step at 50 ºC for 5 min before qPCR was performed.

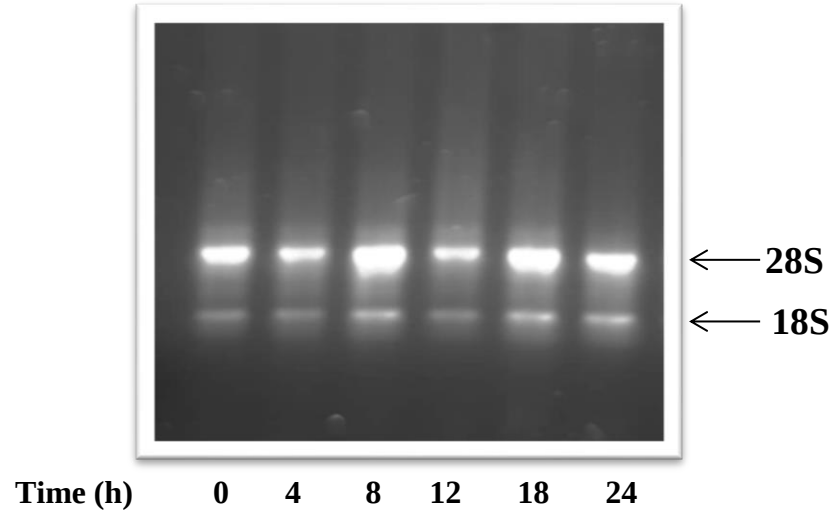

Figure 2.4 Determination of RNA integrity, using gel electrophoresis. Total RNA from each samples were run on 1% agarose gel and stained with Syber® Safe nucleic acid gel stain to evaluate the RNA integrity. The intact RNA (high quality RNA) shows two ribosomal RNA (rRNA) bands- 28S and 18S- with one approximately double the size of the other.

qPCR was performed to quantify specific mRNA using a SYBR® green detection kit according to the manufacturer's instructions (Sigma-Aldrich, Poole, UK). The qPCR analysis was carried out using an Applied Biosystems Step-One Plus real-time PCR system with Step-One^{TM} software (v2.2.2; Applied BioSystems). The cDNA product was utilized in the reaction mixture containing 0.4 nM of specific forward/reverse primer sets along with 0.025 U/µl reaction of SYBR®-Green Jumpstart Taq ready mix (Sigma-Aldrich, Poole, UK) in a total volume of 20µl. The reactions were performed under the following thermocycling conditions: denaturation at 94 ºC for 1min and final elongation step at 72 ºC for 30s. To verify the purity of PCR products, all samples were subjected to melting curve analysis to test for single amplification of a specific product. The primers used for qPCR are listed in table 2.4 (overleaf). The sequence of primers for all target genes were checked using primer express software (v2.2.2; Applied BioSystems).

Table 2.4 The primer sequences of selective genes in NAD^+ metabolism pathway

Target genes	Sequence (5'⟶3')	Primer size (bp)	Annealing Temperature (°C)	Product size (bp)
GAPDH	For: CCCACTCCTCCACCTTTGAC	20	56	100
	Rev: CTGTTGCTGTAGCCAAATTCGT	22	56	
CD38	For: GCACCACCAAGCGCTTTC	18	57	100
	Rev:TCCCATACACTTTGGCAGTCTACA	24	56	
CD157	For: GGGAAGGCAGCATGAAAGTC	20	56	105
	Rev: GGTCCACGCACTGTAAGAGCTT	22	57	
IDO	For: GCCTGCGGGAAGCTTATG	18	56	100
	Rev: TGGCTTGCAGGAATCAGGAT	20	57	
NMNAT	For: TCATTCAATCCCATCACCAACA	22	56	105
	Rev: AGGAGAGATGATGCCTTTGACAA	23	57	
NAMPT	For: TCCGGCCCGAGATGAAT	17	57	105
	Rev: TGCTTGTGTTGGGTGGATATTG	22	56	

The relative amounts of mRNA for each target transcript were normalized according to the expression of the house-keeping gene, glyceraldehyde-3-phosphate dehydrogenase (GAPDH). This gene was chosen because it was stably expressed in both M1-like and M2-like differentiated macrophages. The values were expressed, using the formula $2^{-\Delta\Delta Ct}$, as fold differences between the stimulated and non-stimulated differentiated cells, and also relative to the value at zero time points of THP-1 cells (Livak and Schmittgen, 2001).

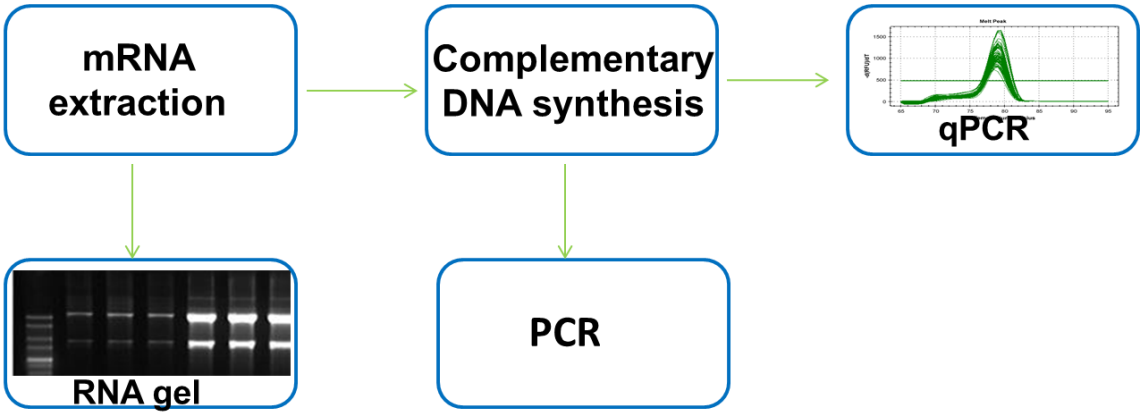

Figure 2.5 Schematic diagram depicting the basic steps of the gene transcription process using real time quantitative PCR (RT qPCR) analysis. The mRNA was extracted from the sample, the integrity of the sample was confirmed using gel electrophoresis, before reverse transcription and finally qPCR were performed. The product was tested for purity using melting curve analysis.

2. 2.11 Agarose gel electrophoresis for RNA analysis

Agarose (0.4 g) was dissolved in 40 ml of1 x TAE buffer which was prepared by mixing 9.68 g Tris, 2.28 ml glacial acetic acid and 4 ml of 0.5 M EDTA (made up to 200 ml distilled water and adjusted to pH 8. The agarose was melted by microwaving for approximately 1-2 mins until boiling and then cooled down by swirling the flask in a cold water bath at temperature (4 ºC). Four microliters of 10,000 x SYBR® Safe nucleic acid gel stain was added to the melted agarose before being poured (about 40 ml) into a tank has buffer in it and fitted with 12 well combs. The gel was left to set at room temperature. The gel was covered with 1x TAE running buffer in an electrophoresis. Samples were diluted appropriately with loading buffer: containing 25 mg Bromophenol Blue, 3 ml glycerol and 7 ml water. Finally, samples were loaded into wells on gel and the gel was run at 80-150V until the dye front had travelled approximately 75-80% along the gel.

2. 2.12 Characterisation of the bioenergetic flux in differentiated macrophages

The cells were seeded at density 40,000 cell/well and differentiated in XF24 (extracellular flux 24) cell culture plate and incubated with LPS- k12 (100 ng/ml) or with medium alone (control). After the indicated times, the cells were washed twice with medium. The medium was removed from each well and replaced with fresh 650 µl glucose-free Krebs-Ringer buffer (KRH) containing 135 mM NaCl, 1 mM HEPES, 0.5 mM $MgCl_2$, 1.5 mM $CaCl_2$, 0.5 mM NaH_2PO_4, 2 mM glutamine and 0.1% w/v BSA, followed by adjustment to pH 7.4 with 0.5 mMsodium phosphate and incubated at 37 °C for 30min. To characterise the bioenergetics flux in differentiated macrophages, a Seahorse extracellular flux analyser was used (Seahorse Bioscience, USA). This system is a fully integrated 24-well instrument that measures in real time the changes in oxygen uptake (oxygen consumption rate, OCR) and proton (extracellular acidification rate, ECAR) in the media surrounding adherent cells. ECAR and OCR were measured using disposable assay kits that contain an XF24 cell culture plate and a solid state sensor cartridge, embedded with 24 dual fluorescent biosensors (detecting O_2 and pH). Each sensor cartridge is also equipped with four drug delivery chambers per well for injecting test agents into wells during an assay. All the test drugs were prepared at appropriate concentrations in the assay buffer. Prior to performing XF24 analysis, the sensor cartridge was loaded with 75 µl of test drugs (oligomycin, retonone/antimycin or 2-deoxy glucose). While the sensor cartridge was calibrated the cell plate was incubated in a 37 ºC non-CO_2 incubator for 30 mins, in order to allow medium temperature and pH to reach equilibrium, before the assay started. After calibration, the cartridge was placed over the plate that contained cells and then transferred to a temperature-controlled 37 ºC seahorse analyser. The plate was then subjected to an equilibration step for 10 mins. The ECAR and OCR baseline (before compounds addition) were measured during 3-4 measurement cycles, each consisting

of a mixing step of 1mins, 2 mins incubation and finally a measuring time of 3min. After the base line measurement, testing drugs were injected into each well to the final working concentration. The first injection was glucose (1mM) and glucose induced-stimulation ECAR or OCR were measured. The second injection was oligomycin (1µM) to inhibit ATP mitochondrial production, with the increase in ECAR after this point representing the capacity of cells to increase glycolysis to maintain ATP production. Finally, 100mM 2-DG (2-deoxy glucose) or a mixture of rotenone/antimycin (1 µM/2 µM, respectively) was added to inhibit glycolysis or complex I and III to correct non-acidification or non-mitochondrial respiration rate, respectively. OCR was expressed as picomoles per minute (pmols/ min) and ECAR as milli-pH per minute (mpH/ min).

2.2.13 Scanning electron microscopy

Cells were seeded on 12 mm glass coverslips in six-well plates and incubated with PMA (25ng/ ml) or Vitamin D_3 (10nM) to generate M1-like and M2-like macrophages as described in section 2.2.2. Non-differentiated THP-1 cells were used as a control. The cells were initially fixed in 2.5% (v/v) glutaraldehyde (Agar scientific, Stansted, UK) in pH 7.2, 0.1 M sodium cacodylate buffer for 2 h. The coverslip was washed four times with 0.1 M cacodylate buffer at pH 7.2 for 10 mins each time. After the washing step, coverslips were then alcohol dehydrated in a graded ethanol series (v/v) in water (30%, 50%, 70%, 90% and 100%) for 15 mins each time. Finally, coverslips were then critically point dried in an Emitech k850 critical point drier before being placed on aluminium stubs (Agar scientific, Stansted, UK) with a carbon infiltrated minitab also known a ‘black spot’ (Agar scientific, Stansted, UK). This was followed by sputter coating with gold/palladium using an Emitech K550 (Quorum Technologies, Laughton, UK) gold sputter coating unit. The stubs were then

examined using a JEOL JSM 6610 LV scanning electron microscope (SEM) using a appropriate magnifications to produce the desired images.

2.2.14 Statistical analysis

Statistical calculations were performed using Statgraphics Centurion XVI (Stat Point Technologies, Inc.) and Minitab 17 Statistical Software. All data were tested for normality using the Anderson-Darling test (with $P < 0.05$ indicating that the data were non-normal). Levene's test was used to check that there were no significant differences in variance between each group ($P < 0.05$ indicated a significant difference in variance between groups). For normally distributed data, significant differences were determined using one way ANOVA followed by Tukey's test while the non-parametric ranking (Kruskal-Wallis) test was performed when data were non-normally distributed. To further investigate the main effects, Bonferroni tests were carried out as *post hoc* multiple comparison tests for normal and non-normal data, respectively. Data were reported as means ± standard error (SE) for triplicate samples from three separate experiments unless otherwise indicated. Differences were considered significant if $P < 0.05$.

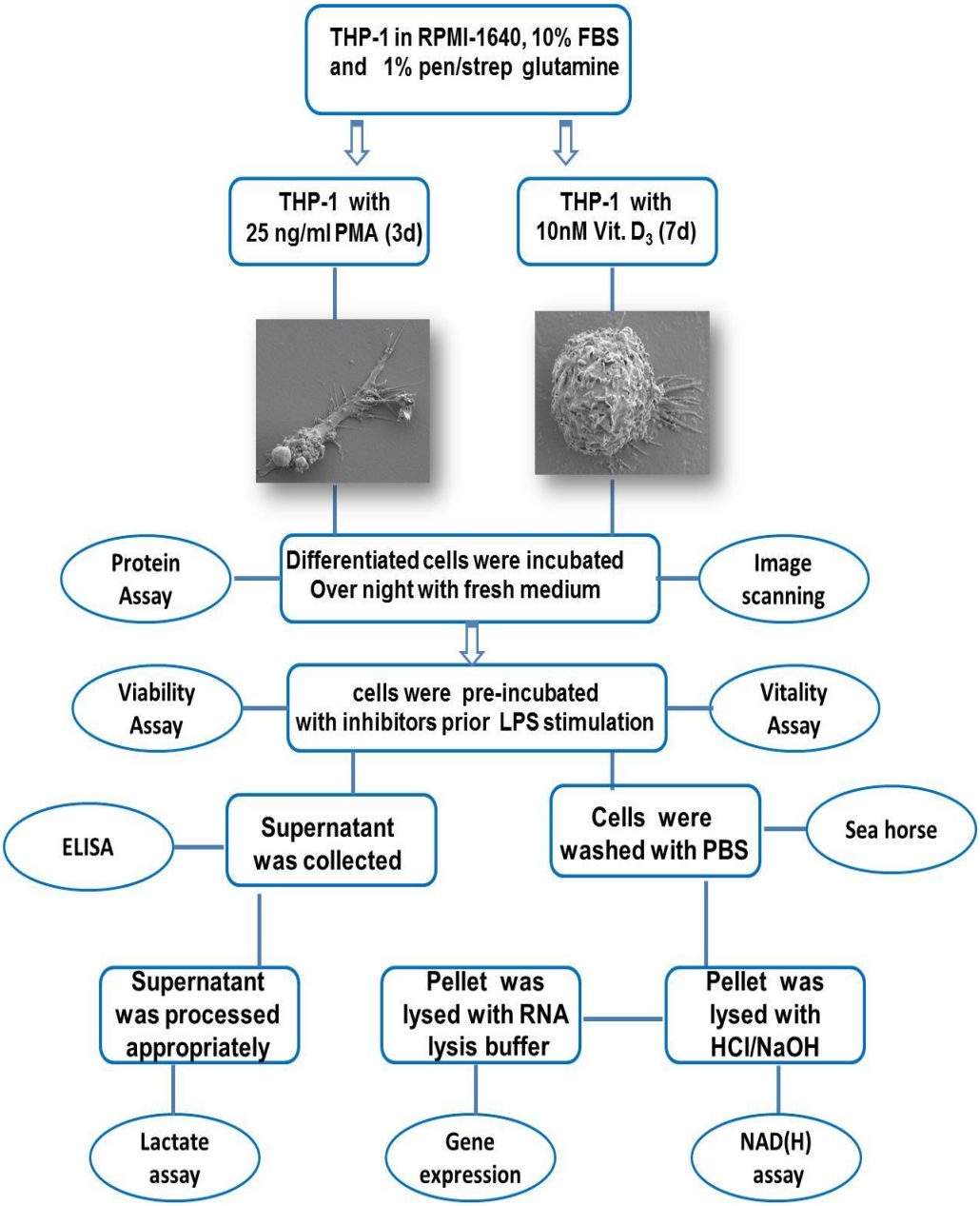

Figure 2.6 General schematic diagrams summarizing the experimental design and the assays carried out during this study. THP-1 cells were differentiated into M1-like and M2-like macrophages using 25 ng/ml PMA and 10 nM vitamin D_3 respectively. The morphological changes were determined using SEM technique as mentioned in section 2.2.13. After stimulation with LPS, the cells were lysed and assayed for NAD^+, protein and kynurenine. The cells free supernatant was used for ELISA, lactate and extracellular kynurenine. Finally, bioenergetics flux was determined in viable cells free medium.

CHAPTER 3

NAD^+ HOMEOSTASIS PROFILE IN PRO-INFLAMMATORY (M1-LIKE) AND ANTI-INFLAMMATORY (M2-LIKE) MACROPHAGES

3.1 Introduction

It is widely accepted that there is a close link between metabolic activity (energy status) of immune cells and their ability to mount appropriate immune responses (Hotamisligil and Erbay, 2008). In particular, classically activated, pro-inflammatory (M1) macrophages obtain their energy largely through glycolysis to support rapid immune responses whereas alternatively activated; anti-inflammatory (M2) macrophages rely mainly on oxidative phosphorylation to support long term-immune functions such as wound healing and tissue repair (Galvan-Pena and O'Neill, 2014). NAD(H) is considered to be crucial as a co-factor to maintain redox balance such that flux through glycolysis can continue. Besides its role as a co-factor, NAD^+ is required for a broad range of metabolic pathways. Indeed, NAD^+ is also involved in a number of signalling processes including calcium signalling and gene transcriptional regulation (Schreiber *et al*., 2006; Malavasi *et al*., 2008; Koch-Nolte *et al*., 2009). In particular, regulation of gene expression by the NAD^+-dependent enzymes, sirtuins, has been shown to play a critical role in modulating of the synthesis of the pro-inflammatory cytokine, TNF-α (van Gool *et al*., 2009). Conversely, it has been shown that TNF-α itself is able to modulate intracellular NAD^+ levels by regulating the expression of selective NAD^+ homeostatic enzymes, probably via a form of feedback regulation, in a model of primary murine macrophages (Iqbal and Zaidi, 2006). In response to TNF-α, these cells have been shown to upregulate the expression of NAMPT, IDO, CD38 and CD157 (Mehta *et al*., 1996; Okuyama *et al*., 1996; Musso *et al*., 2001; Nua *et al*., 2002; Rongvaux *et al*., 2003; Iqbal and Zaidi, 2006). Among the NAD^+ homeostasis enzymes, CD157 and CD38 have shown contrasting expression patterns on immune cells where CD157 is expressed in mature monocytes whereas CD38 is expressed on macrophages suggesting an important role in cell maturation and differentiation (Okuyama *et al*., 1996; Frasca *et al*., 2006). In macrophage and

monocytic cell lines, the induction of CD38 expression, has been shown to increase their antigen presenting ability and the ability to secrete pro-inflammatory cytokines (Funaro *et al*., 1990; Lund *et al*., 1995). Furthermore, LPS has also been shown to mediate the expression of NAMPT (nicotinamide phosphoribosyl transferase, a key enzyme in the NAD^+ recycling pathway) in activated monocytes and macrophages. Indeed, inhibition of NAMPT by FK866, also called APO866 or WK175; (E-N-[4-(1-benzoyl piperidine)-4-yl) butyl] acrylamide-3-pryridin-3-yl), which is a non-competitive inhibitor NAMPT, led to the increase in intracellular NAD^+ being blocked in macrophages (Hasmann and Schemainda, 2003). The upregulation of NAMPT expression was interpreted as a physiological response to provide adequate intracellular NAD^+ levels for optimal TNF-α production in activated macrophages (van Gool *et al*., 2009). However, despite these interesting observations and the intrinsic link between NAD^+ and immune regulation, the potential roles of NAD^+ homeostasis in macrophages and their relationship to the cell phenotype effector functions is not yet completely understood. Understanding NAD^+ synthesis/consumption in macrophages is important to underline and develop potential effective treatment strategies in the context of tumours. Tumour microenvironments are composed of tumour cells as well as other infiltrated immune cells including circulating monocytes and macrophages that are recruited by tumours. While recruiting, M2 cells are polarized resulting in promotion of tumour progression (Chanmee *et al*., 2014). Therefore, a recent focus in the switch from M2 polarization (pro-tumour) into M1 polarization (anti-tumour) has been suggested as a better pharmaceutical strategy for targeting tumours (Chanmee *et al*., 2014). Indeed, it has recently been shown that polarization from an M2 to an M1 phenotype suppressed mammary tumour growth and angiogenesis *in vivo* (Zhang *et al*., 2013; Foey, 2015). To understand more about and NAD^+ levels in macrophages, we have investigated NAD^+ homeostasis using THP-1 cell

line-derived M1-like MΦs and M2-like MΦs. The results showed that NAD^+ levels differ markedly between M1-like and M2-like macrophages with M1s having much higher basal levels. Also, both phenotypes display differential expression profile of selective NAD^+-homeostasis enzymes in the resting state as well as in the activated state. This could suggest that NAD^+ homeostasis enzyme expression and activity as an additional tool in discriminating macrophage maturation and differentiation.

3.2 Results

3.2.1 M1-like and M2-like macrophage subsets differ in their morphology and the ability to secrete cytokines in response to LPS stimulation

The links between TNF-α and NAD^+ levels are well documented. This link might represent a novel regulatory mechanism controlling TNF-α synthesis by the cells of the immune system. In order to investigate this link further, we made use of the differentiation of THP-1, a monocytic cell line. THP-1 cells have become commonly used for the study of macrophage differentiation and immune responses due to (i) the similarity with blood primary monocyte cells, (ii) the difficulty in obtaining primary cells from patient blood and (iii) the fact that phenotypically, these cells are more stable than primary monocytes/ macrophages since it has been reported that THP-1 minimizes the genetic variation in the phenotype (Cousins *et al*., 2003; Rogers *et al*, 2003). We investigated whether THP-1 can be used as a model to generate cells with characteristics of M1-like and M2-like macrophages (MΦs) by using PMA and vitamin D_3, respectively. To verify whether THP-1 was useful model for differentiated macrophages, both the pro-inflammatory TNF-α release and the release of regulatory IL-6 was measured following differentiation. The morphology of the generated macrophages was investigated using scanning electron microscopy (SEM), as described in

section 2.2.13. SEM images of resting cells showed clear differences between PMA-differentiated (M1-like) THP-1 MΦs in comparison to vitamin D_3– differentiated (M2-like) THP-1 MΦs and non-differentiated THP-1 cells. M1-like MΦs became adherent and changed their morphology to become more flat, amoeboid in shape and developed long pseudopodia extensions resembling classically activated MΦs in their appearance (Figure 3.1). Also, PMA caused the cells to become attached to the cell culture plate, requiring trypsin treatment to remove them. In contrast, non-differentiated THP-1s maintained their shape and did not adhere to the culture plate surface. Similarly, there were no appreciable differences in the external morphology of M2-like cells, which stayed rounded and spherical in shape, although the cells developed a ruffled membrane and increased their size relative to untreated THP-1s (Figure 3.1). Given that macrophage heterogeneity is influenced by differentiation state, we investigated potential differences in immune responses, particularly in cytokine production between the two subsets. Differentiated macrophages were stimulated with lipopolysaccharide (LPS) and both TNF-α and IL-6 secretion was measured. LPS, an outer membrane component of Gram negative bacteria, is known to mediate monocyte and macrophage activation (Meng and Lowell, 1997). As expected, M1-like released TNF-α, but little IL-6 while the opposite was true for M2-like cells (Figure 3.2 A, B). Significant increases in TNF-α levels started soon after stimulation (4 h, $P = 0.007$) compared to the control (unstimulated) and peaked at 8 h ($P = 0.004$) before declining after 24 h ($P = 0.07$) as shown in figure 3.2 A. In contrast, M2-like MΦs released TNF-α after 4 h of LPS stimulation, but 10-fold lower than that secreted by M1s as in figure 3.2 A. M2-like MΦs showed significantly increased IL-6 levels during LPS stimulation compared to M1-like cells with the magnitude 8-fold lower than that of the M2-like cells. Indeed, IL-6 levels increased within 4 h ($P = 0.03$) compared to the control (unstimulated) cells, peaking at 8 h ($p = 0.001$),

after which time they started to decline during the stimulation period (24 h). However, IL-6 release in M1-like cells was within the range of unstimulated levels of that for M2-like cells during LPS stimulation (Figure 3.2 B). Neither of the differentiated non-stimulated subsets released any detectable cytokines into the culture medium without LPS stimulation. In addition, non-differentiated, stimulated THP-1s released a detectable amount of TNF-α after 4 h (data not shown) under LPS challenge. Taken together, the data suggests that PMA-differentiated THP-1 exhibited M1-like characteristic due the changes in morphology and TNF-α secretion whereas differentiation with vitamin D_3 induces less morphological changes and TNF-α secretion. Therefore, our observations suggest that THP1-derived macrophages differentiated by PMA or vitamin D_3 could be a useful strategy for generating a reliable model of differentiated macrophages to study macrophage immune responses.

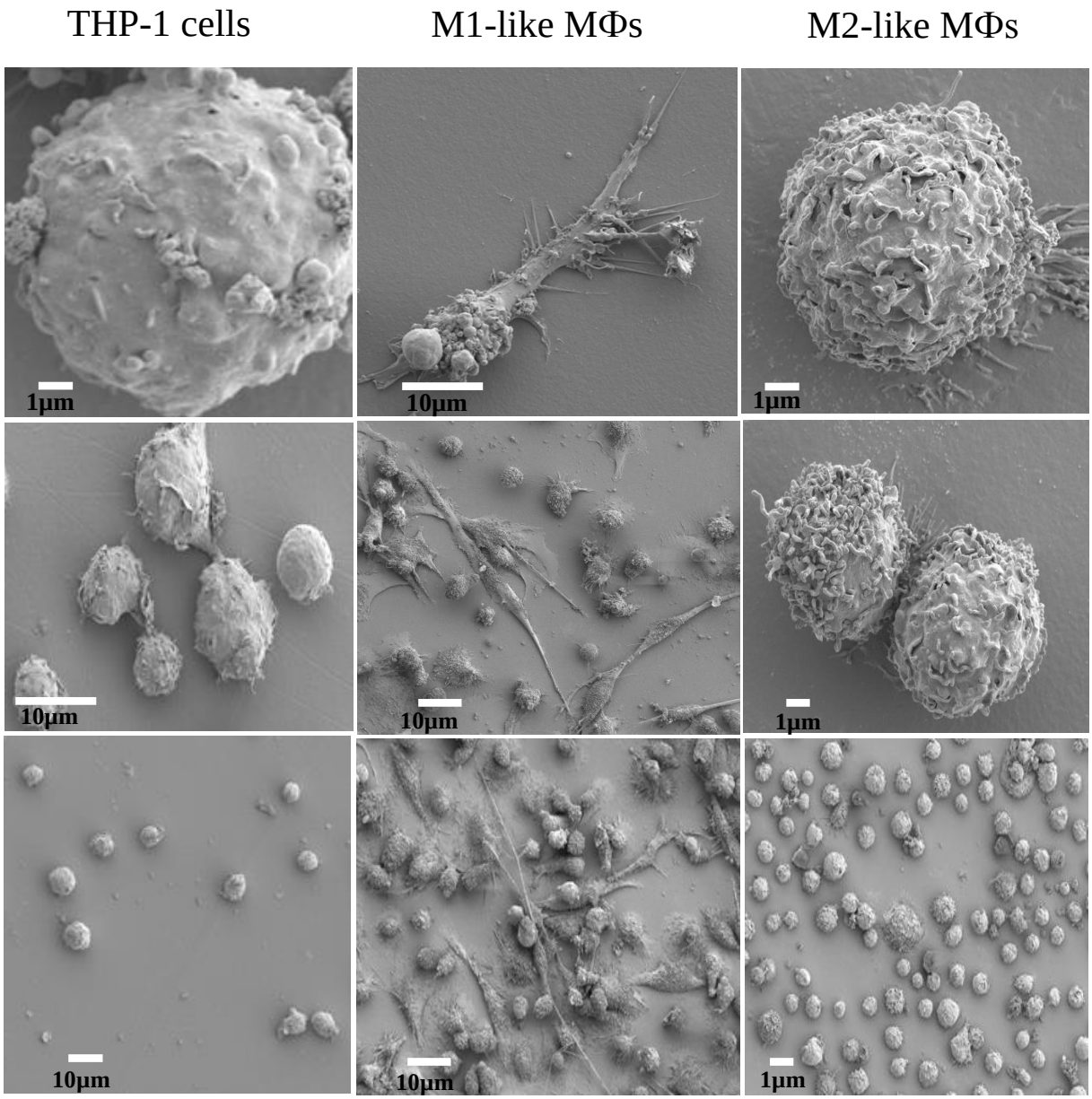

Figure 3.1 Scanning electron micrographs showing the morphological changes of differentiated macrophages compared to non-differentiated THP-1 cells. THP-1 cells were differentiated with either 25 ng/ml PMA or 10 nM vitamin D_3. Scale bars=1 and 10 µm.

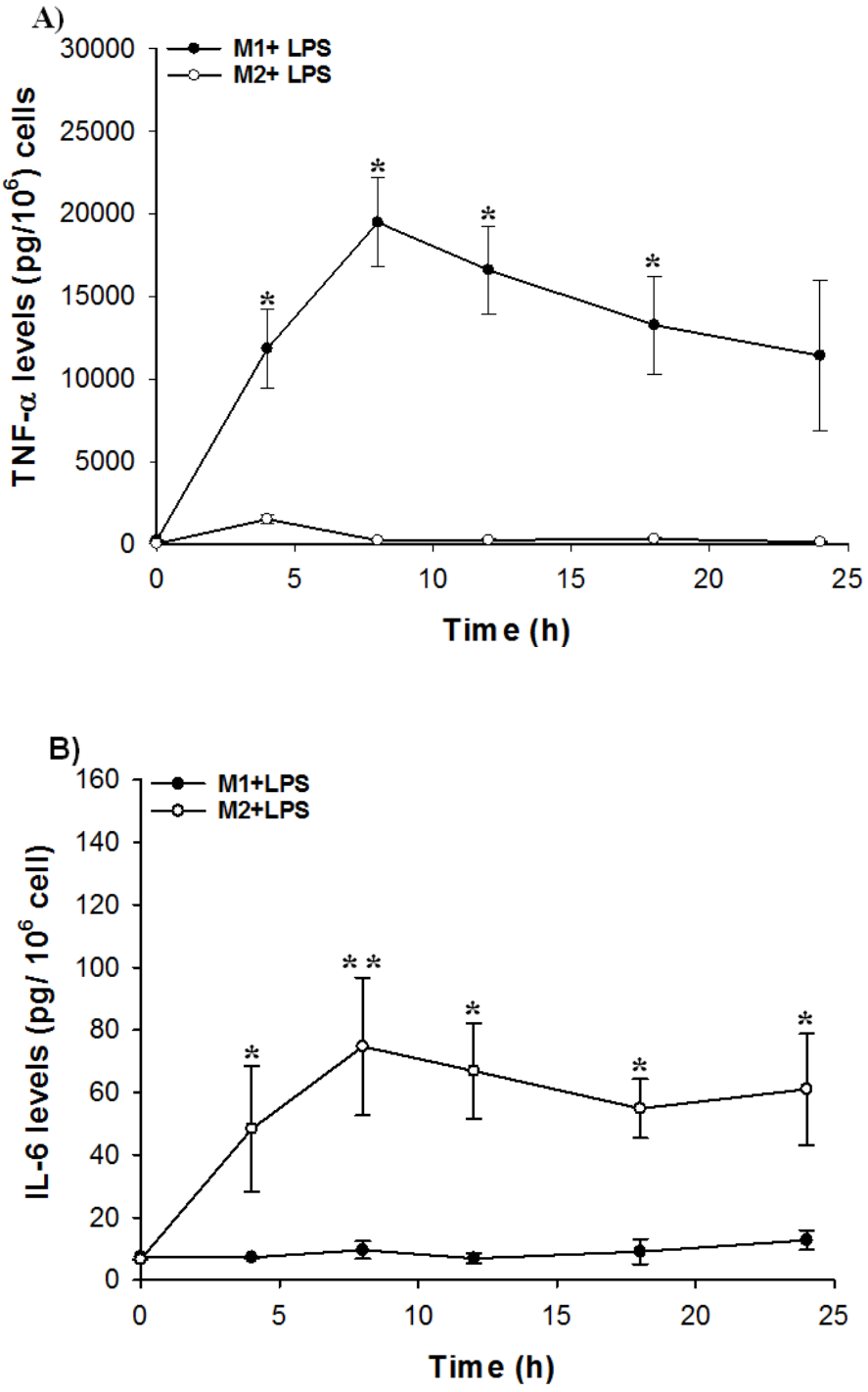

Figure 3.2 LPS stimulation induces differential cytokine secretion profiles in M1-like and M2-like MΦs. THP-1 cells were differentiated into M1-like and M2-like macrophages using either PMA (25 ng/ml) or vitamin D_3 (10nM), respectively. Differentiated cells were then stimulated with LPS-K12 (100 ng/ml). Cytokine production is expressed in pg/10^6 cells for (A) TNFα and (B) IL-6. Data are the mean ± SE of three biological experiments, n=3-4. The data were analysed by two-way ANOVA with Bonferroni test. Significant differences in cytokine production between activated M1 and M2 MΦs are indicated as *P < 0.05, **P< 0.01, ***P < 0.001.

3.2.2 The association between LPS stimulation and NAD^+ levels in differentiated macrophages

The link between NAD^+ metabolism and inflammation is well established in macrophages. To test this link further, we first investigated NAD^+ levels in resting macrophages and compared to THP-1 cells (control) prior stimulation with LPS. Our data show that M1-like MΦs display significantly higher basal NAD^+ levels (P= 0.0001; Figure 3.3 A) compared to resting M2-like MΦs and control THP-1s (P = 0.004). Importantly, we observed no significant differences in NAD^+ levels between M2-like MΦs and the control cells. It is known that LPS induces TNF-α release in a TLR4-dependent manner and to understand whether NAD^+ is also involved, the NAD^+ levels were measured in both subsets during LPS stimulation. While LPS caused a significant increase in NAD^+ levels in M1-like MΦs (P = 0.0001; Figure 3.3 A) it failed to affect NAD^+ levels in both THP-1 and M2-like MΦs with both stimulated and non-stimulated cells showing similar levels of NAD^+ throughout the experiment (Figure 3.3 A). Upon stimulation with LPS, M1-like MΦs showed a large biphasic increase in intracellular NAD^+ levels with a significant distinct peak after 30 min (P = 0.0001) followed by a second significant but lower peak at 4 h (P = 0.001) that remained high and lasted for several hours, starting to return to unstimulated levels at 24 h (Figure 3.3 B). M1-like stimulated with LPS for 4 h significantly increased NAD^+ compared to non-stimulated M1-like macrophages (0 h, P = 0.002 and 4 h, P = 0.0002). These results suggest that LPS affects NAD^+ levels differently in the two subsets with NAD^+ levels being associated with LPS stimulation only in M1-like MΦs, suggesting that M1-like MΦs might be characterised by NAD^+ changes. Also, these observations could suggest that NAD^+ levels might have a critical role for LPS mediated TLR4-induced signalling pathways in pro-inflammatory M1-like cells.

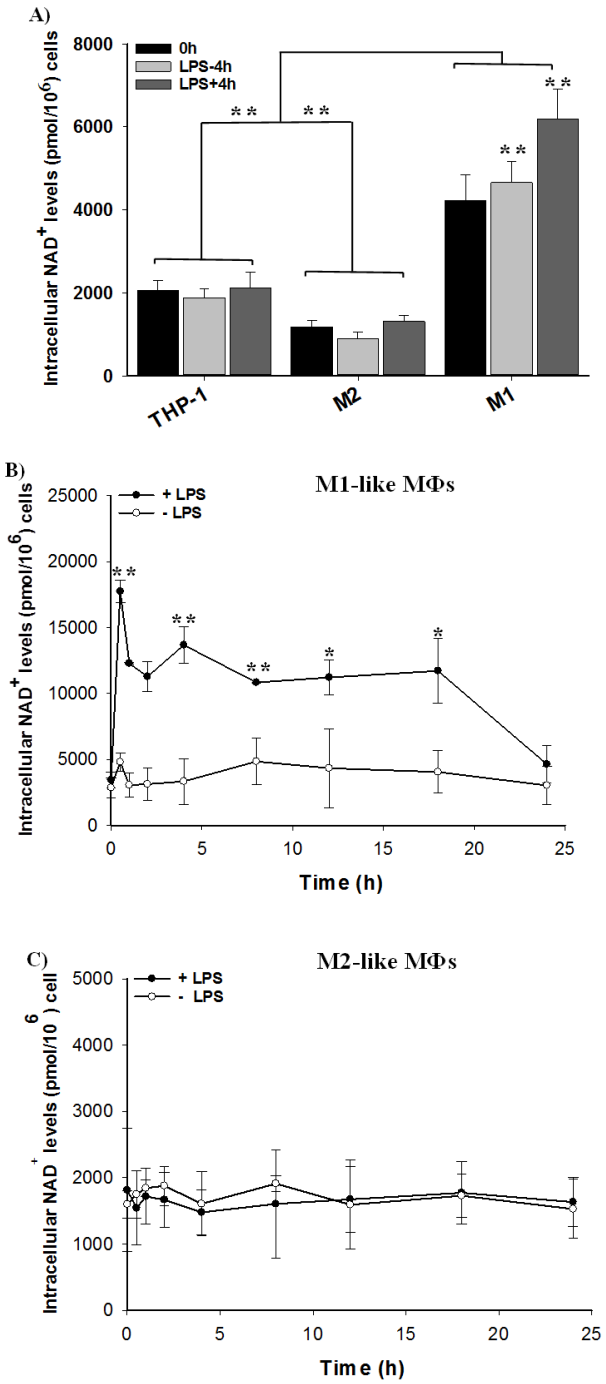

Figure 3.3 LPS stimulation increases NAD^+ levels in pro-inflammatory M1-like macrophages. Differentiated macrophages were induced by incubation with PMA and vitamin D_3 prior to stimulation with LPS. Pellets were harvested at intervals for NAD^+ analysis using NAD^+ cycling assay (A) Differential profile of basal NAD^+ levels in differentiated and non-differentiated (control) cells. NAD^+ levels increased in M1-like cells (B), while it was not affected in M2-like macrophages under LPS challenge (C). Data shown are mean ± SE of three biological experiments (n = 3). Results are significantly different (*P < 0.05, **P < 0.01, ***P < 0.001) when analysed by two-way and one way ANOVA followed by *post hoc* multiple pairwise Bonferroni comparisons compared to the control.

3.2.3 Differential profiles of NAD^+ homeostasis in resting macrophages

We showed that NAD^+ levels clearly differ between M1-like and M2-like MΦs during LPS stimulation, therefore we were interested whether these two subsets differ in the way they perform NAD^+ production. To achieve this, both subsets were treated with either FK866, an inhibitor of NAD^+ synthesis (via inhibition of NAMPTase), nicotinamide (a dietary NAD^+ precursor) or quinolate (an NAD^+ precursor formed via the IDO pathway; Figure 3.4). The concentrations used in this study were chosen based on preliminary experiments and the literature (Grant and Kapoor, 1998; Busso *et al*., 2008; Bowlby *et al*., 2012). THP-1 cells were incubated over 24h with a range of different agents (Figure 3.4 A, B, C). The FK866 treatment was able to significantly decrease NAD^+ levels within the range 1-1000 nM at different times ($P = 0.001$). However, 100 nM FK866 at 2 h was chosen for all experiments because we were interested in early NAD^+ response. Indeed, this concentration is commonly used for NAMPT inhibition (Busso *et al*., 2008; Bowlby *et al*., 2012). Also, differentiated MΦs were incubated with nicotinamide and quinolate (10-300 µM) for up to 3 days (Figure 3.4 B, C). Both nicotinamide and quinolate significantly increased NAD^+ levels at 300 µM after 24 h ($P = 0.001$), therefore, this concentration was chosen for the other experiments. It has been reported that higher micromolar concentrations of nicotinamide and quinolate caused increases in NAD^+ generation (Grant and Kapoor, 1998). Interestingly, FK866 caused a drop in NAD^+ levels in M2-like MΦs (Figure 3.5 B), while it conversely caused an NAD^+ increase in M1-like MΦs (Figure 3.5 A). M1-like MΦs were able to gradually and significantly increase NAD^+ levels ($P = 0.02$) within 4 h of FK866 treatment, reaching maximum levels after 12 h ($p = 0.0014$). In M2-like cells, the decrease was not significant and occurred within 2 h of FK866 treatment, continuing steadily during the entire experiment. This might suggest that the NAD^+ consumption rate is high in M2-like MΦs as

FK866 blocks NAD^+ recycling while the opposite is true for M1-like MΦs. Coupled with this, NAD^+ synthesis from the NAD^+ precursor nicotinamide was high in M1-like cells after 24 h treatment but low in M2-like cells (Figure 3.5 C), again supporting the rapid change in NAD^+ levels in M1-like cells. M1s were able to significantly increase NAD^+ levels by almost 45% after nicotinamide treatment compared to the control ($P = 0.01$). In contrast, nicotinamide treatment failed to induce a significant increase in NAD^+ generation in M2-like MΦs. These data fit well with observations showing that M1-like MΦs are able to rapidly increase their NAD^+ levels while M2-like are not. This might support the assumption suggesting that NAD^+ recycling is low in M2-like cells compared to M1-like cells. On the other hand, quinolate treatment did not induce significant changes in either subset (Figure 3.5 D). Collectively, these observations might suggest that the two phenotypes differ in the way they handle NAD^+ homeostasis, highlighting that this might be phenotype-specific. Therefore, the gene expression of selected regulators of NAD^+ homeostatic enzymes (IDO, NAMPT, CD38, CD157 and NMNAT) was investigated to further understand differences between the two subsets.

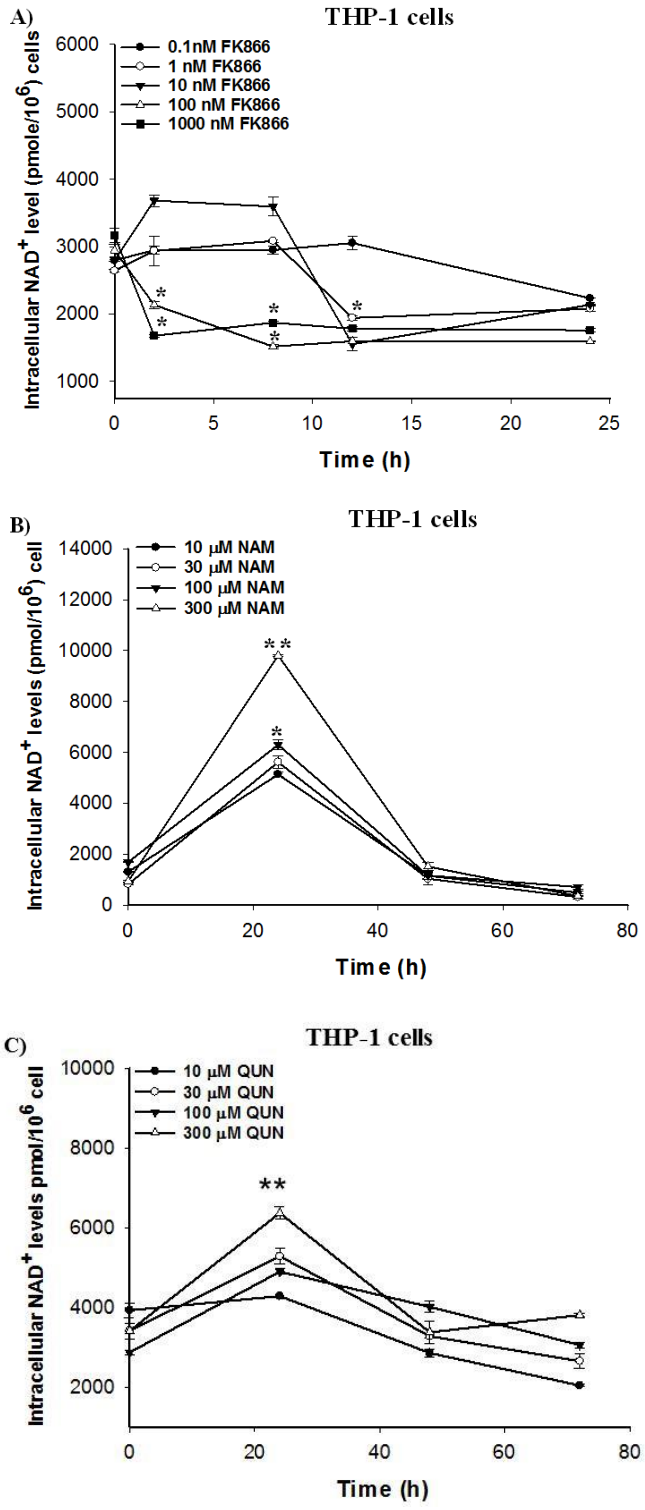

Figure 3.4 The effect of FK866, nicotinamide (NAM) and giunolate (QUN) on NAD^+ levels in undifferentiated THP-1 cells over time. THP-1 cells were incubated with (A) FK866 (0.1-1000 nM), (B) nicotinamide (10-1000) µM for 1-3 days and finally with (C) quinolate (10-300) µM for 1-3 days. Data shown are mean ± SE of three replicate samples (n = 3). Results are significantly different (*P< 0.05, **P < 0.01, ***P < 0.001) analysed by one way ANOVA followed by Bonferroni *post hoc* test compared to the control.

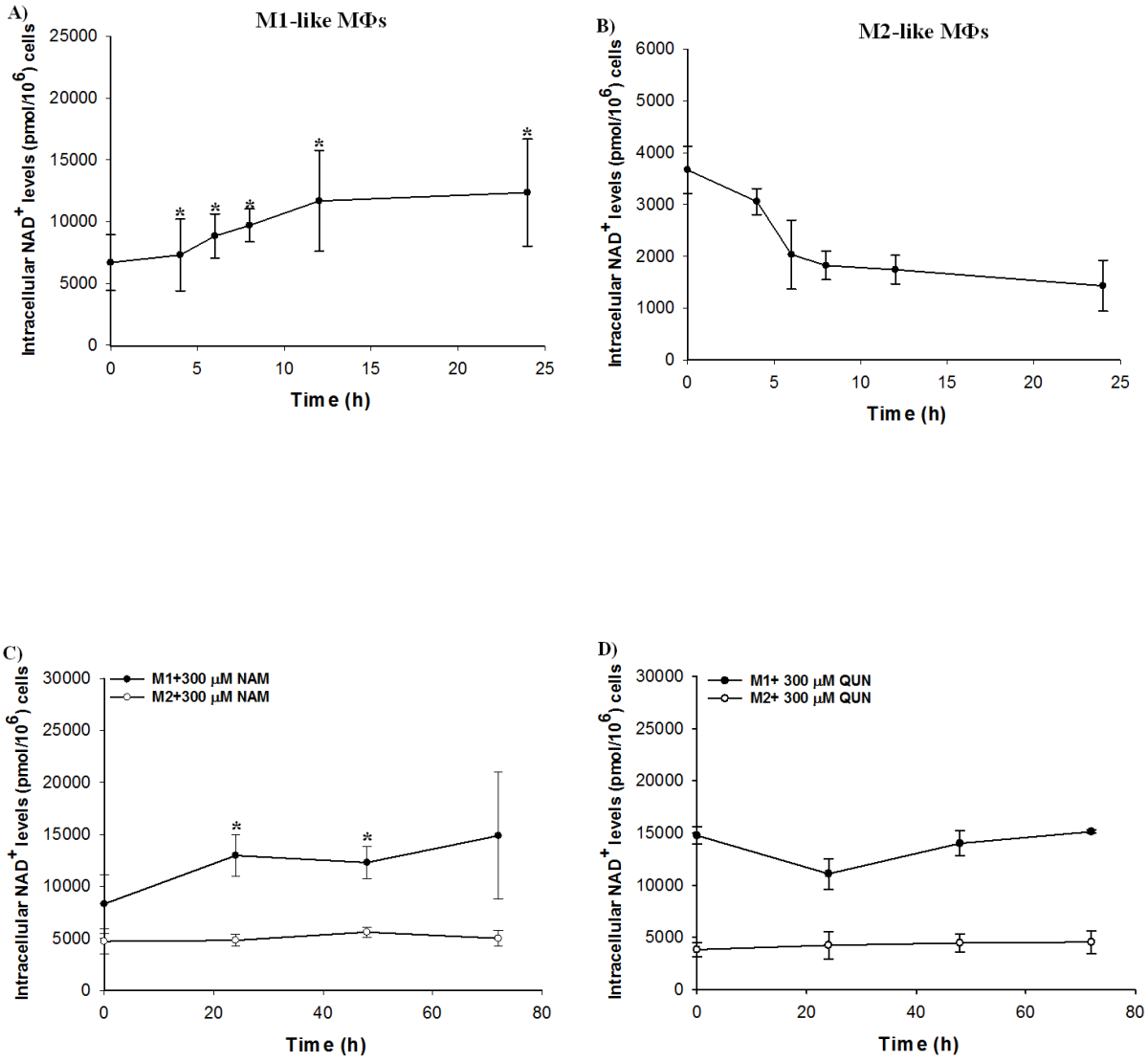

Figure 3.5 Resting macrophages exhibit differential profiles of NAD^+ levels. Differentiated MΦs were incubated with 100 nM FK866 and then the NAD^+ content was measured in unit of pmol/10^6 cells in (A) M1-like MΦs and (B) M2-like MΦs over 24 h. Differentiated MΦs were incubated with 300 μM nicotinamide for 1-3 days and NAD^+ levels were measured in (C) M1- and M2-like MΦs. Similarly, 300 μM was chosen and differentiated MΦs were incubated for the same time and NAD^+ levels were measured in (D) M1- and M2-like cells. Data shown are mean ± SE of three separate experiments (n = 3). Results are significantly different (*P < 0.05, **P < 0.01, ***P < 0.001) when data were analysed by one way and two way ANOVA followed by Bonferroni *post hoc* test compared to the control.

3.2.4 Macrophage differentiation induces gene expression of selected NAD^+ homeostatic enzymes

We have shown that NAD^+ status clearly differs in both subsets in resting and activated states. To address these differences in NAD^+ levels between the two phenotypes, we investigated the gene expression profile of some key regulators for NAD^+ homeostasis, using RT-qPCR, compared to expression in the monocytic progenitor THP-1 cell line (Figure 3.6). In this analysis, the mRNA expression levels of IDO, NAMPT, CD38, CD157 and NMNAT were determined. Upon differentiation with PMA or vitamin D_3, however, both subsets showed a significant increase in IDO expression compared to THP-1 ($P = 0.03$; Figure 3.6 C). Indeed, IDO expression showed the significant highest fold change among the analysed enzyme genes. The NADase CD38, which mediates NAD^+ degradation and can generate cADPR, $NAADP^+$ and ADP-ribose (Lee, 2006; Howard *et al*., 1993), was significantly (upregulated in M1-like cells ($P = 0.02$; Figure 3.6 A) and down-regulated in M2-like cells (Figure 3.6 B), while the opposite was true for CD157, a homologue of CD38 (Ferrero *and* Malavasi, 1997). Finally, NMNAT (nicotinamide mononucleotide adenylyl transferase), which catalyses the final step in NAD^+ biosynthesis (Magni *et al*., 1999), was slightly upregulated in both subsets (Figure 3.6 C), while NAMPT was significantly upregulated only in M1-like cells ($P = 0.04$; Figure 3.6 B). These data indicate that NAD^+ homeostasis enzyme expression changes clearly during differentiation state and this might confirm previous observations showing the difference of NAD^+ levels between differentiated and undifferentiated THP-1 cells. The findings from the current study might suggest that the enzymes involved in NAD^+ metabolism might be associated with macrophage differentiation and activation.

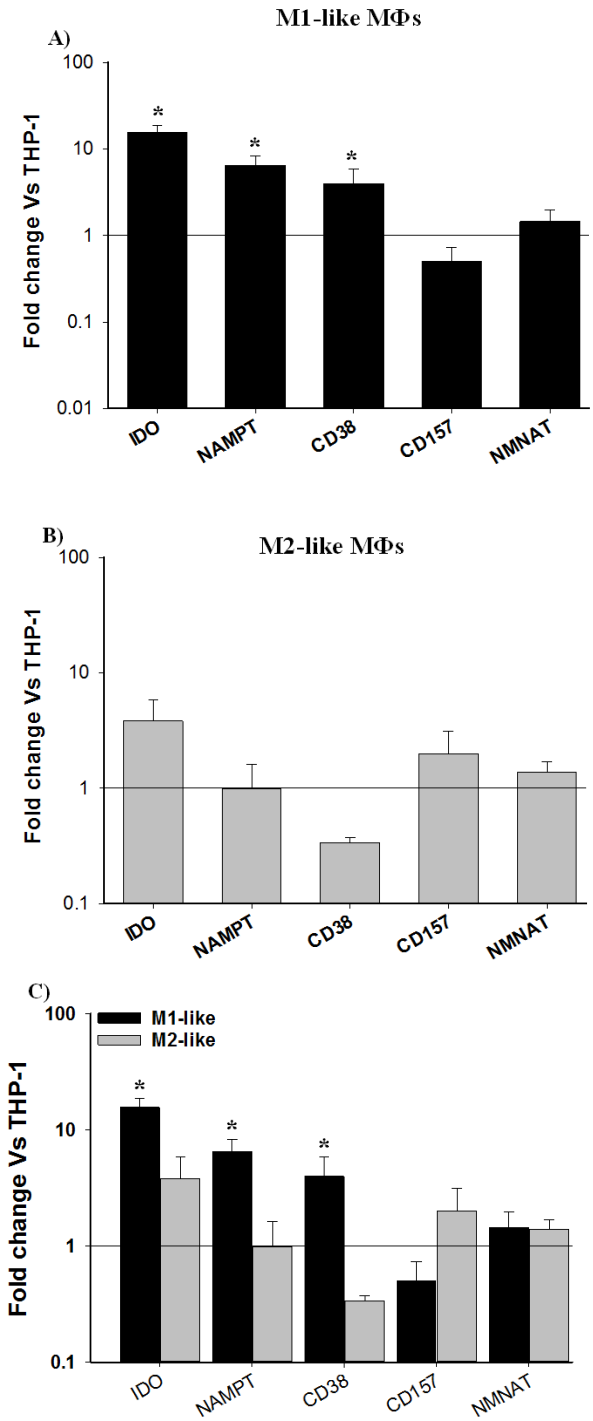

Figure 3.6 The expression of NAD^+ homeostasis enzyme genes in both macrophage subsets in the resting state. The expression of genes relating to the activity of selected enzymes of NAD metabolism were analysed in (A) M1-like (B) M2-like and (C) M1/M2-like MΦs. Data shown are mean ± SE of three separate experiments (n = 3-4). The data were analysed by one way ANOVA followed by Bonferroni test, *P < 0.05.

3.2.5 LPS-induces differential gene expression profile of human M1-like versus M2-like differentiation

We wanted to assess whether LPS stimulation could affect the expression of some key regulators of NAD^+ homeostasis over 24 h. In M1-like cells, LPS stimulation caused a significant increase in IDO mRNA, with a maximal expression after 12 h ($P = 0.02$) during LPS stimulation and with smaller increases in CD38, CD157 and NAMPT expression within 4 h of the stimulation while NMNAT expression was unaffected (Figure 3.7 A). Despite LPS not being able to stimulate NAD^+ changes in M2-like cells, LPS stimulation caused upregulation of all genes examined except CD157. We observed a similar but significant increase in IDO after 4 h of stimulation ($P = 0.01$). NAMPT expression was significantly increased within 4 h ($p = 0.02$) and maintained a rise for the entire stimulation time unlike M1s, where NAMPT reached its maximum expression after 4 h before declining back to almost unstimulated levels after 24 h (Figure 3.7 A, B). On the other hand, NMNAT reached its maximal expression after 24 h of LPS stimulation ($P = 0.017$). Surprisingly, the expression of CD157 was largely unaffected. The current results suggest that NAD^+ homeostasis enzymes are highly sensitive to LPS stimulation highlighting important immune regulatory role for NAD^+ and its metabolism in differentiated macrophages.

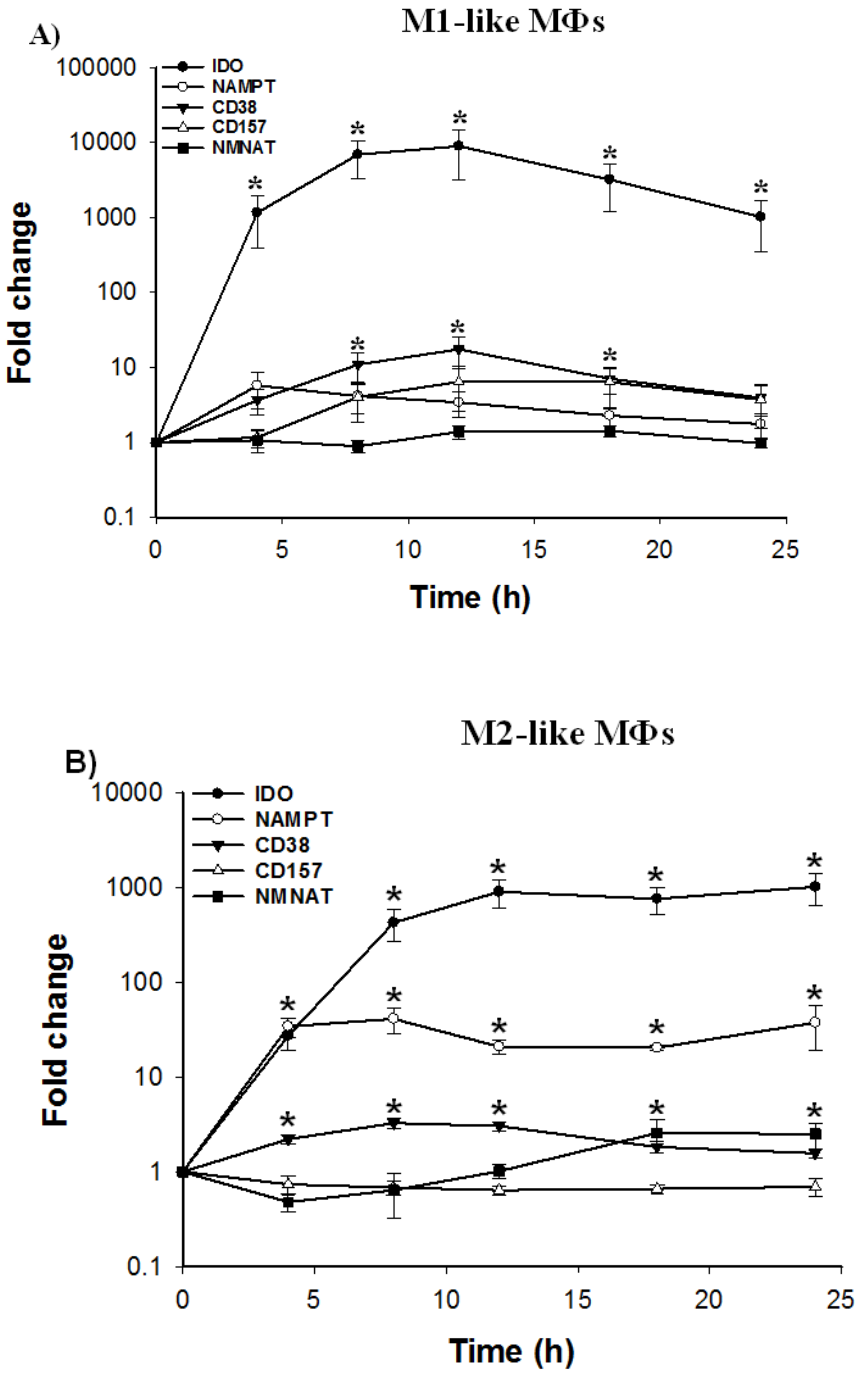

Figure 3.7 The kinetic expression profiles of NAD^+ homeostasis enzymes in (A) M1-like MΦs and (B) M2-like MΦs during LPS stimulation. Differentiated cells were stimulated with LPS (100ng/ml) and the gene expression levels measured using RT-qPCR. . Data shown are mean ± SE of three separate experiments (n = 3-4). The data were analysed by one way ANOVA plus Bonferroni *post hoc* test *P < 0.05.

3.3 Discussion

The tight link between metabolic activity and cellular phenotype is well established, with anti-inflammatory macrophages (M2s) relying on oxidative phosphorylation for energy production, the pro-inflammatory (M1) macrophages relying primarily on glycolysis (Galvan-Pena and O'Neill, 2014). NAD(H) is necessary for glycolysis, thus it was thought that investigating NAD^+ levels might be useful in order to understand more about the metabolism and immune responses in macrophages. Therefore, we decided to investigate NAD^+ and the NAD^+ homeostasis profile in macrophages during LPS stimulation using THP-1 derived macrophage differentiation as a study model. THP-1 cells can be differentiated into macrophage-like cells using PMA and vitamin D_3 and differentiated macrophages were characterised by observing both morphological changes as well as TNF-α and IL-6 secretion. As described previously, and as we show here, PMA treatment induces clear changes in cell morphology, as cells start to adhere to culture plates, developing long pseudopodial extensions and becoming comparable to differentiated macrophage subsets (Traore *et al*., 2005; Schwende *et al*., 1996; Daigneault *et al*., 2010). On the other hand, vitamin D_3 treatment did not greatly affect the morphology of THP-1 as the cells remained spherical and non-adherent although they only increased in size. The observed changes in morphology were supported by the observation of distinct cytokine profiles. In keeping with others, we also have shown that TNF-α and IL-6 secretion differ greatly between M1-like cells and M2-like cells with M1-like cells showing a larger increase in TNF-α release but not IL-6, while M2-like cells display larger increase in IL-6 but only a little of TNF-α (Schwende *et al*., 1996; Daigneault *et al*., 2010). These results suggest that M2-like might resemble M2b features on the sliding sale of macrophage polarization (Figure 1.1) due to TNF-α and IL-6 secretion.

In addition, the results showed that PMA, treatment caused a drop in THP-1 proliferation whereas vitamin D_3 did not. PMA is well known to activate protein kinases (PKCs), in PMA-treated THP-1 cells (Schwende *et al*., 1996), which has been shown to induce cell cycle arrest in a ROS-dependent manner during both G0-G1 and G2 phases (Traore *et al*., 2005). In M1-like cells, TNF-α increases in response to LPS since ROS is known to regulate TNF-α expression in NF-kB-dependent manner (Collart *et al*., 1990; Shakhov *et al*., 1990; Trede *et al*., 1995). The NF-κB accumulation is induced in cytoplasm of M1-like cells, allowing rapid secretion of pro-inflammatory TNF-α in response to LPS stimulation (Takashiba *et al*., 1999). This might explain, at least in part, the large increase in TNF-α secretion by M1-like. This is possibly occurring due to the fact that PMA induces metalloproteinases (MMP-9) that are required for TNF-α release (Ismair *et al*., 1998). However, MMP-9 expression was shown to be inhibited by vitamin D_3 in primary macrophages (Coussens *et al*., 2009) following inflammatory signals which might partially explain the differential trend in TNF-α response in M1-like but not in M2-like cells (Mohler *et al*., 1994; Gearing *et al*., 1994; McGeehan *et al*., 1994). One possible explanation is that vitamin D_3 may be able to suppress the expression and protein of TLR2 and TLR4 in human monocytes in a time- and a dose-dependent manner resulting in hypo-responsive towards pathogens (Sadeghi *et al*., 2006). In contrast, PMA has been shown to enhance TLR2 responses suggesting important role in macrophages differentiation (Daigneault *et al*., 2010). Enhancement of TNF-α secretion by macrophages during monocytes differentiation is well established (Gessani *et al*., 1993).

It seems that both NF-κB and MMP induction by PMA treatment caused an increase in TNF-α release in M1-like MΦs. Vitamin D_3 treatment, on the other hand, showed an opposing effect on IL-6 release in response to LPS challenge. The data in this study seems to be in line with other works (Daigneault *et al*. 2010; Foey and Crean, 2013, Hmama *et al*., 1999)

showing that vitamin D_3 was capable of increasing IL-6 release following LPS stimulation. Indeed, vitamin D_3 has been shown to support HL-60 and U937 cells towards monocyte/macrophage differentiation but not into granulocytes. This is mediated either via induction of alpha-naphthyl acetate esterase activity, a typical marker of monocyte-macrophages or via receptor-mediated monocytic maturation (Tanaka, *et al*., 1983; Mangelsdorf, 1984; Collins, 1987). It is important to note that IL-6 secretion is not only known to mediate pro-inflammatory responses via recruiting mononuclear cells and inhibiting Treg. proliferation but is also implicated in the anti-inflammatory response via activation of STAT3-mediated signalling pathways (Scheller *et al*., 2011). STAT3 has recently emerged as a vital mediator for M2 differentiation (Chávez-Galán *et al*., 2015). In addition, macrophage stimulation with IL-6 led to downregulated IDO expression which might explain the reason as to why M2s display low IDO expression compared to M1s in both the resting and activated states (Figure 3.6). Thus, it appears likely that IL-6 secretion might support the M2 phenotype versus M1 phenotype.

There were some differences between macrophages and THP-1 derived differentiated macrophages with respect to pattern expression of certain genes. For instance, while both apolipoprotein-E and MMP 9 are induced in primary macrophages and M1-like cells, the induction of IL-1β is conversely upregulated in M1-like MΦs but not in primary macrophages (Kohro *et al*., 2004) suggesting that caution must be taken in interpreting results when experiments are done with THP-1 under different conditions. However, collectively, the results from this study and the previous research that we referred to in this section seem to provide further evidence suggesting that THP-1 is a reliable and suitable model to generate cells that might be very close to pro-inflammatory M1-like or anti- inflammatory M2-like MΦs. It has been reported that NAD^+ homeostasis plays a pivotal role in transcriptional

modulation of pro-inflammatory cytokines produced by immune cells. For example, NAD^+-mediated sirtuin activity has been shown to modulate the production of the pro-inflammatory cytokine, TNF-α in pro-inflammatory MΦs (van Gool *et al*., 2009). In the current study, it has been demonstrated that NAD^+ levels differ significantly between differentiated and non-differentiated MΦs with pro-inflammatory M1-like MΦs having higher basal NAD^+ levels, suggesting that NAD^+ are pro-inflammatory (Figure 3.3 A). It seems that M1-like MΦs exhibit higher NAD^+ synthesis rates than M2-like MΦs. This was confirmed by the increase observed in NAD^+ levels after nicotinamide application in M1-like compared to M2-like (Figure 3.5 C). This might account for the upregulation in NAMPT expression we observed in resting M1-like MΦs compared to THP-1 and M2-like MΦs (Figure 3.6 A) whereby both cells display similar NAMPT expression. This might explain why both cells show similar NAD^+ levels as in Figure 3.3 A. Indeed, NAMPT is the rate limiting enzyme in the NAD^+ recycling pathway (Revollo *et al*., 2004) and this pathway is the most active of the three known pathways that lead to NAD^+ synthesis; the others being the *de novo* IDO pathway (Magni *et al*., 2004) and the nicotinamide riboside kinase (NRK) pathway (Bieganowski and Brenner, 2004). The increases in NAMPT in M1-like MΦs would suggest that the cells are priming themselves for NAD^+ production. The induction of NAMPT expression has previously been shown in primary murine macrophages (Iqbal and Zaidi, 2006). The increase in NAMPT expression might be linked to the findings showing that M1-like MΦs are mainly glycolytic (Vazquez *et al*., 2010; Galvan-Pena and O'Neill, 2014) and thus high NAD^+ levels are required to maintain glycolytic activity. In contrast, M2-like MΦs were not able to alter NAD^+ levels under same the same conditions suggesting that M2-like MΦs exhibit low NAD^+ synthesis capacity compared to M1-like. This complemented the results showing NAD^+ production was not affected by both NAM and quinolate treatment. Furthermore, we

observed an opposite effect on NAD^+ levels between the two subsets. In M2-like MΦs, FK866 treatment decreased the levels of NAD^+ over time as it would be expected due to inhibition of NAD^+ synthesis suggesting that M2-like MΦs might have high NAD^+ consumption rate but low synthesis capacity as M2-like failed to increase NAD^+ after NAM and quinolate application. In contrast, FK866 treatment gradually increased NAD^+ levels in M1-like MΦs (Figure 3.5 A). It is not exactly clear as to how this increase might occur. However, we can speculate that these rather contradictory results may be explained as the NAD^+ generation might occur partially via NAMPT recycling pathway as it has been shown in different results that NADH oxidation via NADPH mechanism could be another source for NAD^+ production in M1-like cells (see Chapter 4). Additionally, it is also possible that the increase in NAD^+ levels, observed in M1-like, could be related to the impact of NAD^+-consuming enzymes on NAD^+ turnover resulting in NAM accumulation. Indeed, the treatment with NAM has been shown to block SIRT-dependent de-acylation and ADP-dependent PARP activity can be inhibited in micromolar range of non-competitive inhibitor NAM (Clark *et al.*, 1971; Shall, 1983; Szabo and Dawson, 1998; Hageman and Stierum, 2001, Sanders *et al.*, 2007). For example, NAM can inhibit deacetylation reactions through interference with the reaction intermediate via a base exchange reaction to reproduce NAD^+ at the expense of protein deacetylation reaction (Sanders *et al.*, 2007). The NAD^+-consuming enzymes are regulated by NAD^+; therefore it has been suggested that NAD^+/NAM plays a critical role in linking and thus modulating the activity of NAD^+-requiring enzymes (reviewed in Hassa and Hottiger, 2008). For instance, limiting NAD^+ by ADP-PARP activity might indirectly led to modulate CD38-depedent mono-ribosylation and SIRT-dependent deacetylation activity (reviewed in Hassa and Hottiger, 2008). Indeed, these proteins have been shown to be highly up-regulated in activated macrophages and this seems to be

associated with NAD^+ catabolism and also the consequence liberation of NAM as end-product of the process (Paine *et al*., 1982; Liu *et al*., 2012). Therefore, treatment with FK866 resulted in decreased NAD^+ depletion in a neuronal model due to inhibition SIRT1 activity, one the main NAD^+-consuming enzymes (reviewed in Hassa and Hottiger, 2008). Reduction in NAD^+ depletion has also been reported in neuronal model following FK866 treatment as a result of inhibiting PARP1 activity, another of the main NAD^+-consuming enzymes (reviewed in Hassa and Hottiger, 2008). These data indicate that both subsets have differential profile of NAD^+ homeostasis and it is likely that these differences might be physiologically relevant. Taken into consideration the differential profile of NAD^+ homeostasis, pharmacological approach has been taken to investigate the source of NAD^+ levels in macrophages during stimulation (see Chapter 4).

The intracellular NAD^+ concentration is often reported to be in the high micromolar range (Hasmann and Schemainda, 2003; Houtkooper *et al*., 2010). The increase in NAD^+ levels has been reported previously in a model of human leukaemia cells such as the HL-60 and THP-1 cell lines (Baranowska-Bosiacka *et al*., 2005), suggesting an important role for NAD^+ in cell maturation and proliferation. We also show here increase in NAD^+ levels whereby M1-like MΦs exhibit significant high NAD^+ levels that are even higher than that for THP-1 cells. It is not clear as to why this important increase occurs. A possible explanation is that macrophages are known to induce ROS production as part of a defence mechanism, which induces PARP activity mediated by DNA damage which is thought to be one of the NAD^+-consuming activities in cells (Rodriguez-Vargas *et al*., 2012; Hassa and Hottiger, 2008; Altmeyer and Hottiger, 2009). As a result, PARPs might partially deplete intracellular NAD^+ levels, thus promoting the fast recycling of NAD^+ either *de novo* or from salvage pathways to maintain cellular viability or to support the activity of other NAD^+-consuming enzymes

(Berger, 1985; Skidmore *et al*., 1979). For instance, PARP-1 binds to the nuclear NAD^+ synthase, NMNAT-1 (the enzyme that catalyses NAD^+ synthesis from nicotinamide mononucleotide (NMN) replenishing NAD^+ and providing sufficient NAD^+ for PARP-1), SIRT1, as well as the main NAD^+-consumer, CD38 (Aksoy *et al*., 2006b; Berger *et al*. 2007; Zhang *et al*. 2009). Interestingly, M1-like cells showed higher levels of the NADase CD38, which might reflect high turnover (Figure 3.6 A). This might explain, at least in part, the observed increase in NAD^+ content that is frequently followed by a steady drop within 1 to 2 h of the initial rise before the second rise that start at 4h (Figure 3.3 B). These data might agree with evidence suggesting that the half-life of NAD^+ is short (estimated to be around 1 to 2 h), forcing the cells to continuously replenish NAD^+ to restore NAD^+ balance inside the cells (Elliott and Rechsteiner, 1975; Rechsteiner *et al*., 1976; Williams *et al*., 1985; Berger, 1985). In fact, there is evidence showing CD38 as an early differentiation marker (Frasca *et al*., 2006). However, M2-like cells displayed higher expression of CD157, the CD38 homologue, NADase and the converse of CD38. These findings are in agreement with the results obtained by Hussain *et al*. (2000), who showed that CD157 expression was upregulated in vitamin D_3-differentiated myeloid cells and conversely downregulated with PMA treatment from the same cells. Although there are differences in some genes between primary macrophages and M1/M2-like MΦs (Kohro *et al*., 2004), the differential regulation of CD157 and CD38 for the two subsets may reflect a similarity to *in vitro* monocyte and macrophages. Indeed, the induction of CD157 expression was shown on myeloid precursors as the cells differentiate towards more mature monocytes/macrophages (Kizaki *et al*., 1991; Okuyama *et al*., 1996; Hussain *et al*., 2000). In addition, the ability of M1-like cells to promote NAD^+ level increases could occur due to the increase in volume of cells caused by PMA treatment, as it has previously been reported that NAD^+ amount production is

associated with an increase in cell volume (Williams *et al*., 1985). The results from the current study show that extracellular application of quinolate had no effect on NAD^+ generation in M1-like MΦs. It is somewhat surprising there was no increase in NAD^+ production after quinolate application, although IDO expression was upregulated in both subsets suggesting that IDO might not be involved in NAD^+ generation in resting state. It is not quite clear as to why this occurs. However, it could be that the concentration of quinolate used here was not enough to affect IDO activity or that IDO/kynurenine might be not efficient under the experimental conditions employed. Given the differences in NAD^+ levels and NAD^+ homeostasis gene expression, the NAD^+ changes were investigated during LPS stimulation in both subsets. M1-like MΦ exposure to LPS stimulation led to significantly increasing NAD^+ levels (Figure 3.3 B). NAD^+ levels display a biphasic response with a rapid peak within 50 minutes followed by a sustained rise that lasted for longer during the stimulation. There exists some evidence of the involvement of LPS in NAD(P)H oxidase activation (Remer *et al.*, 2003), in a TLR4 dependent manner (oxidative burst) which catalyses the NAD^+ oxidation from NAD(P)H (Riebel *et al*., 2002). The sustained rise in NAD^+ levels also suggests that NAD^+ synthesis occurs as it would be expected that the cell would return the redox balance after the oxidative burst relatively rapidly so as to maintain the NAD^+/NADH ratio. Given that classical activation (M1s) induces glycolysis to support fast and rapid response while M2s (alternative) utilize oxidative metabolism to support the long phase response (Vazquez *et al*., 2010; Galvan-Pena and O'Neill, 2014)our data could suggest a critical role for the NAD^+ increase in the rapid response reflected by the initial rise that end with a drop after 24 h to allow the second and long phase of the response, highlighting important role for NAD^+ levels in cells phenotype effector function. Indeed, it has been shown that NAD^+ behaves like pro-inflammatory cytokine, recruiting granulocytes

at the site of inflammation (Bruzzone *et al*., 2006). Together, these findings suggest that LPS affects NAD^+ homeostasis differently in the two phenotypes with pro-inflammatory M1-like cells are characterized by changes in NAD^+ while anti-inflammatory M2-like MΦs are not. Also, the gene expression of NAD^+ homeostasis enzymes was investigated during LPS stimulation in both subsets. The greatest increase in expression, compared to parent THP-1 cells, was in IDO in both phenotypes and it might be expected that the *de novo* pathway would, thus, be the biggest contributor to NAD^+ levels. However, this pathway is known to contribute little to the intracellular NAD^+ pools with as little as 1 in 60 molecules of NAD^+ being derived from tryptophan (Horwitt *et al*., 1956). The IDO has been shown to play a key role in mediating the flux between pro- and anti-inflammatory cytokines production (Pilotte *et al*., 2012). It seems that the increase in IDO expression is to regulate macrophage immune function in the second phase of the response.

In M1-like cells, mRNA expression of all enzymes except NMNAT increased significantly within 4h of LPS stimulation with the largest effects on IDO and CD38. In agreement with this, it was found that LPS was able to induce increase in IDO and CD38 expression in NF-kB-dependent manner (Fedele *et al*., 2004; Jung *et al*., 2007). It is likely that the TNF-α released during the experiment is partially responsible for the expression observed and thus why the results largely follow the same trend (Figure 3.7 A) This assumption seems to be in line with Iqbal and Zaidi (2006) who revealed that TNF-α application to macrophages increased the expression of the same enzymes. M2-like MΦs, that secreted a lesser amount of TNF-α, showed subtle differences in expression profiles of the enzymes. While IDO and CD38 both significantly increased, CD157 remained unchanged in M2-like (Figure 3.7 B). Most striking was the differential regulation of NMNAT and NAMPT mRNA expression. While we have been unable to measure long-term effects after LPS stimulation due to

limitations in the cell model, it is tempting to postulate that changes in NAD^+ homeostasis caused by these changes in gene expression, might contribute to changes in cell phenotype and immune function post-infection. It is tempting to speculate that the change in NAD^+ homeostasis gene expression might be required for the initial phase of response which takes few hours to day since the genes expression results seem to follow the same trend of TNF-α. Therefore, future work must be directed to investigate the NAD^+ homeostasis in the macrophage during the second phase of response.

In conclusion, the current findings have shown that pro-inflammatory M1-like cells were subject to significant NAD^+ changes compared to anti-inflammatory M2-like MΦs. The intracellular NAD^+ levels increased with NAM and FK866 in M1-like MΦs unlike M2-like MΦs suggesting a differential profile of NAD^+ synthesis/consumption rate between the two subsets. Therefore, on the basis of the obtained results, it seems that the two subsets clearly differ in the way that they perform NAD^+ homeostasis and this may reflect different needs for NAD^+. Additionally, both subsets differ in the expression profiles of a number of NAD^+ homeostasis enzymes in both basal and activated state. We have shown that expression of CD38 and CD157 are differentially regulated in resting and activated state for both subsets. This could add to list of molecules that discriminate between M1-like and M2-like MΦs (as illustrated in Figure 3.8). The current findings might open the door for pharmacological approach by which we would be able to regulate the immune function for primary MΦs.

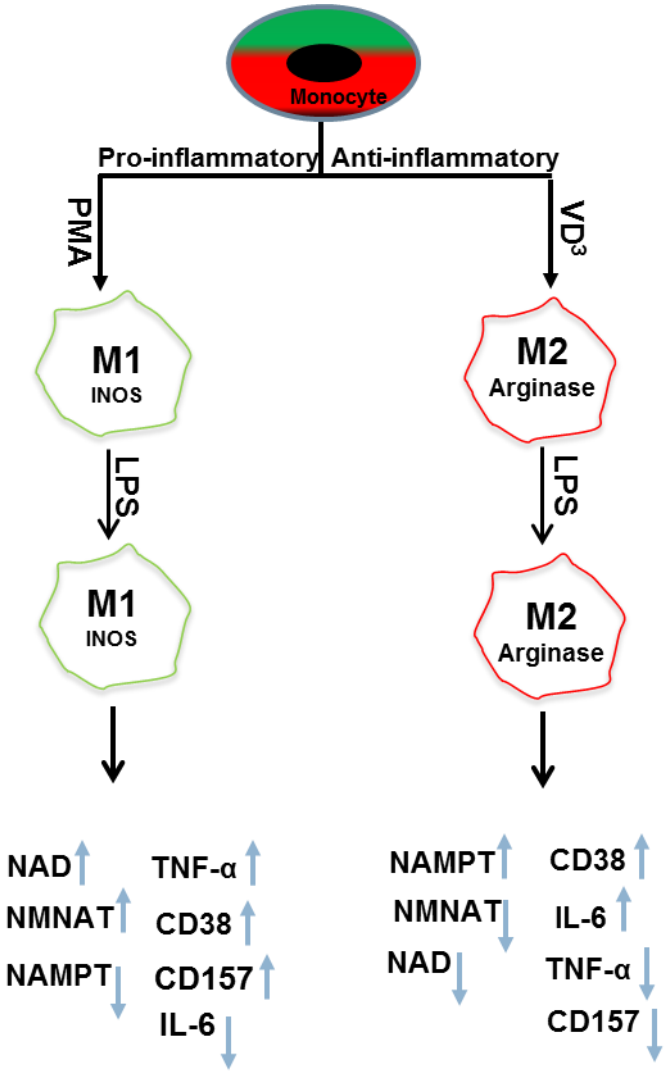

Figure 3.8 Schematic diagram depicting the differences in NAD^+ homeostasis and cytokine production between M1-like and M2-like MΦs during LPS stimulation. M1-like cells displayed higher levels of NAD^+ and TNF-α compared to M2-like cells which displayed high levels of IL-6 in response to LPS. These are also observed by others (Daigneault *et al*., 2010; Foey and Crean, 2013). M1-like MΦs increase the expression of CD38, CD157, NAMPT and NMNAT which might reflect the unusual changes in NAD^+ levels. On the other hand, M2-like cells increase the expression of NAMPT, CD38 but not CD157 and NMNAT in response to LPS challenge compared to M1-like cells.

CHAPTER 4

PHARMACOLOGICAL MODULATION OF NAD^+ LEVELS CONTROLS TNF-α SECRETION IN DIFFERENTIATED MACROPHAGES

4.1 Introduction

TNF-α is mainly produced by proteolytic cleavage of a larger protein by macrophages which play a pivotal role in both innate immunity and adaptive immunity upon inflammation induction (Grivennikov *et al*., 2005; Classen *et al*., 2009). TNF-α is critically involved in a variety of inflammatory effects (Hehlgans and Pfeffer, 2005). Despite TNF-α being crucial for macrophage immune function and host defence (Parameswaran and Patial, 2010), excessive production of TNF-α can lead to pro-inflammatory cascades resulting in a potentially fatal cytokine storm (Finlay and McFadden, 2006) leading to damage of the host. Therefore, a regulatory system must have evolved to dampen the damaging impact of TNF-α in such conditions. TNF-α synthesis is initially triggered by LPS-induced TLR4 signalling resulting on activation of the MAPKs (ERK 1, 2), P38, JNKs pathways along with the transcription factors NF-κB and AP-1 (Sanghera *et al*., 1996; Tsushima and Mori, 2001; Beutler and Rietschel, 2003; Karin, 2009). TNF-α is produced as a 26 kDa pro-form, which is membrane associated (mTNF-α) and which either stays on the cell surface or can be processed to release a 17 kDa soluble product (sTNF-α) via proteolytic cleavage referred to as ectodomain shedding (Beutler and Cerami, 1989; Moss *et al*., 1997; Peschon *et al*., 1998). This process is defined as the proteolytic cleavage of a wide range of transmembrane proteins, such as TNF-α, to release an extracellular domain from the cells (Peschon *et al*., 1998). The shedding is induced by PMA in a PKC-dependent manner (Nakada-Tsukui *et al*., 1999). Indeed, PKC mediates the shedding of a number of membrane proteins including pro-TNF-α, pro-TGF-β, CD14, CD16, CD44, IL-6 and the receptors for TNFα (Bazil, 1995; Hooper *et al*., 1997; Peschon *et al*., 1998). Several studies have shown that the shedding process is mediated by a disintegrin and metalloproteinases (ADAM) family such as TNF-α converting enzyme (TACE) in several cell line systems (Black *et al*., 1997; Reddy *et al*.,

2000; Peschon *et al*., 1998). Indeed, ADAM 10 has been shown to cleave TNF-α and its receptor in THP-1 (Rosendahl *et al*., 1997), whereas ADAM 17 has been shown to be a sheddase of TNF-α and its receptor in macrophages and neutrophils (Bell *et al*., 2007). However, there is evidence that, rather than ADAM, serine proteases are also involved in the shedding of TNF-α (Kim *et al.*, 1993; Nakada-Tsukui *et al*., 1999). Interestingly, since TNF-α is a fatty acylated protein (Stevenson *et al*., 1993) it is believed that TNF-α can also be shed by SIRT6 via removal of the fatty acyl group (Jiang *et al*., 2013). This is perhaps not surprising because SIRT6 plays a crucial role in the regulation of TNF-α synthesis via intracellular NAD^+. Indeed, a key role has been shown for NAD^+ in the positive control of TNF-α transcription, via the de-acylation of the Rel A/p65 subunit of NF-kB, in an NAD^+-sirtuin dependent manner and thus the reduction in NAD^+ levels or SIRT6 knock out blocks synthesis of TNF-α (van Gool *et al*., 2009). Sirtuins comprise a family of seven conserved members (SIRT1 to 7) that use NAD^+ (Heltweg *et al*., 2006) to regulate multiple biological processes from gene transcription/translation (Vaquero *et al.*, 2004) to cell differentiation (Fulco *et al*., 2003). Sirtuin-dependent acetylation has been shown to modulates the immune response via its substrate NAD^+ (Magni *et al*., 2004) and its sensitivity to NAD^+/NADH ratio (Picard *et al*., 2004; Yeung *et al*., 2004). It has recently been shown that pharmacological inhibition of sirtuins caused a reduction in secretion of selective inflammatory cytokines including IL-6 and TNF-α due to blockage of NF-κB activity and IκBa phosphorylation in J774 macrophages (Fernandes *et al*., 2012). Besides the sirtuins, the inflammatory responses can be also regulated via NADPH oxidase which mediates reactive oxygen species (ROS) production and oxidative burst (Chiarugi *et al*., 2012). NADPH oxidase has been shown to regulate the NF-κB signalling pathway and the consequence production of pro-inflammatory TNFα (Kaul and Forman, 1996). Despite the well-established link between NAD^+ and TNF-

α, there is still a need to elucidate the mechanisms that mediate how NAD^+ levels and TNF-α are linked and whether pharmacological NAD^+ manipulation can modulate macrophage inflammatory responses, in particular, TNF-α.. An interest in the pharmacological modulation of NAD^+ levels to regulate pro-inflammatory responses. In particular, focus has grown on the modulation of NAD^+ homeostasis as a way of decreasing NAD^+ levels, reducing the activity of NAD^+-dependent immune function. Indeed, the inhibition of NAMPT-mediated NAD^+ generation by FK866 blocked the increase of NAD^+ content and inhibited LPS-mediated TNF-α secretion in THP-1 cells, human monocytes and macrophages (van Gool *et al*., 2009; Schilling *et al*., 2012). In addition, in the light of the role of *de novo* NAD^+ synthesis in maintaining NAD^+ levels, Braidly and his team (2011) have investigated the pharmacological inhibition of IDO activity using an IDO inhibitor, 1D-MT (1D-methyl tryptophan), with the ability to decrease NAD^+ levels, highlighting the importance of IDO activity in sustaining NAD^+ availibity during inflammation. Despite the role of IDO in NAD^+ production, IDO is known for its role in immune suppression and therefore 1D-MT-mediated IDO inhibition led to blockage of host-mediated immunosuppression and enhanced antitumour immunity in dendritic cells (Hou *et al*., 2007). We show here that NAD^+ levels are correlated with TNF-α secretion in pro-inflammatory M1-like but not in anti-inflammatory M2-like cells during LPS stimulation. Also, we found that NAD^+ is produced partially via NADH oxidation and partially via the NAD^+ recycling pathway suggesting that the mechanism linking NAD^+ and TNF-α is complex and requires a combination of pathways.

4.2 Results

4.2.1 Toxicity assessment of inhibitors

We performed pharmacological inhibition to elucidate how NAD^+ modulation controls TNF-α responses using a number of specific inhibitors includes DPI (diphenylene iodonium), a competitive inhibitor for NADPH oxidase, 1-MT (1-methyl tryptophan, a competitive inhibitor of IDO (indole amine 2,3-dioxygenase), FK866, an inhibitor of NAMPT and sirtinol, a sirtuin inhibitor (Table 4.1). We initially sought to test the toxicity of inhibitors used in this study in order to select a non-toxic concentration and thus to exclude non-specific cellular toxicity. The inhibitor concentrations were chosen according to the literature and primary optimization. Thus, the MTT assay was performed on differentiated cells following incubation with different concentrations of the inhibitors used in our study (Figure 4.1). Although, the MTT assay showed reduction in viability with DPI after 12 h, the trypan blue assay did not show any reduction in cell viability before 18 h. This is because the MTT assay is based on the activity of dehydrogenases, which might be already affected by DPI treatment. The remaining inhibitors had no toxic impact on the cells under the experimental conditions (Figure 4.1) and this was confirmed by the trypan blue assay. It has been shown that DPI is able to block NADPH oxidase activity at 100 µM (Riganti *et al*., 2004), so we used this concentration because we wanted to achieve sufficient inhibition. In addition, our rationale is that we were interested in the very early stages of the LPS response. It has been reported that the inhibition of NAMPT activity was achieved with 100 nM (Hasmann and Schemainda, 2003; Billington *et al*., 2008), while IDO inhibition was achieved with 1-MT at 200 µM for 2 h according to Opitz *et al*. (2011a) and sirtuin inhibition with 25 µM sirtinol for 24 h according to Fernandes *et al.* (2012).

Table 4.1 The chemical structure and solvents used for the inhibitors used in this study

Inhibitors	Action	Solvents	Chemical Structures
1-methyl-L-Tryptophan (1-MT)	Competitive IDO inhibitor	0.1 N NaOH to give 200µM final concentration	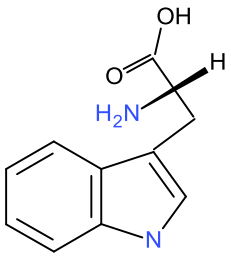
FK866 (APO866, Daporinad)	Non-competitive inhibitor	DMSO (dimethyl sulfoxide) to give 100nM final concentration	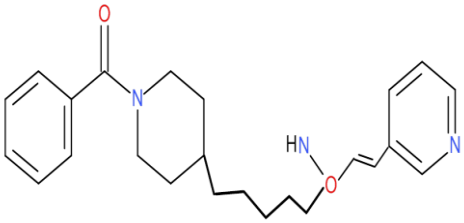
DPI (Diphenyl iodonium chloride)	Uncompetitive inhibitors of flavoenzyme	DMSO (dimethyl sulfoxide) to give 100 µM final concentration	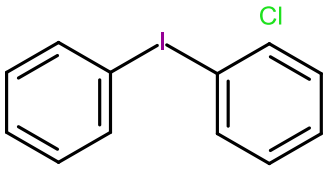
Sirtinol 2-[(2 Hydroxynaphthalen-1-ylmethylene) amino]-N-(1phenethyl)benzamide	inhibitor of sirtuin family members	DMSO (dimethyl sulphoxide) to give 25 µM final concentration	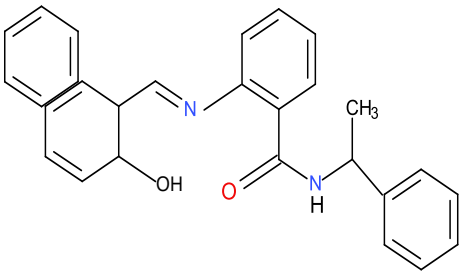

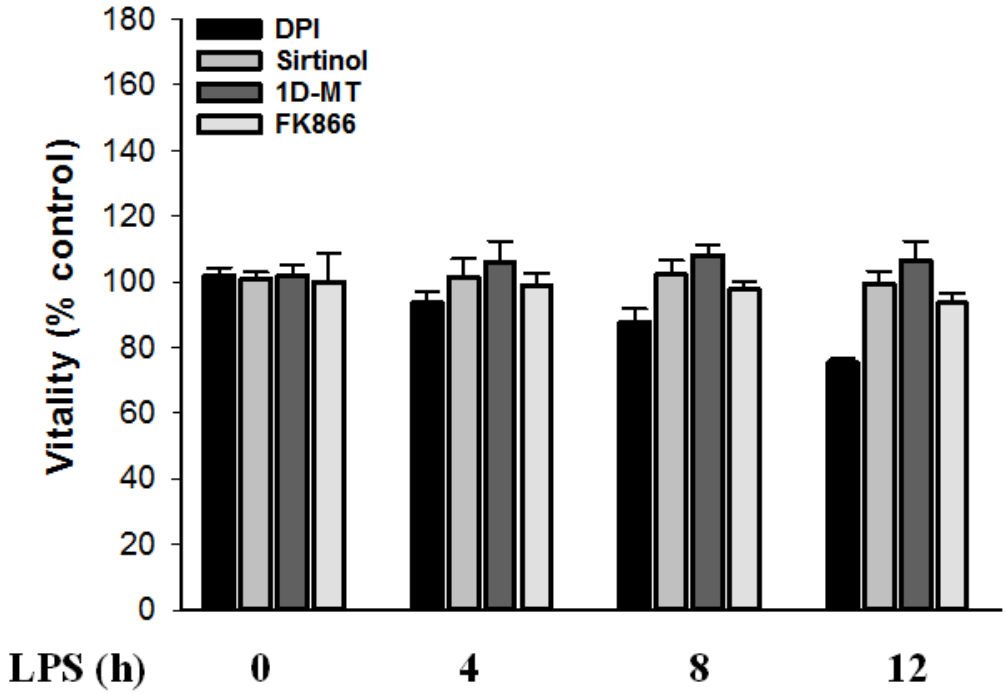

Figure 4.1 Cell vitality was determined using the MTT assay. Differentiated cells were pre-incubated with 100 µM DPI, (0.5 h) or 25 µM sirtinol, (24 h) or 200 µM 1-MT, (2 h) or FK886 100 nM, (1 h) prior to stimulation with LPS. Results were analysed by two way ANOVA followed by the Bonferroni test. Significantly different results are indicated as follows: *P<0.05, **P<0.01, ***P<0.001.

4.2.2 Elevated NAD^+ levels are associated with TNF-α secretion in response to LPS stimulation

The link between NAD^+ levels and TNF-α is well established with NAD^+ being shown to modulate TNF-α synthesis in a sirtuin-dependent manner (van Gool *et al*., 2009). The authors showed that intracellular NAD^+ levels are required for TNF-α synthesis regulation as sirtuin deacetylase-6 (SIRT6) uses NAD^+ to regulate TNF-α expression at the transcriptional level. It has been previously shown that TNF-α secretion is triggered by LPS stimulation in MΦs (Tracey and Cerami, 1994). We showed earlier (Chapter 3) that M1-like MΦs display high NAD^+ levels in response to LPS challenge; therefore we reinvestigated the link between NAD^+ and TNF-α and whether TNF-α release is associated with the observed changes in NAD^+. To do this, we initially investigated TNF-α release in differentiated MΦs following stimulation with and without LPS over 24 h (Figure 4.2). As expected, M1-like MΦs showed significant TNF-α release, under LPS challenge, that peaked within 4 h compared to the control ($P = 0.001$) and was sustained at 8 h before decaying back to basal levels by 24 h ($P = 0.001$; Figure 4.2 A). In contrast, M2-like cells secreted a relatively small but significant amount of TNF-α which corresponded to less than 10% of that secreted by M1-like cells (Figure 4.2 B). In M2-like cells, the levels of TNF-α peaked at 4 h compared to the control ($P = 0.01$) but this was short lived and TNF- α had returned to almost basal levels by 8 h. However, there was a lower level of TNF-α which persisted to beyond 18 h. It seems that TNF-α levels paralleled LPS-induced NAD^+ changes in pro-inflammatory M1-like MΦs (see Chapter 3) while this is not the case with anti-inflammatory M2-like MΦs. In order to investigate this link further, differentiated macrophages were incubated with and without sirtinol, a well-known sirtuin inhibitor, and both NAD^+ and TNF-α levels were measured. The stimulation with LPS caused a robust TNF-α release, as expected, where TNF-α reached

its maximum levels after 8 h while sirtinol significantly reduced TNF-α cells after 8 h in treated MΦs compared to non-treated MΦs (P = 0.001; Figure 4.2 C). This only occurred after 24 h of incubation confirming recent results (Fernandes *et al*., 2012). In contrast, 1 h pre-treatment with sirtinol surprisingly failed to reduce TNF-α release and rather significantly increased TNF-α to reach its maximum levels after 12 h in treated MΦs compared to non-treated cells (P = 0.002; Figure 4.2 D) suggesting that the effect might be at the transcription/translation level rather than the release levels. The incubation with sirtinol for 1 h increased LPS-induced TNF-α release almost 3-fold higher after 12 h following LPS stimulation. Similarly, sirtinol was capable of increasing NAD^+ levels, which also started to significantly increase after 4 h of stimulation to reach maximum levels after 12 h of LPS stimulation (P = 0.02; Figure 4.2 E) highlighting that NAD^+ may cover the response phase of TNF-α. Together, these data might suggest that TNF-α secretion is correlated with NAD^+ changes in M1-like cells highlighting that NAD^+ is required for TNF-α secretion. Therefore, the data from this study confirm and further strengthen the existing link between NAD^+ and TNF-α and thus metabolism and pro-inflammatory responses.

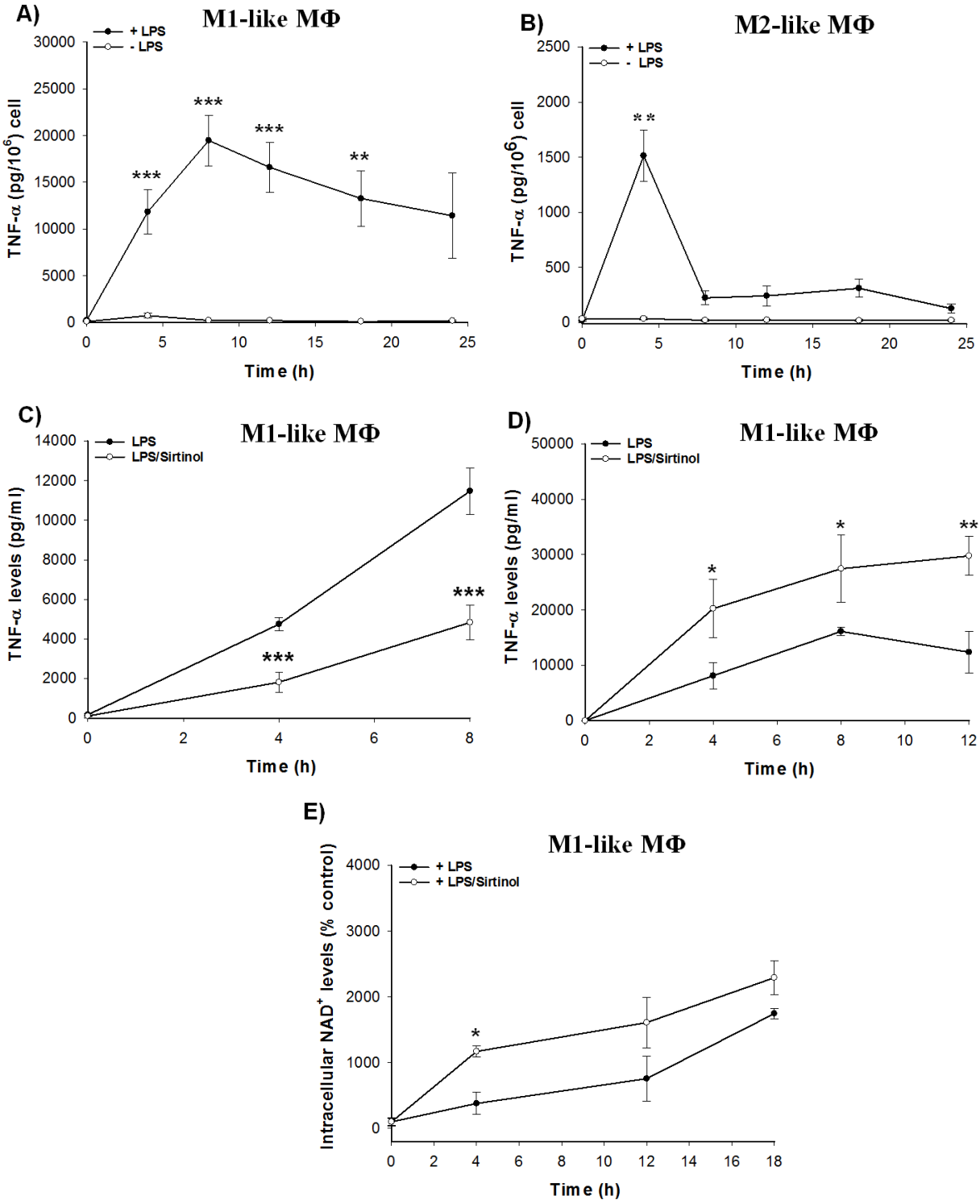

Figure 4.2 NAD^+ levels are associated with TNF-α release in differentiated macrophages during LPS stimulation. LPS increases TNF-α release in M1-like cells (A) but not in M2-like macrophages (B). Pro-inflammatory M1-like macrophages were pre-incubated with sirtinol prior LPS stimulation (C) Sirtinol (25 µM, 24 h) treatment caused decrease in TNF-α release in response to LPS stimulation. However, incubation M1-like with 25 µM sirtinol for 1 h prior to LPS stimulation led to increase in both (D) TNF-α and (E) NAD^+ levels over the experiment. Data shown are means ± SE of three separate experiments (n = 3). Results were analysed by two way ANOVA followed by the Bonferroni *post hoc* test. Significantly different results are indicated as follows: *P<0.05, **P<0.01, ***P<0.001.

4.2.3 DPI treatment decreases both NAD^+ and TNF-α levels in M1-like MΦs but only TNF-α in M2-like MΦs during LPS stimulation

Given that LPS induced unusual changes in gene expression of NAD^+ homeostasis and that NAD^+ levels are correlated with TNF-α release, we decided to investigate the source of NAD^+ generation and whether NAD^+ manipulation can control TNF-α release in differentiated cells. NAD(P)H oxidase is required for macrophage activation because it is involved in TNF-α production via ROS-mediated NF-κB activation (Forman, 1996 and Forman and Torres, 2002; Kaul). Therefore, we were interested in investigating the potential role of NAD(H) oxidation in NAD^+ generation using the inhibitor DPI. DPI is a well-known NADPH oxidase inhibitor that covalently binds to the catalytic subunit of NOX2 enzymes (Cross and Jones, 1986). Indeed, it was found that DPI was capable of abolishing NAD(P)H oxidase-mediated ROS generation in monocytes/macrophage cells (Li and Dinauer, 1998). It is known that NAD(P)H oxidase (Remer *et al*., 2003) is activated in response to LPS in a TLR4-dependent manner and catalyses the oxidation of NAD(P)H to $NAD(P)^+$ (Riebel *et al*., 2002). It has recently been shown that NADPH plays a critical role in supporting elevated glycolysis, by facilitating additional NAD^+ production in cancer cells (Lu *et al*., 2012).

Differentiated macrophages were pre-incubated with 100 μM DPI for 0.5 h prior to LPS stimulation and both NAD^+ and TNF-α were measured, with the results shown in figure 4.3. M1-like cell exposure to DPI caused an inhibition in LPS-induced TNF-α and NAD^+ but only TNF-α in M2s as in this case, DPI might block NADPH oxidase mediated ROS-induced NF-κB activation resulted in inhibition of TNF-α release. In M1s, DPI was able to significantly attenuate both the initial NAD^+ peak ($P = 0.023$) and the sustained rise caused by LPS ($P = 0.014$) suggesting that one source of the NAD^+ is the oxidation of NADH during the

respiratory burst as might be expected (Figure 4.3 A). The decrease was 80% and 50% for the initial peak and the sustained rise, respectively, in comparison to the control. However, NAD^+ levels were not affected by DPI treatment in M2-like cells in response to LPS challenge. Most striking was the effect of the DPI treatment on TNF-α release. In fact, DPI was able to almost completely abolish TNF-α secretion although a small amount was secreted over 8-24 h but significantly less than in the absence of DPI (Figure 4.3 C, D). Indeed, incubation of M1-like MΦs with DPI caused a significant reduction in TNF-α release compared to stimulated non-treated macrophages (4 h, $P = 0.001$). In M2-like MΦs, however, TNF-α release was significantly impaired (4 h, $p = 0.014$) whereas NAD^+ levels were not affected under the same conditions. These data might indicate that the TNF-α response is independent of NAD^+ in M2-like MΦs. This is consistent with data showing that M2-like MΦs secreted a lower amount of TNF-α and showed a modest change in NAD^+ generation (Chapter 3). Taken together, our data suggested that NAD^+ generation might occur partially via NADH oxidation and that NAD^+ might regulate TNF-α release via a DPI-dependent mechanism in M1-like MΦs which further strengthen the link between NAD^+ and TNF-α.

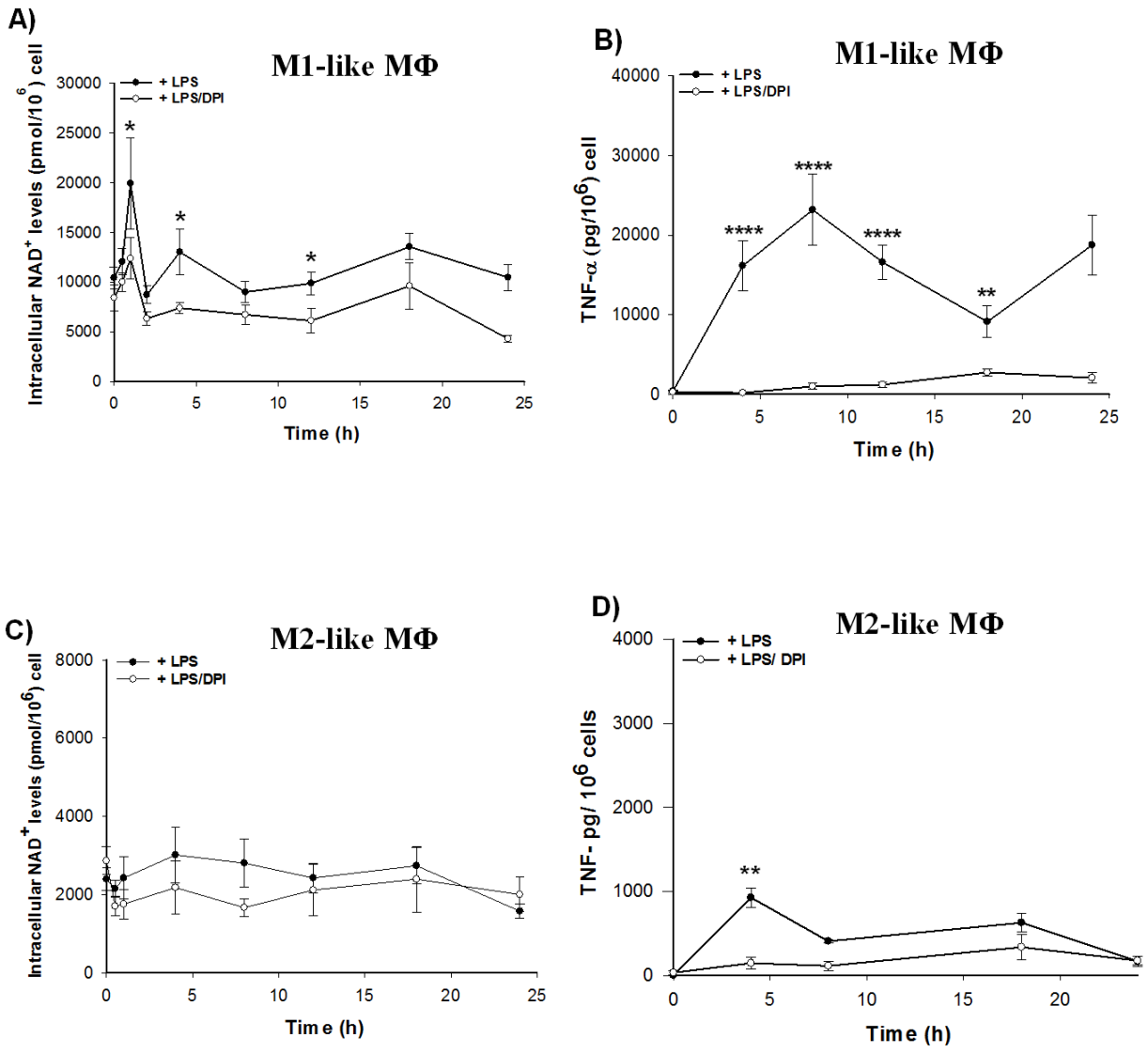

Figure 4.3 DPI treatment blocks LPS-induced NAD^+ levels and TNF-α release in differentiated macrophages. The cells were incubated in the presence or absence of 100 µM, 0.5 h DPI prior LPS challenge. Incubation of M1-like MΦs with DPI led to inhibited NAD^+ levels (B) and TNF-α (C) while in M2-like cells it did not affect NAD^+ levels (C) but did affect TNF-α levels (D) during LPS stimulation. Data shown are mean ± SE of separate experiments in triplicate (n = 3-4). Results were analysed by two way ANOVA followed by the Bonferroni *post hoc* test, and significant results are indicated as follows:*P < 0.05, **P < 0.01, ***P < 0.001.

4.2.4 FK866 stops the increase of both NAD^+ and TNF-α release in M1-like but not in M2-like macrophages in response to LPS challenge

In mammalian cells, NAD^+ is resynthesized preferentially by NAMPT, using nicotinamide, a by-product of the enzymatic cleavage of NAD^+, the rate limiting step for NAD salvage pathways. Since we have shown earlier the upregulation of NAMPT expression (Chapter 3) and considering the importance of the salvage pathway, we next decided to investigate the impact of NAMPT blockage on NAD^+ recycling and TNF-α secretion by using FK866, an inhibitor of NAMPT. It has been recently reported that monocytes rely on this pathway to mount an appropriate inflammatory response, in particular, TNF-α (Schilling *et al*., 2012). Therefore, we made use of FK866, an inhibitor of NAMPT, to investigate the impact of the salvage pathway blockage on TNF-α release in order to test whether lowering NAD^+ levels by FK866 might alter TNF-α response in differentiated macrophages. To acheive this, differentiated macrophages were pre-incubated with 100 nM FK866 for 1 h prior to stimulation with LPS, versus control cells.

As seen in figure 4.4 A, incubation of M1-like MΦs with FK866 resulted in the significant decrease in NAD^+ levels by 40% and 70% for both the initial (1 h, $P = 0.02$) and sustained rise (4 h, $P = 0.014$), respectively, with the greatest effect over the longer term. To investigate whether the decrease in NAD^+ level was correlated with TNF-α, we measured TNF-α release under the same experimental conditions to verify whether FK88-mediated NAD^+ inhibition could negatively affect TNF-α release. TNF-α did still increase, but FK866 was able to significantly reduce the amount released (Figure 4.4 B). FK866 significantly inhibited LPS-induced TNF-α release in time-dependent manner (8 h, $P = 0.023$). TNF-α was decreased by 40% in M1-like MΦs compared to the control.

In M2-like MΦs, however, FK866 caused both NAD^+ and TNF-α to decrease slightly but not significantly after 4 h of LPS stimulation (Figure 4.4 C, D). In M1-like MΦs, it seems that FK88 mediated-NAD^+ inhibition modulates LPS-induced TNF-α secretion suggesting that both are correlated. These data could also suggest NAD^+ re-generation via NAMPT, at least in part, plays an important in identifying the link between NAD^+ and pro-inflammatory TNF-α response suggesting that NAD^+ might be required for TNF-α release.

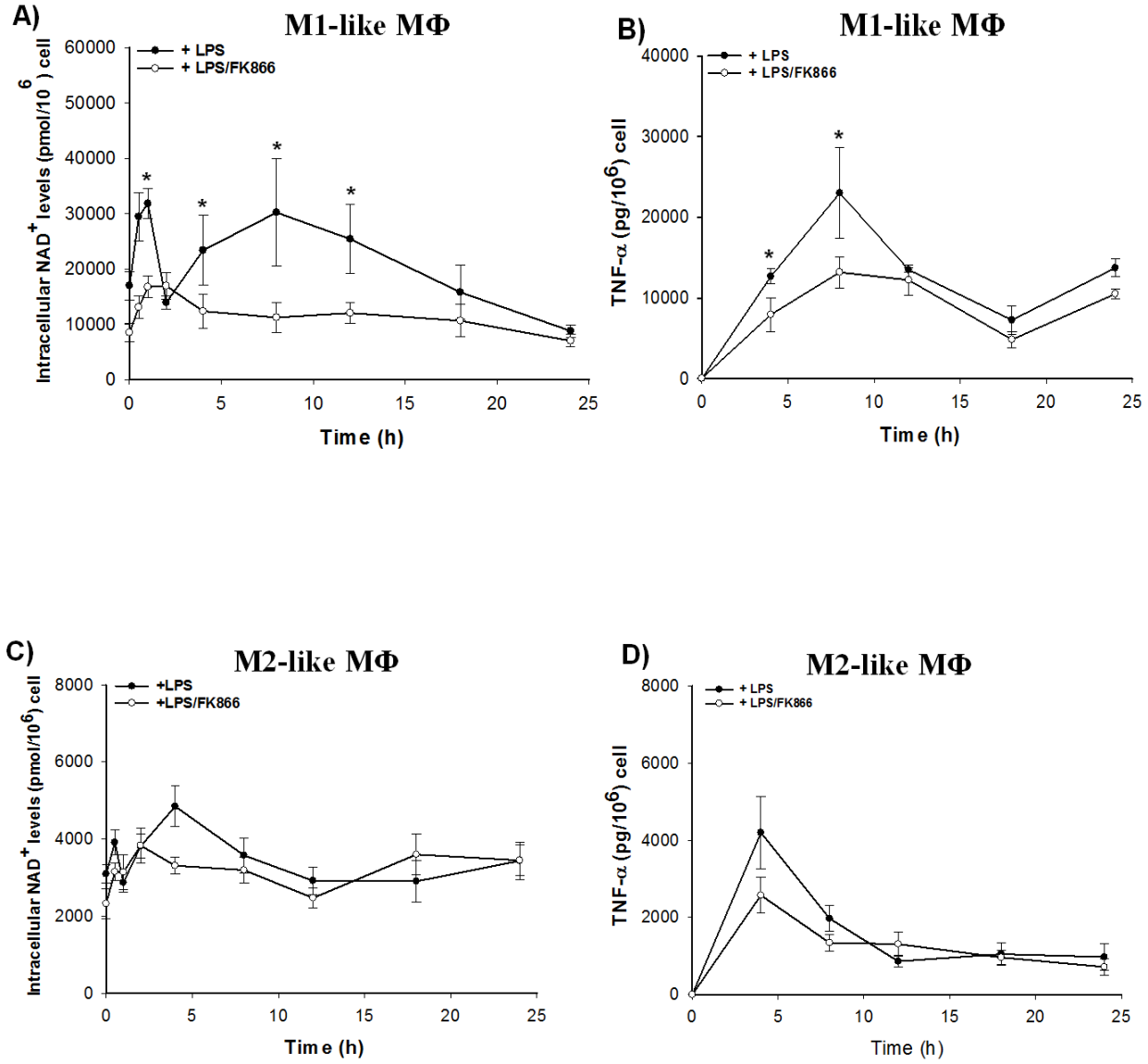

Figure 4.4 FK866 inhibits LPS-induces NAD^+ levels and TNF-α release in pro-inflammatory differentiated (M1-like) macrophages and not in anti-inflammatory (M2-like) macrophages. Differentiated macrophages pre-incubated with and without 100nM FK866 (1h) prior LPS stimulation for the indicated time points. Cells were then harvested for NAD determination and supernatant were collected, from the same sample, for TNF-α measurement. FK866 treatment reduced in time dependent manner (A) NAD^+ levels and (B) TNF-α in M1-like while it did not affect (C) NAD^+ levels and (D) TNF-α in M2-like under LPS challenge. Data shown are means ± SE of three separate experiments (n = 3). Results were analysed by two way ANOVA followed by the Bonferroni *post hoc* test. Significantly different results are indicated as follows:*P < 0.05, **P < 0.01, *** P < 0.001).

4.2.5 Inhibition of IDO with 1-MT attenuates NAD^+ levels but does not affect TNF-α release in differentiated macrophages during stimulation

The IDO pathway, also known as the IDO-kynurenine pathway, is reported to play an important role in *de novo* NAD^+ generation via the oxidation of the essential amino acid tryptophan (Mellor and Munn, 1999; Orabona *et al.*, 2006). Given the involvement of IDO in NAD^+ supply as suggested by Grant and Kapoor (2003) and the remarkable upregulation in IDO expression which we observed previously (chapter 3), we decided to investigate the impact of IDO inhibition on LPS-induced TNF-α and NAD^+ levels in differentiated MΦs. To verify this role, we blocked the enzymatic activity of IDO using the IDO inhibitor, 1D-methyl tryptophan (1D-MT). Differentiated macrophages were pre-incubated in the presence and absence of 200 µM for 2 h prior stimulation with LPS, and both NAD and TNF-α were measured (Figure 4.5). While 1-MT was able to significantly decrease intracellular NAD^+ levels, it did not affect TNF-α responses (Figure 4.5 A, B). Interestingly, 1-MT also inhibited the initial rise of NAD^+ with a longer effect on the sustained rise in M1-like MΦs. In M1-like MΦs, the decrease in NAD^+ levels in stimulated cells treated with 1-MT was 40% (1 h, $P = 0.01$) and 60% (4 h, $P = 0.001$) for the initial and sustained rise, respectively. On the other hand, when M2-like cells were incubated with 1-MT, both NAD^+ and TNF-α levels were slightly but not significantly affected under the same conditions (Figure 4.5 C, D). These data could suggest that the IDO inhibition largely affects NAD^+ generation in M1-like MΦs and it does not affect LPS-induced TNF-α production.

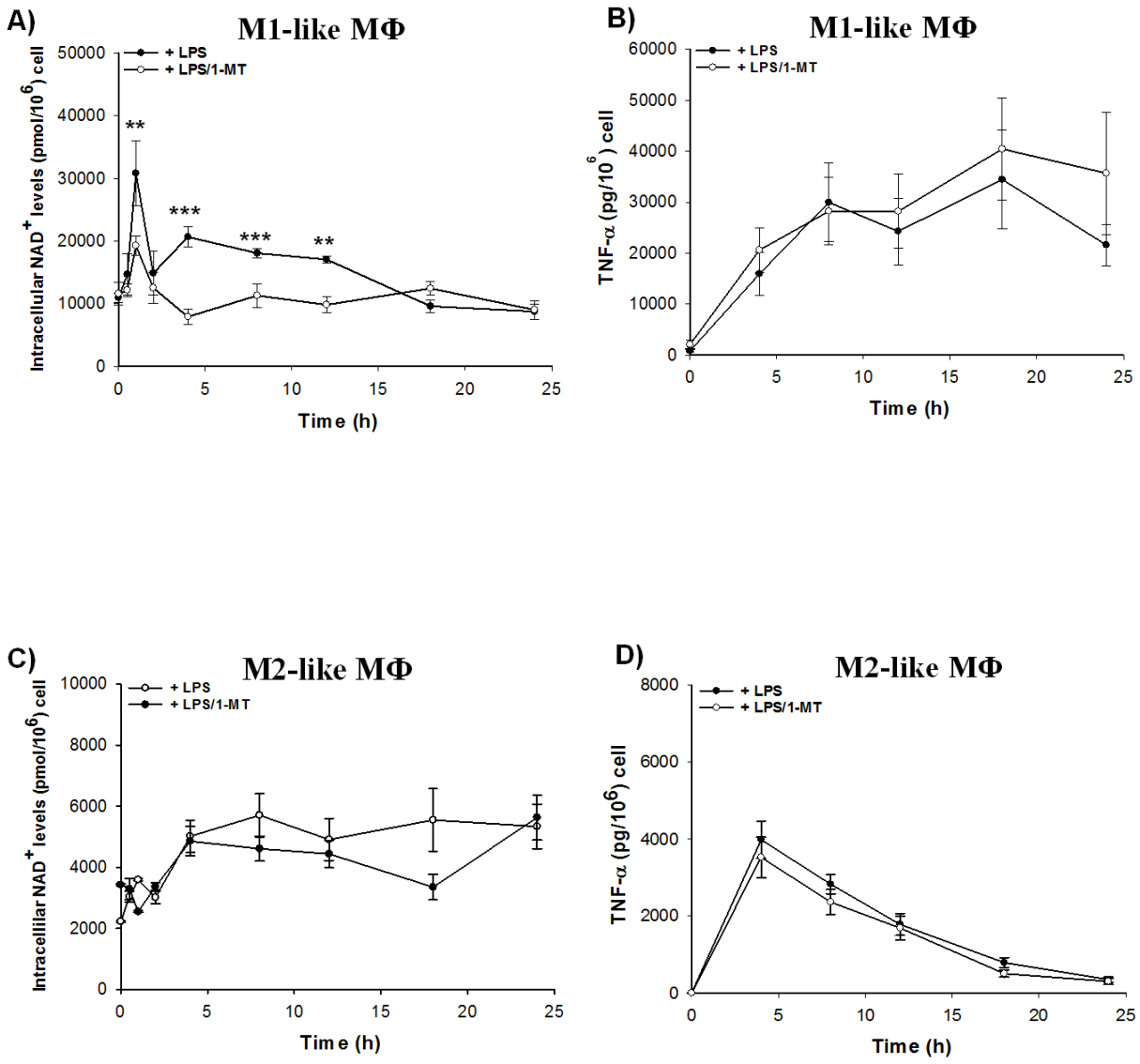

Figure 4.5 1-MT (1-methyl tryptophan) pre-treatment for LPS stimulated pro-inflammatory (M1-like) differentiated macrophages reduced NAD^+ levels but not TNF-α release while anti-inflammatory (M2-like) macrophages were not affected. After differentiation, macrophages were stimulated with LPS post-incubation with and without 200 µM 1-MT (2 h). 1-MT treatment reduced in time-dependent manner (A) NAD^+ levels but not TNF-α (B) in M1-like cells while it did not affect (C) NAD^+ levels and (D) TNF-α in M2-like MΦs. Data shown are means ± SE of three separate experiments (n = 3). Results were analysed by two way ANOVA followed by the Bonferroni *post hoc* test. Significantly different results are indicated as follows:*P < 0.05, **P < 0.01, *** P < 0.001).

4.2.6 Determination of IDO-kynurenine pathway (IDO-KP) activity in differentiated macrophage-like subsets

It is known that IDO catalyses the conversion of tryptophan, via the IDO-kynurenine pathway, into number of immune regulatory metabolites collectively known as kynurenines before ultimately NAD^+ formation (Munn *et al*., 1998). Given that 1-MT inhibits IDO activity mediated NAD^+ production and to further verify the activity of IDO, we next decided to investigate the effect of 1-MT on kynurenine pathway in both macrophage subsets. Differentiated macrophages were pre-incubated with 200 µM 1-MT prior stimulation with LPS and extracellular kynurenine was measured (Figure 4.6). While 1-MT was able to significantly decrease NAD^+ levels, surprisingly, it caused a slight but not significant increase in extracellular kynurenine formation in M1-like MΦs (Figure 4.6 B). We observed no effect on kynurenine levels in 1-MT treated M1-like MΦs in the early stages of LPS stimulation as the levels were comparable to those measured in cells without 1-MT but reached levels even higher than those without treatment and started to increase slightly but not significantly after 18 h and 24 h of LPS stimulation. On the other hand, 1-MT treatment did not affect kynurenine levels in M2-like MΦs. Also, kynurenine consumption rate was quantified in cell lysate from both phenotypes after the indicated times (Figure 4.6 C). Both subsets displayed a very low consumption rate of kynurenine (Figure 4.6 D). These data, collectively, suggest that kynurenine metabolism might be regulated by different pathway in M1-like MΦs and could also suggest that 1-MT has partial effect on kynurenine metabolism.

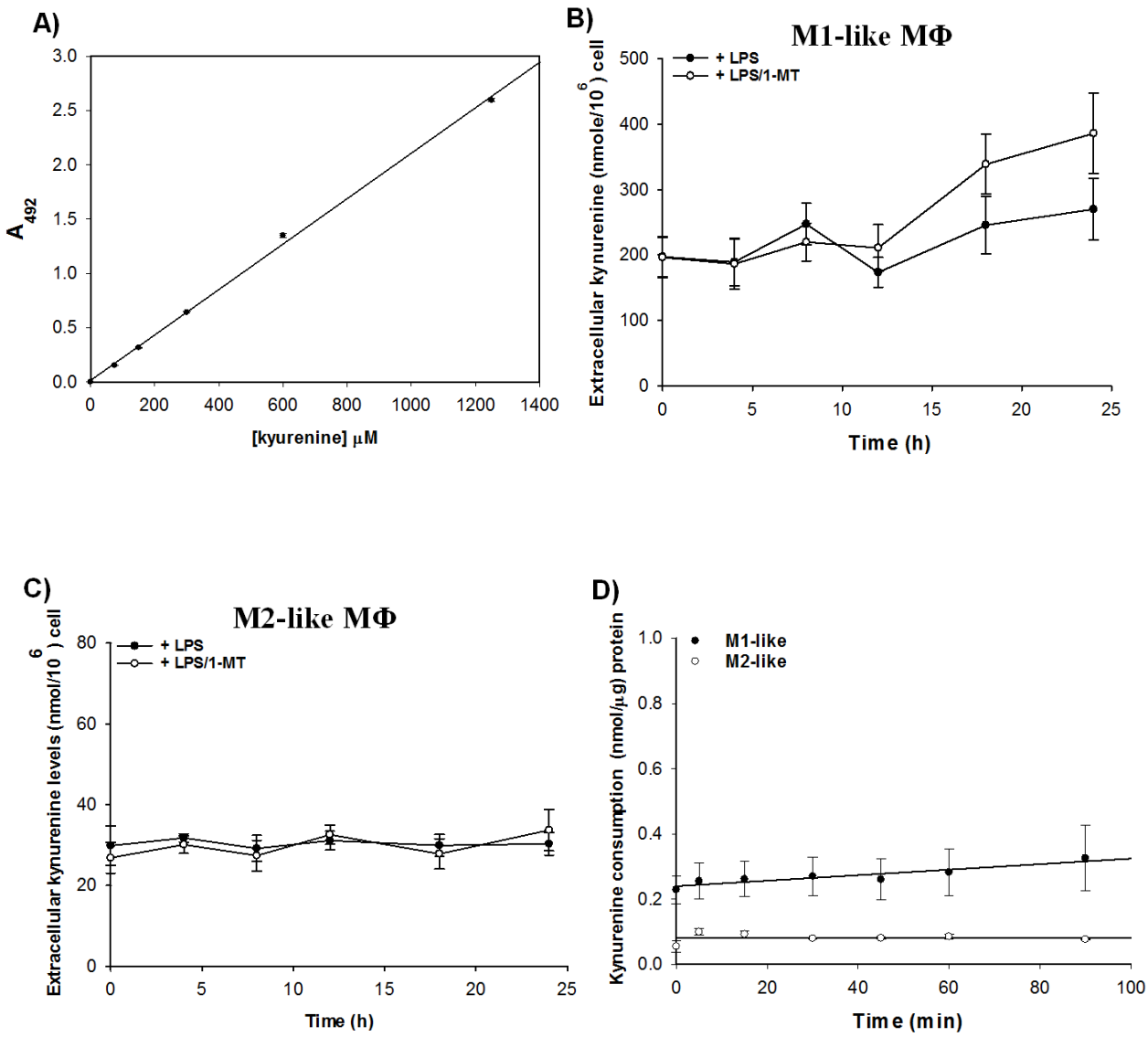

Figure 4.6 The 1-MT treatment does not affect kynurenine formation during LPS stimulation in differentiated macrophages. (A) The linearity of kynurenine standards using the Ehrlich assay. The kynurenine was dissolved in 0.5 M HCl and serial dilutions were prepared. The effect of 1-MT treatment on extracellular kynurenine levels in (B) M1-like and (C) M2-like cells during LPS stimulation is also shown. After differentiation, macrophages were incubated with kynurenine and the rate of kynurenine consumption was measured. (D) The kynurenine consumption in resting macrophages. Data shown are means ± SE of four separate experiments (n = 3-4). Results were analysed by two way ANOVA followed by the Bonferroni test. Significantly different results are indicated as follows:*P < 0.05, **P < 0.01, *** P < 0.001).

4.3 Discussion

It is becoming clear that there is a close relationship between NAD^+ metabolism and inflammatory responses in innate immune cells, in particular, in macrophages (van Gool *et al*., 2009). One of the best studied links is that between NAD(H) and TNF-α with NAD(H) levels known to regulate TNF-α synthesis (van Gool *et al*., 2009) and conversely TNF-α levels are known to regulate expression of NAD(H) homeostasis enzymes (Iqbal and Zaidi, 2006). This study was designed to understand how pharmacological manipulation of NAD^+ homeostasis can control TNF-α release by macrophages. Our data show that LPS stimulation of M1-like macrophages caused significant changes (Chapter 3) in NAD^+ levels while in M2-like cells this was not the case. Also, we demonstrated that TNF-α level also increased in pro-inflammatory M1-like MΦs suggesting that they might be linked. Therefore, to understand more about this link, we investigated the unusual NAD^+ changes and the source of the LPS-induced changes as well as the link to TNF-α release in both subsets. LPS stimulation of differentiated cells was performed in the presence of DPI (commonly used to inhibit NADPH oxidase), FK866 (a NAMPT inhibitor) or 1D-MT (an IDO inhibitor) and sirtinol (a sirtuin inhibitor). We demonstrate that both DPI and FK866 are also able to inhibit the observed initial and the sustained rise in M1-like MΦs (Figures 3 B and 4 A). This decrease might be caused, in part, via direct and indirect inhibition of the NADPH oxidase by DPI and FK866 treatment, respectively. Indeed, it has been recently shown that DPI and FK866 treatment was able to inhibit oxidative burst through inhibition of NAD(P)H activity (Malam *et al*., 2011; Lu *et al*., 2012).

The current results might suggest that NAD^+ levels are lowered as consequence of inhibition of NADPH oxidase mediated NADH oxidation via DPI suggesting NADH oxidation as an important source of NAD^+ production as well as NAMPT-mediated NAD^+ recycling. In addition, our results show that the decrease in NAD^+ production following FK866 and DPI was correlated with a reduction in TNF-α levels in M1-like but not in M2-like MΦs (Figure 3, 4). Since TNF-α is required for LPS-induced IDO activity in the THP-1 model (Fujigaki *et al*., 2001) and considering the role of IDO in NAD^+ production, one might speculate that 1D-MT mediated inhibition of NAD^+-dependent IDO activity could affect TNF-α release from THP-1-derived macrophages. Interestingly, we observed no effect of IDO inhibition on TNF-α release and this could be explained, in part, by the fact that IDO contributes only a little to the intracellular NAD^+ pool as 1 NAD^+ molecule out of 60 molecules comes from this pathway. These assumptions are supported by Grant and Kapoor (2003), who showed that IDO activity functions to maintain NAD^+ levels during inflammation. M2-like MΦs, however, display only a small TNF-α increase after 4 h of LPS stimulation and clearly this was not linked to NAD^+ in M2-like MΦs (Figure 4.2 B). It seems that NAD^+ levels are correlated with TNF-α secretion in M1-like cells and not in M2-like cells, confirming the existing link between NAD^+ and macrophage inflammatory responses, in particular the TNF-α response. We initially investigated the link between NAD^+ and TNF-α in our model via using sirtinol, a sirtuin inhibitor. The role of sirtuins and NAD^+ dependent mediated cytokine production is well established (Landry *et al*., 2000a; Jackson and Denu, 2002; van Gool *et al*., 2009). Our data confirmed previous findings showing that synthesis of TNF-α is sirtuin dependent (van Gool *et al*., 2009). Sirtinol treatment was able to inhibit the secretion of TNF-α when cells pre-incubated overnight prior LPS stimulation (Figure 4.2 C). These findings are in accordance with a recent study showing that sirtuin inhibition blocks LPS-induced TNF-α

release in an NF-κB-dependent manner in stimulated macrophages (Fernandes *et al*., 2012). However, pre-incubation with sirtinol for 1 h prior to stimulation led to a block in the time-dependent decrease in TNF-α release during LPS stimulation with TNF-α levels not decreasing in 24 h as in the control (Figure 4.2 D). It is perhaps not surprising that TNF-α release is modulated by a sirtuin inhibitor as TNF-α synthesis was shown to be regulated by NAD^+ in SIRT6-dependent manner (van Gool *et al*., 2009).

In fact, the second phase of the NAD^+ increase, that we observed under LPS stimulation, is prolonged and covers the period of the TNF-α decay phase suggesting they may be correlated and thus that NAD^+ levels mediate the decay phase of TNF-α. This assumption is supported by the results showing that NAD^+ levels also not decreasing over 24 h after 1 h sirtinol treatment prior to stimulation (Figure 4.2 E). The contradictory effect of sirtinol on TNF-α in this study is not quite clear. Although, it is difficult to explain the discrepancy in these results- we could speculate that there is a counter-regulatory mechanism between sirtuin family members, including SIRT1 and SIRT6. It seems that TNF-α production is not only regulated by SIRT6 because SIRT1 has also been shown to regulate TNF-α production in response to LPS stimulation in monocytes (Niederer *et al*., 2011). In this study, the authors showed SIRT1 overexpression led to a modest but significant increase in LPS-induced TNF-α secretion while inhibition or downregulation by SIRT1 siRNA caused TNF-α release to be halted in the same cells (Niederer *et al*., 2011). Also, It has recently been shown that SIRT1 contributes to TNF-α secretion by up-regulation the expression of TLR 2, 4 (Lee *et al*., 2012) that are required for cytokine release (Andersson and Tracey, 2011). On the other hand, a converse relationship between SIRT1 and the capacity for TNF-α production, via the ability to dampen inflammatory process through inhibition of NF-κB in cultured macrophages, has been observed previously (Shen *et al*., 2009). Indeed, knockdown of SIRT1 or inhibition led

to largely activate the JNK and IKK inflammatory pathways in a model of the mouse macrophage RAW264.7 cell line and in intraperitoneal macrophages resulted in augmented TNF-α secretion (Yoshizaki *et al*., 2010). In the same respect, SIRT6 has been shown to positively regulate TNF-α production at the transcription/translation level (van Gool *et al*., 2009). Despite these findings, it has been suggested that SIRT6 exerts opposing effect on expression of pro-inflammatory mediators via negatively regulating the transcriptional activity of NF-κB (Kawahara *et al*., 2009).

It seems that SIRT1 and SIRT6 roles are not straightforward with regards to the TNFα response as they exert contradictory effects on TNFα, indicating that sirtuin's role in this signalling pathway is more complex than previously thought. It is possible, therefore, that these findings may partially explain the observed increase in TNF-α release, following sirtinol treatment in the current study. This increase could be explained in part by selective inhibition for SIRT1 by sirtinol which has higher affinity for SIRT1 than other family member (Heltweg and Jung, 2002; Heltweg *et al*., 2006; Braidy *et al*., 2011) and thus sustains NAD^+ availibity for SIRT6-mediated TNF-α secretion. This assumption is strongly supported by recent observations showing that SIRT6 enhances TNF-α secretion, in a fatty acyl modification mechanism, via the removal of the fatty acyl groups on K19 and K20 of TNF-α (Jiang *et al*., 2013). It is believed that TNF-α release is mediated via acyl modification since TNF-α is one of the fatty acylated proteins (Stevenson *et al*., 1993). Furthermore, TNF-α release is alternatively regulated by a shedding proteolytic process, rather than SIRT6-mediated fatty acyl modification, that is mediated by a disintegrin and metalloproteinases including TACE in a model of human alveolar macrophages (Rosendahl *et al*., 1997; Moss *et al*., 1997; Armstrong *et al*., 2006) in a PKC-dependent manner in macrophages (Nakada-Tsukui *et al*., 1999). TNF-α is initially synthesised as a precursor protein of 26 kDa which

can be processed by a metalloproteinases that specifically cleave the polypeptide at a site between the amino acid Val^{76} and Ala^{77}, to a secrete a soluble TNF-α into the cell culture medium (Rosendahl *et al*., 1997). Indeed, ADAM 10 has been shown to cleave TNF-α in THP-1 whereas ADAM17 is required for the processing of TNF-α and its receptor in macrophages (Rosendahl *et al*., 1997; Bell *et al*., 2007). Furthermore, several studies revealed that sheddases other than ADAM are required for TNF-α release including matrix metalloproteinase enzymes (MMPs; Haro *et al*., 2000) from peritoneal macrophages due their ability to cleave extracellular domain of many surface-proteins. Therefore, pharmacological inhibition by an hydroxomic acid-based MMP inhibitor led to the blockage of TNF-α proteolytic shedding (McGeehan *et al*., 1994; Solomon *et al*., 1997). Given that MMP expression is activated in M1-like MΦs via PMA, it is likely that sirtinol mediated SIRT1 inhibition led to up-regulated MMP expression resulting in TNF-α release induction (Ismair *et al*., 1998; Wang *et al*., 2003). In fact, SIRT1 has been shown to negatively regulate MMP9 expression and MMP9 promoter activation and that SIRT1 activation by small pharmacological activators blocks the MMP9 expression in U937 cells line suggesting a critical regulatory role for SIRT1 on MMP9 expression (Nakamaru *et al*., 2009). These assumptions, therefore, strongly agree with recent evidence by Shen *et al*. (2009) who found that sirtinol addition or SIRT1 knockdown by siRNA led to augmented TNF-α secretion suggesting the involvement of SIRT1 in impairment of TNF-α release.

In addition, these observations are further supported by findings showing that SIRT1 deletion or inhibition was associated with a compensatory elevation in SIRT6 expression in macrophages in response to environmental stress, suggesting important immune regulatory roles for sirtuins in myeloid cells (Schug *et al*., 2010). Future work is needed to investigate the role of SIRT6 in regulating MMP expression in macrophages. Other possible mechanism

might be related to SIRT1 role mediated the reprogramming switch from glycolysis to oxidative metabolism in THP-1 cells line (Liu *et al*. 2012). It may be the case that selective inhibition of SIRT1 by sirtinol might block a SIRT1 mediated shift towards oxidative metabolism leading to increased incidence of glycolysis which is required for TNF-α release (Dietl *et al*., 2010). This assumption is supported by TNF-α increase following a 1 h incubation of cells with sirtinol (Figure 4.2 D). Collectively, these results further confirm the link between NAD^+, the immune response and metabolism highlighting the importance of an immune regulatory role for NAD^+ and thus SIRT1, 6 in macrophages. Therefore, further study is required to investigate the NAD^+-sirtuin axis in M1-like MΦs and whether this link could be useful approach for developing a therapeutic strategy for inflammation associated tumours. It is known that NAD(P)H oxidase activation occurred both in *vitro* and *in vivo* via LPS stimulation in TLR4-dependent manner during macrophage activation resulting in a marked increase in oxidative burst activity and the generation of reactive oxygen species (ROS; Kaul and Forman, 1996; Remer *et al*., 2003). Our data show that the increase in NAD^+ levels was also inhibited by blocking NADH oxidation via the flavoenzyme, NAD(P)H oxidase (Figure 4.3 A). This may explain, at least in part, the rapid peak that was observed in NAD^+ levels as this was partially inhibited by the NAD(P)H oxidase inhibitor DPI. Therefore, our findings strongly agree with others showing that DPI treatment caused NAD(P)H oxidase (NOX) inhibition and led to lower NAD^+ levels suggesting a critical role for NADPH oxidase in supporting glycolysis activity in cancer cells via providing additional NAD^+ (Lu *et al*., 2012). Interestingly, the initial peak was also inhibited after FK866 treatment (Figure 4.4 A). Indeed, it has been shown recently that FK866 treatment was able to decrease NADP(H) levels, which is required for NADPH oxidase, as well as the production of ROS, in a time and dose-dependent manner (Roberts *et al*., 2013). In line with

these findings, a recent study has also shown that a reduction in ROS production have been observed in FK866-treated monocytes (Schilling *et al*., 2012), highlighting the involvement of FK866 in the inhibition of NADPH oxidase activity.

Additionally, we showed here that FK866 treatment limited the second NAD^+ rise (after 4 h) similar to others in a model of monocytic cells (Busso *et al*., 2008; Schilling *et al*., 2012). These data fit nicely with previous results showing that M1-like induced NAMPT expression after 4 h of LPS stimulation (chapter 3). Similarly, TNF-α levels were also inhibited by both FK866 and DPI in M1-like MΦs. The effect of DPI on TNF-α was striking (Figure 4.3 B) as DPI treatment mediated NAD(P)H oxidase inhibition led to almost completely knock out TNF-α release. Our results seem to be line with others who reported that DPI blocked NADPH oxidase-derived IL-6 and TNF-α release (Turchan-Cholewo *et al*., 2009). It is likely that both NAD^+ and perhaps the free radicals generated by NAD(P)H oxidase might partially contribute to TNF-α secretion. These assumptions are supported by others showing that DPI treatment inhibited the oxidation of NAD(P)H to $NAD(P)^+$ via NAD(P)H oxidase (Riebel *et al*., 2002) and it also has been shown that DPI was able to inhibit the NADPH oxidase-mediated (oxidative burst) ROS production (Babior, 1999). The induction of ROS has previously been shown in neutrophils following PMA stimulation (Kobayashi *et al*., 1998; Babior, 1999). As a consequence, PMA-induced monocyte/macrophage activation caused ROS to activate the transcription factor (NF-κB; Kaul and Forman, 1996). Therefore, it is perhaps not surprising that NADPH oxidase activation has been involved in NF-κB-mediated TNF-α production (Kaul and Forman, 1996) which, in turn, catalyses ROS production via the activation of NADPH oxidases (Kim *et al*., 2007). On the other hand, the effect of FK866 on TNF-α release was not striking although it was able to reduce TNF-α release (Figure 4.4 B). These data are supported by several studies showing that FK886 inhibiting intracellular

NAD^+ levels led to block LPS-induced TNF-α release in activated monocyte while we here show it in activated macrophages (Rongvaux *et al*., 2002; Busso *et al*., 2008; Schilling *et al*., 2012). Although the mechanism that links FK866 to NAD^+ inhibition and the blockage in TNF-α release is not fully explained, there is some evidence implicating NAD^+, via NAD^+-dependent enzymes, in a number of immune regulatory pathways including transcriptional regulation processes. In particular, the immune regulatory role for sirtuin deacetylase in cytokine production has been described (Ziegler, 2000; Guarente, 2006). By using NAD^+, SIRT6 can control the cytokine production via acting as co-activator of NF-κB during inflammation (Oliver *et al*., 1999; Bai and Virág, 2012). Therefore, FK866 treatment might indirectly affect SIRT activity by decreasing NAD^+ availability resulting in alteration in the expression of pro-inflammatory cytokines. In agreement with this, Bruzzone *et al.* (2009) showed that the exposure of immune cells to FK866 impaired SIRT6 activity-mediated TNF-α production. It has been consistently shown that SIRT6 blocking or knockdown affects post-transcriptional expression of TNF-α (van Gool *et al*., 2009). An alternative mechanism might be through the blocking of NAM conversion into NAD^+, via FK866-mediated NAMPT inhibition, resulting in NAM build-up which is known for its anti-inflammatory effect on pro-inflammatory cytokine production (Ungerstedt *et al*, 2003). In line with this, Heine *et al.* (1995) reported that blocking of PARP activity by NAM led to inhibited LPS-initiated phosphorylation of p36/38 and that this was accompanied by an inhibition of TNF-α and IL-6 mRNA as well as protein production. Furthermore, NAM displays anti-inflammatory properties as it has been shown to protect mice from endotoxin toxicity by preventing TNF-α secretion during LPS stimulation (LeClaire *et al*., 1996; Fukuzawa *et al*., 1997). Although M2-like cells showed a significant increase in NAMPT expression (Chapter 3) the FK866 treatment exert slight but not significant effect on both NAD^+ and TNF-α secretion (Figure

4.4 C, D). The reason for this discrepancy is not clear and thus further study is required to understand the mechanism which underlies these responses. However, we can postulate that TLRs and MMP are differentially regulated in both subsets. While PMA was shown to upregulate both MMP and TLR4 expression the vitamin D_3 was shown to negatively regulate MMP and TL4, 2 expressions. Therefore, in M1-like cells, LPS induced a robust secretion of TNF-α which was almost completely blocked by DPI and partially inhibited by FK866, suggesting that NAD^+ is also derived from a number of different syntheses and recycling pathways.

Conversely, M2-like cells responded to LPS by releasing a relatively small amount of TNF-α. Crucially, this was not associated with any changes in NAD^+ levels, suggesting that the signalling between TLR4 and TNF-α release is via a different pathway compared to M1-like cells. TLR4 is known to signal via different intracellular pathways, one of which is NAD(P)H oxidase dependent which causes the oxidative burst and ROS production (Park *et al*.,2004) and converts NADH to NAD^+ (Riebel *et al*., 2002). Our data suggest that the link between NAD^+ and TNF-α secretion is perhaps complex and may require both NAD^+ and the activity of NAD(P)H oxidase and could also suggest that NAD^+ is required for glycolysis to mount appropriate immune response. It has been recently reported that TNF-α release requires active glycolysis and thus, the LPS-induced increase in NAD^+ levels suggest that this may occur in order to provide NAD^+ for glycolysis perhaps to partially support TNF-α release (Dietl *et al*., 2010). Therefore, further work is required to investigate the impact of NAD^+ modulation on glycolysis mediated TNF-α response. The effect of 1D-MT on NAD^+ was not correlated with TNFα release as the 1D-MT was able to significantly decrease NAD^+ whereas it showed no effect on TNF-α response. While 1L-MT (1-levo-methyl tryptophan) was shown to inhibit IDO1 (Hou *et al*., 2007) in cancer cells, 1D-MT was shown to selectively inhibit the IDO2

activity (Metz *et al*., 2007). Whilst both isomers block tryptophan activity, the L-isomer exhibits a modest effect on tryptophan metabolism compared to the D-isomer which has a stronger, more specific effect on IDO activity (Metz *et al*., 2007; Hou *et al*., 2007). For these reasons, it was chosen in this study. We showed here that 1D-MT was able to decrease NAD^+ levels in M1-like under LPS challenge. However, it was unable to inhibit the TNF-α rise, suggesting that IDO activation is possibly to maintain NAD^+ supply. Macrophage exposure to LPS enhances the conversion of tryptophan into NAD^+ in macrophages via IDO activity (Wirthgen *et al*, 2014; Heyes *et al*., 1997) which is correlated with ROS production that occurs in response to PMA and LPS (Babior, 1999; Kaul and Forman, 1996). This might explain, at least in part, the increase in NAD^+ production which was inhibited by 1D-MT treatment (Figure 4.5 A). In agreement with this, a recent report has recently shown that the inhibition of IDO activity was achieved following 1D-MT treatment resulted in decrease NAD^+ levels (Braidy *et al*., 2011). In this study, the authors showed that NAD^+ production was attenuated in primary astrocyte cells following 1D-MT application resulted in inhibited SIRT1 activation. Given that SIRT1 is known to mediate anti-inflammatory state and IDO is known to regulate the flux between pro- and anti-inflammatory cytokine production pathways (Pilotte *et al*., 2012), the current data might support our hypothesis suggesting that the inhibition of SIRT1 block anti-inflammatory response as TNF-α release was not inhibited after 24 h. Alternatively, IDO activity is known to critically contribute to immune-regulatory mechanism in tumour conditions. Inhibition of IDO activity might therefore block immune suppression and conversely enhance effective anti-tumour immunity; this might explain, at least in part, the results showing that TNF-α was not affected by 1D-MT treatment (Munn and Mellor, 2007). 1D-MT was shown to differentially regulate IDO isoforms and that IDO1 is upregulated with 1D-MT while IDO2 was downregulated (Opitz *et al*., 2011a) and this

might account to the decrease NAD^+ production and TNF-α being not affected. Indeed, the induction of IDO1 expression by 1D-MT was interpreted to support anti-tumour activity (pro-inflammation) in immune cells (Opitz *et al*., 2011a; Metz *et al*., 2007) and that 1D-MT blocks the IDO-mediated immunosuppression mechanism which might partially explain why TNF-α release was not affected. In addition, it has previously been reported that IDO expression induction is associated with L-isomer but not with D-isomer (Lob *et al*., 2008). These findings might support the superior-anti tumour activity of D-isomer (Opitz *et al*., 2011a; Hou *et al*., 2007). Interestingly, while 1-MT treatment inhibited NAD^+ levels, it did not affect kynurenine production and it conversely caused a slight increase in the measured levels in M1-like MΦs (Figure 4.6 B) suggesting that kynurenine production might occur through different pathway. The discrepancy between the effect of 1D-MT on NAD^+ and kynurenine levels might be related to the induction of a compensatory mechanism that increases IDO expression and activity following 1D-MT treatment (Boasso *et al*., 2009). Similarly, Boasso *et al*. (2009) observed an increase rather than a decrease in kynurenine levels after 1D-MT and related the lack of 1-MT effect on kynurenine to the increase in IDO1 mRNA expression in model was very similar to human model. Also, an increase in kynurenine production and IDO1 expression has been shown by Opitz *et al*. (2011a) who related this discrepancy to the superior anti-tumour activity of 1D-MT. Recent studies reported that human IDO2 (hIDO2) plays pivotal role in regulating hIDO1 activation suggesting a useful therapeutic strategy for immune regulatory disorders (Lee *et al*., 2014). Therefore, further research might be required to understand the immune-regulatory role of IDO isoforms in pro-inflammatory M1-like macrophages.

In summary, we have demonstrated that pharmacological modulation of NAD^+ controlled TNF-α release. These data serve to reinforce the link between NAD^+, TNF-α and inflammatory responses. NAD^+ has previously been shown to have an intimate relationship with TNF-α at the transcriptional level and we have further confirmed this link at the release level by showing that sirtinol blocks the time-dependent decrease in TNF-α and NAD^+ after LPS stimulation. It seems that lowering NAD^+ might have an anti-inflammatory effect on inflammation and thus might be a useful therapeutic tool for inflammation-associated cancers. Further clarification of the exact mechanisms involved will be required before pharmacological approaches can be tested for immunomodulatory effects. Given that TNF-α plays critical role in differentiation, proliferation and apoptosis (Fiers *et al*., 1999; Karin and Lin, 2002), it would be interesting to look at the NAD^+-TNF-α axis in modulating these cellular events in immune cells. In addition, recent focus has shifted to the link between metabolism and innate immune responses, with NAD^+ a key player both as a indication of the metabolic status of a cell and as a signalling molecule. While NAD^+ is central to the links between metabolism and immunology there has been precious little work on NAD^+ homeostasis in this context. We believe this may be an interesting avenue to pursue regarding different aspects of immune responses. Therefore, we investigated whether NAD^+ manipulation can modulate metabolic activity in our model (Chapter 5).

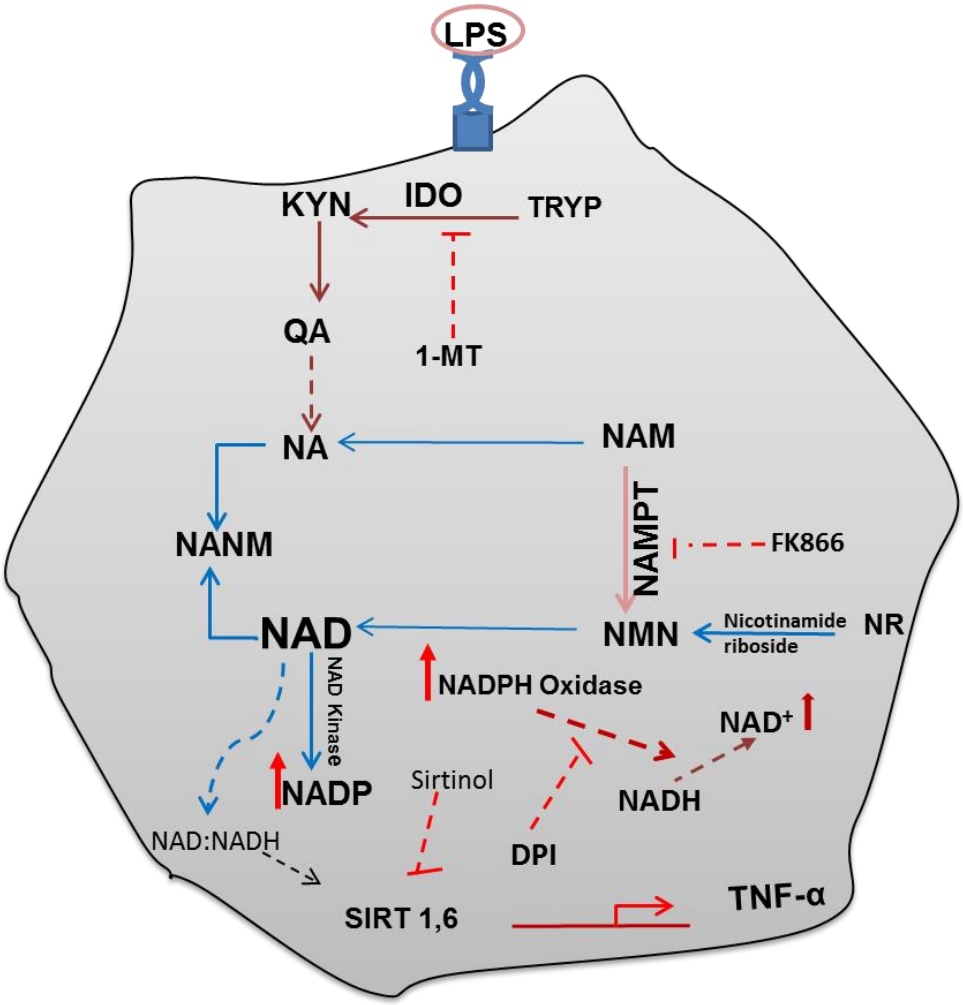

Figure 4.7 The stimulation of macrophages with LPS promotes NAD^+ level-mediated TNF-α release which in turns activates macrophages for its secretion. FK866 inhibits NAMPT activation resulted in inhibition of NAD^+ levels and TNF-α release. NAD kinase uses NAD^+ to produce NADP. NADP serves as substrate for NADPH oxidase activity that activates TNF-α release in an NF-κB dependent manner. The inhibition of NADPH oxidase by DPI (an NADPH oxidase inhibitor) blocks TNF-α release. The secretion of TNF-α is regulated by NAD-dependent sirtuin activity. Sirtuin activation is inhibited by sirtinol causing a reduction in TNF-α release.

CHAPTER 5

MODULATION OF NAD^+ LEVELS MODULATES GLYCOLYTIC FLUX IN PRO-INFLAMMATORY M1-LIKE MACROPHAGES

5.1 Introduction

Recent work has revealed the close link between metabolic state and the phenotype of immune cells. Indeed, classically activated, pro-inflammatory (M1) macrophages rely mainly on glycolysis whereas alternatively activated, anti-inflammatory (M2) macrophages utilise oxidative phosphorylation (Galvan-Pena and O'Neill, 2014). Despite NAD^+ being required for glycolysis activity, little is known about the role of NAD^+ homeostasis in driving the glycolytic phenotype in macrophages. Glycolysis is an inefficient way of generating ATP followed by lactate production and it has been found that tumour cells rely mainly on glycolysis to generate energy in a phenomenon termed as the Warburg effect (Warburg, 1956; Van-der Heiden *et al*., 2009). For the glycolytic flux to be maintained in any type of cell, it is essential that NAD^+ is regenerated from NADH to eliminate the imbalance in the redox ratio (NAD: NADH) caused by glycolysis activity (Locasale and Cantley, 2011). This can occur via active oxidation phosphorylation (OXPHOS) whereby the malate aspartate shuttle gives rise to cytosolic NAD^+ providing a supply for mitochondrial NADH to support OXPHOS under normal conditions (Locasale and Cantley, 2011).

During non-normal conditions, however, where the glucose uptake increases due to HIF-1α activity, this malate-aspartate shuttle gets saturated and thus is no longer able to replenish cytosolic NAD^+. Therefore, NAD^+ can be alternatively regenerated via LDH which catalyses the conversion of pyruvate into lactate (Locasale and Cantley, 2011). LDH overexpression has been shown to maintain high levels of glycolysis via increased NAD^+ regeneration supporting the Warburg effect in cells. It is now recognised that glycolysis is induced in classically activated (M1) macrophages upon activation which helps to increase a glucose uptake as well as the conversion of pyruvate to lactate. This scenario is thought to be

committed in classical M1 cells due to the activity of hypoxia inducible factor 1α (HIF-1α), as cells are frequently exposed to hypoxic microenvironments, which have been shown to play a pivotal role in directing the conversion of pyruvate either to acetyl-CoA or to lactate (Kim *et al*., 2006; Papandreou *et al*., 2006). In fact, HIF-1α controls this mechanism via upregulation of the expression of LDH thus facilitating the conversion of pyruvate into lactate (Semenza *et al*., 1996) and conversely downregulation of pyruvate dehydrogenase (Papandreoue *et al*., 2006) reducing the conversion of pyruvate to acetyl-CoA. As a consequence, the tricarboxylic acid (TCA) cycle activity is limited in activated macrophages. Also, HIF-1α is known to increase glucose uptake to support glycolytic flux in activated macrophages through the up-regulation of glucose transporter 1 (GLUT-1; Chen *et al*., 2005). Indeed, GLUT-1 has been shown to mediate glucose metabolism and ROS production supporting the effector phenotype in macrophages (Freemerman *et al*., 2014).

In contrast, alternatively activated (M2) macrophages are known to be regulated by OXPHOS (Lacy-Hulbert and Moore, 2006). Interestingly, M2 macrophages prefer to use OXPHOS which can be induced for longer phases during LPS stimulation (Vats *et al*., 2006; Rodriguez-Prados, 2010). Stimulation of M2s with LPS decreases the expression of adenosine monophosphate activated protein kinase (AMPK) which supports the metabolic switch from glycolysis to OXPHOS (Sag *et al*., 2008; Krawczyk *et al*., 2010). AMPK promotes the switch towards OXPHOS via upregulating enzymes involved in mitochondrial activity (Winder *et al*., 2000) including succinate dehydrogenase (SDH) as well as proteins involved in mitochondrial biogenesis (Vats *et al*., 2006) such as peroxisome proliferator-activated receptor (PPAR-γ). While M2s utilize OXPHOS because this helps with their longer-term immune functions (Galvan-Pena and O'Neill, 2014), M1s favour glycolysis because it is 100-times faster but less efficient than OXPHOS for faster responses and macromolecule

synthesis (Figure 5.1; Pfeiffer *et al*., 2001). Notably, LPS stimulation also increases the activity of the pentose phosphate pathway (PPP) where glucose is directed at an early branch point in the glycolysis pathway to feed into the PPP. The PPP is essential for pentose sugar production, which is required for nucleotide biosynthesis (Borregaard and Herlin, 1982) as well as for the production of NADPH. NADPH is a critical coenzyme for NADPH oxidase-mediated ROS production and respiratory burst (Aktan, 2004).

Recent reports have shown that NADPH oxidase drives glycolysis activity in cancer cells by providing additional NAD^+ (Lu *et al.,* 2012). Suppression of NAD(P)H oxidase by chemical inhibitors or knock-down by genetic modification caused a decrease in NADH oxidation lowering NAD^+ levels leading to a decrease in cellular glycolysis (Lu *et al*., 2012). Moreover, pharmacological modulation of NAD^+ recycling (NAMPT pathway) by FK866 led to a decrease in intracellular NAD(H) resulting in inhibition of glycolysis (Venter *et al*., 2012). On the other hand, inhibition of NAD^+ *de novo* synthesis by 1D-MT showed the opposite effect on glycolytic flux and oxidative metabolism activity in human lymphocytes (Eleftheriadis *et al*., 2012).

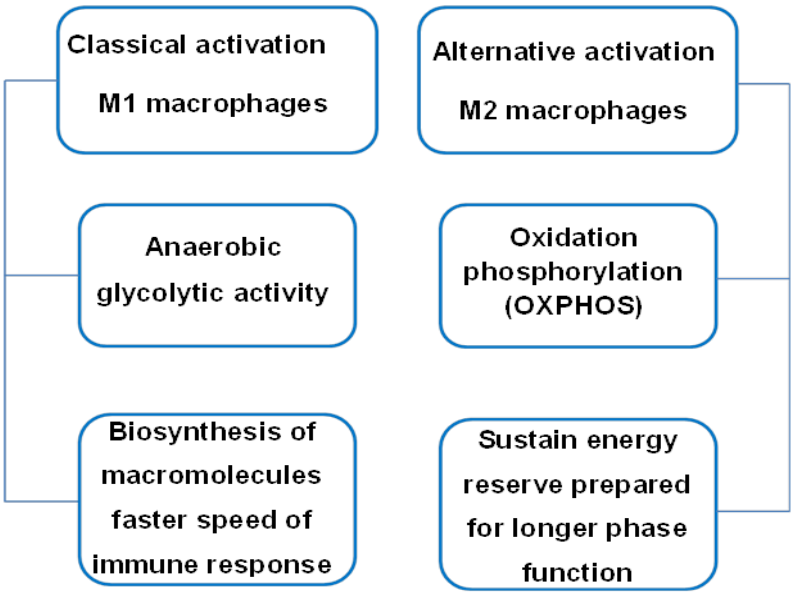

Figure 5.1 Schematic diagrams depicting the bioenergetics of the metabolism in classical (M1) macrophages versus alternative activation (M2) macrophages. Classical M1s utilize anaerobic glycolysis for rapid response and to generate new nucleotides as well as pentose phosphate pathway (PPP)-mediated NADPH production, while alternative M2s use oxidative phosphorylation to build up reserves of ATP for longer-term function.

We have shown in Chapter 3 that NAD^+ levels increased in M1-like cells during LPS stimulation, so here we investigated the bioenergetics flux in stimulated M1-like cells using an extracellular flux analyser that depends on pH and oxygen sensors to measure ECAR (extracellular acidification rate) and OCR (oxygen consumption rate). We have shown here, that M1-like MΦs increase glycolysis activity, which might support the increase in NAD^+ we showed earlier, whereas oxidative metabolism is decreased in response to LPS stimulation confirming previous findings showing that classical M1s mainly rely on glycolysis for energy generation. Our data show that both DPI and FK866, but not 1-MT, were capable of decreasing glycolysis activity suggesting that NAD^+ and thus NAD^+ homeostasis might partially regulate glycolysis activity in macrophages. Given that glycolysis is required to support the effector phenotype, pharmacological modulation of NAD^+ levels might affect at least in part the macrophages metabolic phenotype and inflammatory response.

5.2. Results

5.2.1 LPS-induced NAD^+ affect the NAD^+/NADH ratio in M1 but not in M2 MΦs

It is well established that classically activated macrophages rely mainly on glycolysis (Calder, 1995) for pro-inflammatory responses (Delmastro-Greenwood and Piganelli, 2013). In order to sustain flux through glycolysis, it is essential that macrophages maintain sufficient concentrations of cytoplasmic NAD^+ and hence the NAD^+/NADH ratio, so that glycolysis can continue (Newsholme, 1986). Given the unusual changes we observed earlier (Chapter 3), we decided to try to understand more about the redox-state and the link to glycolysis in differentiated macrophages. Therefore, the concentration of NAD^+ and NADH, plus the NAD^+/NADH ratio, in response to LPS stimulation, was investigated in both macrophage subsets. Stimulation with LPS regulates NAD^+ and NADH levels differentially in a time-dependent manner in M1-like but not in M2-like MΦs (Figure 5.2). In M1-like MΦs, NAD^+ levels showed an early peak after 0.5 h of stimulation, followed by a second sustained rise after 4 h, before decaying back after 24 h. However, NADH levels showed a smaller increase than NAD^+ levels after 4 h in response to LPS stimulation before they decreased and stayed low for almost the entire period of stimulation. While NAD^+ levels increased (Figure 5.2 A) by almost 60% compared to NADH levels in M1- like MΦs, in M2-like MΦs both NAD^+ and NADH levels were unaffected by LPS stimulation (Figure 5.2 B). The observed increase in NAD^+ levels in M1-like cells might be due to the conversion of NADH to NAD^+ confirming our hypothesis that NADH oxidation might be another source of NAD^+ generation (Chapter 4) and thus sustain the intracellular redox ratio. This assumption was supported by NAD^+/NADH ratio results that showed a similar pattern to that of NAD^+ levels after LPS stimulation in M1-like cells only (Figure 5.2 C) with ratio of almost twice as high as that in M2-like cells. In these cells, the NAD^+/NADH ratio was not affected by LPS stimulation.

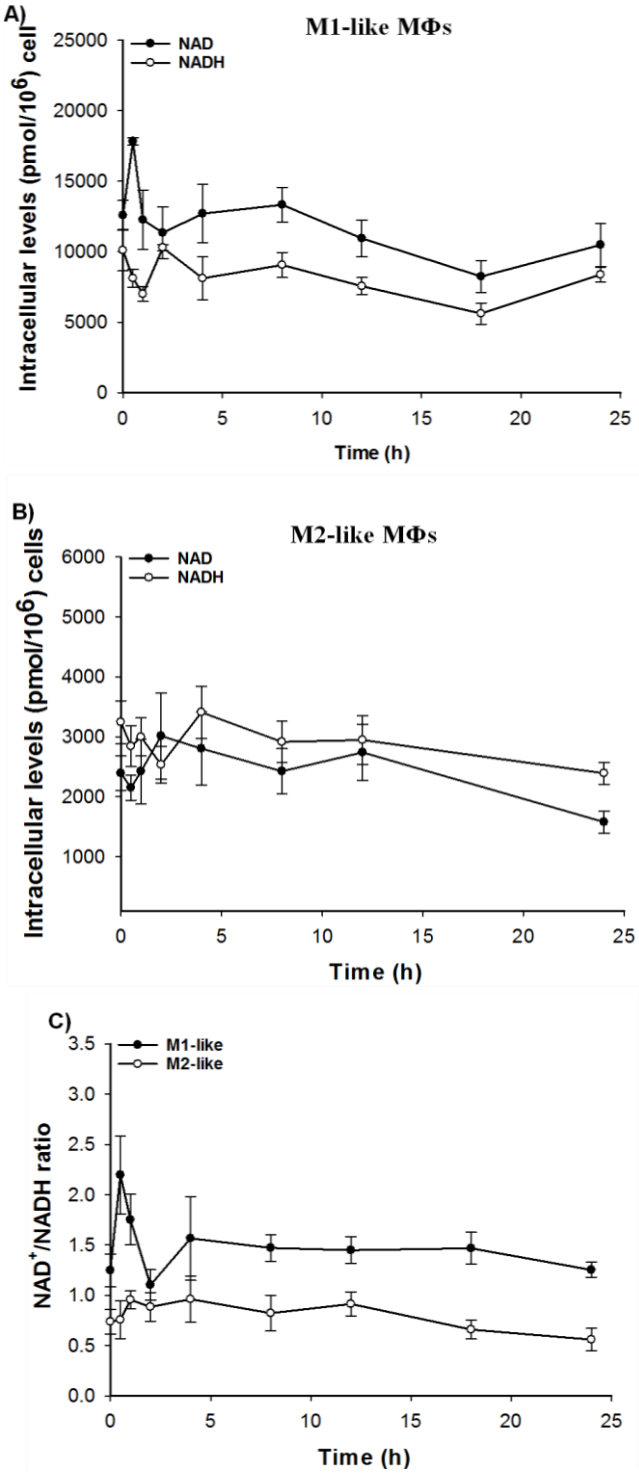

Figure 5.2 LPS stimulation regulates NAD^+, NADH and NAD^+/NADH ratio differentially in M1- and M2-like macrophages. Differentiated macrophages were stimulated with 100 ng ml^{-1} LPS-K12 for the indicated time periods and intracellular NAD^+/NADH was measured. (A) LPS increases NAD^+ levels in M1-like MΦs in a time-dependent manner. (B) LPS does not affect NAD^+ levels in M2-like MΦs. (C) LPS stimulation increases NAD^+/NADH ratio in M1-like but not in M2-like MΦs. Data are means ± SE from three independent experiments performed in triplicate.

5.2.2 LPS enhances ECAR but not OCR in M1-like macrophages

We suspected that the increase in NAD^+ and the subsequent increase in redox-balance might lead to distinct glycolytic activity. Therefore, a Seahorse X24 extracellular flux analyser was used to test the metabolic profile in differentiated macrophages (see Chapter 2, section 2.2.12). We decided to continue the current study with the main focus being on M1-like MΦs because of the limitation of using only M2-like cells for the Seahorse protocol, as M2-like cells do not adhere [see chapter 3] to the Seahorse plate.

The ECAR and OCR were measured after the sequential additions of specific inhibitors (Figure 5.3 A, B) including 2-deoxy glucose (an inhibitor of glycolysis), oligomycin (ATP synthase inhibitor), rotenone (complex I inhibitor) and antimycin A (complex III inhibitor). ECAR measures glycolysis independently of oxygen. To test whether glucose affects ECAR and OCR, glucose was added and both ECAR and OCR were measured (Figure 5.3 C, D). The increase in ECAR, after glucose addition, reflects the glycolysis rate (see Figure 5.3 A, B).

After oligomycin (an inhibitor of mitochondrial ATP synthase) is injected, the additional increase in ECAR is used to calculate maximum glycolytic flux. The treatment with oligomycin caused the cells to augment their glycolysis flux to make ATP because of the loss in mitochondrial ATP production and so restore cellular ATP homeostasis (Wu *et al*., 2007). However, the injection of 2-DG completely shuts down glycolysis and thus might provide additional information about the non-glycolytic acidification. We demonstrated that LPS significantly increased all ECAR parameters including maximum glycolytic flux ($P = 0.03$), glycolysis rate ($p = 0.012$) and glycolysis reserve ($p = 0.02$) while it significantly decreased

($p = 0.018$) non-glycolytic ECAR in M1s compared to the resting state (Figure 5.3 E). On the other hand, OCR measures oxygen devoted to generate ATP from mitochondrial respiration. The measurement after glucose addition represents glucose-stimulated respiration whereas oligomycin injection allows calculation of the oxygen used for mitochondrial ATP synthesis. The injection of the two inhibitors, rotenone and antimycin A, inhibited the electron flux through ETC as well as the TCA cycle and thus provided data about the non-mitochondrial oxygen consumption. Our data show that all OCR parameters (coupling efficiency, respiration rate and reserve) as well as non-mitochondrial OCR were not affected by LPS stimulation (Figure 5.3 F). These data might suggest that glycolysis accounts for the majority of the ECAR observed in macrophages post-stimulation with LPS.

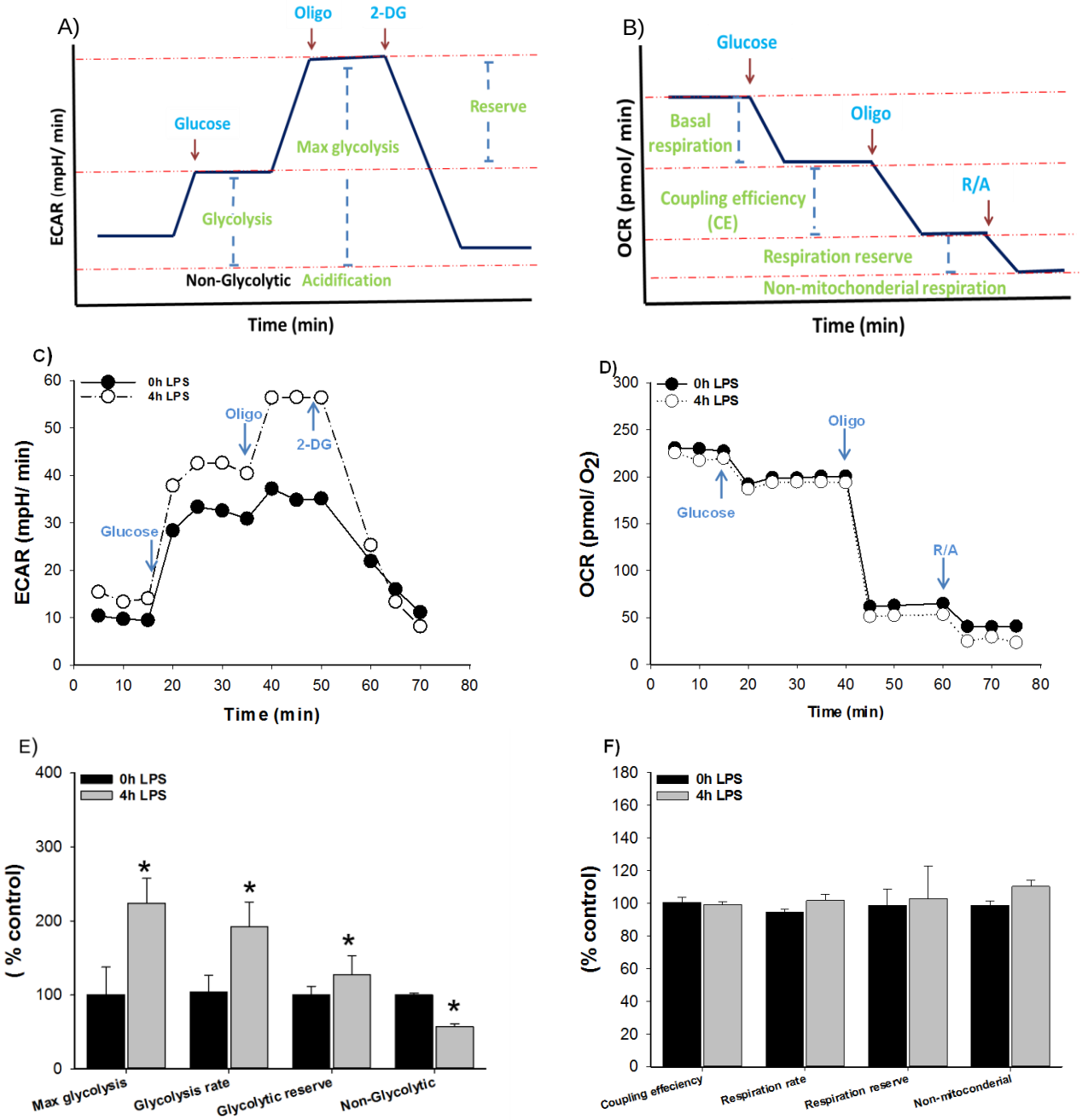

Figure 5.3 LPS stimulation of macrophages promotes ECAR induction but not OCR in M1-like MΦs. Differentiated MΦs were checked for OCR and ECAR with or without 100 ng/ml LPS (the later representing the control). OCR is expressed as the absolute rate in pmol/min, while ECAR is expressed in mpH/ min. Both ECAR and OCR were measured after sequential interferences with specific inhibitors, using Seahorse XF-24 extracellular flux technology, for glycolysis and respiration, respectively. (A) and (B) provide an overview of ECAR and OCR measurement, respectively. The baseline refers to ECAR and OCR in the saturation state prior to inhibitor injection. The glycolysis and respiration activity was obtained after glucose injection whereas 100 mM 2-DG, an inhibitor of glycolysis, was added to correct for non-glycolytic acidification. After inhibition with oligomycin (Oligo, 1 µM), an inhibitor of mitochondrial ATP production, maximum glycolysis and coupling efficiency (CE) were obtained. LPS stimulation increases ECAR (C) while it decreases OCR (D) in M1-like MΦs. LPS increases ECAR (E) but not OCR parameters (F). The data are averaged means ± SE from 3-4 wells of a single XF24 microplate. Each set of data was measured in triplicates. The data were analysed by one way ANOVA followed by the Bonferroni *post hoc* test and significant differences are indicated as *P < 0.05, **P < 0.01, ***P < 0.001.

5.2.3 LPS stimulation increases glycolytic flux and glycolysis capacity in M1-like macrophages

It has recently been reported that exposure of macrophages to LPS leads to a switch from mainly OXPHOS to predominantly glycolysis activity for energy production (Krawczyk *et al*., 2010; Galvan-Pena and O'Neill, 2014). As expected, M1-like cells showed clear glycolysis activity in response to LPS activation whereas mitochondrial respiration was not affected in M1s. When glucose was added to the M1-like MΦs the cells exhibited a clear increase in ECAR which was inhibited after 2-DG injection eliminating the glucose effect on ECAR.

The results show that glycolytic capacity, glycolysis rate and glycolytic reserve significantly increased after 4 h ($P = 0.014$) reaching maximum levels after 12 h (where maximum was $P = 0.02$, glycolysis was $P = 0.027$ and reserve was $P = 0.021$) of LPS stimulation compared to the control (zero time). Meanwhile, respiration activity (coupling efficiency, CE), respiration rate and respiration reserve showed no sensitivity to LPS stimulation (Figure 5.4 A, B, C). Indeed, LPS stimulation promoted glycolytic rate and maximum glycolytic capacity 2.5 fold more than control samples compared to mitochondrial respiration activity. Therefore, the current data strongly agree with others showing that the increase observed in ECAR is accounted for by glycolysis activity (Winer and Wu, 2014).

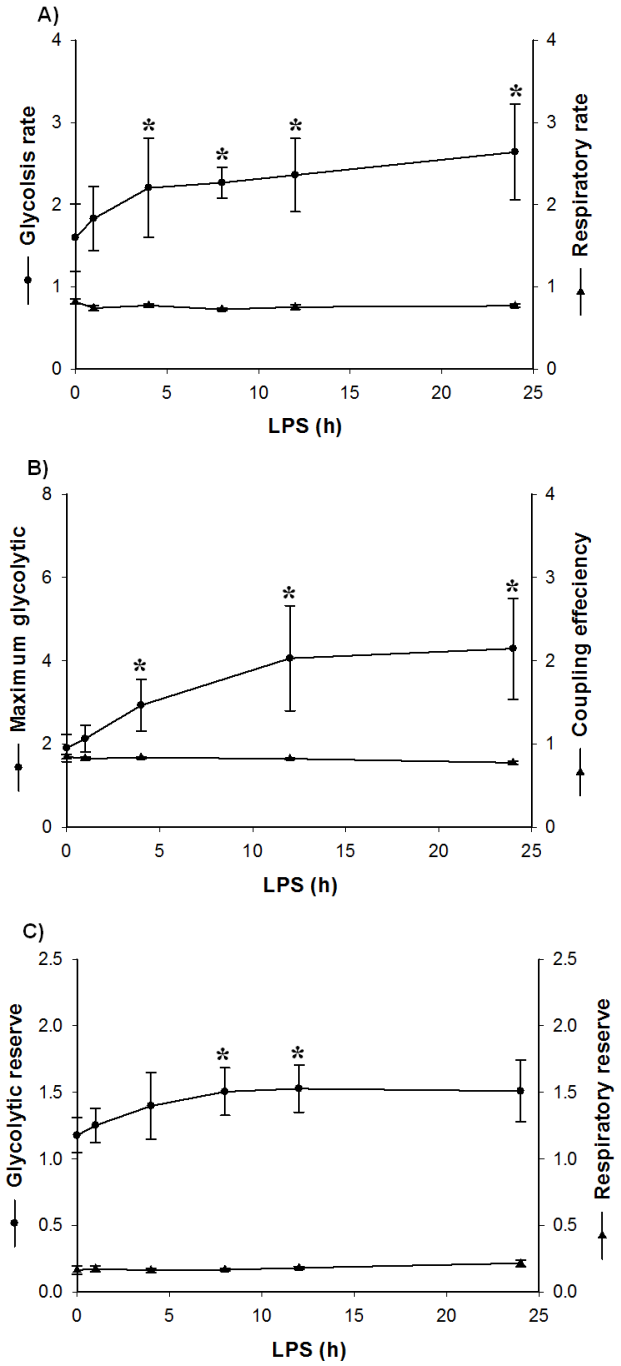

Figure 5.4 LPS stimulation of macrophages induces glycolytic metabolism. (A) Glycolysis rate and (B) maximum glycolytic activity were induced by LPS exposure whereas coupling efficiency and respiration activity was not affected. Inhibition with rotenone/antimycin A (R/A, 1 µM/ 2 µM), inhibitors of complex II and III, respectively, were used to calculate reserve capacity. (C) LPS stimulation increases glycolytic reserve and do not affect respiratory reserve in M1-like macrophages. Each data point represent mean value ± SE, n = 3-4 independent experiments performed in 3-4 wells/ treatment. The data were analysed by one way ANOVA followed by the Bonferroni *post hoc* test and significant differences are indicated as *P < 0.05, **P< 0.01, ***P < 0.001.

5.2.4 LPS-induced lactate production increases in M1-like but not in M2-like macrophages

Given that glycolysis increases during LPS stimulation, we measured lactate production to confirm that this increase is due to lactate production since the lactate reflects glycolytic metabolism. Accordingly, a significant increase in lactate production was observed in M1-like MΦs following LPS stimulation ($P = 0.03$; Figure 5.5 A).

The lactate production increased during the early stages of stimulation before declining back into almost unstimulated levels after 24 h. On the other hand, LPS failed to increase lactate levels in M2-like MΦs, suggesting that M2-like cells do not produce the majority of their ATP via glycolysis (Figure 5.5 B). We show here that lactate levels parallel that of ECAR and thus glycolysis increase in response to LPS stimulation. These findings suggest that LPS stimulation enhances lactate production due to glycolysis activity in M1-like MΦs highlighting that M1-like MΦs might switch to glycolytic metabolism for energy production.

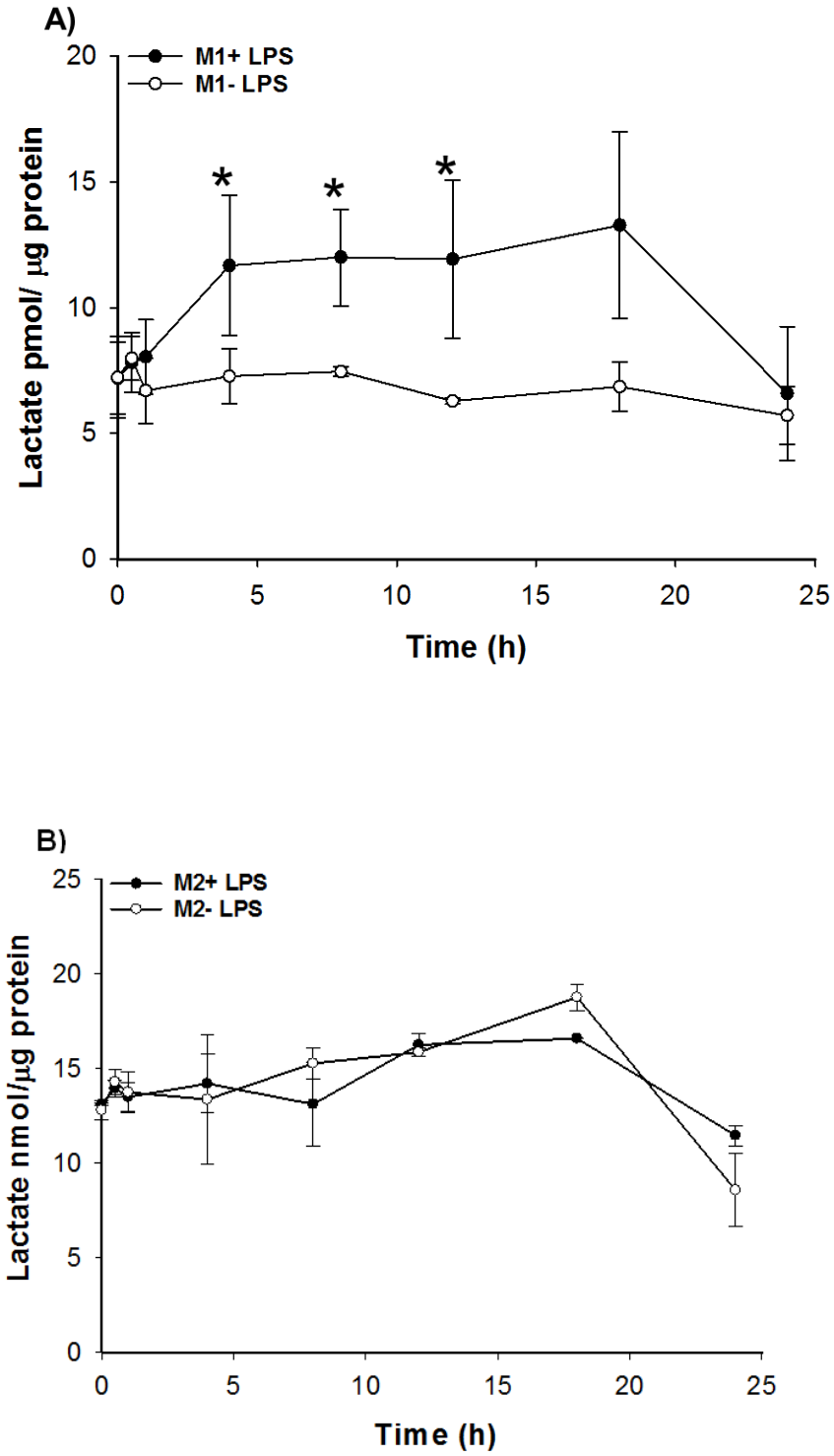

Figure5.5 LPS stimulation of macrophages promotes lactate production in M1-like macrophages during LPS stimulation. In response to LPS stimulation, lactate production was increased in M1-like macrophages (A) while it was not affected in M2-like macrophages (B). Each data point represents mean ± SE, n = 3-4 independent experiments performed in 3-4 wells/ treatment. The data were analysed by one way ANOVA followed by the Bonferroni *post hoc* test and significant differences are indicated as *P < 0.05, **P < 0.01, ***P < 0.001.

5.2.5 FK866 and DPI treatment block LPS-induced increases in the NAD^+/NADH ratio in differentiated macrophages

The conversion of pyruvate, into lactate, helps to maintain the cytoplasmic NAD^+ and thus NAD^+/NADH ratio needed to maintain glycolysis activity. It has been reported that SIRT can regulate metabolic reprogramming in MΦs by sensing the changes in NAD^+/NADH ratio, showing that NAD^+-dependent sirtuin activity mediates the link between metabolism and immune response during LPS stimulation in a model of THP-1 sepsis (Liu *et al*., 2012). Therefore, we tested the impact of inhibition by DPI and FK866 on the NAD^+/NADH ratio and on whether it can control flux through glycolysis in M1s during LPS stimulation.

The NAD^+/NADH ratio was significantly decreased with both FK866 and DPI, with DPI showing higher impact from the early stages of the experiment at 0.5 h, compared to the control ($P = 0.02$), for DPI and FK866 treatment, respectively (Figure 5.6 A). These data fit nicely with previous results showing that both the initial peak and the second peak of NAD^+ levels were inhibited in M1-like cells treated with DPI and FK866, respectively. It seems that NAD^+ level decrease affected the redox ratio resulting in a clear decrease following treatment. These results showed that both DPI and FK866 treatment caused a decrease in NAD^+/NADH ratio due to limitation of NAD^+ from NADH oxidation and the recycling pathway, respectively. In view of these results and the NAD^+ availability, we suspect that NAD^+ manipulation might regulate the flux through glycolysis in pro-inflammatory M1-like macrophages, so we next decided to investigate the glycolysis activity using the same inhibitors.

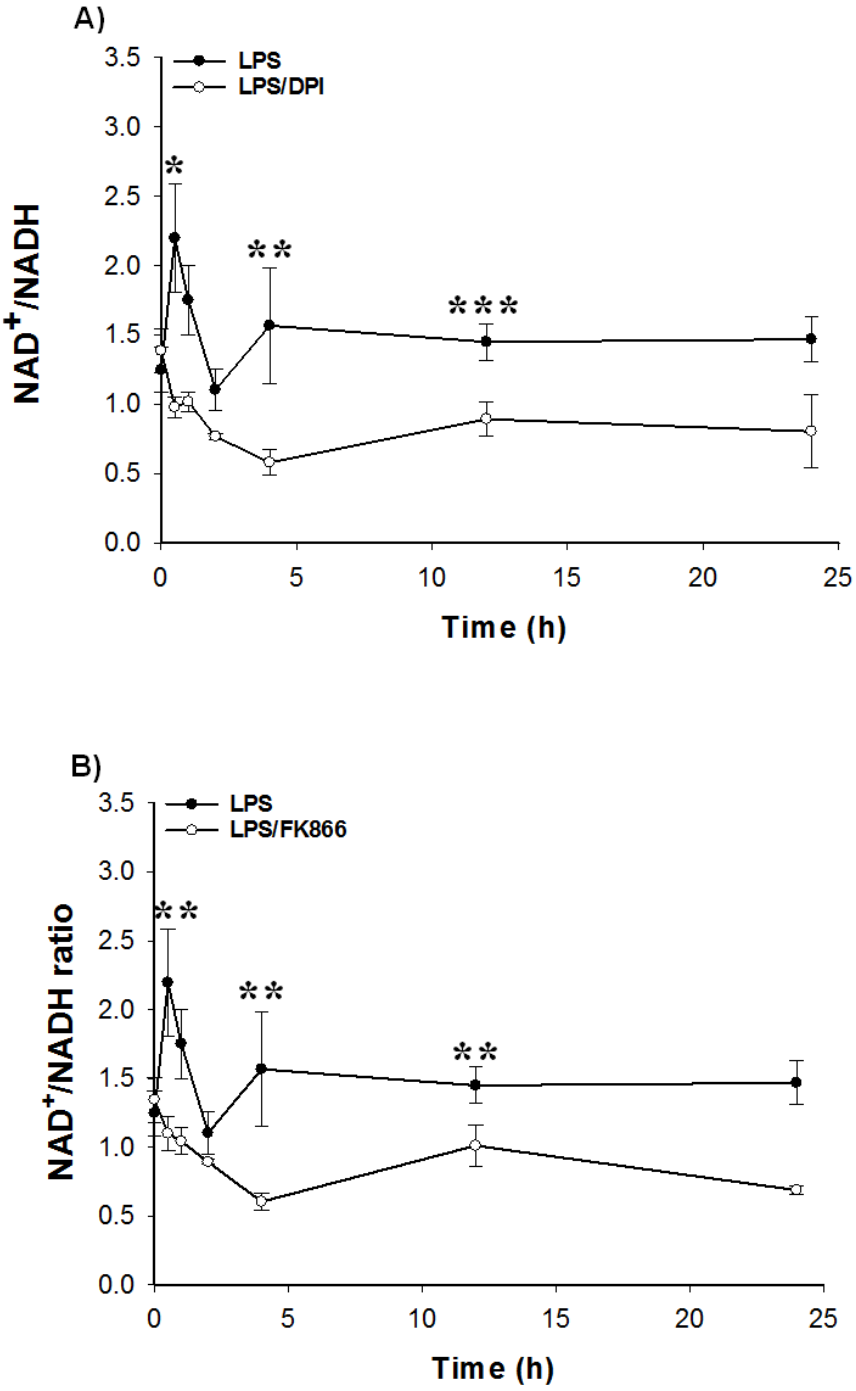

Figure 5.6 Pharmacological modulation with DPI (A) and FK866 (B) decreases the NAD^+/NADH ratio in response to LPS stimulation in pro-inflammatory M1-like MΦs. Differentiated M1s were pre-incubated with DPI (100 µM) or FK866 (100 nM) for 0.5 h and 1 h, respectively, prior to LPS stimulation. LPS-induced NAD^+/ NADH ratio increase is inhibited with (A) DPI and (B) FK866. Each data point represents mean ± SE, (n = 3) independents experiments performed in triplicate. The data were analysed by one way ANOVA followed by Bonferroni *post-hoc* test and significant differences are indicated as *P < 0.05, **P < 0.01, ***P < 0.001.

5.2.6 DPI inhibits LPS-induced glycolysis activity increase in M1-like macrophages

Since we observed that NAD^+ and the NAD^+/NADH ratio were decreased by DPI treatment in M1-like cells, we suspected that blockage of NADH oxidation might affect the glycolytic flux during LPS stimulation and therefore DPI was used in this study. Macrophages were pre-incubated with 100 µM DPI for 0.5 h prior to LPS stimulation. DPI treatment confirmed our prediction as maximum glycolysis and glycolysis rate were significantly inhibited in a time-dependent manner after 0.5 h (where maximum was $P = 0.036$, glycolysis was $P = 0.02$ and reserve was $P = 0.006$) while coupling efficiency, respiration rate and reserve were not affected as shown in figure 5.7. The decrease in maximum glycolysis, glycolysis and glycolytic reserve decreased to less than 70%, 60% and 50%, respectively (Figure 5.7 A, B, C).

These results are consistent with previous findings showing that glycolysis was inhibited by DPI-mediated NADPH oxidase inhibition (Liu *et al*., 2012). Based on our previous results that showed DPI treatment blocks NAD^+ production, the observed inhibition in glycolytic parameters might be due to limit NAD^+ availability via DPI-sensitive mechanism. Consistently, we observed no effect on the respiratory parameters and this because the latter is limited in M1-like macrophages and could also suggest that NAD^+ production is not linked to OXPHOS activity.

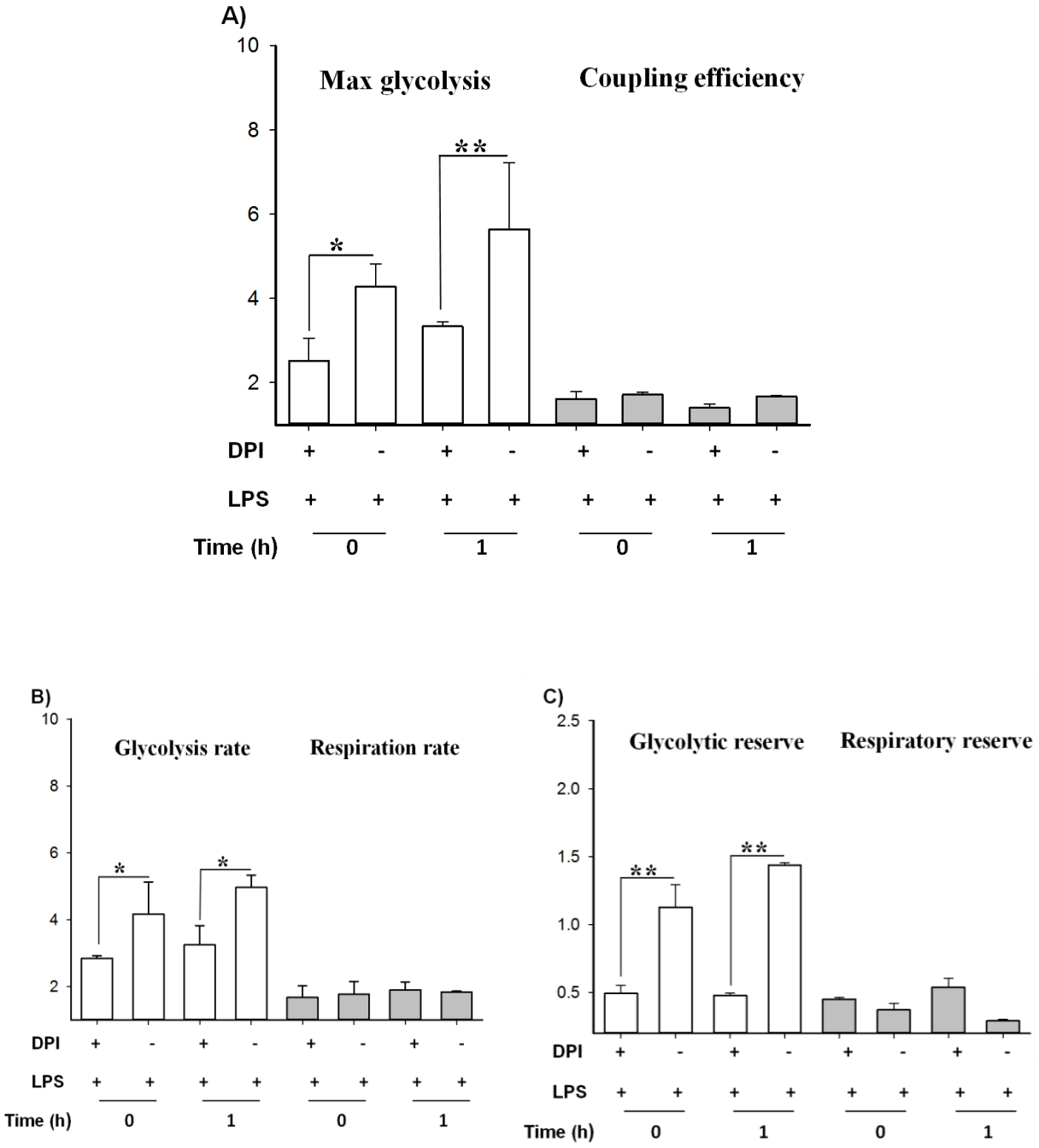

Figure 5. 7 DPI treatment decreased glycolytic activity in M1-like macrophages. Differentiated cells were pre-incubated with DPI (100 µM) or with culture medium for 0 h and 0.5 h prior to stimulation with LPS. Both OCR and ECAR were measured in seeded cells after sequential addition of glucose (11 µM), oligomycin 1 µM), 2-DG (100 mM) and finally (rotenone/antimycin (1 µM/ 2 µM, respectively). The effect of DPI on LPS induced (A) max glycolytic and coupling efficiency, (B) glycolysis and respiration rate, (C) glycolytic and respiration reserve. In each case, +/- indicates addition/non-addition of DPI/LPS. Data shown are the means ± SE of (n = 3-4) independent experiments performed in triplicate. The data were analysed by one way ANOVA followed by the Bonferroni test and significant differences are indicated as *P < 0.05, **P < 0.01, ***P < 0.001.

5.2.7 FK866 inhibits LPS-induced glycolytic activity increase but not OXPHOS activity following LPS stimulation in M1-like macrophages

Next, we decided to test the impact of FK866 treatment mediated NAD^+ recycling on glycolytic flux in M1-like cells. As we observed that NAD^+ production and the redox ratio were clearly sensitive to FK866-mediated NAD^+ inhibition, we assumed that FK866 might also affect glycolysis. FK866 is a well-known drug that has entered clinical trials to treat tumours (Hasmann and Schemainda, 2003). Venter and others (2012) have recently reported that FK886-mediated NAMPT inhibition attenuated glycolysis activity but it did not affect OXPHOS in a model of macrophages. We show a similar picture here, with glycolysis significantly inhibited with FK866 treatment whereas OXPHOS was not affected in M1-like macrophages (Figure 5.8).

The inhibition with FK866 caused a significant decrease in maximum glycolytic (60%, $P = 0.02$) and glycolysis rate (50%, $P = 0.012$) but it had no pronounced effect on glycolysis reserve suggesting that glycolysis is partially dependent on NAMPT-mediated NAD^+ production. Indeed, we have shown previously that FK866 treatment blocks NAD^+ production under LPS challenge (Chapter 4). It seems that the decrease in NAD^+ impairs redox balance and tips the balance to NADH which might lead to inhibition of glycolysis activity. However, FK866 was not able to inhibit glycolysis in resting macrophages. This might fit nicely with previous results showing that NAD^+ increases gradually after FK866 treatment and further confirm that M1-like are glycolytic. On the other hand, FK866 treatment does not affect respiration parameters (Figure 8 A, B and C).

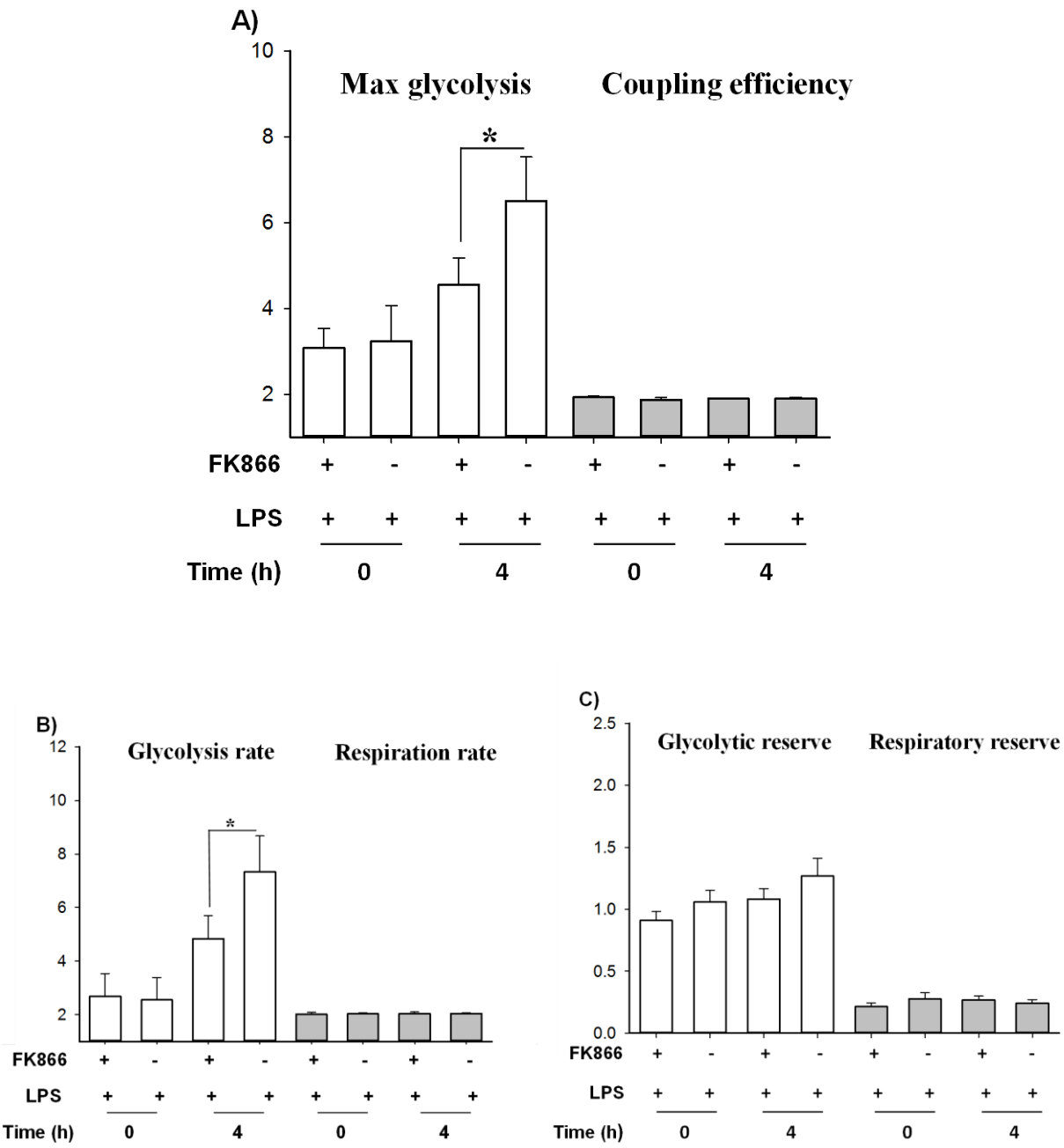

Figure 5.8 FK866 treatment decreased LPS-induced glycolysis, but had no effect on mitochondrial respiration. Differentiated cells were incubated with the presence of FK866(100 nM) or with culture medium for 1 h prior to stimulation with LPS for 0 h and 4 h. ECAR and OCR were calculated as previously described in Materials and Methods (chapter 2, section 2.2.12). FK866 treatment decreases LPS-induced maximum glycolysis activity but not coupling efficiency (A), glycolysis and not respiratory rate (B) and glycolytic reserve while it does not affect respiratory reserve in macrophages (C). In each case, +/- indicates addition/non-addition of FK866/LPS. Data shown are the means ± SE, (n = 3) independent experiments performed in triplicate. The data were analysed by one way ANOVA followed by the Bonferroni test and significant differences are indicated as *P < 0.05, **P < 0.01, ***P < 0.001.

5.2.8 1D-MT treatment does not affect LPS-induced glycolytic activity in M1-like macrophages

To further investigate the link between NAD^+ availibity and glycolysis, 1-MT has been used as inhibitor for IDO activity, the rate limiting step for NAD^+ *de novo* pathway. It is well-known that IDO supports immune regulatory mechanisms through tryptophan depletion and/or immune regulatory metabolites produced by kynurenine pathway (Orabona *et al*., 2006; Pilotte *et al*., 2012). Our data show that 1-MT treatment has no effect on glycolysis activity (Figure 5.9) suggesting that NAD^+ *de novo* synthesis plays an insignificant role in regulating glycolysis flux in M1-like cells. These results might be because NAD^+ *de novo* synthesis contributes less to NAD^+ production as only one NAD^+ molecule in 60 can be produced through the IDO pathway. Also, our data show that 1-MT treatment had no effect on respiration parameters. These observations contradict some other recent findings in which the investigators reported that IDO activity inhibition with 1D-MT led to decrease glycolysis activity while conversely increased mitochondrial metabolism in a model of lymphocytes (Eleftheriadis *et al*., 2012). The contradiction in the results might be cell-type dependent response.

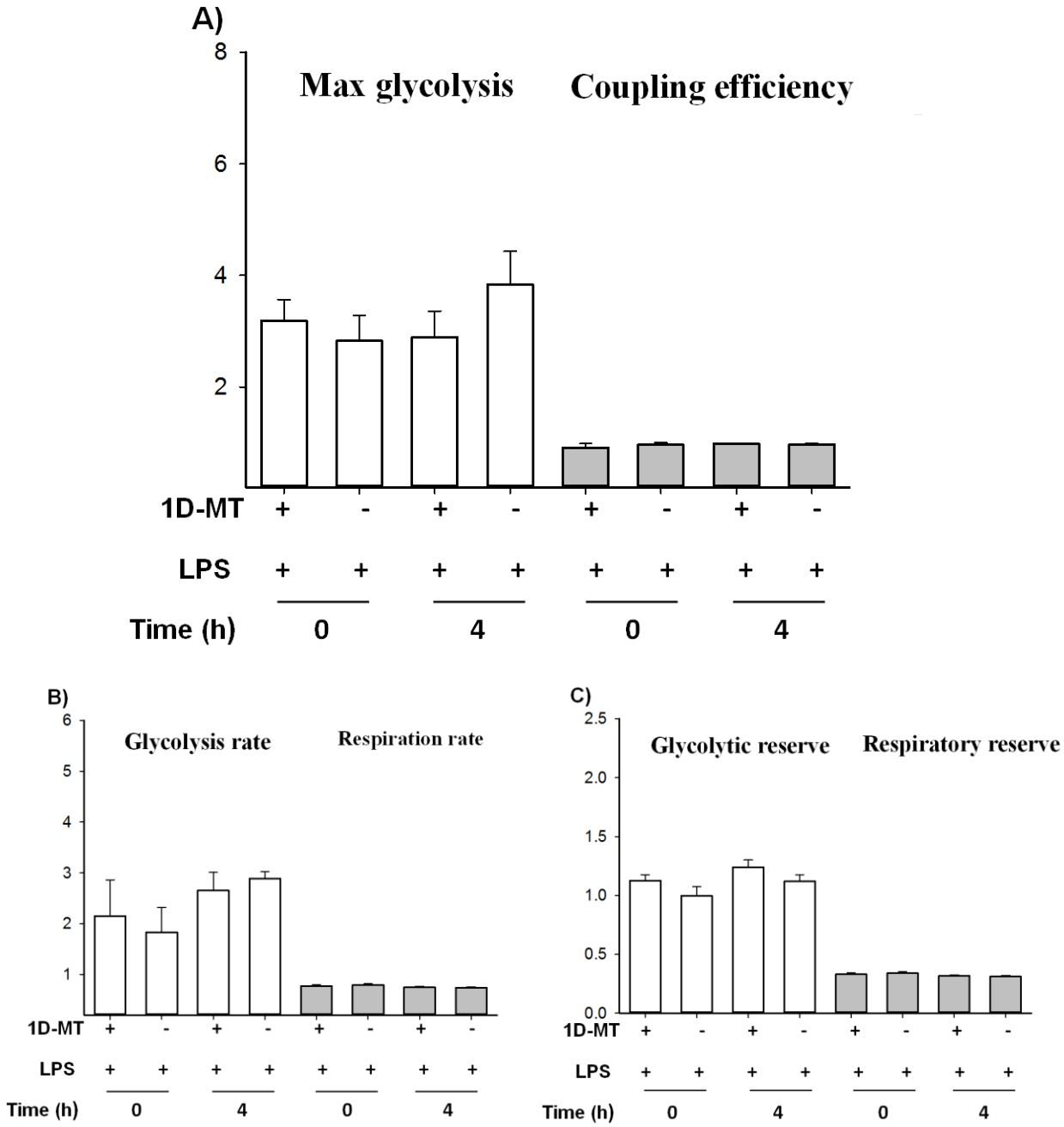

Figure 5.9 1D-MT treatment causes no effect on anaerobic glycolytic and mitochondrial respiration during LPS stimulation in differentiated macrophages. Cells were seeded in a Seahorse V7 plate and allowed to differentiate for 72 h prior to ECAR/ OCR measurement. Prior to stimulation with LPS, for 0 h and 4 h, differentiated cells were pre-incubated with 1D-MT (200 µM) for 2 h. The effect of 1D-MT treatment on LPS induce max glycolytic actvity and coupling efficiency (A), glycolysis rate and respiration rate (B) and finally glycolytic reserve and respiratory reserve in macrophages (C). In each case, +/- indicates addition/ non-addition of 1D-MT/LPS Data shown are the means ± SE, (n = 3) independent experiments performed in triplicate.

5.3 Discussion

It is now known that classical (M1) macrophages depend strongly on glycolysis while M2s (alternative) are known to utilize OXPHOS for energy production. In order to achieve this, macrophages need to maintain the redox state (NAD^+/ NADH ratio) and maintain sufficient quantities of NAD(H) in the cytoplasm (Newsholme, 1986). We have shown here that NAD(H) levels, at least in part, might affect glycolytic activity in pro-inflammatory macrophages suggesting that NAD^+ levels and thus NAD^+ metabolism as another factor influencing the regulation of energy metabolism under LPS challenge. Our results demonstrate that LPS stimulation increases NAD(H) levels and the NAD^+/NADH ratio in differentiated macrophages (Figure 5.2). This increase might be accounted for by the NADPH oxidase activity as this increase was inhibited with DPI, an NADPH oxidase inhibitor (Figure 5.6 A). These assumptions are confirmed by a recent report in which the authors have shown that NAD(P)H oxidase plays a key role in supporting glycolysis by increasing NAD^+ generation in a model of cancer cells (Lu *et al*., 2012). In this study, the authors relate the decrease in NAD^+ production to the reduction in NADH oxidation caused by DPI treatment leading to a decrease in glycolysis activity. Indeed, our results show that NADH levels follow the same trend as that observed for NAD^+ although NADH levels were slightly lower but also might mean that NADH is oxidised to give rise to NAD^+ in M1-like cells during LPS stimulation (Figure 5.2 A). In contrast, the NAD(H) levels and the NAD^+/NADH ratio were not sensitive to DPI treatment in M2-like cells and this might be accounted for being NADPH oxidase role missing in this subset. Alternatively, M2-like MΦs are known to use OXPHOS for energy production. Therefore, LPS failed to induce significant changes in NAD(H) levels and hence the NAD/NADH ratio in this subset (Figure 5.2 B, C). These findings fit well with our previous data showing that DPI treatment was able

to block the NAD^+ increase in M1-like but not in M2-like macrophages. The current data might confirm our assumptions suggesting that NADH oxidation through NADPH oxidase activity could be another source of NAD^+ production in M1-like macrophages. We have shown here that FK866 treatment caused a decrease in redox (NAD/NADH) ratio (Figure 5.6 B); this is in agreement with Venter *et al*. (2014). This could be explained in a variety of ways, such as (i) the cellular redox ratio was highly sensitive to FK866 inhibition in M1-like cells since the latter produces high levels of NAD^+ as we have shown previously (Chapter 3). (ii) The redox ratio was affected in M1-like cells because pro-inflammatory macrophages depend on glycolytic metabolism to produce energy (Galvan-Pena and O'Neill, 2014) and it is known that NAMPT-mediated NAD^+ production supports glycolysis. Therefore NAD^+ levels and thus the NAD/NADH ratio were sensitive to FK866 treatment. While studying macrophages using the inhibitor FK866, Vento-Gerad and his colleagues (2014) also observed that FK866 was able to decrease NAD^+ levels and redox ratio in a model of RAW 264.7 macrophages. They pointed out that cells with a high metabolic activity, such as tumour cells, are more sensitive to FK866 treatment because these cells have high NAD^+ turnover. Given that NAD^+ levels are a central link to glycolysis, we decided to evaluate metabolic flux in our model using Seahorse technology as we suspected that the increase in NAD^+ we observed might lead to an increase in glycolysis flux in M1-like macrophages.

The ECAR was investigated while sequentially injecting glucose, oligomycin and 2-DG whereas we concurrently measured OCR, replacing 2-DG with a combination of rotenone/antimycin. When glucose was added to cells, the ECAR showed a significant increase while OCR was not affected with glucose treatment. Our data are consistent with others showing that glucose augments ECAR and this was attributed to increased glycolysis activity (Winer and Wu, 2014). Oligomycin injection caused M1-like MΦs to induce an

ECAR increase; this might be attributed to compensation for the loss of mitochondrial ATP, due to oligomycin treatment, via the generation of more ATP through glycolysis in order to maintain the required cellular ATP levels (Winer and Wu, 2014). In this study, the authors found that when cancer cells experience high energy demand due to loss in mitochondrial ATP, under hypoxic condition or exposure to oligomycin, cells maintained energy homeostasis by boosting glycolysis activity as an alternative mechanism to adapt and survive under hypoxic conditions.

The data shows that LPS stimulation caused an induction of glycolysis parameters (maximum glycolytic, glycolysis rate and reserve) and conversely a down-regulation of OXPHOS parameters (mitochondrial capacity, respiration rate and respiration reserve) in M1-like MΦs (Figure 5.4). Accordingly, our data show that glucose failed to increase OCR under the experimental conditions and this is supported by recent work (Winer and Wu, 2014). It is tempting to speculate that metabolic reprogramming was induced towards glycolytic activity by LPS stimulation, suggesting that M1-like MΦs are regulated by active glycolysis and not OXPHOS. Accordingly, these results are in line with recent reports in which Krawczyk and colleagues (2010) reported that TLR-activation mediates metabolic reprogramming in dendritic cells (DCs) from OXPHOS to highly active glycolysis. In this pathway, NADH is converted back into NAD^+ via the conversion of pyruvate to lactate (Pearce and Pearce, 2013). Interestingly, this can occur under conditions where OXPHOS is inhibited (Locasale and Cantley, 2011). In fact, this reaction restores NAD^+/NADH balance which help to maintain the NAD^+ supply for glycolysis (Venter *et al*., 2014). NAD(H) plays a key role in the glycolysis pathway. For instance, it is used as a coenzyme for the GAPDH reaction that is mediated the flux through glycolysis (Ying, 2006). As lactate is an alternative measure of anaerobic glycolysis (Keuper *et al.*, 2014), we measured lactate production. We demonstrate

that lactate increase paralleled glycolysis increase in response to an LPS challenge. Of note, TCA-mediated CO_2 production can contribute to ECAR, therefore, this could be ruled out by observing lactate production, which served to confirm that the observed acidification (ECAR) was not due to TCA activity. In response to LPS stimulation, the lactate production was increased by 40% compared to the resting state while it was not affected in M2-like MΦs in both the resting and the activated states (Figure 5.5 A, B). Notably, there was an argument that the TCA cycle activity and CO_2 release might contribute to extracellular acidification rate (ECAR) as a result of CO_2 being converted to bicarbonate (Keuper *et al*, 2014).We and others have shown that glycolysis was highly active unlike OXPHOS and this might mean that glycolysis pathway is the main source of lactate production (Jensen *et al*., 1990). Indeed, it was reported that if the glucose does not affect or inhibit OCR, as we showed earlier, then this might mean that there is no glucose- derived CO_2 production (Winer and Wu, 2014). In a similar way to DCs and T-cells, pro-inflammatory MΦs rapidly utilize glycolysis but not oxidative metabolism. Several possible mechanisms might be involved. For example, PMA has been reported to promote the induction of the phosphatidyl inositol 3'-kinase/Akt pathway (PI3K/Akt; Nishizuka, 1995; Busca *et al*., 2014) that is required for glycolysis. Indeed, PI3K/Akt activity has been shown to enhance TLR-induced glycolysis activity while monophosphate (AMP)-activated protein kinase (AMPK) has been shown to antagonise glycolysis (Busca *et al*., 2014). It has been reported that AMPK is regulated by vitamin D_3 treatment is involved in supporting oxidative metabolism in M2s (Sag *et al*., 2008; Wu *et al*., 2015). Although the reason as to why macrophages utilize glycolysis is largely unknown, it has recently been speculated that using glycolysis is beneficial from the bioenergetics point of view. While glycolysis ability is less efficient at producing ATP than OXPHOS, it actively supports an immune response in immune cells because glycolysis is 100 times faster than

oxidative metabolism. Also, it was suggested that increased glycolytic metabolism might be useful in maintaining immune cell activity during inflammation where ATP production could also occur anaerobically. One study has reported that HIF-1α plays a crucial role for DC activation in inflammatory states by enhancing LPS- induced glycolysis (Jantsch *et al*, 2008). HIF-1α induces glycolysis flux in activated macrophages by mediating the expression and up-regulation of the glucose transporter, GLUT-1 leading to increase glucose uptake (Chen *et al*., 2005). It has been shown that GLUT-1 is translocated from the cytoplasm to the cell surface under energy stress, promoting rapid glucose uptake (Artemov *et al*., 1998; Rivenzon-Segal *et al*., 2003). Indeed, GLUT-1 mediated glucose metabolism induces ROS production which supports pro-inflammatory phenotypes in macrophages (Freemerman *et al*., 2014). The current findings might suggest that in M1-like MΦs NAD^+ increases might partially support the glycolytic phenotype and perhaps explain why these cells are committed to anaerobic glycolysis. Also, the increase in glycolysis flux might be accounted for by a different mechanism according to Winer and Wu (2014), who suggested that inhibition of mitochondrial ATP synthesis by oligomycin might direct pyruvate away from TCA to lactate production. To investigate whether modulation of NAD^+ availability can control glycolysis, we measured LPS–induced glycolytic metabolism in the presence of DPI, an NAD(P)H oxidase inhibitor. Interestingly, examination of glycolysis in the presence of DPI led to a decrease in maximum glycolysis, glycolysis rate and glycolytic reserve. The maximum glycolysis and glycolysis was reduced 2.5-fold in DPI-treated macrophages compared to non-treated cells. The decrease in maximum glycolytic metabolism is perhaps due to the fact that DPI-mediated inhibition limits NAD^+ availability, allowing reduction of the flux through glycolysis pathway. This assumption is supported by NAD^+/NADH ratio results in which the ratio was inhibited by 60% after treatment with DPI. While DPI inhibition did not affect the

respiration rate, it was able to slightly increase the respiratory reserve. The observed increase in respiratory reserve was probably due to the fact that oxidative phosphorylation still occurs because it is necessary for functionality to compensate for the energy required for cell viability. Our results might suggest DPI-sensitive NAD^+ inhibition as a potential approach to control glycolysis flux in macrophages. NAD^+ can be generated via *de novo* synthesis from tryptophan or via three salvage pathways, and NAMPT salvage is more preferable. To further investigate the importance of NAD^+ availability for glycolytic metabolism, we have investigated NAD^+ biosynthesis pathways by using FK866, NAMPT (salvage pathway) inhibitor or 1D-MT, an inhibitor for IDO (*de novo* pathway). We have demonstrated here that FK866-mediated NAD^+ inhibition was able to attenuate glycolytic metabolism in differentiated macrophages. Our results seems to be in agreement with Tan and his team (2013), who showed that FK866-mediated NAMPT inhibition caused a reduction in glycolysis as a result of the inhibition in NAD^+ availability for the glyceraldehyde 3-phosphate dehydrogenase enzyme. Collectively, the inhibitory effect of FK866 on aerobic metabolism, in macrophages, is probably due to the fact that cytoplasmic NAD^+ levels are high in activated macrophages, and it has been found that the NAD^+ pool in cytoplasm is highly sensitive to FK866-mediated NAMPT inhibition (Pittelli *et al*., 2010). On the other hand, mitochondrial respiration seems to not be sensitive to FK866 inhibition. One possible explanation is that the mitochondrial NAD^+ pool is independent of NAMPT activity (Yang *et al*., 2007 and Pittelli *et al*., 2010). In agreement with these findings, Tan and others (2013) reported that mitochondrial NAD^+ represents a small fraction of the total NAD^+ pool, and therefore FK866-mediated NAMPT inhibition may only affect the cytoplasmic NAD^+ pool (Pittelli *et al*., 2010). Together, both FK866 and DPI treatments were able to inhibit NAD^+ production (Chapter 4) as well as glycolytic activity with M1s not being able to boost their

OXPHOS activity to meet their energy demands. These findings further confirm that the ATP generation is glycolysis-dependent in macrophages, and suggest that NAD^+ metabolism as a potential approach to pharmacologically modulate bioenergetics metabolism in pro-inflammatory differentiated MΦs.

Finally, the glycolysis and OXPHOS profiles were also investigated using 1D-MT under LPS challenge. While 1D-MT-mediated IDO inhibition was able to attenuate NAD^+ levels the inhibitory effect of 1D-MT on glycolytic metabolism was less pronounced. These observations might be due to the IDO pathway being less efficient at building up a sufficient cytoplasmic NAD^+ pool to derive glycolytic activity in our model. Indeed, it has been reported that one in 60 molecules of NAD^+ is derived from tryptophan pathway (Horwitt *et al*., 1956), and this could be accounted for by 1D-MT's effect on energy production in M1-like macrophages. The treatment with 1D-MT did not affect OXPHOS activity and this could be attributed to OXPHOS activity already being inhibited in M1-like macrophages. In contrast, a recent study has been conducted on lymphocytes in which the investigators showed that 1D-MT was able to induce glycolysis an increase while conversely suppressing oxidative metabolism (Eleftheriadis *et al*., 2012). These findings might be somewhat limited as the glycolysis profile in this study is represented by the lactate production which might be not sufficient as both TCA and glycolysis could contribute to lactate production. However, the discrepancy in the results could be accounted i several ways, namely (i) cell- dependent response as M1-like macrophages differ from lymphocytes since these cells are known to utilize both TCA and glycolysis for energy production, whereas M1s are mainly glycolytic, (ii) different experimental conditions were used in the two studies; we treated our cells with 1D-MT for 2 h, while Eleftheriadis *et al*. (2012) incubated the cells with 1D-MT for 96 h and finally (iii) there may be differential expression of IDO isoforms (IDO1/IDO2) in response to

1D-MT treatment. Opitz and his colleagues (2011b) reported that 1D-MT was capable of upregulating IDO mRNA and protein expression in T cells. Further work might be required to investigate the counter-regulatory impact of IDO1/IDO2 isoforms on glycolysis activity in macrophages.

In this study, we focussed on how NAD^+ manipulation modulates glycolysis activity in pro-inflammatory M1-like macrophages. The most striking findings to emerge were that disturbing NAD^+ production either from NADH oxidation or from NAD^+ recycling pathway caused a decrease in glycolytic metabolism in M1-like macrophages. Also, LPS stimulation did not affect oxidative respiration in M1-like macrophages and this might suggest a switch towards glycolysis activity. This switch might occur to compensate for energy demand and to support M1-like cell immune function, confirming previous findings (Galvan-Pena and O'Neill, 2014) in showing that M1 are mainly glycolytic. The impact of NAD^+ homeostasis on glycolysis is not yet fully understood, therefore further study is necessary to address how modulation NAD^+ homeostasis affects glycolytic enzyme activities. The current results may assist in identifying pharmacological targeting for NAD^+ homeostasis as a useful molecular mechanism to modulate bioenergetics metabolism and thus offer a novel approach that might assist in restoring metabolic disorder-associated diseases.

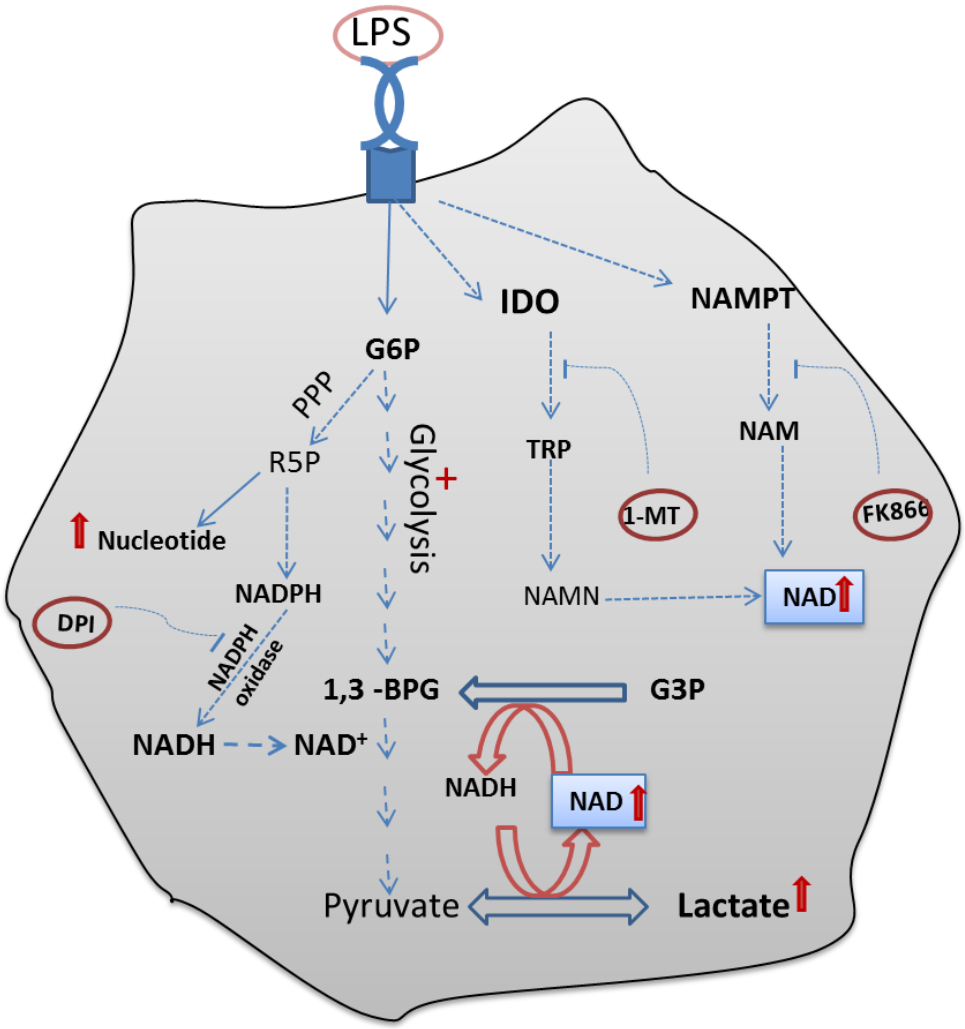

Figure 5.10 Pharmacological modulation of NAD metabolism controls glycolysis metabolism in pro-inflammatory macrophages. FK866 and DPI (but not 1-MT) inhibits LPS-induced glycolytic capacity by controlling the availability of NAD^+ that is required for deriving glycolysis pathway. FK866= inhibitor of nicotinamide phosphoribosyl transferase (NAMPT); DPI = diphenylene iodonium, an inhibitor of NADPH oxidase. 1-MT= 1-methyl tryptophan, an inhibitor of IDO pathway; G6P= glucose-6-phosphate, G3P= glyceryl aldehyde-3-phosphate; PPP = pentose phosphate pathway.

CHAPTER 6

GENERAL DISCUSSION

6.1 Discussion

This study aimed to explore NAD^+ levels and NAD^+ homeostasis in differentiated macrophages and during LPS stimulation to see whether pharmacological manipulation of NAD^+ can control TNF-α release in differentiated MΦs using a monocytic THP-1 cell line. Whilst THP-1 cells are usually non-adhesive cells that grow in suspension, THP-1 are widely used for macrophage differentiation as these cells can be easily differentiated into cells with features of MΦ-like subsets. Accordingly, the macrophages used in this study were generated using pro-monocytic THP-1 differentiation towards macrophages (MΦs) with M1-like and M2-like characteristics using PMA and vitamin D_3, respectively (Figure 6.1). This is supported by the changes in cytokine secretion as TNF-α largely increased in M1-like MΦs in addition to the gene expression profile of NAD^+ homeostasis enzymes reflected by upregulation in CD38 and CD157 that are known as markers of macrophages maturation and activation (Frasca *et al*., 2006). Exploring NAD^+ homeostasis gene expression revealed that M1-like MΦs exhibit a differential profile in the resting state and also when stimulated with LPS as both CD38 and CD157 expression, well known differentiation markers, were upregulated in M1-like MΦs while this was not the case with M2-like MΦs (chapter 3). In support of this, it has been shown that vitamin D_3 treatment was capable of upregulating CD157 expression. Conversely, PMA was found to downregulate CD157 expression. TNF-α release was also increased in M1-like MΦs; this is supported by Takashiba *et al*., (1999) suggesting that PMA mediates NF-kB accumulation, metalloproteinases and TLR2/TLR4 expression (Figure 6.1) that are required for LPS-induced TNF-α secretion. However, TNF-α release increased slightly for a short time in M2-like MΦs and this might be explained by vitamin D_3 treatment which was shown to negatively regulate MMPs and TLR4 expression in time dependent manner.

Several studies have shown that THP-1 cells are the most commonly used cells to study monocyte-macrophage immune function since THP-1 cells behave similarly to PBMCs (Sharif *et al*., 2007; Qin, 2008). Indeed, THP-1 cells synthesise and secrete MCSF, IL-8 and apolipoprotein E (Menju *et al*., 1989). Also, THP-1 is similar to primary macrophages with regards to LPS-induced gene expression (Verreck *et al*, 2006). Furthermore, THP-1 represents a better system than PBMCs as technically speaking; THP-1 minimizes the degree of variability in the cell phenotype. Additionally, by following an appropriate procedure, this cell line can be recovered without any obvious effect on monocyte-macrophage features and cell viability. Using THP-1 as a model offers some advantages that it avoids the difficulties of obtaining sufficient quantities of human primary monocytes/macrophages. In addition, donor variability and accessibility are additional reasons as to why using THP-1 cells is more advantageous over using PBMCs. However, some differences and dissimilarities were observed between macrophages and THP-1 derived macrophages in that LPS stimulated the expression of certain genes. In fact, Kohro *et al*. (2004) showed that both apolipoprotein-E and MMP 9 are induced in primary macrophages and M1-like MΦs whereas the expression of IL-1β is conversely upregulated between M1-like MΦ and primary macrophages suggesting careful interpretation of the results is required before they can be generalised to monocytes and macrophages when experiments are done with THP-1 under different conditions. There is also a striking difference in the redox balance between THP-1 and primary monocyte as suggested recently by Carta *et al* (2011). The authors reported that THP-1 cells show large increase in anti-oxidants systems with high activity of cystine/cysteine cycle whereas primary monocytes display low levels of antioxidant systems with both cells having low amounts of ROS. Additionally, both ROS and anti-oxidants are induced in stimulated primary monocyte while the opposite was true in THP-1, suggesting an

important role for redox balance in inflammation. In a study investigating the role of redox balance in inflammatory response, Tassi *et al.* (1999) showed that anti-oxidant enzymes are required for regulating ROS-induced IL-1β secretion. Indeed, superoxide dismutase 1 (SOD 1), a well know anti-oxidant enzyme, has been proven to regulate caspase-1 and consequently IL-1β signalling (Meissner *et al*., 2008).

On the other hand, Sharif and his team (2007) showed that LPS-induced gene expression in THP-1 cells, but not in U937-derived macrophages, are very similar to PBMC-derived macrophages, suggesting that THP-1 cells have some value for the study of LPS- and NF-kB-dependent gene expression. Taken together, it can be concluded that THP-1 cells provide a valid and reasonable model for the study of monocyte-macrophage differentiation, polarization and immune function. The current study showed that differentiated macrophages displayed a differential profile of NAD^+ levels/NAD^+ homeostasis in the resting state and in response to LPS stimulation, with M1-like MΦs showing higher NAD^+ levels in both the resting and stimulated states this might suggest that NAD^+ is pro-inflammatory and that NAD^+ is required for macrophages immune function, particularly, the TNF-α response (chapter 3). It was hypothesised that NAD^+ might be of high importance regarding characterization of both subsets. By comparing the effect of FK866 on both subsets in the resting state, it was found that FK866 caused a drop in NAD^+ levels in M2-like MΦs, while it conversely caused an increase in NAD^+ levels in M1-like MΦs. This might suggest that the rate of NAD^+ consumption is high in M2-like MΦs as FK866 blocks NAD^+ recycling while it is low in M1-like MΦs. These data are consistent with the observation that M1-like MΦs significantly increase NAD^+ while M2-like MΦs do not. This is evident as NAD^+ generation significantly increases in M1-like MΦs following NAM application; this was not the case with M2-like MΦs, again supporting the rapid increase in NAD^+ levels seen in M1-like MΦs.

Based on these observations, it can be concluded that the rate of NAD^+ synthesis/consumption might reflect the cellular phenotype and thus the need for a particular type of immune response. The study reported in chapter 4 explored the source of NAD^+ in both subsets. Both DPI and FK866 decreased NAD^+ levels in M1-like MΦs but not in M2-like MΦs in response to LPS stimulation, suggesting that NAD^+ is produced partially via NADH oxidation and partially through the NAD^+ recycling pathway (Figure 6.1) which further confirmed the existence of a link between NAD^+ and the immune response. While it has previously been shown that TNF-α is controlled by NAD^+-dependent sirtuin activity at the transcription/translational level (van Gool *et al*., 2009), the data presented herein show that NAD^+ levels seem to correlate with TNF-α secretion levels in M1-like MΦs but not in M2-like MΦs. van Gool and his team (2009) showed that intracellular NAD^+, via NAMPT-mediated NAD^+ salvage pathway, is required for optimal TNF-α synthesis. This study was the first to report that NAD^+ regulates TNF-α production in a SIRT6-dependent manner, suggesting a link between NAD^+ metabolism and inflammation. However, it was not clear how NAD^+ and TNF-α are linked. Therefore, we showed this link is complex as it is required in a combination of pathways including NAD(H) oxidation-dependent mechanisms and NAD^+ salvage-dependent mechanisms suggesting that this link is even more intimate than first thought but this time at TNF-α secretion levels and this may also suggest that NAD^+ is partially required for TNF-α secretion. Collectively, these results might further strengthen the link between NAD^+ homeostasis, inflammation and metabolism in what it has recently become known as 'immunometabolism'. The increase in NAD^+ levels was supported by the increase in glycolysis that we showed in chapter 5 in M1-like MΦs during LPS stimulation (Figure 6.1). In support of this, glycolysis activity is decreased when NAD^+ availability is reduced by blocking either NADH oxidation or NAD^+ recycling in M1-like MΦs (chapter 5).

In fact, it has been reported that glycolysis is required for TNF-α production since TNF-α secretion and glycolysis was inhibited by lactic acid and acidification (Dietl *et al*., 2010). In chapter 5, LPS stimulation caused an increase in glycolysis parameters (maximum glycolytic rate, glycolysis rate and reserve) and conversely decreases in OXPHOS parameters (mitochondrial capacity, respiration rate and respiration reserve) in M1-like MΦs. In the interest of investigating NAD^+ involvement, we used the same inhibitors for NAD^+ generation and glycolysis activity was explored (chapter 5). Although, the mechanism which mediates glycolysis increase is not yet fully understood, it is believed that the glycolysis pathway is induced in classically activated (M1) macrophages, resulting in lactate production (Figure 6.1). Indeed, M1-like MΦs always exist in a hypoxic microenvironment and it has been shown that they are able to upregulate HIF-1α expression, which supports glycolysis flux via the activation of LDH-mediated conversion of pyruvate into lactate. HIF-1α increases glucose uptake via upregulation of GLUT-1 expression (Figure 6.1) to support glycolytic flux in activated macrophages. In contrast, due to AMPK induction, a switch towards OXPHOS occurs in M2-like (alternatively activated) MΦs via the upregulation of enzymes involved in mitochondrial activity such as succinate dehydrogenases in addition to proteins involved in mitochondrial biogenesis such as PPAR-γ (Figure 6.1). Moreover, in chapter 5 it was also reported that glycolysis was inhibited by FK866 treatment. Clearly, the inhibition of NAMPT-mediated NAD^+ recycling by FK866 caused a decrease in intracellular NAD(H) and the consequent inhibition in glycolysis activity. Similar to other studies, our data showed that NAD(P)H oxidase inhibition by DPI caused to decrease NAD^+ levels-mediated glycolysis activity. Together, these data might further strengthen the link between NAD^+, the immune response and metabolism and suggest that NAD^+ might be partially involved in TNF-α secretion. It has been reported recently that many metabolic disorders are

associated with inflammation. Indeed, immunometabolism is linked to numerous diseases such as diabetes, cardiovascular disease and some cancers (Steinberg and Schertzer *et al*., 2014). The effects of immunometabolism in macrophages are well known (Steinberg and Schertzer *et al*., 2014). The immunometabolism field is an area of research which has recently grown, being associated with metabolic reprograming in MΦs which is required for their immune function (O'neill *et al*., 2016). Therefore, it is perhaps not surprising that macrophages have recently been shown to play a key role in metabolic disorders (Chawla *et al*., 2011). In fact, sirtuin-mediated deacetylation has been shown to regulate the metabolic switch in TLR4-stimulated THP-1 (Liu *et al*., 2012). The authors of this study showed that SIRT1 uses NAD^+ to regulate the switch from increased glycolysis, supported by HIF-1α mediated the up-regulation of GLUT-1, to increased oxidative metabolism, supported by PGC-1 α, β and CD36, highlighting a critical for NAD^+ in metabolic reprogramming in MΦs. SIRT1, via sensing NAD^+ availability, has also been linked to a switch from early to the late inflammatory response via regulating TNF-α/IL-1β secretion in NF-KB dependent manner (Liu *et al*., 2011). These observations suggest that NAD^+/sirtuin might be partially required for the link between metabolism and the inflammatory response. Intracellular NAD^+ and thus the NAD^+/NADH has been implicated in range of metabolism-associated diseases including diabetes and obesity due to its role as co-factor in regulating metabolism and sirtuin activity, (Srivastava, 2016). The pathology of these diseases has also been associated with elevated levels of TNF-α (Swaroop *et al*., 2012). We showed that NAD^+ levels are associated with elevated TNF-α secretion and that the decrease in NAD^+ levels caused to decrease glycolytic activity. Therefore, modulation of NAD^+ levels might be a potential therapeutic means for managing MΦ functions and thus metabolic diseases. Increasing evidence suggests that boosting NAD^+ levels, via precursor supplementation (NMN, NA and NR) or by inhibiting

NAD^+-consuming enzymes (CD38, PARP), may have a clinically beneficial influence on multiple mitochondrial as well as age-associated disorders (reviewed in Srivastava, 2016). Studying the correlation between NAD^+ and TNF-α in MΦs might contribute to our understanding of immunometabolism which might open the door for treatment for MΦs-derive pathology of chronic diseases including rheumatoid arthritis and Crohn's disease.

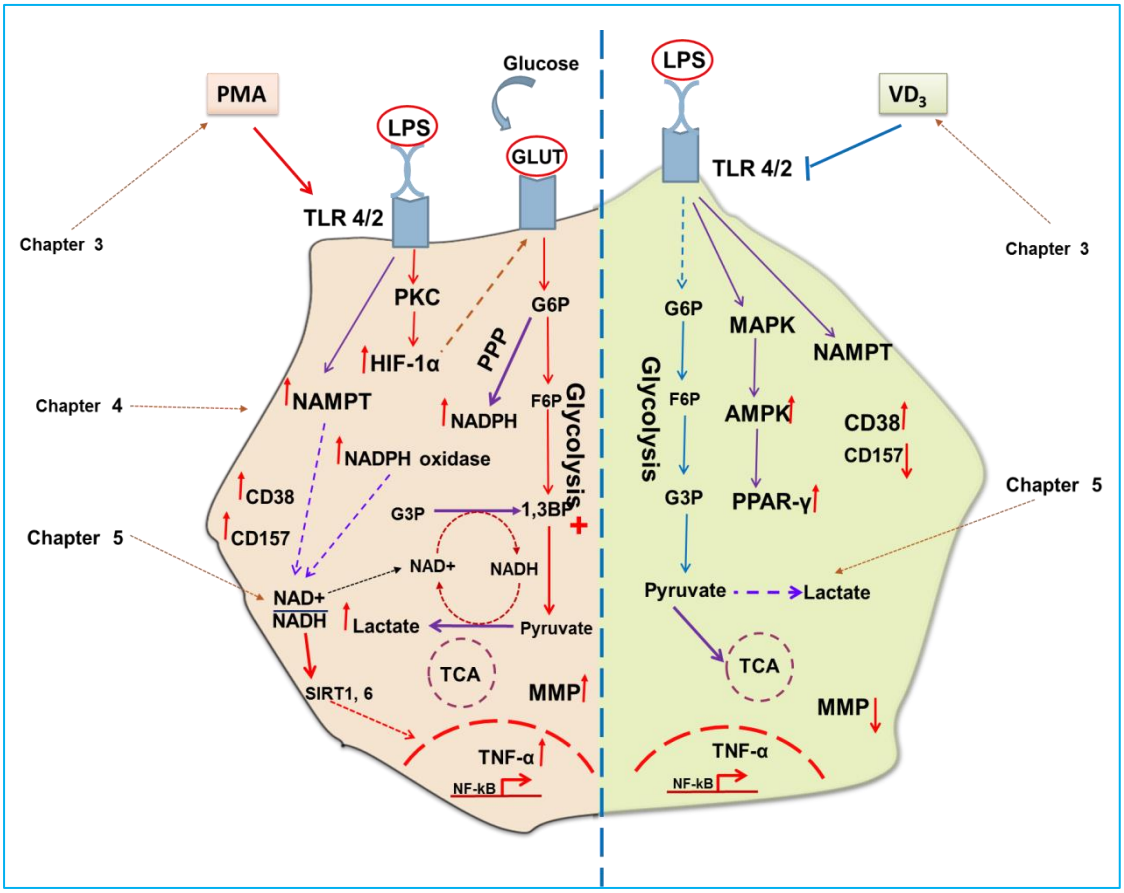

Figure 6.1 Metabolic profiles differ between M1-like (classical) and M2-like (alternative) macrophages during LPS stimulation. In M1-like macrophages, PMA induces TLR 4, 2 expression and NAMPT activity resulting in TNF-α release induction being supported. TNF-α release is regulated by MMP and SIRT 1, 6 activities which are sensitive to NAD^+/NADH ratio. LPS also increase PPP (pentose phosphate pathway) mediated NADPH generation that is required for NADPH oxidase activity. This enzyme regulates glycolysis via providing additional NAD^+. Moreover, HIF-1α increases glucose uptake to support glycolysis activity in classical M1s. In M2-like macrophages, TLRs are down-regulated by vitamin D_3 resulting in decrease TNF-α release. Similarly, MMP expression is downregulated in vitamin D_3 -treated cells. In addition, treatment with vitamin D_3 leads to upregulated AMPK which is required to drive mitochondrial activity in M2s (alternative) via up-regulation of PPAR-γ.

6.2 Future work

TNF-α production is implicated in numerous autoimmune and inflammatory diseases including rheumatoid arthritis and Crohn's disease. TNF-α is mainly produced by macrophages and therefore it is perhaps not surprising that macrophage-derived TNF-α can be deleterious to health. Therefore, given their role in a wide range of diseases, targeting macrophage responses, specifically TNF-α secretion, might be beneficial for therapeutic intervention.

Modulation of macrophage responses via the NAD^+ homeostasis pathway, by lowering NAD^+ levels, might represent an exciting therapeutic aspect for treating a number of chronic inflammatory diseases. It was recently shown that manipulating NAD^+ levels has a potential therapeutic impact on metabolic associated disorders (Mouchiroud *et al*., 2013). Since NAD(H) plays important role in regulating metabolic pathways, changes in NAD^+ levels have emerged as a powerful therapeutic tool for metabolic-related conditions via sirtuin activity (reviewed in Hall *et al*., 2013). In addition, NAD(H) has also been linked to pro-inflammatory TNF-α production via sirtuin activity in MΦs (van Gool *et al*., 2009). We have recently shown that pro-inflammatory MΦs display unusual changes in NAD^+ levels suggesting that NAD^+ levels are pro-inflammatory. The results from this study revealed that lowering NAD^+ levels, by modulating NAD^+ homeostasis, limited TNF-α secretion in a time-dependent manner in pro-inflammatory MΦs, highlighting a potential therapeutic tool for the treatment of MΦs-derive inflammatory pathologies. Notably, the link between pro-inflammatory MΦs and chronic disease, including Crohn's disease (CD) and rheumatoid arthritis (RA), has been known for some time (Kinne *et al*., 2000; Grip *et al*., 2003). Indeed, pro-inflammatory MΦs have the ability to contribute to the pathology of RA via the

production of a plethora of inflammatory mediators including pro-inflammatory cytokines (IL-6, IL-8, IL-18, IL-1β and TNF-α) and matrix metalloproteinases (MMP-1 and MMP-3; reviewed in Kinne *et al*., 2000). It is also worth noting that, MΦs derive cytokine production results in Th1/Th17 axis that produces IL-17/IL-15 which, in turn, supports MΦ activation, resulting in a positive feedback loop and thus sustaining the severity of the diseases (Mcinnes *et al*., 1997; Aarvak *et al*., 1999).

The M1 pro-inflammatory cytokine, TNF-α, has been shown to have primary role in the pathology of RA via ROS production (Miesel *et al*., 1996) as well as stimulation of MMP-1, -2, -3 secretion mediated articular destruction (reviewed in Maruotti *et al*, 2007). Similarly, IL-1β secretion is responsible for the synovial destruction in RA by inhibiting proteoglycan synthesis and degradation proteoglycan (von den Hoff *et al*., 1995) and the secretion of MMP-1 and MMP-3 (Arend *et al*., 1998). Therefore, manipulating NAD^+ homeostasis might offer a conventional anti-cytokine therapy towards TNF-α/IL-1β, produced by pro-inflammatory M1s, for the treatment of M1-mediated RA. Since NAD^+ levels are limiting for sirtuin activity which is required for TNF-α secretion, lowering its levels, either via NADH-oxidation or NAD^+-salvage dependent mechanism as we have shown previously, might offer a powerful therapy for treatment of RA or any inflammation-related disease. In fact, over expression of SIRT1 led to increase TNF-α secretion in rheumatoid arthritis synovium, as was found by Niederer *et al*. (2011). The authors found that SIRT1 is constitutively up-regulated in synovial tissue and thus SIRT1 silencing via siRNA or inhibition of enzymatic activity via SIRT inhibitors decreased LPS-induced TNF-α in monocyte freshly isolated from RA synovial tissue. In fact, blockage of TNF-α, via antibody neutralisation treatment, has been proven to inhibit collagen-mediated arthritis and supress inflammation in human/murine arthritis (Schadlich *et al*., 1999) suggesting a critical role for this cytokine in progression of

RA. Indeed, it has been hypothesised that therapeutic targeting of TNF-α has major importance for RA as TNF-α inhibition inhibited pro-inflammatory cytokines including IL-1, suggesting that RA might be TNF-α dependent (Feldmann *et al*., 1996). In addition, M1s are also responsible for RA via the chemokines secretion including CXCL13, also known as B cell-attracting chemokine 1 (BCA-1), which is constitutively expressed in RA tissue, suggesting a pathogenic role (Carlsen *et al*., 2004). The chemokine signalling is controlled by CD38, which has been shown to regulate chemotaxis signalling to CCL2, CCL19, CCL21, and CXCL12 in immature and mature DCs highlighting a regulatory role for CD38 on adaptive immunity by controlling DCs trafficking (Partida-Sanchez *et al*., 2004). We have shown that M1s largely express CD38 in both the activated and the resting state. As CD38 acts one of the main NAD^+ consuming enzymes, its manipulation via lowering NAD^+ levels might offer a powerful therapeutic means for regulating MΦ trafficking and consequently adaptive immunity. Given that NAD^+ levels are associated with TNF-α response in pro-inflammatory MΦs and that NAD^+ levels are required for NAD^+-dependent (sirtuin/CD38) activity, lowering its levels is a promising therapeutic regimen for anti-macrophage function which can also involve in regulation of adaptive immunity as a treatment for chronic diseases, in particular, RA. It is reported that NAD^+ levels differ between M1-like (pro-inflammatory) and M2-like (anti-inflammatory) macrophages. What is now needed is further systematic characterisation of NAD^+ homeostasis during macrophage differentiation. Therefore, it would be of interest to explore similar studies to those reported in this thesis on naturally occurring M1s, M2s and the sliding scale of functionally polarized subsets (M2a, M2b and M2c). Glycolysis is required for M1s (classical activation) and this was inhibited in this study in the FK866-mediated NAD^+ recycling mechanism and in the DPI-mediated NADH oxidation mechanism. To expand this, it would be of interest to explore NAD^+

therapeutic targeting on bioenergetics metabolism mediated M1 polarization. Recent work has shown that metabolic reprogramming is essential for M1-like and M2-like polarization and activation (Haschemi *et al*., 2012). In a similar context, further work needs to be done to establish whether manipulation of NAD^+ homeostasis could modulate macrophage differentiation and maturation. The results in this study showed that the trend of NAD^+ homeostasis gene expression was similar to that of TNF-α response, suggesting that both might be correlated. The next step would be to explore the role of NAD^+ homeostasis gene expression over longer time points and whether this can contribute to endotoxin tolerance in macrophages. A recent report has shown that elevation of NAD^+ and sirtuin is required for epigenetic reprogramming during endotoxin tolerance in a model of human sepsis (Liu *et al*., 2011). More research is needed to truly understand the role of NAD^+ and thus NAD^+ homeostasis in TAMs and whether NAD^+ targeting would be of interest for anti-cancer therapies. For example, a switch in polarization between M1s and M2s, via boosting NAD^+ levels activates sirtuin-mediated metabolic reprogramming, might be a useful tool for anti-cancer therapy. According to the results reported in chapter 4, NAD^+ increases after 1h sirtinol treatment which further confirm the contradictory effect of sirtuin on pro-/anti-inflammatory responses and raise the importance of the NAD^+-sirtuin axis in treating inflammation-associated tumour conditions. It has recently been shown that sirtuin 1, 6 activity are linked to metabolism reprogramming in activated macrophages (Liu *et al*., 2012). Since NAD^+ is a central link between metabolism and inflammation, the NAD^+-sirtuin axis may be critical for coupling metabolism reprogramming to the immune response. It would be worthwhile to further investigate this link and to understand this process and whether it could be useful for a potential pharmaceutical strategy that may target immune function in macrophages. Given the data show that NAD^+ levels are not decreasing after 1h sirtinol

treatment, it is tempting to investigate the effect of NAD^+ on TNF-α gene expression during the experimental studies. Our data might shed light on the importance of intracellular NAD(H) changes in supporting the energetic profile to mount an effective immune response in MΦs. A recent study has revealed the importance of glycolysis metabolism in pro-inflammatory cytokine signalling (Delmastro-Greenwood and Piganelli, 2013). Given that NAD^+ sensing by sirtuin activity is critical in linking inflammatory response and metabolic reprogramming (Liu *et al*., 2012), further studies need to be carried out in order to investigate NAD^+ and glycolysis and formulate a useful strategy to modulate macrophage polarization and inflammatory immune functions such as cytokine production, phagocytosis and migration, etc. We found both CD38 and CD157 display differential expression between M1-like and M2-like MΦs. It would be of interest to explore expression and over-expression of those proteins in reverting M1/M2 polarization in TAMs, which are known to play a pivotal role in linking inflammatory response to tumours and are characterised by M2 polarisation-mediated tumour progression. Thus, it would be interesting to assess the effect of CD157 and CD38 overexpression in reprogramming M1/M2 polarisation to hopefully provide anti-tumour treatment. Furthermore, it would be interesting to know the effect of CD38 on TNF-α response in both subsets. One way to expand our knowledge on this enzyme would be to silence its expression by using small interfering RNA (siRNA). Also, further work regarding the impact of CD38 deletion macrophages or inhibition in both *in vivo* and *in vitro* model on macrophages differentiation, migration and polarization would be beneficial. NAD^+ was reported to achieve immune regulatory function. For instance, it was reported that NAD^+ can function occasionally as a cytokine and that this occurs when the secretion of NAD^+ increases intracellular calcium in neighbouring cells resulting in an increase in their proliferation. In addition, CD38 is reported to be functionally involved in IL-12 induction in human

monocyte-derived DCs (Fedele *et al*., 2004). It perhaps not surprising that CD38 is implicated in immune regulation since CD38 is known to regulate the metabolism of adenine based-second messenger mediated calcium signalling (Fliegert *et al*., 2007). Therefore, future work should be directed towards understanding the role of CD38 in LPS-induced expression and the release of TNF-α *in vivo* and *in vitro* in macrophages. Additionally, we observed in this study that FK866 induced NAD^+ rises or inhibited NAD^+ turnover in M1-like but not in M2-like (chapter 3) macrophages suggesting a fundamental difference in NAD^+ homeostasis between the two subsets. Further research is required as to how this occurs and also further research needs to be carried out in order to understand whether the differences in NAD^+ homeostasis are related to the effector phenotype. This might open the door for pharmacological studies to achieve the switch between subsets M1-like to M2-like macrophages which might be useful for treating diseases that have been associated with one phenotype or another. Finally, according to results reported in chapter 4, the inhibition of IDO by 1D-MT decreased LPS-induced NAD^+ levels while it failed to affect the kynurenine pathway. In fact, IDO exists in two isoforms; IDO1 represents the classical form that is involved in the kynurenine pathway in addition to possessing anti-tumour activity. The two isoforms have been shown to display counter-regulatory roles in different inflammatory settings, mediating the flux between pathways that lead to pro-/anti-inflammatory cytokine production (Opitz *et al*., 2011a; Pilotte *et al*., 2012), understanding the cooperation between IDO1 and IDO2 could be useful strategy in order to characterise macrophage polarisation and thus further work is required to address this issue. Also, the opposing effect of IDO on glycolysis has been recently reported (Eleftheriadis *et al*., 2012). Therefore, future work may seek to understand the NAD^+-IDO axis on glycolysis in primary macrophages.

REFERENCES

References

Aarvak, T., Chabaud, M., Miossec, P. & Natvig, J. B. 1999. IL-17 is produced by some pro-inflammatory Th1/Th0 cells but not by Th2 cells. *J Immunol,* 162, 1246-51.

Abe, E., Miyaura, C., Tanaka, H., Shiina, Y., Kuribayashi, T., Suda, S., Nishii, Y., Deluca, H. F. & Suda, T. 1983. 1 alpha,25-dihydroxyvitamin D3 promotes fusion of mouse alveolar macrophages both by a direct mechanism and by a spleen cell-mediated indirect mechanism. *Proc Natl Acad Sci U S A,* 80**,** 5583-7.

Aksoy, P., Escande, C., White, T. A., Thompson, M., Soares, S., Benech, J. C. & Chini, E. N. 2006a. Regulation of SIRT 1 mediated NAD-dependent deacetylation: a novel role for the multifunctional enzyme CD38. *Biochem Biophys Res Commun,* 349**,** 353-9.

Aksoy, P., White, T. A., Thompson, M. & Chini, E. N. 2006b. Regulation of intracellular levels of NAD: a novel role for CD38. *Biochem Biophys Res Commun,* 345**,** 1386-92.

Aktan, F. 2004. iNOS-mediated nitric oxide production and its regulation. *Life Sci,* 75**,** 639-53.

Al-Abady, Z. N., Durante, B., Moody, A. J. & Billington, R. A. 2013. Large changes in NAD^+ levels associated with CD38 expression during HL-60 cell differentiation. *Biochem Biophys Res Commun,* 442**,** 51-5.

Alappat, L., Valerio, M. & Awad, A. B. 2010. Effect of vitamin D and beta-sitosterol on immune function of macrophages. *Int Immunopharmacol,* 10**,** 1390-6.

Altmeyer, M. & Hottiger, M. O. 2009. Poly(ADP-ribose) polymerase 1 at the crossroad of metabolic stress and inflammation in aging. *Aging (Albany NY),* 1**,** 458-69.

Andersen, H. U., Jorgensen, K. H., Egeberg, J., Mandrup-Poulsen, T. & Nerup, J. 1994. Nicotinamide prevents interleukin-1 effects on accumulated insulin release and nitric oxide production in rat islets of Langerhans. *Diabetes,* 43**,** 770-7.

Anderson, C. F. & Mosser, D. M. 2002. A novel phenotype for an activated macrophage: the type 2 activated macrophage. *J Leukoc Biol,* 72**,** 101-6.

Anderson, R. M., Bitterman, K. J., Wood, J. G., Medvedik, O. & Sinclair, D. A. 2003. Nicotinamide and PNC1 govern lifespan extension by calorie restriction in Saccharomyces cerevisiae. *Nature,* 423**,** 181-185.

Andersson, U. & Tracey, K. J. 2011. HMGB1 is a therapeutic target for sterile inflammation and infection. *Annu Rev Immunol,* 29**,** 139-62.

Arend, W. P., Malyak, M., Guthridge, C. J. & Gabay, C. 1998. Interleukin-1 receptor antagonist: role in biology. *Annu Rev Immunol,* 16**,** 27-55.

Armstrong, L., Godinho, S. I., Uppington, K. M., Whittington, H. A. & Millar, A. B. 2006. Contribution of TNF-alpha converting enzyme and proteinase-3 to TNF-alpha processing in human alveolar macrophages. *Am J Respir Cell Mol Biol,* 34**,** 219-25.

Arner, P. 2006. Visfatin--a true or false trail to type 2 diabetes mellitus. *J Clin Endocrinol Metab,* 91**,** 28-30.

Artemov, D., Bhujwalla, Z. M., Pilatus, U. & Glickson, J. D. 1998. Two-compartment model for determination of glycolytic rates of solid tumors by in vivo 13C NMR spectroscopy. *NMR Biomed,* 11**,** 395-404.

Auwerx, J. 1991. The human leukemia cell line, THP-1: a multifacetted model for the study of monocyte-macrophage differentiation. *Experientia,* 47**,** 22-31.

Babior, B. M. 1999. NADPH oxidase: an update. *Blood,* 93**,** 1464-76.

Bai, P. & Virág, L. 2012. Role of poly(ADP-ribose) polymerases in the regulation of inflammatory processes. *FEBS Letters,* 586**,** 3771-3777.

Ball, H. J., Sanchez-Perez, A., Weiser, S., Austin, C. J., Astelbauer, F., Miu, J., Mcquillan, J. A., Stocker, R., Jermiin, L. S. & Hunt, N. H. 2007. Characterization of an indoleamine 2,3-dioxygenase-like protein found in humans and mice. *Gene,* 396**,** 203-13.

Baranowska-Bosiacka, I., Machalinski, B. & Tarasiuk, J. 2005. The purine nucleotide content in human leukemia cell lines. *Cell Mol Biol Lett,* 10**,** 217-26.

Basset, C., Holton, J., O'mahony, R. & Roitt, I. 2003. Innate immunity and pathogen-host interaction. *Vaccine,* 21 Suppl 2**,** S12-23.

Bazil, V. 1995. Physiological enzymatic cleavage of leukocyte membrane molecules. *Immunol Today,* 16**,** 135-40.

Beckers, A., Organe, S., Timmermans, L., Vanderhoydonc, F., Deboel, L., Derua, R., Waelkens, E., Brusselmans, K., Verhoeven, G. & Swinnen, J. V. 2006. Methotrexate enhances the antianabolic and antiproliferative effects of 5-aminoimidazole-4-carboxamide riboside. *Mol Cancer Ther,* 5**,** 2211-7.

Bedard, K. & Krause, K. H. 2007. The NOX family of ROS-generating NADPH oxidases: physiology and pathophysiology. *Physiol Rev,* 87**,** 245-313.

Belenky, P., Bogan, K. L. & Brenner, C. 2007. NAD^+ metabolism in health and disease. *Trends Biochem Sci,* 32**,** 12-9.

Bell, E. L. & Guarente, L. 2011. The SirT3 divining rod points to oxidative stress. *Mol Cell,* 42**,** 561-8.

Bell, J. H., Herrera, A. H., Li, Y. & Walcheck, B. 2007. Role of ADAM17 in the ectodomain shedding of TNF-alpha and its receptors by neutrophils and macrophages. *J Leukoc Biol,* 82**,** 173-6.

Berger, F., Lau, C., Dahlmann, M. & Ziegler, M. 2005. Subcellular compartmentation and differential catalytic properties of the three human nicotinamide mononucleotide adenylyltransferase isoforms. *J Biol Chem,* 280**,** 36334-41.

Berger, F., Lau, C. & Ziegler, M. 2007. Regulation of poly(ADP-ribose) polymerase 1 activity by the phosphorylation state of the nuclear NAD biosynthetic enzyme NMN adenylyl transferase 1. *Proc Natl Acad Sci U S A,* 104**,** 3765-70.

Berger, F., Ramirez-Hernandez, M. H. & Ziegler, M. 2004. The new life of a centenarian: signalling functions of NAD(P). *Trends Biochem Sci,* 29**,** 111-8.

Berger, N. A. 1985. Poly(ADP-ribose) in the cellular response to DNA damage. *Radiat Res,* 101**,** 4-15.

Beutler, B. & Rietschel, E. T. 2003. Innate immune sensing and its roots: the story of endotoxin. *Nat Rev Immunol,* 3**,** 169-76.

Bieganowski, P. & Brenner, C. 2004. Discoveries of nicotinamide riboside as a nutrient and conserved NRK genes establish a Preiss-Handler independent route to NAD^+ in fungi and humans. *Cell,* 117**,** 495-502.

Billington, R. A., Travelli, C., Ercolano, E., Galli, U., Roman, C. B., Grolla, A. A., Canonico, P. L., Condorelli, F. & Genazzani, A. A. 2008. Characterization of NAD uptake in mammalian cells. *J Biol Chem,* 283**,** 6367-74.

Bingle, L., Brown, N. J. & Lewis, C. E. 2002. The role of tumour-associated macrophages in tumour progression: implications for new anticancer therapies. *J Pathol,* 196**,** 254-65.

Bingle, L., Lewis, C. E., Corke, K. P., Reed, M. W. & Brown, N. J. 2006. Macrophages promote angiogenesis in human breast tumour spheroids in vivo. *Br J Cancer,* 94**,** 101-7.

Bitterman, K. J., Anderson, R. M., Cohen, H. Y., Latorre-Esteves, M. & Sinclair, D. A. 2002. Inhibition of silencing and accelerated aging by nicotinamide, a putative negative regulator of yeast sir2 and human SIRT1. *J Biol Chem,* 277**,** 45099-107.

Black, R. A., Rauch, C. T., Kozlosky, C. J., Peschon, J. J., Slack, J. L., Wolfson, M. F., Castner, B. J., Stocking, K. L., Reddy, P., Srinivasan, S., Nelson, N., Boiani, N., Schooley, K. A., Gerhart, M., Davis, R., Fitzner, J. N., Johnson, R. S., Paxton, R. J., March, C. J. & Cerretti, D. P. 1997. A metalloproteinase disintegrin that releases tumour-necrosis factor-alpha from cells. *Nature,* 385**,** 729-33.

Boasso, A., Vaccari, M., Fuchs, D., Hardy, A. W., Tsai, W.-P., Tryniszewska, E., Shearer, G. M. & Franchini, G. 2009. Combined Effect of Antiretroviral Therapy and Blockade of IDO in SIV-Infected Rhesus Macaques. *J Immunol,* 182**,** 4313-4320.

Bogan, K. L. & Brenner, C. 2008. Nicotinic acid, nicotinamide, and nicotinamide riboside: a molecular evaluation of NAD^+ precursor vitamins in human nutrition. *Annu Rev Nutr,* 28**,** 115-30.

Borregaard, N. & Herlin, T. 1982. Energy metabolism of human neutrophils during phagocytosis. *J Clin Invest,* 70**,** 550-7.

Bosisio, D., Polentarutti, N., Sironi, M., Bernasconi, S., Miyake, K., Webb, G. R., Martin, M. U., Mantovani, A. & Muzio, M. 2002. Stimulation of toll-like receptor 4 expression in human mononuclear phagocytes by interferon-gamma: a molecular basis for priming and synergism with bacterial lipopolysaccharide. *Blood,* 99**,** 3427-31.

Bouma, G. & Strober, W. 2003. The immunological and genetic basis of inflammatory bowel disease. *Nat Rev Immunol,* 3**,** 521-33.

Bowlby, S. C., Thomas, M. J., D'agostino, R. B., Jr. & Kridel, S. J. 2012. Nicotinamide phosphoribosyl transferase (Nampt) is required for de novo lipogenesis in tumor cells. *PLoS One,* 7**,** e40195.

Bozza, M., Satoskar, A. R., Lin, G., Lu, B., Humbles, A. A., Gerard, C. & David, J. R. 1999. Targeted disruption of migration inhibitory factor gene reveals its critical role in sepsis. *J Exp Med,* 189**,** 341-6.

Brachmann, C. B., Sherman, J. M., Devine, S. E., Cameron, E. E., Pillus, L. & Boeke, J. D. 1995. The SIR2 gene family, conserved from bacteria to humans, functions in silencing, cell cycle progression, and chromosome stability. *Genes Dev,* 9**,** 2888-902.

Braidy, N., Guillemin, G. J. & Grant, R. 2011. Effects of Kynurenine Pathway Inhibition on NAD^+ Metabolism and Cell Viability in Human Primary Astrocytes and Neurons. *Int J Tryptophan Res,* 4**,** 29-37.

Braun, D., Longman, R. S. & Albert, M. L. 2005. A two-step induction of indoleamine 2,3 dioxygenase (IDO) activity during dendritic-cell maturation. *Blood,* 106**,** 2375-81.

Bruzzone, S., Fruscione, F., Morando, S., Ferrando, T., Poggi, A., Garuti, A., D'urso, A., Selmo, M., Benvenuto, F., Cea, M., Zoppoli, G., Moran, E., Soncini, D., Ballestrero, A., Sordat, B., Patrone, F., Mostoslavsky, R., Uccelli, A. & Nencioni, A. 2009. Catastrophic NAD^+ depletion in activated T lymphocytes through Nampt inhibition reduces demyelination and disability in EAE. *PLoS One,* 4**,** e7897.

Bruzzone, S., Moreschi, I., Guida, L., Usai, C., Zocchi, E. & De Flora, A. 2006. Extracellular NAD^+ regulates intracellular calcium levels and induces activation of human granulocytes. *Biochem J,* 393**,** 697-704.

Busca, A., Saxena, M., Iqbal, S., Angel, J. & Kumar, A. 2014. PI3K/Akt regulates survival during differentiation of human macrophages by maintaining NF-kappaB-dependent expression of antiapoptotic Bcl-xL. *J Leukoc Biol,* 96**,** 1011-22.

Busso, N., Karababa, M., Nobile, M., Rolaz, A., van Gool, F., Galli, M., Leo, O., So, A. & De Smedt, T. 2008. Pharmacological inhibition of nicotinamide phosphoribosyltransferase/visfatin enzymatic activity identifies a new inflammatory pathway linked to NAD. *PLoS One,* 3**,** e2267.

Buttgereit, F., Burmester, G. R. & Brand, M. D. 2000. Bioenergetics of immune functions: fundamental and therapeutic aspects. *Immunol Today,* 21**,** 192-9.

Byles, V., Covarrubias, A. J., Ben-Sahra, I., Lamming, D. W., Sabatini, D. M., Manning, B. D. & Horng, T. 2013. The TSC-mTOR pathway regulates macrophage polarization. *Nat Commun,* 4**,** 2834.

Calandra, T., Echtenacher, B., Roy, D. L., Pugin, J., Metz, C. N., Hultner, L., Heumann, D., Mannel, D., Bucala, R. & Glauser, M. P. 2000. Protection from septic shock by neutralization of macrophage migration inhibitory factor. *Nat Med,* 6**,** 164-70.

Calder, P. C. 1995. Fuel utilization by cells of the immune system. *Proc Nutr Soc,* 54**,** 65-82.

Canto, C. & Auwerx, J. 2012. Targeting sirtuin 1 to improve metabolism: all you need is $NAD(^+)$? *Pharmacol Rev,* 64**,** 166-87.

Canto, C., Gerhart-Hines, Z., Feige, J. N., Lagouge, M., Noriega, L., Milne, J. C., Elliott, P. J., Puigserver, P. & Auwerx, J. 2009. AMPK regulates energy expenditure by modulating NAD^+ metabolism and SIRT1 activity. *Nature,* 458**,** 1056-1060.

Carlsen, H. S., Baekkevold, E. S., Morton, H. C., Haraldsen, G. & Brandtzaeg, P. 2004. Monocyte-like and mature macrophages produce CXCL13 (B cell–attracting chemokine 1) in inflammatory lesions with lymphoid neogenesis. *Blood,* 104**,** 3021-3027.

Carta, S., Tassi, S., Pettinati, I., Delfino, L., Dinarello, C. A. & Rubartelli, A. 2011. The Rate of Interleukin-1β Secretion in Different Myeloid Cells Varies with the Extent of Redox Response to Toll-like Receptor Triggering. *The Journal of Biological Chemistry,* 286**,** 27069-27080.

Cavaillon, J. M. 2011. The historical milestones in the understanding of leukocyte biology initiated by Elie Metchnikoff. *J Leukoc Biol,* 90**,** 413-24.

Chalkiadaki, A. & Guarente, L. 2012. Sirtuins mediate mammalian metabolic responses to nutrient availability. *Nat Rev Endocrinol,* 8**,** 287-96.

Chanmee, T., Ontong, P., Konno, K. & Itano, N. 2014. Tumor-associated macrophages as major players in the tumor microenvironment. *Cancers (Basel),* 6**,** 1670-90.

Chávez-Galán, L., Olleros, M. L., Vesin, D. & Garcia, I. 2015. Much More than M1 and M2 Macrophages, There are also CD169(+) and TCR(+) Macrophages. *Frontiers in Immunology,* 6**,** 263.

Chawla, A., Nguyen, K. D. & Goh, Y. P. S. 2011. Macrophage-mediated inflammation in metabolic disease. *Nature Reviews. Immunology,* 11**,** 738-749.

Chen, C., Pore, N., Behrooz, A., Ismail-Beigi, F. & Maity, A. 2001. Regulation of glut1 mRNA by hypoxia-inducible factor-1. Interaction between H-ras and hypoxia. *J Biol Chem,* 276**,** 9519-25.

Chen L, B. I., Feld J, Sun J, Tannis Ll, Coltescu C, Heathcote J, Edwards Am, Mcgilvray Id. 2005. Hepatic gene expression discriminates responders and nonresponders in treatment of chronic hepatitis C viral infection. *Gastroenterology.,* 128(5):**,** 1437-44.

Chen, Z. J. 2005. Ubiquitin signalling in the NF-kappaB pathway. *Nat Cell Biol,* 7**,** 758-65.

Chiarugi, A., Dolle, C., Felici, R. & Ziegler, M. 2012. The NAD^+ metabolome [mdash] a key determinant of cancer cell biology. *Nat Rev Cancer,* 12**,** 741-752.

Clark, J. B., Ferris, G. M. & Pinder, S. 1971. Inhibition of nuclear NAD nucleosidase and poly ADP-ribose polymerase activity from rat liver by nicotinamide and 5'-methyl nicotinamide. *Biochim Biophys Acta,* 238**,** 82-5.

Classen, A., Lloberas, J. & Celada, A. 2009. Macrophage activation: classical versus alternative. *Methods Mol Biol,* 531**,** 29-43.

Cleeter, M. W., Cooper, J. M., Darley-Usmar, V. M., Moncada, S. & Schapira, A. H. 1994. Reversible inhibition of cytochrome c oxidase, the terminal enzyme of the mitochondrial respiratory chain, by nitric oxide. Implications for neurodegenerative diseases. *FEBS Lett,* 345**,** 50-4.

Clementi, E., Brown, G. C., Feelisch, M. & Moncada, S. 1998. Persistent inhibition of cell respiration by nitric oxide: crucial role of S-nitrosylation of mitochondrial complex I and protective action of glutathione. *Proc Natl Acad Sci U S A,* 95**,** 7631-6.

Collart, M. A., Baeuerle, P. & Vassalli, P. 1990. Regulation of tumor necrosis factor alpha transcription in macrophages: involvement of four kappa B-like motifs and of constitutive and inducible forms of NF-kappa B. *Mol Cell Biol,* 10**,** 1498-506.

Collins, S. J. 1987. The HL-60 promyelocytic leukemia cell line: proliferation, differentiation, and cellular oncogene expression. *Blood,* 70**,** 1233-44.

Conte, D., Holcik, M., Lefebvre, C. A., Lacasse, E., Picketts, D. J., Wright, K. E. & Korneluk, R. G. 2006. Inhibitor of apoptosis protein cIAP2 is essential for lipopolysaccharide-induced macrophage survival. *Mol Cell Biol,* 26**,** 699-708.

Cousins, R. J., Blanchard, R. K., Popp, M. P., Liu, L., Cao, J., Moore, J. B. & Green, C. L. 2003. A global view of the selectivity of zinc deprivation and excess on genes expressed in human THP-1 mononuclear cells. *Proc Natl Acad Sci U S A,* 100**,** 6952-7.

Coussens, A., Timms, P. M., Boucher, B. J., Venton, T. R., Ashcroft, A. T., Skolimowska, K. H., Newton, S. M., Wilkinson, K. A., Davidson, R. N., Griffiths, C. J., Wilkinson, R. J. & Martineau, A. R. 2009. 1alpha,25-dihydroxyvitamin D3 inhibits matrix metalloproteinases induced by Mycobacterium tuberculosis infection. *Immunol,* 127**,** 539-48.

Cramer, T., Yamanishi, Y., Clausen, B. E., Forster, I., Pawlinski, R., Mackman, N., Haase, V. H., Jaenisch, R., Corr, M., Nizet, V., Firestein, G. S., Gerber, H. P., Ferrara, N. & Johnson, R. S. 2003. HIF-1alpha is essential for myeloid cell-mediated inflammation. *Cell,* 112**,** 645-57.

Cross, A. R. & Jones, O. T. 1986. The effect of the inhibitor diphenylene iodonium on the superoxide-generating system of neutrophils. Specific labelling of a component polypeptide of the oxidase. *Biochem J,* 237**,** 111-6.

Daigneault, M., Preston, J. A., Marriott, H. M., Whyte, M. K. & Dockrell, D. H. 2010. The identification of markers of macrophage differentiation in PMA-stimulated THP-1 cells and monocyte-derived macrophages. *PLoS One,* 5**,** e8668.

Dali-Youcef, N., Lagouge, M., Froelich, S., Koehl, C., Schoonjans, K. & Auwerx, J. 2007. Sirtuins: the 'magnificent seven', function, metabolism and longevity. *Ann Med,* 39**,** 335-45.

Delmastro-Greenwood, M. M. & Piganelli, J. D. 2013. Changing the energy of an immune response. *Am J Clin Exp Immunol,* 2**,** 30-54.

Delude, R. L., Fenton, M. J., Savedra, R., Jr., Perera, P. Y., Vogel, S. N., Thieringer, R. & Golenbock, D. T. 1994. CD14-mediated translocation of nuclear factor-kappa B induced by lipopolysaccharide does not require tyrosine kinase activity. *J Biol Chem,* 269**,** 22253-60.

Denko, N. C. 2008. Hypoxia, HIF1 and glucose metabolism in the solid tumour. *Nat Rev Cancer,* 8**,** 705-713.

Dietl, K., Renner, K., Dettmer, K., Timischl, B., Eberhart, K., Dorn, C., Hellerbrand, C., Kastenberger, M., Kunz-Schughart, L. A., Oefner, P. J., Andreesen, R., Gottfried, E. & Kreutz, M. P. 2010. Lactic acid and acidification inhibit TNF secretion and glycolysis of human monocytes. *J Immunol,* 184**,** 1200-9.

Djano, J., Griffin, B., Van Bruggen, I. & Mcmenamin, P. G. 1999. Environmental scanning electron microscopic study of macrophages associated with the tunica vasculosa lentis in the developing rat eye. *Brit J Ophthalmol,* 83**,** 1384-1385.

Drach, J., Mcqueen, T., Engel, H., Andreeff, M., Robertson, K. A., Collins, S. J., Malavasi, F. & Mehta, K. 1994. Retinoic acid-induced expression of CD38 antigen in myeloid cells is mediated through retinoic acid receptor-alpha. *Cancer Res,* 54**,** 1746-52.

Drapier, J. C. & Hibbs, J. B., Jr. 1988. Differentiation of murine macrophages to express nonspecific cytotoxicity for tumor cells results in L-arginine-dependent inhibition of mitochondrial iron-sulfur enzymes in the macrophage effector cells. *J Immunol,* 140**,** 2829-38.

Drexler, S. K., Kong, P. L., Wales, J. & Foxwell, B. M. 2008. Cell signalling in macrophages, the principal innate immune effector cells of rheumatoid arthritis. *Arthritis Res Ther,* 10**,** 216.

Eleftheriadis, T., Pissas, G., Karioti, A., Antoniadi, G., Liakopoulos, V., Dafopoulou, K., Pournaras, S., Koukoulis, G. & Stefanidis, I. 2012. The indoleamine 2,3-dioxygenase inhibitor 1-methyl-tryptophan suppresses mitochondrial function, induces aerobic glycolysis and decreases interleukin-10 production in human lymphocytes. *Immunol Invest,* 41**,** 507-20.

Elliott, G. & Rechsteiner, M. 1975. Pyridine nucleotide metabolism in mitotic cells. *J Cell Physiol,* 86 Suppl 2**,** 641-51.

Emanuelli, M., Carnevali, F., Saccucci, F., Pierella, F., Amici, A., Raffaelli, N. & Magni, G. 2001. Molecular cloning, chromosomal localization, tissue mRNA levels, bacterial expression, and enzymatic properties of human NMN adenylyltransferase. *J Biol Chem,* 276**,** 406-12.

Fedele, G., Frasca, L., Palazzo, R., Ferrero, E., Malavasi, F. & Ausiello, C. M. 2004. CD38 is expressed on human mature monocyte-derived dendritic cells and is functionally involved in CD83 expression and IL-12 induction. *Eur J Immunol,* 34**,** 1342-50.

Feldmann, M., Brennan, F. M. & Maini, R. N. 1996. Role of cytokines in rheumatoid arthritis. *Annu Rev Immunol,* 14**,** 397-440.

Fernandes, C. A., Fievez, L., Neyrinck, A. M., Delzenne, N. M., Bureau, F. & Vanbever, R. 2012. Sirtuin inhibition attenuates the production of inflammatory cytokines in lipopolysaccharide-stimulated macrophages. *Biochem Biophys Res Commun,* 420**,** 857-61.

Ferrero, E. & Malavasi, F. 1997. Human CD38, a leukocyte receptor and ectoenzyme, is a member of a novel eukaryotic gene family of nicotinamide adenine dinucleotide+-converting enzymes: extensive structural homology with the genes for murine bone marrow stromal cell antigen 1 and aplysian ADP-ribosyl cyclase. *J Immunol,* 159**,** 3858-65.

Fiers, W., Beyaert, R., Declercq, W. & Vandenabeele, P. 1999. More than one way to die: apoptosis, necrosis and reactive oxygen damage. *Oncogene,* 18**,** 7719-30.

Finlay, B. B. & Mcfadden, G. 2006. Anti-immunology: evasion of the host immune system by bacterial and viral pathogens. *Cell,* 124**,** 767-82.

Finnin, M., Hamilton, J. A. & Moss, S. T. 1999. Characterization of a CSF-induced proliferating subpopulation of human peripheral blood monocytes by surface marker expression and cytokine production. *J Leukoc Biol,* 66**,** 953-60.

Fleit, H. B. & Kobasiuk, C. D. 1991. The human monocyte-like cell line THP-1 expresses Fc gamma RI and Fc gamma RII. *J Leukoc Biol,* 49**,** 556-65.

Fliegert, R., Gasser, A. & Guse, A. H. 2007. Regulation of calcium signalling by adenine-based second messengers. *Biochem Soc Trans,* 35**,** 109-14.

Foey, A. D. 2015. Macrophage Polarisation: A collaboration of Differentiation, Activation and Pre-Programming? *J Clin Cell Immunol* 6:293.

Foey, A. D. & Brennan, F. M. 2004. Conventional protein kinase C and atypical protein kinase Czeta differentially regulate macrophage production of tumour necrosis factor-alpha and interleukin-10. *Immunol,* 112**,** 44-53.

Foey, A. D. & Crean, S. 2013. Macrophage subset sensitivity to endotoxin tolerisation by Porphyromonas gingivalis. *PLoS One,* 8**,** e67955.

Forman, H. J. & Torres, M. 2001. Redox signaling in macrophages. *Mol Aspects Med,* 22**,** 189-216.

Forman, H. J. & Torres, M. 2002. Reactive oxygen species and cell signaling: respiratory burst in macrophage signaling. *Am J Respir Crit Care Med,* 166**,** S4-8.

Frasca, L., Fedele, G., Deaglio, S., Capuano, C., Palazzo, R., Vaisitti, T., Malavasi, F. & Ausiello, C. M. 2006. CD38 orchestrates migration, survival, and Th1 immune response of human mature dendritic cells. *Blood,* 107**,** 2392-9.

Freemerman, A. J., Johnson, A. R., Sacks, G. N., Milner, J. J., Kirk, E. L., Troester, M. A., Macintyre, A. N., Goraksha-Hicks, P., Rathmell, J. C. & Makowski, L. 2014. Metabolic reprogramming of macrophages: glucose transporter 1 (GLUT1)-mediated glucose metabolism drives a proinflammatory phenotype. *J Biol Chem,* 289**,** 7884-96.

Friebe, D., Neef, M., Kratzsch, J., Erbs, S., Dittrich, K., Garten, A., Petzold-Quinque, S., Bluher, S., Reinehr, T., Stumvoll, M., Bluher, M., Kiess, W. & Korner, A. 2011. Leucocytes are a major source of circulating nicotinamide phosphoribosyltransferase (NAMPT)/pre-B cell colony (PBEF)/visfatin linking obesity and inflammation in humans. *Diabetologia,* 54**,** 1200-11.

Frumento, G., Rotondo, R., Tonetti, M., Damonte, G., Benatti, U. & Ferrara, G. B. 2002. Tryptophan-derived catabolites are responsible for inhibition of T and natural killer cell proliferation induced by indoleamine 2,3-dioxygenase. *J Exp Med,* 196**,** 459-68.

Fujigaki, S., Saito, K., Sekikawa, K., Tone, S., Takikawa, O., Fujii, H., Wada, H., Noma, A. & Seishima, M. 2001. Lipopolysaccharide induction of indoleamine 2,3-dioxygenase is mediated dominantly by an IFN-γ-independent mechanism. *Eur J Immunol,* 31**,** 2313-2318.

Fukata, M., Vamadevan, A. S. & Abreu, M. T. 2009. Toll-like receptors (TLRs) and Nod-like receptors (NLRs) in inflammatory disorders. *Semin Immunol,* 21**,** 242-53.

Fukuhara, A., Matsuda, M., Nishizawa, M., Segawa, K., Tanaka, M., Kishimoto, K., Matsuki, Y., Murakami, M., Ichisaka, T., Murakami, H., Watanabe, E., Takagi, T., Akiyoshi, M., Ohtsubo, T., Kihara, S., Yamashita, S., Makishima, M., Funahashi, T., Yamanaka, S., Hiramatsu, R., Matsuzawa, Y. & Shimomura, I. 2005. Visfatin: a protein secreted by visceral fat that mimics the effects of insulin. *Science,* 307**,** 426-30.

Fukuzawa, M., Satoh, J., Muto, G., Muto, Y., Nishimura, S., Miyaguchi, S., Qiang, X. L. & Toyota, T. 1997. Inhibitory effect of nicotinamide on in vitro and in vivo production of tumor necrosis factor-alpha. *Immunol Lett,* 59**,** 7-11.

Fulco, M., Schiltz, R. L., Iezzi, S., King, M. T., Zhao, P., Kashiwaya, Y., Hoffman, E., Veech, R. L. & Sartorelli, V. 2003. Sir2 regulates skeletal muscle differentiation as a potential sensor of the redox state. *Mol Cell,* 12**,** 51-62.

Funaro, A., Spagnoli, G. C., Ausiello, C. M., Alessio, M., Roggero, S., Delia, D., Zaccolo, M. & Malavasi, F. 1990. Involvement of the multilineage CD38 molecule in a unique pathway of cell activation and proliferation. *J Immunol,* 145**,** 2390-6.

Gaffney, E. V., Dell'aquila, M. L., Lingenfelter, S. E., Huffnagle, G. B. & Wiest, D. L. 1986. Characterization of a colony-stimulating factor produced by the human monocytic leukemia cell line, THP-1. *J Leukoc Biol,* 39**,** 409-21.

Galli, M., van Gool, F., Rongvaux, A., Andris, F. & Leo, O. 2010. The nicotinamide phosphoribosyltransferase: a molecular link between metabolism, inflammation, and cancer. *Cancer Res,* 70**,** 8-11.

Galvan-Pena, S. & O'neill, L. A. 2014. Metabolic reprograming in macrophage polarization. *Front Immunol,* 5**,** 420.

Garten, A., Petzold, S., Korner, A., Imai, S. & Kiess, W. 2009. Nampt: linking NAD biology, metabolism and cancer. *Trends Endocrinol Metab,* 20**,** 130-8.

Gearing, A. J., Beckett, P., Christodoulou, M., Churchill, M., Clements, J., Davidson, A. H., Drummond, A. H., Galloway, W. A., Gilbert, R., Gordon, J. L. & Et Al. 1994. Processing of tumour necrosis factor-alpha precursor by metalloproteinases. *Nature,* 370**,** 555-7.

Geppert, T. D., Whitehurst, C. E., Thompson, P. & Beutler, B. 1994. Lipopolysaccharide signals activation of tumor necrosis factor biosynthesis through the ras/raf-1/MEK/MAPK pathway. *Mol Med,* 1**,** 93-103.

Gessani, S., Testa, U., Varano, B., Di Marzio, P., Borghi, P., Conti, L., Barberi, T., Tritarelli, E., Martucci, R., Seripa, D. & Et Al. 1993. Enhanced production of LPS-induced cytokines during differentiation of human monocytes to macrophages. Role of LPS receptors. *J Immunol,* 151**,** 3758-66.

Gibbs, D. F., Warner, R. L., Weiss, S. J., Johnson, K. J. & Varani, J. 1999. Characterization of matrix metalloproteinases produced by rat alveolar macrophages. *Am J Respir Cell Mol Biol,* 20**,** 1136-44.

Goerdt, S. & Orfanos, C. E. 1999. Other functions, other genes: alternative activation of antigen-presenting cells. *Immunity,* 10**,** 137-42.

Gordon, S. 2003. Alternative activation of macrophages. *Nat Rev Immunol,* 3**,** 23-35.

Gordon, S. & Taylor, P. R. 2005. Monocyte and macrophage heterogeneity. *Nat Rev Immunol,* 5**,** 953-64.

Granger, D. L., Hibbs, J. B., Jr., Perfect, J. R. & Durack, D. T. 1988. Specific amino acid (L-arginine) requirement for the microbiostatic activity of murine macrophages. *J Clin Invest,* 81**,** 1129-36.

Grant, R. & Kapoor, V. 2003. Inhibition of indoleamine 2,3-dioxygenase activity in IFN-gamma stimulated astroglioma cells decreases intracellular NAD^+ levels. *Biochem Pharmacol,* 66**,** 1033-6.

Grant, R. S. & Kapoor, V. 1998. Murine glial cells regenerate NAD, after peroxide-induced depletion, using either nicotinic acid, nicotinamide, or quinolinic acid as substrates. *J Neurochem,* 70**,** 1759-63.

Green, S. P. & Phillips, W. A. 1994. Activation of the macrophage respiratory burst by phorbol myristate acetate: Evidence for both tyrosine-kinase-dependent and -independent pathways. *Biochimica et Biophysica Acta (BBA) - Mol Cell Res,* 1222**,** 241-248.

Grip, O., Janciauskiene, S. & Lindgren, S. 2003. Macrophages in inflammatory bowel disease. *Curr Drug Targets Inflamm Allergy,* 2**,** 155-60.

Grivennikov, S. I., Tumanov, A. V., Liepinsh, D. J., Kruglov, A. A., Marakusha, B. I., Shakhov, A. N., Murakami, T., Drutskaya, L. N., Forster, I., Clausen, B. E., Tessarollo, L., Ryffel, B., Kuprash, D. V. & Nedospasov, S. A. 2005. Distinct and nonredundant in vivo functions of TNF produced by t cells and macrophages/neutrophils: protective and deleterious effects. *Immunity,* 22**,** 93-104.

Grohmann, U., Fallarino, F. & Puccetti, P. 2003. Tolerance, DCs and tryptophan: much ado about IDO. *Trends Immunol,* 24**,** 242-8.

Guarente, L. 2006. Sirtuins as potential targets for metabolic syndrome. *Nature,* 444**,** 868-74.

Hageman, G. J. & Stierum, R. H. 2001. Niacin, poly(ADP-ribose) polymerase-1 and genomic stability. *Mutat Res/Fundamental and Molecular Mechanisms of Mutagenesis,* 475**,** 45-56.

Haigis, M. C. & Sinclair, D. A. 2010. Mammalian sirtuins: biological insights and disease relevance. *Annu Rev Pathol,* 5**,** 253-95.

Hall, J. A., Dominy, J. E., Lee, Y. & Puigserver, P. 2013. The sirtuin family's role in aging and age-associated pathologies. *The Journal of Clinical Investigation,* 123**,** 973-979.

Hara, N., Yamada, K., Shibata, T., Osago, H. & Tsuchiya, M. 2011. Nicotinamide phosphoribosyltransferase/visfatin does not catalyze nicotinamide mononucleotide formation in blood plasma. *PLoS One,* 6**,** e22781.

Haro, H., Crawford, H. C., Fingleton, B., Shinomiya, K., Spengler, D. M. & Matrisian, L. M. 2000. Matrix metalloproteinase-7-dependent release of tumor necrosis factor-alpha in a model of herniated disc resorption. *J Clin Invest,* 105**,** 143-50.

Haschemi, A., Kosma, P., Gille, L., Evans, C. R., Burant, C. F., Starkl, P., Knapp, B., Haas, R., Schmid, J. A., Jandl, C., Amir, S., Lubec, G., Park, J., Esterbauer, H., Bilban, M., Brizuela, L., Pospisilik, J. A., Otterbein, L. E. & Wagner, O. 2012. The sedoheptulose kinase CARKL directs macrophage polarization through control of glucose metabolism. *Cell Metab,* 15**,** 813-26.

Hasmann, M. & Schemainda, I. 2003. FK866, a highly specific noncompetitive inhibitor of nicotinamide phosphoribosyltransferase, represents a novel mechanism for induction of tumor cell apoptosis. *Cancer Res,* 63**,** 7436-42.

Hassa, P. O. & Hottiger, M. O. 2008. The diverse biological roles of mammalian PARPS, a small but powerful family of poly-ADP-ribose polymerases. *Front Biosci,* 13**,** 3046-82.

Hawley, S. A., Fullerton, M. D., Ross, F. A., Schertzer, J. D., Chevtzoff, C., Walker, K. J., Peggie, M. W., Zibrova, D., Green, K. A., Mustard, K. J., Kemp, B. E., Sakamoto, K., Steinberg, G. R. & Hardie, D. G. 2012. The ancient drug salicylate directly activates AMP-activated protein kinase. *Science,* 336**,** 918-22.

Hegyi, J., Schwartz, R. A. & Hegyi, V. 2004. Pellagra: dermatitis, dementia, and diarrhea. *Int J Dermatol,* 43**,** 1-5.

Hehlgans, T. & Pfeffer, K. 2005. The intriguing biology of the tumour necrosis factor/tumour necrosis factor receptor superfamily: players, rules and the games. *Immunol,* 115**,** 1-20.

Heine, H., Ulmer, A. J., Flad, H. D. & Hauschildt, S. 1995. Lipopolysaccharide-induced change of phosphorylation of two cytosolic proteins in human monocytes is prevented by inhibitors of ADP-ribosylation. *J Immunol,* 155**,** 4899-908.

Heltweg, B., Gatbonton, T., Schuler, A. D., Posakony, J., Li, H., Goehle, S., Kollipara, R., Depinho, R. A., Gu, Y., Simon, J. A. & Bedalov, A. 2006. Antitumor activity of a small-molecule inhibitor of human silent information regulator 2 enzymes. *Cancer Res,* 66**,** 4368-77.

Heltweg, B. & Jung, M. 2002. A microplate reader-based nonisotopic histone deacetylase activity assay. *Anal Biochem,* 302**,** 175-83.

Heyes, M. P., Chen, C. Y., Major, E. O. & Saito, K. 1997. Different kynurenine pathway enzymes limit quinolinic acid formation by various human cell types. *Biochem J,* 326 (Pt 2)**,** 351-6.

Highfill, S. L., Rodriguez, P. C., Zhou, Q., Goetz, C. A., Koehn, B. H., Veenstra, R., Taylor, P. A., Panoskaltsis-Mortari, A., Serody, J. S., Munn, D. H., Tolar, J., Ochoa, A. C. & Blazar, B. R. 2010. Bone marrow myeloid-derived suppressor cells (MDSCs) inhibit graft-versus-host disease (GVHD) via an arginase-1-dependent mechanism that is up-regulated by interleukin-13. *Blood,* 116**,** 5738-47.

Hirata, Y., Tabata, M., Kurobe, H., Motoki, T., Akaike, M., Nishio, C., Higashida, M., Mikasa, H., Nakaya, Y., Takanashi, S., Igarashi, T., Kitagawa, T. & Sata, M. 2011. Coronary Atherosclerosis Is Associated With Macrophage Polarization in Epicardial Adipose Tissue. *J Am Coll Cardiology,* 58**,** 248-255.

Hiromatsu, Y., Sato, M., Tanaka, K., Ishisaka, N., Kamachi, J. & Nonaka, K. 1993. Inhibitory effects of nicotinamide on intercellular adhesion molecule-1 expression on cultured human thyroid cells. *Immunol,* 80**,** 330-2.

Hmama, Z., Nandan, D., Sly, L., Knutson, K. L., Herrera-Velit, P. & Reiner, N. E. 1999. 1alpha,25-dihydroxyvitamin D(3)-induced myeloid cell differentiation is regulated by a vitamin D receptor-phosphatidylinositol 3-kinase signaling complex. *J Exp Med,* 190**,** 1583-94.

Holscher, C., Atkinson, R. A., Arendse, B., Brown, N., Myburgh, E., Alber, G. & Brombacher, F. 2001. A protective and agonistic function of IL-12p40 in mycobacterial infection. *J Immunol,* 167**,** 6957-66.

Hooper, N. M., Karran, E. H. & Turner, A. J. 1997. Membrane protein secretases. *Biochem J,* 321 (Pt 2)**,** 265-79.

Horwitt, M. K., Harvey, C. C., Rothwell, W. S., Cutler, J. L. & Haffron, D. 1956. Tryptophan-Niacin Relationships in Man: Studies with Diets Deficient in Riboflavin and Niacin, Together with Observations on the Excretion of Nitrogen and Niacin Metabolites. *J Nutr,* 60**,** 1-43.

Hou, D. Y., Muller, A. J., Sharma, M. D., Duhadaway, J., Banerjee, T., Johnson, M., Mellor, A. L., Prendergast, G. C. & Munn, D. H. 2007. Inhibition of indoleamine 2,3-dioxygenase in dendritic cells by stereoisomers of 1-methyl-tryptophan correlates with antitumor responses. *Cancer Res,* 67**,** 792-801.

Houtkooper, R. H., Canto, C., Wanders, R. J. & Auwerx, J. 2010. The secret life of NAD^+: an old metabolite controlling new metabolic signaling pathways. *Endocr Rev,* 31**,** 194-223.

Howard, M., Grimaldi, J. C., Bazan, J. F., Lund, F. E., Santos-Argumedo, L., Parkhouse, R. M., Walseth, T. F. & Lee, H. C. 1993. Formation and hydrolysis of cyclic ADP-ribose catalyzed by lymphocyte antigen CD38. *Science,* 262**,** 1056-9.

Huang, C., Wang, Y., Li, D., Li, Y., Luo, J., Yuan, W., Ou, Y., Zhu, C., Zhang, Y., Wang, Z., Liu, M. & Wu, X. 2004. Inhibition of transcriptional activities of AP-1 and c-Jun by a new zinc finger protein ZNF394. *Biochem Biophys Res Commun,* 320**,** 1298-305.

Hume, D. A. 2006. The mononuclear phagocyte system. *Curr Opin Immunol,* 18**,** 49-53.

Hussain, A. M., Lee, H. C. & Chang, C. F. 2000. Modulation of CD157 expression in multi-lineage myeloid differentiation of promyelocytic cell lines. *Eur J Cell Biol,* 79**,** 697-706.

Iqbal, J. & Zaidi, M. 2006. TNF regulates cellular NAD^+ metabolism in primary macrophages. *Biochem Biophys Res Commun,* 342**,** 1312-8.

Iqbal, J. & Zaidi, M. 2007. CD38 is required for priming by TNF-alpha: a mechanism for extracellular coordination of cell fate. *Am J Physiol Renal Physiol,* 292**,** F1283-90.

Ismair, M. G., Ries, C., Lottspeich, F., Zang, C., Kolb, H. J. & Petrides, P. E. 1998. Autocrine regulation of matrix metalloproteinase-9 gene expression and secretion by tumor necrosis factor-alpha (TNF-alpha) in NB4 leukemic cells: specific involvement of TNF receptor type 1. *Leukemia,* 12**,** 1136-43.

Iwasaki, A. & Medzhitov, R. 2004. Toll-like receptor control of the adaptive immune responses. *Nat Immunol,* 5**,** 987-95.

Jackson, M. D. & Denu, J. M. 2002. Structural identification of 2'- and 3'-O-acetyl-ADP-ribose as novel metabolites derived from the Sir2 family of beta -NAD^+-dependent histone/protein deacetylases. *J Biol Chem,* 277**,** 18535-44.

Jacobson, E. L., Dame, A. J., Pyrek, J. S. & Jacobson, M. K. 1995. Evaluating the role of niacin in human carcinogenesis. *Biochimie,* 77**,** 394-8.

Janeway, C. A., Jr. 1989. Approaching the asymptote? Evolution and revolution in immunology. *Cold Spring Harb Symp Quant Biol,* 54 Pt 1**,** 1-13.

Janeway, C. A., Jr. & Medzhitov, R. 2002. Innate immune recognition. *Annu Rev Immunol,* 20**,** 197-216.

Jantsch, J., Chakravortty, D., Turza, N., Prechtel, A. T., Buchholz, B., Gerlach, R. G., Volke, M., Glasner, J., Warnecke, C., Wiesener, M. S., Eckardt, K. U., Steinkasserer, A., Hensel, M. &

Willam, C. 2008. Hypoxia and hypoxia-inducible factor-1 alpha modulate lipopolysaccharide-induced dendritic cell activation and function. *J Immunol,* 180**,** 4697-705.

Jensen, J. C., Buresh, C. & Norton, J. A. 1990. Lactic acidosis increases tumor necrosis factor secretion and transcription in *vitro*. *J Surg Res,* 49**,** 350-3.

Jha, A. K., Huang, S. C., Sergushichev, A., Lampropoulou, V., Ivanova, Y., Loginicheva, E., Chmielewski, K., Stewart, K. M., Ashall, J., Everts, B., Pearce, E. J., Driggers, E. M. & Artyomov, M. N. 2015. Network integration of parallel metabolic and transcriptional data reveals metabolic modules that regulate macrophage polarization. *Immunity,* 42**,** 419-30.

Jiang, H., Khan, S., Wang, Y., Charron, G., He, B., Sebastian, C., Du, J., Kim, R., Ge, E., Mostoslavsky, R., Hang, H. C., Hao, Q. & Lin, H. 2013. SIRT6 regulates TNF-alpha secretion through hydrolysis of long-chain fatty acyl lysine. *Nature,* 496**,** 110-3.

Jing, E., Gesta, S. & Kahn, C. R. 2007. SIRT2 regulates adipocyte differentiation through FoxO1 acetylation/deacetylation. *Cell Metab,* 6**,** 105-14.

Jones, R. G., Plas, D. R., Kubek, S., Buzzai, M., Mu, J., Xu, Y., Birnbaum, M. J. & Thompson, C. B. 2005. AMP-activated protein kinase induces a p53-dependent metabolic checkpoint. *Mol Cell,* 18**,** 283-93.

Joos, L. & Tamm, M. 2005. Breakdown of pulmonary host defense in the immunocompromised host: cancer chemotherapy. *Proc Am Thorac Soc,* 2**,** 445-8.

Jounai, N., Kobiyama, K., Takeshita, F. & Ishii, K. J. 2012. Recognition of damage-associated molecular patterns related to nucleic acids during inflammation and vaccination. *Front Cell Infect Microbiol,* 2**,** 168.

Jung, I. D., Lee, C.-M., Jeong, Y.-I., Lee, J. S., Park, W. S., Han, J. & Park, Y.-M. 2007. Differential regulation of indoleamine 2,3-dioxygenase by lipopolysaccharide and interferon gamma in murine bone marrow derived dendritic cells. *FEBS Letters,* 581**,** 1449-1456.

Kabelitz, D. & Medzhitov, R. 2007. Innate immunity--cross-talk with adaptive immunity through pattern recognition receptors and cytokines. *Curr Opin Immunol,* 19**,** 1-3.

Karin, M. 2009. NF-kappaB as a critical link between inflammation and cancer. *Cold Spring Harb Perspect Biol,* 1**,** a000141.

Karin, M. & Lin, A. 2002. NF-kappaB at the crossroads of life and death. *Nat Immunol,* 3**,** 221-7.

Kaul, N. & Forman, H. J. 1996. Activation of NF kappa B by the respiratory burst of macrophages. *Free Radic Biol Med,* 21**,** 401-5.

Kawahara, T. L., Michishita, E., Adler, A. S., Damian, M., Berber, E., Lin, M., Mccord, R. A., Ongaigui, K. C., Boxer, L. D., Chang, H. Y. & Chua, K. F. 2009. SIRT6 links histone H3 lysine 9 deacetylation to NF-kappaB-dependent gene expression and organismal life span. *Cell,* 136**,** 62-74.

Kawai, T. & Akira, S. 2007. Signaling to NF-kappaB by Toll-like receptors. *Trends Mol Med,* 13**,** 460-9.

Kellett, D. N. 1966. 2-Deoxyglucose and inflammation. *J Pharm Pharmacol,* 18**,** 199-200.

Kelly, B. & O'neill, L. A. 2015. Metabolic reprogramming in macrophages and dendritic cells in innate immunity. *Cell Res,* 25**,** 771-84.

Keuper, M., Jastroch, M., Yi, C. X., Fischer-Posovszky, P., Wabitsch, M., Tschop, M. H. & Hofmann, S. M. 2014. Spare mitochondrial respiratory capacity permits human adipocytes to maintain ATP homeostasis under hypoglycemic conditions. *Faseb J,* 28**,** 761-70.

Kielian, M. C. & Cohn, Z. A. 1981. Phorbol myristate acetate stimulates phagosome-lysosome fusion in mouse macrophages. *J Exp Med,* 154**,** 101-11.

Kim, J. W., Tchernyshyov, I., Semenza, G. L. & Dang, C. V. 2006. HIF-1-mediated expression of pyruvate dehydrogenase kinase: a metabolic switch required for cellular adaptation to hypoxia. *Cell Metab,* 3**,** 177-85.

Kim, K. U., Kwon, O. J. & Jue, D. M. 1993. Pro-tumour necrosis factor cleavage enzyme in macrophage membrane/particulate. *Immunol,* 80**,** 134-9.

Kim, M. Y., Zhang, T. & Kraus, W. L. 2005. Poly(ADP-ribosyl)ation by PARP-1: 'PAR-laying' NAD^+ into a nuclear signal. *Genes Dev,* 19**,** 1951-67.

Kim, Y. S., Morgan, M. J., Choksi, S. & Liu, Z. G. 2007. TNF-induced activation of the Nox1 NADPH oxidase and its role in the induction of necrotic cell death. *Mol Cell,* 26**,** 675-87.

Kinne, R. W., Bräuer, R., Stuhlmüller, B., Palombo-Kinne, E. & Burmester, G.-R. 2000. Macrophages in rheumatoid arthritis. *Arthrit Res,* 2**,** 189-202.

Kirkland, J. B. 2009. Niacin status, NAD distribution and ADP-ribose metabolism. *Curr Pharm Des,* 15**,** 3-11.

Kizaki, M., Norman, A., Bishop, J., Lin, C., Karmakar, A. & Koeffler, H. 1991. 1,25-Dihydroxyvitamin D3 receptor RNA: expression in hematopoietic cells. *Blood,* 77**,** 1238-1247.

Kobayashi, T., Robinson, J. M. & Seguchi, H. 1998. Identification of intracellular sites of superoxide production in stimulated neutrophils. *J Cell Sci,* 111**,** 81-91.

Koch-Nolte, F., Haag, F., Guse, A. H., Lund, F. & Ziegler, M. 2009. Emerging roles of NAD^+ and its metabolites in cell signaling. *Sci Signal,* 2**,** mr1.

Kohro, T., Tanaka, T., Murakami, T., Wada, Y., Aburatani, H., Hamakubo, T. & Kodama, T. 2004. A comparison of differences in the gene expression profiles of phorbol 12-myristate 13-acetate differentiated THP-1 cells and human monocyte-derived macrophage. *J Atheroscler Thromb,* 11**,** 88-97.

Krausgruber, T., Blazek, K., Smallie, T., Alzabin, S., Lockstone, H., Sahgal, N., Hussell, T., Feldmann, M. & Udalova, I. A. 2011. IRF5 promotes inflammatory macrophage polarization and TH1-TH17 responses. *Nat Immunol,* 12**,** 231-8.

Krauss, S., Brand, M. D. & Buttgereit, F. 2001. Signaling takes a breath--new quantitative perspectives on bioenergetics and signal transduction. *Immunity,* 15**,** 497-502.

Krawczyk, C. M., Holowka, T., Sun, J., Blagih, J., Amiel, E., Deberardinis, R. J., Cross, J. R., Jung, E., Thompson, C. B., Jones, R. G. & Pearce, E. J. 2010. Toll-like receptor-induced changes in glycolytic metabolism regulate dendritic cell activation. *Blood,* 115**,** 4742-9.

Kudo, Y. & Boyd, C. a. R. 2000. Human placental indoleamine 2,3-dioxygenase: cellular localization and characterization of an enzyme preventing fetal rejection. *Biochimica et Biophysica Acta (BBA) - Molecular Basis of Disease,* 1500**,** 119-124.

Kwidzinski, E., Bunse, J., Aktas, O., Richter, D., Mutlu, L., Zipp, F., Nitsch, R. & Bechmann, I. 2005. Indolamine 2,3-dioxygenase is expressed in the CNS and down-regulates autoimmune inflammation. *Faseb J,* 19**,** 1347-9.

Lacy-Hulbert, A. & Moore, K. J. 2006. Designer macrophages: oxidative metabolism fuels inflammation repair. *Cell Metab,* 4**,** 7-8.

Lambrecht, B. N. 2006. Alveolar macrophage in the driver's seat. *Immunity,* 24**,** 366-8.

Lan, F., Cacicedo, J. M., Ruderman, N. & Ido, Y. 2008. SIRT1 modulation of the acetylation status, cytosolic localization, and activity of LKB1. Possible role in AMP-activated protein kinase activation. *J Biol Chem,* 283**,** 27628-35.

Land, S. C. & Tee, A. R. 2007. Hypoxia-inducible factor 1alpha is regulated by the mammalian target of rapamycin (mTOR) via an mTOR signaling motif. *J Biol Chem,* 282, 20534-43.

Landry, J., Slama, J. T. & Sternglanz, R. 2000a. Role of NAD(+) in the deacetylase activity of the SIR2-like proteins. *Biochem Biophys Res Commun,* 278, 685-90.

Landry, J., Sutton, A., Tafrov, S. T., Heller, R. C., Stebbins, J., Pillus, L. & Sternglanz, R. 2000b. The silencing protein SIR2 and its homologs are NAD-dependent protein deacetylases. *Proc Natl Acad Sci U S A,* 97, 5807-11.

Lau, C., Niere, M. & Ziegler, M. 2009. The NMN/NaMN adenylyltransferase (NMNAT) protein family. *Front Biosci* (Landmark Ed), 14, 410-31.

Leclaire, R. D., Kell, W., Bavari, S., Smith, T. J. & Hunt, R. E. 1996. Protective effects of niacinamide in staphylococcal enterotoxin-B-induced toxicity. *Toxicology,* 107, 69-81.

Lee, H. C. 2006. Structure and enzymatic functions of human CD38. *Mol Med,* 12, 317-23.

Lee, J., Ryu, H., Ferrante, R. J., Morris, S. M., Jr. & Ratan, R. R. 2003. Translational control of inducible nitric oxide synthase expression by arginine can explain the arginine paradox. *Proc Natl Acad Sci U S A,* 100, 4843-8.

Lee, J. C. & Young, P. R. 1996. Role of CSB/p38/RK stress response kinase in LPS and cytokine signaling mechanisms. *J Leukoc Biol,* 59**,** 152-7.

Lee, S. I., Park, K. H., Kim, S. J., Kang, Y. G., Lee, Y. M. & Kim, E. C. 2012. Mechanical stress-activated immune response genes via Sirtuin 1 expression in human periodontal ligament cells. *Clin Exp Immunol,* 168**,** 113-24.

Lee, Y.-K., Lee, H. B., Shin, D.-M., Kang, M. J., Yi, E. C., Noh, S., Lee, J., Lee, C., Min, C.-K. & Choi, E. Y. 2014. Heme-binding-mediated negative regulation of the tryptophan metabolic enzyme indoleamine 2,3-dioxygenase 1 (IDO1) by IDO2. *Exp Mol Med,* 46**,** e121.

Legutko, A., Lekeux, P. And Bureau, F. 2009. NAD^+-Consuming Enzymes in the Regulation of Lung Immune Responses. *The Open Immunol J,* 2, 42-51.

Legutko, A., Marichal, T., Fievez, L., Bedoret, D., Mayer, A., De Vries, H., Klotz, L., Drion, P. V., Heirman, C., Cataldo, D., Louis, R., Thielemans, K., Andris, F., Leo, O., Lekeux, P., Desmet, C. J. & Bureau, F. 2011. Sirtuin 1 promotes Th2 responses and airway allergy by repressing peroxisome proliferator-activated receptor-gamma activity in dendritic cells. *J Immunol,* 187**,** 4517-29.

Leonardo, M. R., Dailly, Y. & Clark, D. P. 1996. Role of NAD in regulating the adhE gene of Escherichia coli. *J Bacteriol,* 178**,** 6013-8.

Levesque, M. C., Chen, Y., Beasley, B. E., O'loughlin, C. W., Gockerman, J. P., Moore, J. O. & Weinberg, J. B. 2006. Chronic lymphocytic leukemia cell CD38 expression and inducible nitric oxide synthase expression are associated with serum IL-4 levels. *Leuk Res,* 30**,** 24-8.

Li, L. L. & Dinauer 1998. Reconstitution of NADPH oxidase activity in human X-linked chronic granulomatous disease myeloid cells after stable gene transfer using a recombinant adeno-associated virus 2 vector. *Blood Cells Mol Dis,* 24**,** 522-38.

Li, Y., Zhang, Y., Dorweiler, B., Cui, D., Wang, T., Woo, C. W., Brunkan, C. S., Wolberger, C., Imai, S. & Tabas, I. 2008. Extracellular Nampt promotes macrophage survival via a nonenzymatic interleukin-6/STAT3 signaling mechanism. *J Biol Chem,* 283**,** 34833-43.

Lim, J. H., Lee, Y. M., Chun, Y. S., Chen, J., Kim, J. E. & Park, J. W. 2010. Sirtuin 1 modulates cellular responses to hypoxia by deacetylating hypoxia-inducible factor 1alpha. *Mol Cell,* 38**,** 864-78.

Liu, G. & Yang, H. 2013. Modulation of macrophage activation and programming in immunity. *J Cell Physiol,* 228**,** 502-12.

Liu, T. F., Vachharajani, V. T., Yoza, B. K. & Mccall, C. E. 2012. NAD^+-dependent sirtuin 1 and 6 proteins coordinate a switch from glucose to fatty acid oxidation during the acute inflammatory response. *J Biol Chem,* 287**,** 25758-69.

Liu, T. F., Yoza, B. K., El Gazzar, M., Vachharajani, V. T. & Mccall, C. E. 2011. NAD^+-dependent SIRT1 deacetylase participates in epigenetic reprogramming during endotoxin tolerance. *J Biol Chem,* 286**,** 9856-64.

Liu, Y., Stewart, K. N., Bishop, E., Marek, C. J., Kluth, D. C., Rees, A. J. & Wilson, H. M. 2008. Unique expression of suppressor of cytokine signaling 3 is essential for classical macrophage activation in rodents in vitro and in vivo. *J Immunol,* 180**,** 6270-8.

Livak, K. J. & Schmittgen, T. D. 2001. Analysis of relative gene expression data using real-time quantitative PCR and the 2(-Delta Delta C(T)) Method. *Methods,* 25**,** 402-8.

Livneh, E. & Fishman, D. D. 1997. Linking protein kinase C to cell-cycle control. *Eur J Biochem,* 248**,** 1-9.

Lob, S., Konigsrainer, A., Schafer, R., Rammensee, H. G., Opelz, G. & Terness, P. 2008. Levo- but not dextro-1-methyl tryptophan abrogates the IDO activity of human dendritic cells. *Blood,* 111**,** 2152-4.

Locasale, J. W. & Cantley, L. C. 2011. Metabolic flux and the regulation of mammalian cell growth. *Cell Metab,* 14**,** 443-51.

Lombard, D. B., Alt, F. W., Cheng, H. L., Bunkenborg, J., Streeper, R. S., Mostoslavsky, R., Kim, J., Yancopoulos, G., Valenzuela, D., Murphy, A., Yang, Y., Chen, Y., Hirschey, M. D., Bronson, R. T., Haigis, M., Guarente, L. P., Farese, R. V., Jr., Weissman, S., Verdin, E. & Schwer, B. 2007. Mammalian Sir2 homolog SIRT3 regulates global mitochondrial lysine acetylation. *Mol Cell Biol,* 27**,** 8807-14.

Lopez-Castejon, G., Baroja-Mazo, A. & Pelegrin, P. 2011. Novel macrophage polarization model: from gene expression to identification of new anti-inflammatory molecules. *Cell Mol Life Sci,* 68**,** 3095-107.

Louis, J., Himmelrich, H., Parra-Lopez, C., Tacchini-Cottier, F. & Launois, P. 1998. Regulation of protective immunity against Leishmania major in mice. *Curr Opin Immunol,* 10**,** 459-64.

Lu, W., Hu, Y., Chen, G., Chen, Z., Zhang, H., Wang, F., Feng, L., Pelicano, H., Wang, H., Keating, M. J., Liu, J., Mckeehan, W., Wang, H., Luo, Y. & Huang, P. 2012. Novel role of NOX in supporting aerobic glycolysis in cancer cells with mitochondrial dysfunction and as a potential target for cancer therapy. *PLoS Biol,* 10**,** e1001326.

Luk, T., Malam, Z. & Marshall, J. C. 2008. Pre-B cell colony-enhancing factor (PBEF)/visfatin: a novel mediator of innate immunity. *J Leukoc Biol,* 83**,** 804-16.

Lund, F., Solvason, N., Grimaldi, J. C., Parkhouse, R. M. & Howard, M. 1995. Murine CD38: an immunoregulatory ectoenzyme. *Immunol Today,* 16**,** 469-73.

Lund, F. E. 2006. Signaling properties of CD38 in the mouse immune system: enzyme-dependent and -independent roles in immunity. *Mol Med,* 12**,** 328-33.

Magni, G., Amici, A., Emanuelli, M., Orsomando, G., Raffaelli, N. & Ruggieri, S. 2004. Enzymology of NAD^+ homeostasis in man. *Cell Mol Life Sci,* 61**,** 19-34.

Magni, G., Amici, A., Emanuelli, M., Raffaelli, N. & Ruggieri, S. 1999. Enzymology of NAD^+ synthesis. *Adv Enzymol Relat Areas Mol Biol,* 73**,** 135-82, xi.

Magni, G., Orsomando, G., Raffelli, N. & Ruggieri, S. 2008. Enzymology of mammalian NAD^+ metabolism in health and disease. *Front Biosci,* 13**,** 6135-54.

Malam, Z., Parodo, J., Waheed, F., Szaszi, K., Kapus, A. & Marshall, J. C. 2011. Pre-B cell colony-enhancing factor (PBEF/Nampt/visfatin) primes neutrophils for augmented respiratory burst activity through partial assembly of the NADPH oxidase. *J Immunol,* 186**,** 6474-84.

Malavasi, F., Deaglio, S., Ferrero, E., Funaro, A., Sancho, J., Ausiello, C. M., Ortolan, E., Vaisitti, T., Zubiaur, M., Fedele, G., Aydin, S., Tibaldi, E. V., Durelli, I., Lusso, R., Cozno, F. & Horenstein, A. L. 2006. CD38 and CD157 as receptors of the immune system: a bridge between innate and adaptive immunity. *Mol Med,* 12**,** 334-41.

Malavasi, F., Deaglio, S., Funaro, A., Ferrero, E., Horenstein, A. L., Ortolan, E., Vaisitti, T. & Aydin, S. 2008. Evolution and Function of the ADP Ribosyl Cyclase/CD38 Gene Family in Physiology and Pathology. *Physiol Rev*. 88 , 841-886.

Mangelsdorf, D. J., Koeffler, H. P., Donaldson, C. A., Pike, J. W. & Haussler, M. R. 1984. 1,25-Dihydroxyvitamin D3-induced differentiation in a human promyelocytic leukemia cell line (HL-60): receptor-mediated maturation to macrophage-like cells. *J Cell Biol,* 98**,** 391-8.

Mantovani, A., Schioppa, T., Porta, C., Allavena, P. & Sica, A. 2006. Role of tumor-associated macrophages in tumor progression and invasion. *Cancer Metastasis Rev,* 25**,** 315-22.

Mantovani, A., Sica, A., Sozzani, S., Allavena, P., Vecchi, A. & Locati, M. 2004. The chemokine system in diverse forms of macrophage activation and polarization. *Trends Immunol,* 25**,** 677-86.

Mantovani, A., Sozzani, S., Locati, M., Allavena, P. & Sica, A. 2002. Macrophage polarization: tumor-associated macrophages as a paradigm for polarized M2 mononuclear phagocytes. *Trends Immunol,* 23**,** 549-55.

Martin, M., Schifferle, R. E., Cuesta, N., Vogel, S. N., Katz, J. & Michalek, S. M. 2003. Role of the phosphatidylinositol 3 kinase-Akt pathway in the regulation of IL-10 and IL-12 by Porphyromonas gingivalis lipopolysaccharide. *J Immunol,* 171**,** 717-25.

Martinez, F. O., Helming, L. & Gordon, S. 2009. Alternative activation of macrophages: an immunologic functional perspective. *Annu Rev Immunol,* 27**,** 451-83.

Maruotti, N., Cantatore, F. P., Crivellato, E., Vacca, A. & Ribatti, D. 2007. Macrophages in rheumatoid arthritis. *Histol Histopathol,* 22**,** 581-6.

Matzinger, P. 2002. The danger model: a renewed sense of self. *Science,* 296**,** 301-5.

Mcgeehan, G. M., Becherer, J. D., Bast, R. C., Boyer, C. M., Champion, B., Connolly, K. M., Conway, J. G., Furdon, P., Karp, S., Kidao, S., Mcelroy, A. B., Nichols, J., Pryzwansky, K. M., Schoenen, F., Sekut, L., Truesdale, A., Verghese, M., Warner, J. & Ways, J. P. 1994. Regulation of tumour necrosis factor-[alpha] processing by a metalloproteinase inhibitor. *Nature,* 370**,** 558-561.

Mcinnes, I. B., Leung, B. P., Sturrock, R. D., Field, M. & Liew, F. Y. 1997. Interleukin-15 mediates T cell-dependent regulation of tumor necrosis factor-alpha production in rheumatoid arthritis. *Nat Med,* 3**,** 189-95.

Mcgettrick, A. F. & O'neill, L. A. 2013. How metabolism generates signals during innate immunity and inflammation. *J Biol Chem,* 288**,** 22893-8.

Medzhitov, R. 2001. Toll-like receptors and innate immunity. *Nat Rev Immunol,* 1**,** 135-45.

Medzhitov, R. & Janeway, C., Jr. 2000. Innate immunity. *N Engl J Med,* 343**,** 338-44.

Mehta, K., Shahid, U. & Malavasi, F. 1996. Human CD38, a cell-surface protein with multiple functions. *Faseb J,* 10**,** 1408-17.

Meissner, F., Molawi, K. & Zychlinsky, A. 2008. Superoxide dismutase 1 regulates caspase-1 and endotoxic shock. *Nat Immunol,* 9**,** 866-72.

Mellor, A. 2005. Indoleamine 2,3 dioxygenase and regulation of T cell immunity. *Biochem Biophys Res Commun,* 338**,** 20-4.

Mellor, A. L. & Munn, D. H. 1999. Tryptophan catabolism and T-cell tolerance: immunosuppression by starvation? *Immunol Today,* 20**,** 469-73.

Mellor, A. L. & Munn, D. H. 2004. IDO expression by dendritic cells: tolerance and tryptophan catabolism. *Nat Rev Immunol,* 4**,** 762-74.

Meng, F. & Lowell, C. A. 1997. Lipopolysaccharide (LPS)-induced macrophage activation and signal transduction in the absence of Src-family kinases Hck, Fgr, and Lyn. *J Exp Med,* 185**,** 1661-70.

Menju, M., Tajima, S. & Yamamoto, A. 1989. Expression of the Apolipoprotein E Gene in a Human Macrophage-Like Cell Line, THP. *J Biochem,* 106**,** 505-510.

Metz, R., Duhadaway, J. B., Kamasani, U., Laury-Kleintop, L., Muller, A. J. & Prendergast, G. C. 2007. Novel tryptophan catabolic enzyme IDO2 is the preferred biochemical target of the antitumor indoleamine 2,3-dioxygenase inhibitory compound D-1-methyl-tryptophan. *Cancer Res,* 67**,** 7082-7.

Michan, S. & Sinclair, D. 2007. Sirtuins in mammals: insights into their biological function. *Biochem J,* 404**,** 1-13.

Michishita, E., Park, J. Y., Burneskis, J. M., Barrett, J. C. & Horikawa, I. 2005. Evolutionarily conserved and nonconserved cellular localizations and functions of human SIRT proteins. *Mol Biol Cell,* 16**,** 4623-35.

Miesel, R., Murphy, M. P. & Kroger, H. 1996. Enhanced mitochondrial radical production in patients which rheumatoid arthritis correlates with elevated levels of tumor necrosis factor alpha in plasma. *Free Radic Res,* 25**,** 161-9.

Mills, C. D., Kincaid, K., Alt, J. M., Heilman, M. J. & Hill, A. M. 2000. M-1/M-2 macrophages and the Th1/Th2 paradigm. *J Immunol,* 164**,** 6166-73.

Mills, C. D., Shearer, J., Evans, R. & Caldwell, M. D. 1992. Macrophage arginine metabolism and the inhibition or stimulation of cancer. *J Immunol,* 149**,** 2709-14.

Mohler, K. M., Sleath, P. R., Fitzner, J. N., Cerretti, D. P., Alderson, M., Kerwar, S. S., Torranee, D. S., Otten-Evans, C., Greenstreet, T., Weerawarna, K., Kronheim, S. R., Petersen, M., Gerhart, M., Kozlosky, C. J., March, C. J. & Black, R. A. 1994. Protection against a lethal dose of endotoxin by an inhibitor of tumour necrosis factor processing. *Nature,* 370**,** 218-220.

Mole, D. R., Blancher, C., Copley, R. R., Pollard, P. J., Gleadle, J. M., Ragoussis, J. & Ratcliffe, P. J. 2009. Genome-wide association of hypoxia-inducible factor (HIF)-1alpha and HIF-2alpha DNA binding with expression profiling of hypoxia-inducible transcripts. *J Biol Chem,* 284**,** 16767-75.

Moss, M. L., Jin, S. L., Milla, M. E., Bickett, D. M., Burkhart, W., Carter, H. L., Chen, W. J., Clay, W. C., Didsbury, J. R., Hassler, D., Hoffman, C. R., Kost, T. A., Lambert, M. H., Leesnitzer, M. A., Mccauley, P., Mcgeehan, G., Mitchell, J., Moyer, M., Pahel, G., Rocque, W., Overton, L. K., Schoenen, F., Seaton, T., Su, J. L., Becherer, J. D. & Et Al. 1997. Cloning of a disintegrin metalloproteinase that processes precursor tumour-necrosis factor-alpha. *Nature,* 385**,** 733-6.

Mosser, D. M. 2003. The many faces of macrophage activation. *J Leukoc Biol,* 73**,** 209-12.

Mosser, D. M. & Edwards, J. P. 2008. Exploring the full spectrum of macrophage activation. *Nat Rev Immunol,* 8**,** 958-69.

Mulherin, D., Fitzgerald, O. & Bresnihan, B. 1996. Synovial tissue macrophage populations and articular damage in rheumatoid arthritis. *Arthritis Rheum,* 39**,** 115-24.

Munn, D. H. & Mellor, A. L. 2007. Indoleamine 2,3-dioxygenase and tumor-induced tolerance. *J Clin Invest,* 117**,** 1147-54.

Munn, D. H., Zhou, M., Attwood, J. T., Bondarev, I., Conway, S. J., Marshall, B., Brown, C. & Mellor, A. L. 1998. Prevention of allogeneic fetal rejection by tryptophan catabolism. *Science,* 281**,** 1191-3.

Musso, T., Deaglio, S., Franco, L., Calosso, L., Badolato, R., Garbarino, G., Dianzani, U. & Malavasi, F. 2001. CD38 expression and functional activities are up-regulated by IFN-gamma on human monocytes and monocytic cell lines. *J Leukoc Biol,* 69**,** 605-12.

Nakada-Tsukui, K., Watanabe, N. & Kobayashi, Y. 1999. Regulation of the processing and release of tumor necrosis factor alpha in a human macrophage cell line. *J Leukoc Biol,* 66**,** 968-73.

Nakamaru, Y., Vuppusetty, C., Wada, H., Milne, J. C., Ito, M., Rossios, C., Elliot, M., Hogg, J., Kharitonov, S., Goto, H., Bemis, J. E., Elliott, P., Barnes, P. J. & Ito, K. 2009. A protein deacetylase SIRT1 is a negative regulator of metalloproteinase-9. *Faseb J,* 23**,** 2810-9.

Nathan, C. F. & Hibbs, J. B. 1991. Role of nitric oxide synthesis in macrophage antimicrobial activity. *Curr Opin Immunol,* 3**,** 65-70.

Nau, G. J., Richmond, J. F., Schlesinger, A., Jennings, E. G., Lander, E. S. & Young, R. A. 2002. Human macrophage activation programs induced by bacterial pathogens. *Proc Natl Acad Sci U S A,* 99**,** 1503-8.

Newsholme, P., Curi, R., Gordon, S. & Newsholme, E. A. 1986. Metabolism of glucose, glutamine, long-chain fatty acids and ketone bodies by murine macrophages. *Biochem J,* 239**,** 121-5.

Newsholme, P., Gordon, S. & Newsholme, E. A. 1987. Rates of utilization and fates of glucose, glutamine, pyruvate, fatty acids and ketone bodies by mouse macrophages. *Biochem J,* 242**,** 631-6.

Niederer, F., Ospelt, C., Brentano, F., Hottiger, M. O., Gay, R. E., Gay, S., Detmar, M. & Kyburz, D. 2011. SIRT1 overexpression in the rheumatoid arthritis synovium contributes to proinflammatory cytokine production and apoptosis resistance. *Ann Rheum Dis,* 70**,** 1866-73.

Nikiforov, A., Kulikova, V. & Ziegler, M. 2015. The human NAD metabolome: Functions, metabolism and compartmentalization. *Crit Revi Biochem Mol Biol***,** 1-14.

Nishizuka, Y. 1995. Protein kinase C and lipid signaling for sustained cellular responses. *Faseb J,* 9**,** 484-96.

O'neill, L. a. J. 2006. How Toll-like receptors signal: what we know and what we don't know. *C CurrOpin Immunol,* 18**,** 3-9.

O'neill, L. a. J., Kishton, R. J. & Rathmell, J. 2016. A guide to immunometabolism for immunologists. *Nat Rev Immunol,* 16**,** 553-565.

Odegaard, J. I., Ricardo-Gonzalez, R. R., Goforth, M. H., Morel, C. R., Subramanian, V., Mukundan, L., Red Eagle, A., Vats, D., Brombacher, F., Ferrante, A. W. & Chawla, A. 2007. Macrophage-specific PPARgamma controls alternative activation and improves insulin resistance. *Nature,* 447**,** 1116-20.

Okuyama, Y., Ishihara, K., Kimura, N., Hirata, Y., Sato, K., Itoh, M., Ok, L. B. & Hirano, T. 1996. Human BST-1 expressed on myeloid cells functions as a receptor molecule. *Biochem Biophys Res Commun,* 228**,** 838-45.

Olesen, U. H., Christensen, M. K., Bjorkling, F., Jaattela, M., Jensen, P. B., Sehested, M. & Nielsen, S. J. 2008. Anticancer agent CHS-828 inhibits cellular synthesis of NAD. *Biochem Biophys Res Commun,* 367**,** 799-804.

Olesen, U. H., Thougaard, A. V., Jensen, P. B. & Sehested, M. 2010. A preclinical study on the rescue of normal tissue by nicotinic acid in high-dose treatment with APO866, a specific nicotinamide phosphoribosyltransferase inhibitor. *Mol Cancer Ther,* 9**,** 1609-17.

Oliver, F. J., Menissier-De Murcia, J., Nacci, C., Decker, P., Andriantsitohaina, R., Muller, S., De La Rubia, G., Stoclet, J. C. & De Murcia, G. 1999. Resistance to endotoxic shock as a consequence of defective NF-kappaB activation in poly (ADP-ribose) polymerase-1 deficient mice. *EMBO J,* 18**,** 4446-54.

Opitz, C. A., Litzenburger, U. M., Opitz, U., Sahm, F., Ochs, K., Lutz, C., Wick, W. & Platten, M. 2011a. The indoleamine-2,3-dioxygenase (IDO) inhibitor 1-methyl-D-tryptophan upregulates IDO1 in human cancer cells. *PLoS One,* 6**,** e19823.

Opitz, C. A., Litzenburger, U. M., Sahm, F., Ott, M., Tritschler, I., Trump, S., Schumacher, T., Jestaedt, L., Schrenk, D., Weller, M., Jugold, M., Guillemin, G. J., Miller, C. L., Lutz, C., Radlwimmer, B., Lehmann, I., Von Deimling, A., Wick, W. & Platten, M. 2011b. An endogenous tumour-promoting ligand of the human aryl hydrocarbon receptor. *Nature,* 478**,** 197-203.

Orabona, C., Puccetti, P., Vacca, C., Bicciato, S., Luchini, A., Fallarino, F., Bianchi, R., Velardi, E., Perruccio, K., Velardi, A., Bronte, V., Fioretti, M. C. & Grohmann, U. 2006. Toward the identification of a tolerogenic signature in IDO-competent dendritic cells. *Blood,* 107**,** 2846-54.

Paine, A. J., Allen, C. M., Durkacz, B. W. & Shall, S. 1982. Evidence that poly(ADP-ribose) polymerase is involved in the loss of NAD from cultured rat liver cells. *Biochem J,* 202**,** 551-3.

Pallotta, M. T., Orabona, C., Volpi, C., Vacca, C., Belladonna, M. L., Bianchi, R., Servillo, G., Brunacci, C., Calvitti, M., Bicciato, S., Mazza, E. M. C., Boon, L., Grassi, F., Fioretti, M. C., Fallarino, F., Puccetti, P. & Grohmann, U. 2011. Indoleamine 2,3-dioxygenase is a signaling protein in long-term tolerance by dendritic cells. *Nat Immunol,* 12**,** 870-878.

Pantel, A., Teixeira, A., Haddad, E., Wood, E. G., Steinman, R. M. & Longhi, M. P. 2014. Direct Type I IFN but Not MDA5/TLR3 Activation of Dendritic Cells Is Required for Maturation and Metabolic Shift to Glycolysis after Poly IC Stimulation. *PLoS Biol,* 12**,** e1001759.

Papadakis, K. A. & Targan, S. R. 2000. Tumor necrosis factor: biology and therapeutic inhibitors. *Gastroenterology,* 119**,** 1148-57.

Papandreou, I., Cairns, R. A., Fontana, L., Lim, A. L. & Denko, N. C. 2006. HIF-1 mediates adaptation to hypoxia by actively downregulating mitochondrial oxygen consumption. *Cell Metab,* 3**,** 187-97.

Parameswaran, N. & Patial, S. 2010. Tumor necrosis factor-alpha signaling in macrophages. *Crit Rev Eukaryot Gene Expr,* 20**,** 87-103.

Park, H. S., Jung, H. Y., Park, E. Y., Kim, J., Lee, W. J. & Bae, Y. S. 2004. Cutting edge: direct interaction of TLR4 with NAD(P)H oxidase 4 isozyme is essential for lipopolysaccharide-induced production of reactive oxygen species and activation of NF-kappa B. *J Immunol,* 173**,** 3589-93.

Partida-Sanchez, S., Goodrich, S., Kusser, K., Oppenheimer, N., Randall, T. D. & Lund, F. E. 2004. Regulation of dendritic cell trafficking by the ADP-ribosyl cyclase CD38: impact on the development of humoral immunity. *Immunity,* 20**,** 279-91.

Pawlus, M. R. & Hu, C. J. 2013. Enhanceosomes as integrators of hypoxia inducible factor (HIF) and other transcription factors in the hypoxic transcriptional response. *Cell Signal,* 25**,** 1895-903.

Pearce, E. L. 2010. Metabolism in T cell activation and differentiation. *Curr Opin Immunol,* 22**,** 314-20.

Pearce, Erika l. & Pearce, Edward j. 2013. Metabolic Pathways in Immune Cell Activation and Quiescence. *Immunity,* 38**,** 633-643.

Pearce, E. L., Poffenberger, M. C., Chang, C.-H. & Jones, R. G. 2013a. Fueling Immunity: Insights into Metabolism and Lymphocyte Function. *Science,* 342.

Peschon, J. J., Slack, J. L., Reddy, P., Stocking, K. L., Sunnarborg, S. W., Lee, D. C., Russell, W. E., Castner, B. J., Johnson, R. S., Fitzner, J. N., Boyce, R. W., Nelson, N., Kozlosky, C. J., Wolfson, M. F., Rauch, C. T., Cerretti, D. P., Paxton, R. J., March, C. J. & Black, R. A. 1998. An essential role for ectodomain shedding in mammalian development. *Science,* 282**,** 1281-4.

Pfeiffer, T., Schuster, S. & Bonhoeffer, S. 2001. Cooperation and competition in the evolution of ATP-producing pathways. *Science,* 292**,** 504-7.

Picard, F., Kurtev, M., Chung, N., Topark-Ngarm, A., Senawong, T., Machado De Oliveira, R., Leid, M., Mcburney, M. W. & Guarente, L. 2004. Sirt1 promotes fat mobilization in white adipocytes by repressing PPAR-gamma. *Nature,* 429**,** 771-6.

Pike Winer, L. S. & Wu, M. 2014. Rapid Analysis of Glycolytic and Oxidative Substrate Flux of Cancer Cells in a Microplate. *PLoS ONE,* 9**,** e109916.

Pilotte, L., Larrieu, P., Stroobant, V., Colau, D., Dolusic, E., Frederick, R., De Plaen, E., Uyttenhove, C., Wouters, J., Masereel, B. & Van Den Eynde, B. J. 2012. Reversal of tumoral immune resistance by inhibition of tryptophan 2,3-dioxygenase. *Proc Natl Acad Sci U S A,* 109**,** 2497-502.

Pittelli, M., Formentini, L., Faraco, G., Lapucci, A., Rapizzi, E., Cialdai, F., Romano, G., Moneti, G., Moroni, F. & Chiarugi, A. 2010. Inhibition of nicotinamide phosphoribosyltransferase: cellular bioenergetics reveals a mitochondrial insensitive NAD^+ pool. *J Biol Chem,* 285**,** 34106-14.

Pollard, J. W. 2009. Trophic macrophages in development and disease. *Nat Rev Immunol,* 9**,** 259-70.

Preiss, J. & Handler, P. 1958. Biosynthesis of diphosphopyridine nucleotide. I. Identification of intermediates. *J Biol Chem,* 233**,** 488-92.

Price, N. L., Gomes, A. P., Ling, A. J., Duarte, F. V., Martin-Montalvo, A., North, B. J., Agarwal, B., Ye, L., Ramadori, G., Teodoro, J. S., Hubbard, B. P., Varela, A. T., Davis, J. G., Varamini, B., Hafner, A., Moaddel, R., Rolo, A. P., Coppari, R., Palmeira, C. M., De Cabo, R., Baur, J. A.

& Sinclair, D. A. 2012. SIRT1 is required for AMPK activation and the beneficial effects of resveratrol on mitochondrial function. *Cell Metab,* 15**,** 675-90.

Prieto, J., Eklund, A. & Patarroyo, M. 1994. Regulated expression of integrins and other adhesion molecules during differentiation of monocytes into macrophages. *Cell Immunol,* 156**,** 191-211.

Qin, Z. 2012. The use of THP-1 cells as a model for mimicking the function and regulation of monocytes and macrophages in the vasculature. *Atherosclerosis,* 221**,** 2-11.

Rechsteiner, M., Hillyard, D. & Olivera, B. M. 1976. Turnover at nicotinamide adenine dinucleotide in cultures of human cells. *J Cell Physiol,* 88**,** 207-17.

Reddy, P., Slack, J. L., Davis, R., Cerretti, D. P., Kozlosky, C. J., Blanton, R. A., Shows, D., Peschon, J. J. & Black, R. A. 2000. Functional analysis of the domain structure of tumor necrosis factor-alpha converting enzyme. *J Biol Chem,* 275**,** 14608-14.

Reinherz, E. L., Kung, P. C., Goldstein, G., Levey, R. H. & Schlossman, S. F. 1980. Discrete stages of human intrathymic differentiation: analysis of normal thymocytes and leukemic lymphoblasts of T-cell lineage. *Proc Natl Acad Sci U S A,* 77**,** 1588-92.

Remer, K. A., Brcic, M. & Jungi, T. W. 2003. Toll-like receptor-4 is involved in eliciting an LPS-induced oxidative burst in neutrophils. *Immunol Lett,* 85**,** 75-80.

Revollo, J. R., Grimm, A. A. & Imai, S. 2004. The NAD^+ biosynthesis pathway mediated by nicotinamide phosphoribosyltransferase regulates Sir2 activity in mammalian cells. *J Biol Chem,* 279**,** 50754-63.

Reyes, L., Davidson, M. K., Thomas, L. C. & Davis, J. K. 1999. Effects of Mycoplasma fermentans incognitus on differentiation of THP-1 cells. *Infect Immun,* 67**,** 3188-92.

Riebel, B. R., Gibbs, P. R., Wellborn, W. B. & Bommarius, A. S. 2002. Cofactor Regeneration of NAD^+ from NADH: Novel Water-Forming NADH Oxidases. *Adv Syn Catal,* 344**,** 1156-1168.

Riganti, C., Gazzano, E., Polimeni, M., Costamagna, C., Bosia, A. & Ghigo, D. 2004. Diphenyleneiodonium inhibits the cell redox metabolism and induces oxidative stress. *J Biol Chem,* 279**,** 47726-31.

Rivenzon-Segal, D., Boldin-Adamsky, S., Seger, D., Seger, R. & Degani, H. 2003. Glycolysis and glucose transporter 1 as markers of response to hormonal therapy in breast cancer. *Int J Cancer,* 107**,** 177-82.

Roberts, K. J., Cross, A., Vasieva, O., Moots, R. J. & Edwards, S. W. 2013. Inhibition of pre-B cell colony-enhancing factor (PBEF/NAMPT/visfatin) decreases the ability of human neutrophils to generate reactive oxidants but does not impair bacterial killing. *J Leukoc Biol,* 94**,** 481-92.

Rodriguez-Prados, J. C., Traves, P. G., Cuenca, J., Rico, D., Aragones, J., Martin-Sanz, P., Cascante, M. & Bosca, L. 2010. Substrate fate in activated macrophages: a comparison between innate, classic, and alternative activation. *J Immunol,* 185**,** 605-14.

Rodriguez-Vargas, J. M., Ruiz-Magana, M. J., Ruiz-Ruiz, C., Majuelos-Melguizo, J., Peralta-Leal, A., Rodriguez, M. I., Munoz-Gamez, J. A., De Almodovar, M. R., Siles, E., Rivas, A. L., Jaattela, M. & Oliver, F. J. 2012. ROS-induced DNA damage and PARP-1 are required for optimal induction of starvation-induced autophagy. *Cell Res,* 22**,** 1181-1198.

Rogers, P. D., Thornton, J., Barker, K. S., Mcdaniel, D. O., Sacks, G. S., Swiatlo, E. & Mcdaniel, L. S. 2003. Pneumolysin-dependent and -independent gene expression identified by cDNA microarray analysis of THP-1 human mononuclear cells stimulated by Streptococcus pneumoniae. *Infect Immun,* 71**,** 2087-94.

Rongvaux, A., Andris, F., van Gool, F. & Leo, O. 2003. Reconstructing eukaryotic NAD^+ metabolism. *Bioessays,* 25**,** 683-90.

Rongvaux, A., Galli, M., Denanglaire, S., van Gool, F., Dreze, P. L., Szpirer, C., Bureau, F., Andris, F. & Leo, O. 2008. Nicotinamide phosphoribosyl transferase/pre-B cell colony-enhancing factor/visfatin is required for lymphocyte development and cellular resistance to genotoxic stress. *J Immunol,* 181**,** 4685-95.

Rongvaux, A., Shea, R. J., Mulks, M. H., Gigot, D., Urbain, J., Leo, O. & Andris, F. 2002. Pre-B-cell colony-enhancing factor, whose expression is up-regulated in activated lymphocytes, is a nicotinamide phosphoribosyltransferase, a cytosolic enzyme involved in NAD^+ biosynthesis. *Eur J Immunol,* 32**,** 3225-3234.

Rosendahl, M. S., Ko, S. C., Long, D. L., Brewer, M. T., Rosenzweig, B., Hedl, E., Anderson, L., Pyle, S. M., Moreland, J., Meyers, M. A., Kohno, T., Lyons, D. & Lichenstein, H. S. 1997. Identification and Characterization of a Pro-tumor Necrosis Factor-α-processing Enzyme from the ADAM Family of Zinc Metalloproteases. *J Biol Chem,* 272**,** 24588-24593.

Sadeghi, K., Wessner, B., Laggner, U., Ploder, M., Tamandl, D., Friedl, J., Zügel, U., Steinmeyer, A., Pollak, A., Roth, E., Boltz-Nitulescu, G. & Spittler, A. 2006. Vitamin D3 down-regulates monocyte TLR expression and triggers hyporesponsiveness to pathogen-associated molecular patterns. *EurJ Immunology,* 36**,** 361-370.

Sag, D., Carling, D., Stout, R. D. & Suttles, J. 2008. Adenosine 5'-monophosphate-activated protein kinase promotes macrophage polarization to an anti-inflammatory functional phenotype. *J Immunol,* 181**,** 8633-41.

Salminen, A., Kauppinen, A., Suuronen, T. & Kaarniranta, K. 2008. SIRT1 longevity factor suppresses NF-kappaB -driven immune responses: regulation of aging via NF-kappaB acetylation? *Bioessays,* 30**,** 939-42.

Sanders, B. D., Zhao, K., Slama, J. T. & Marmorstein, R. 2007. Structural basis for nicotinamide inhibition and base exchange in Sir2 enzymes. *Mol Cell,* 25**,** 463-72.

Sanghera, J. S., Weinstein, S. L., Aluwalia, M., Girn, J. & Pelech, S. L. 1996. Activation of multiple proline-directed kinases by bacterial lipopolysaccharide in murine macrophages. *J Immunol,* 156**,** 4457-65.

Sauve, A. A., Wolberger, C., Schramm, V. L. & Boeke, J. D. 2006. The biochemistry of sirtuins. *Annu Rev Biochem,* 75**,** 435-65.

Schadlich, H., Ermann, J., Biskop, M., Falk, W., Sperling, F., Jungel, A., Lehmann, J., Emmrich, F. & Sack, U. 1999. Anti-inflammatory effects of systemic anti-tumour necrosis factor α treatment in human/murine SCID arthritis. *Annals of the Rheumatic Diseases,* 58**,** 428-434.

Scheller, J., Chalaris, A., Schmidt-Arras, D. & Rose-John, S. 2011. The pro- and anti-inflammatory properties of the cytokine interleukin-6. *Biochimica et Biophysica Acta (BBA) - Molecular Cell Research,* 1813**,** 878-888.

Scherberich, J. E., Kellermeyer, M., Ried, C. & Hartinger, A. 2005. 1-alpha-calcidol modulates major human monocyte antigens and toll-like receptors TLR 2 and TLR4 in vitro. *Eur J Med Res,* 10**,** 179-82.

Schilling, E., Wehrhahn, J., Klein, C., Raulien, N., Ceglarek, U. & Hauschildt, S. 2012. Inhibition of nicotinamide phosphoribosyltransferase modifies LPS-induced inflammatory responses of human monocytes. *Innate Immun,* 18**,** 518-30.

Schug, T. T., Xu, Q., Gao, H., Peres-Da-Silva, A., Draper, D. W., Fessler, M. B., Purushotham, A. & Li, X. 2010. Myeloid deletion of SIRT1 induces inflammatory signaling in response to environmental stress. *Mol Cell Biol,* 30**,** 4712-21.

Schwende, H., Fitzke, E., Ambs, P. & Dieter, P. 1996. Differences in the state of differentiation of THP-1 cells induced by phorbol ester and 1,25-dihydroxyvitamin D3. *J Leukoc Biol,* 59**,** 555-61.

Semenza, G. L., Jiang, B. H., Leung, S. W., Passantino, R., Concordet, J. P., Maire, P. & Giallongo, A. 1996. Hypoxia response elements in the aldolase A, enolase 1, and lactate dehydrogenase A gene promoters contain essential binding sites for hypoxia-inducible factor 1. *J Biol Chem,* 271**,** 32529-37.

Semenza, G. L., Nejfelt, M. K., Chi, S. M. & Antonarakis, S. E. 1991. Hypoxia-inducible nuclear factors bind to an enhancer element located 3' to the human erythropoietin gene. *Proc Natl Acad Sci U S A,* 88**,** 5680-4.

Shakhov, A. N., Collart, M. A., Vassalli, P., Nedospasov, S. A. & Jongeneel, C. V. 1990. Kappa B-type enhancers are involved in lipopolysaccharide-mediated transcriptional activation of the tumor necrosis factor alpha gene in primary macrophages. *J Exp Med,* 171**,** 35-47.

Shall, S. 1983. ADP-ribosylation, DNA repair, cell differentiation and cancer. *Princess Takamatsu Symp,* 13**,** 3-25.

Sharif, O., Bolshakov, V. N., Raines, S., Newham, P. & Perkins, N. D. 2007. Transcriptional profiling of the LPS induced NF-kappaB response in macrophages. *BMC Immunol,* 8**,** 1.

Shen, Z., Ajmo, J. M., Rogers, C. Q., Liang, X., Le, L., Murr, M. M., Peng, Y. & You, M. 2009. Role of SIRT1 in regulation of LPS- or two ethanol metabolites-induced TNF-alpha production in cultured macrophage cell lines. *Am J Physiol Gastrointest Liver Physiol,* 296**,** G1047-53.

Shubinsky, G. & Schlesinger, M. 1997. The CD38 lymphocyte differentiation marker: new insight into its ectoenzymatic activity and its role as a signal transducer. *Immunity,* 7**,** 315-24.

Si-Tahar, M., Touqui, L. & Chignard, M. 2009. Innate immunity and inflammation--two facets of the same anti-infectious reaction. *Clin Exp Immunol,* 156**,** 194-8.

Sindrilaru, A., Peters, T., Wieschalka, S., Baican, C., Baican, A., Peter, H., Hainzl, A., Schatz, S., Qi, Y., Schlecht, A., Weiss, J. M., Wlaschek, M., Sunderkotter, C. & Scharffetter-Kochanek, K. 2011. An unrestrained proinflammatory M1 macrophage population induced by iron impairs wound healing in humans and mice. *J Clin Invest,* 121**,** 985-97.

Skidmore, C. J., Davies, M. I., Goodwin, P. M., Halldorsson, H., Lewis, P. J., Shall, S. & Zia'ee, A. A. 1979. The involvement of poly(ADP-ribose) polymerase in the degradation of NAD caused by gamma-radiation and N-methyl-N-nitrosourea. *Eur J Biochem,* 101**,** 135-42.

Skokowa, J., Lan, D., Thakur, B. K., Wang, F., Gupta, K., Cario, G., Brechlin, A. M., Schambach, A., Hinrichsen, L., Meyer, G., Gaestel, M., Stanulla, M., Tong, Q. & Welte, K. 2009. NAMPT is essential for the G-CSF-induced myeloid differentiation via a NAD^+-sirtuin-1-dependent pathway. *Nat Med,* 15**,** 151-158.

Smith, J. S., Brachmann, C. B., Celic, I., Kenna, M. A., Muhammad, S., Starai, V. J., Avalos, J. L., Escalante-Semerena, J. C., Grubmeyer, C., Wolberger, C. & Boeke, J. D. 2000. A phylogenetically conserved NAD^+-dependent protein deacetylase activity in the Sir2 protein family. *Proc Natl Acad Sci U S A,* 97**,** 6658-63.

Smith, J. W., Gamelli, R. L., Jones, S. B. & Shankar, R. 2006. Immunologic responses to critical injury and sepsis. *J Intensive Care Med,* 21**,** 160-72.

Solomon, K. A., Covington, M. B., Decicco, C. P. & Newton, R. C. 1997. The fate of pro-TNF-alpha following inhibition of metalloprotease-dependent processing to soluble TNF-alpha in human monocytes. *J Immunol,* 159**,** 4524-31.

Srivastava, S. 2016. Emerging therapeutic roles for NAD^+ metabolism in mitochondrial and age-related disorders. *Clin Transl Med,* 5**,** 25.

Steinberg, G. R. & Schertzer, J. D. 2014. AMPK promotes macrophage fatty acid oxidative metabolism to mitigate inflammation: implications for diabetes and cardiovascular disease. *Immunol Cell Biol,* 92**,** 340-5.

Stephens, J. M. & Vidal-Puig, A. J. 2006. An update on visfatin/pre-B cell colony-enhancing factor, an ubiquitously expressed, illusive cytokine that is regulated in obesity. *Curr Opin Lipidol,* 17**,** 128-31.

Stevenson, F. T., Bursten, S. L., Fanton, C., Locksley, R. M. & Lovett, D. H. 1993. The 31-kDa precursor of interleukin 1 alpha is myristoylated on specific lysines within the 16-kDa N-terminal propiece. *Proc Natl Acad Sci U S A,* 90**,** 7245-9.

Stockinger, B. & Veldhoen, M. 2007. Differentiation and function of Th17 T cells. *Curr Opin Immunol,* 19**,** 281-6.

Stone, T. W. & Darlington, L. G. 2002. Endogenous kynurenines as targets for drug discovery and development. *Nat Rev Drug Discov,* 1**,** 609-20.

Strauss-Ayali, D., Conrad, S. M. & Mosser, D. M. 2007. Monocyte subpopulations and their differentiation patterns during infection. *J Leukoc Biol,* 82**,** 244-52.

Sun, S. C. & Ley, S. C. 2008. New insights into NF-kappaB regulation and function. *Trends Immunol,* 29**,** 469-78.

Swantek, J. L., Cobb, M. H. & Geppert, T. D. 1997. Jun N-terminal kinase/stress-activated protein kinase (JNK/SAPK) is required for lipopolysaccharide stimulation of tumor necrosis factor alpha (TNF-alpha) translation: glucocorticoids inhibit TNF-alpha translation by blocking JNK/SAPK. *Mol Cell Biol,* 17**,** 6274-82.

Swaroop, J. J., Rajarajeswari, D. & Naidu, J. N. 2012. Association of TNF-α with insulin resistance in type 2 diabetes mellitus. *The Indian Journal of Medical Research,* 135**,** 127-130.

Sweet, M. J. & Hume, D. A. 1996. Endotoxin signal transduction in macrophages. *J Leukoc Biol,* 60**,** 8-26.

Szabo, C. & Dawson, V. L. 1998. Role of poly(ADP-ribose) synthetase in inflammation and ischaemia-reperfusion. *Trends Pharmacol Sci,* 19**,** 287-98.

Takashiba, S., Van Dyke, T. E., Amar, S., Murayama, Y., Soskolne, A. W. & Shapira, L. 1999. Differentiation of monocytes to macrophages primes cells for lipopolysaccharide stimulation via accumulation of cytoplasmic nuclear factor kappaB. *Infect Immun,* 67**,** 5573-8.

Takeuch, O. & Akira, S. 2011. Epigenetic control of macrophage polarization. *Eur J Immunol,* 41**,** 2490-3.

Takikawa, O., Yoshida, R., Kido, R. & Hayaishi, O. 1986. Tryptophan degradation in mice initiated by indoleamine 2,3-dioxygenase. *J Biol Chem,* 261**,** 3648-53.

Tan, B., Young, D. A., Lu, Z. H., Wang, T., Meier, T. I., Shepard, R. L., Roth, K., Zhai, Y., Huss, K., Kuo, M. S., Gillig, J., Parthasarathy, S., Burkholder, T. P., Smith, M. C., Geeganage, S. & Zhao, G. 2013. Pharmacological inhibition of nicotinamide phosphoribosyltransferase (NAMPT), an enzyme essential for NAD^+ biosynthesis, in human cancer cells: metabolic basis and potential clinical implications. *J Biol Chem,* 288**,** 3500-11.

Tanaka, H., Abe, E., Miyaura, C., Shiina, Y. & Suda, T. 1983. 1 alpha,25-dihydroxyvitamin D3 induces differentiation of human promyelocytic leukemia cells (HL-60) into monocyte-macrophages, but not into granulocytes. *Biochem Biophys Res Commun,* 117**,** 86-92.

Tannahill, G. M., Curtis, A. M., Adamik, J., Palsson-Mcdermott, E. M., Mcgettrick, A. F., Goel, G., Frezza, C., Bernard, N. J., Kelly, B., Foley, N. H., Zheng, L., Gardet, A., Tong, Z., Jany, S. S., Corr, S. C., Haneklaus, M., Caffrey, B. E., Pierce, K., Walmsley, S., Beasley, F. C., Cummins, E., Nizet, V., Whyte, M., Taylor, C. T., Lin, H., Masters, S. L., Gottlieb, E., Kelly, V. P., Clish, C., Auron, P. E., Xavier, R. J. & O/'Neill, L. a. J. 2013. Succinate is an inflammatory signal that induces IL-1[bgr] through HIF-1[agr]. *Nature,* 496**,** 238-242.

Tassi, S., Carta, S., Vene, R., Delfino, L., Ciriolo, M. R. & Rubartelli, A. 2009. Pathogen-induced interleukin-1beta processing and secretion is regulated by a biphasic redox response. *J Immunol,* 183**,** 1456-62.

Taylor, M. W. & Feng, G. S. 1991. Relationship between interferon-gamma, indoleamine 2,3-dioxygenase, and tryptophan catabolism. *Faseb J,* 5**,** 2516-22.

Ting, J. P. Y., Kastner, D. L. & Hoffman, H. M. 2006. CATERPILLERs, pyrin and hereditary immunological disorders. *Nat Rev Immunol,* 6**,** 183-195.

Tobias, P. S., Soldau, K., Kline, L., Lee, J. D., Kato, K., Martin, T. P. & Ulevitch, R. J. 1993. Cross-linking of lipopolysaccharide (LPS) to CD14 on THP-1 cells mediated by LPS-binding protein. *J Immunol,* 150**,** 3011-21.

Tracey, K. J. & Cerami, A. 1994. Tumor necrosis factor: a pleiotropic cytokine and therapeutic target. *Annu Rev Med,* 45**,** 491-503.

Traore, K., Trush, M. A., George Jr, M., Spannhake, E. W., Anderson, W. & Asseffa, A. 2005. Signal transduction of phorbol 12-myristate 13-acetate (PMA)-induced growth inhibition of human monocytic leukemia THP-1 cells is reactive oxygen dependent. *Leukemia Res,* 29**,** 863-879.

Trede, N. S., Tsytsykova, A. V., Chatila, T., Goldfeld, A. E. & Geha, R. S. 1995. Transcriptional activation of the human TNF-alpha promoter by superantigen in human monocytic cells: role of NF-kappa B. *J Immunol,* 155**,** 902-8.

Tsuchiya, S., Kobayashi, Y., Goto, Y., Okumura, H., Nakae, S., Konno, T. & Tada, K. 1982. Induction of maturation in cultured human monocytic leukemia cells by a phorbol diester. *Cancer Res,* 42**,** 1530-6.

Tsuchiya, S., Yamabe, M., Yamaguchi, Y., Kobayashi, Y., Konno, T. & Tada, K. 1980. Establishment and characterization of a human acute monocytic leukemia cell line (THP-1). *Int J Cancer,* 26**,** 171-6.

Tsushima, H. & Mori, M. 2001. Involvement of protein kinase C and tyrosine kinase in lipopolysaccharide-induced anorexia. *Pharmacol Biochem Behav,* 69**,** 17-22.

Turchan-Cholewo, J., Dimayuga, V. M., Gupta, S., Gorospe, R. M., Keller, J. N. & Bruce-Keller, A. J. 2009. NADPH oxidase drives cytokine and neurotoxin release from microglia and macrophages in response to HIV-Tat. *Antioxid Redox Signal,* 11**,** 193-204.

Ulevitch, R. J. & Tobias, P. S. 1995. Receptor-dependent mechanisms of cell stimulation by bacterial endotoxin. *Annu Rev Immunol,* 13**,** 437-57.

Ungerstedt, J. S., Blomback, M. & Soderstrom, T. 2003. Nicotinamide is a potent inhibitor of proinflammatory cytokines. *Clin Exp Immunol,* 131**,** 48-52.

Vallabhapurapu, S. & Karin, M. 2009. Regulation and function of NF-kappaB transcription factors in the immune system. *Annu Rev Immunol,* 27**,** 693-733.

Van Beijnum, J. R., Moerkerk, P. T., Gerbers, A. J., De Bruine, A. P., Arends, J. W., Hoogenboom, H. R. & Hufton, S. E. 2002. Target validation for genomics using peptide-specific phage antibodies: a study of five gene products overexpressed in colorectal cancer. *Int J Cancer,* 101**,** 118-27.

Van Der Bruggen, T., Nijenhuis, S., Van Raaij, E., Verhoef, J. & Van Asbeck, B. S. 1999. Lipopolysaccharide-induced tumor necrosis factor alpha production by human monocytes involves the raf-1/MEK1-MEK2/ERK1-ERK2 pathway. *Infect Immun,* 67**,** 3824-9.

Van Ginderachter, J. A., Movahedi, K., Hassanzadeh Ghassabeh, G., Meerschaut, S., Beschin, A., Raes, G. & De Baetselier, P. 2006. Classical and alternative activation of mononuclear phagocytes: picking the best of both worlds for tumor promotion. *Immunobiology,* 211**,** 487-501.

Van Gool, F., Galli, M., Gueydan, C., Kruys, V., Prevot, P. P., Bedalov, A., Mostoslavsky, R., Alt, F. W., De Smedt, T. & Leo, O. 2009. Intracellular NAD^+ levels regulate tumor necrosis factor protein synthesis in a sirtuin-dependent manner. *Nat Med,* 15**,** 206-10.

Vander Heiden, M. G., Cantley, L. C. & Thompson, C. B. 2009. Understanding the Warburg effect: the metabolic requirements of cell proliferation. *Science,* 324**,** 1029-33.

Vaquero, A., Scher, M., Lee, D., Erdjument-Bromage, H., Tempst, P. & Reinberg, D. 2004. Human SirT1 interacts with histone H1 and promotes formation of facultative heterochromatin. *Mol Cell,* 16**,** 93-105.

Vassalli, P. 1992. The pathophysiology of tumor necrosis factors. *Annu Rev Immunol,* 10**,** 411-52.

Vats, D., Mukundan, L., Odegaard, J. I., Zhang, L., Smith, K. L., Morel, C. R., Wagner, R. A., Greaves, D. R., Murray, P. J. & Chawla, A. 2006. Oxidative metabolism and PGC-1beta attenuate macrophage-mediated inflammation. *Cell Metab,* 4**,** 13-24.

Vazquez, A., Liu, J., Zhou, Y. & Oltvai, Z. N. 2010. Catabolic efficiency of aerobic glycolysis: the Warburg effect revisited. *BMC Syst Biol,* 4**,** 58.

Vega, M. A., Corbí, A. L., 2006. Human macrophage activation: Too many functions and phenotypes for a single cell type. *Inmunologia,* 25, **,** 248-272.

Venter, G., Oerlemans, F. T., Willemse, M., Wijers, M., Fransen, J. A. & Wieringa, B. 2014. NAMPT-mediated salvage synthesis of NAD^+ controls morphofunctional changes of macrophages. *PLoS One,* 9**,** e97378.

Verreck, F. A., De Boer, T., Langenberg, D. M., Van Der Zanden, L. & Ottenhoff, T. H. 2006. Phenotypic and functional profiling of human proinflammatory type-1 and anti-inflammatory type-2 macrophages in response to microbial antigens and IFN-gamma- and CD40L-mediated costimulation. *J Leukoc Biol,* 79**,** 285-93.

Von Den Hoff, H., De Koning, M., Van Kampen, J. & Van Der Korst, J. 1995. Interleukin-1 reversibly inhibits the synthesis of biglycan and decorin in intact articular cartilage in culture. *J Rheumatol,* 22**,** 1520-6.

Wang, B. W., Chang, H., Lin, S., Kuan, P. & Shyu, K. G. 2003. Induction of matrix metalloproteinases-14 and -2 by cyclical mechanical stretch is mediated by tumor necrosis factor-alpha in cultured human umbilical vein endothelial cells. *Cardiovasc Res,* 59**,** 460-9.

Wang, F., Wang, L. Y., Wright, D. & Parmely, M. J. 1999. Redox imbalance differentially inhibits lipopolysaccharide-induced macrophage activation in the mouse liver. *Infect Immun,* 67**,** 5409-16.

Wang, N., Tabas, I., Winchester, R., Ravalli, S., Rabbani, L. E. & Tall, A. 1996. Interleukin 8 is induced by cholesterol loading of macrophages and expressed by macrophage foam cells in human atheroma. *J Biol Chem,* 271**,** 8837-42.

Wang, Q., Zhang, Y., Yang, C., Xiong, H., Lin, Y., Yao, J., Li, H., Xie, L., Zhao, W., Yao, Y., Ning, Z. B., Zeng, R., Xiong, Y., Guan, K. L., Zhao, S. & Zhao, G. P. 2010. Acetylation of metabolic enzymes coordinates carbon source utilization and metabolic flux. *Science,* 327**,** 1004-7.

Wang, Q., Zhao, Y., Sun, M., Liu, S., Li, B., Zhang, L. & Yang, L. 2014. 2-Deoxy-D-glucose attenuates sevoflurane-induced neuroinflammation through nuclear factor-kappa B pathway in vitro. *Toxicol In Vitro,* 28**,** 1183-9.

Warburg, O. 1956. On the origin of cancer cells. *Science,* 123**,** 309-14.

Warrington, R., Watson, W., Kim, H. L. & Antonetti, F. R. 2011. An introduction to immunology and immunopathology. *Allergy Asthma Clin Immunol,* 7 Suppl 1**,** S1.

Watanabe, Y., Fujiwara, M., Yoshida, R. & Hayaishi, O. 1980. Stereospecificity of hepatic L-tryptophan 2,3-dioxygenase. *Biochem J,* 189**,** 393-405.

Watson, M., Roulston, A., Belec, L., Billot, X., Marcellus, R., Bedard, D., Bernier, C., Branchaud, S., Chan, H., Dairi, K., Gilbert, K., Goulet, D., Gratton, M. O., Isakau, H., Jang, A., Khadir, A., Koch, E., Lavoie, M., Lawless, M., Nguyen, M., Paquette, D., Turcotte, E., Berger, A., Mitchell, M., Shore, G. C. & Beauparlant, P. 2009. The small molecule GMX1778 is a potent inhibitor of NAD^+ biosynthesis: strategy for enhanced therapy in nicotinic acid phosphoribosyltransferase 1-deficient tumors. *Mol Cell Biol,* 29**,** 5872-88.

Wellen, K. E. & Thompson, C. B. 2010. Cellular metabolic stress: considering how cells respond to nutrient excess. *Mol Cell,* 40**,** 323-32.

Williams, G. T., Lau, K. M., Coote, J. M. & Johnstone, A. P. 1985. NAD^+ metabolism and mitogen stimulation of human lymphocytes. *Exp Cell Res,* 160**,** 419-26.

Winder, W. W., Holmes, B. F., Rubink, D. S., Jensen, E. B., Chen, M. & Holloszy, J. O. 2000. Activation of AMP-activated protein kinase increases mitochondrial enzymes in skeletal muscle. *J Appl Physiol (1985),* 88**,** 2219-26.

Wirthgen, E., Tuchscherer, M., Otten, W., Domanska, G., Wollenhaupt, K., Tuchscherer, A. & Kanitz, E. 2014. Activation of indoleamine 2,3-dioxygenase by LPS in a porcine model. *Innate Immun,* 20**,** 30-9.

Wu, M., Neilson, A., Swift, A. L., Moran, R., Tamagnine, J., Parslow, D., Armistead, S., Lemire, K., Orrell, J., Teich, J., Chomicz, S. & Ferrick, D. A. 2007. Multiparameter metabolic analysis reveals a close link between attenuated mitochondrial bioenergetic function and enhanced glycolysis dependency in human tumor cells. *Am J Physiol Cell Physiol,* 292**,** C125-36.

Wu, Y., Song, P., Zhang, W., Liu, J., Dai, X., Liu, Z., Lu, Q., Ouyang, C., Xie, Z., Zhao, Z., Zhuo, X., Viollet, B., Foretz, M., Wu, J., Yuan, Z. & Zou, M.-H. 2015. Activation of AMPK[alpha]2 in adipocytes is essential for nicotine-induced insulin resistance in vivo. *Nat Med,* 21**,** 373-382.

Xie, H., Valera, V. A., Merino, M. J., Amato, A. M., Signoretti, S., Linehan, W. M., Sukhatme, V. P. & Seth, P. 2009. LDH-A inhibition, a therapeutic strategy for treatment of hereditary leiomyomatosis and renal cell cancer. *Mol Cancer Ther,* 8**,** 626-35.

Yamazaki, F., Kuroiwa, T., Takikawa, O. & Kido, R. 1985. Human indolylamine 2,3-dioxygenase. Its tissue distribution, and characterization of the placental enzyme. *Biochem J,* 230**,** 635-8.

Yang, H., Yang, T., Baur, J. A., Perez, E., Matsui, T., Carmona, J. J., Lamming, D. W., Souza-Pinto, N. C., Bohr, V. A., Rosenzweig, A., De Cabo, R., Sauve, A. A. & Sinclair, D. A. 2007. Nutrient-sensitive mitochondrial NAD^+ levels dictate cell survival. *Cell,* 130**,** 1095-107.

Yang, Z., Kahn, B. B., Shi, H. & Xue, B. Z. 2010. Macrophage alpha1 AMP-activated protein kinase (alpha1AMPK) antagonizes fatty acid-induced inflammation through SIRT1. *J Biol Chem,* 285**,** 19051-9.

Yeung, F., Hoberg, J. E., Ramsey, C. S., Keller, M. D., Jones, D. R., Frye, R. A. & Mayo, M. W. 2004. Modulation of NF-kappaB-dependent transcription and cell survival by the SIRT1 deacetylase. *EMBO J,* 23**,** 2369-80.

Ying, W. 2006. NAD^+ and NADH in cellular functions and cell death. *Front Biosci,* 11**,** 3129-48.

Yoshizaki, T., Schenk, S., Imamura, T., Babendure, J. L., Sonoda, N., Bae, E. J., Oh, D. Y., Lu, M., Milne, J. C., Westphal, C., Bandyopadhyay, G. & Olefsky, J. M. 2010. SIRT1 inhibits

inflammatory pathways in macrophages and modulates insulin sensitivity. *Am J Physiol Endocrinol Metab,* 298**,** E419-28.

Zea, A. H., Rodriguez, P. C., Atkins, M. B., Hernandez, C., Signoretti, S., Zabaleta, J., Mcdermott, D., Quiceno, D., Youmans, A., O'neill, A., Mier, J. & Ochoa, A. C. 2005. Arginase-producing myeloid suppressor cells in renal cell carcinoma patients: a mechanism of tumor evasion. *Cancer Res,* 65**,** 3044-8.

Zhang, T., Berrocal, J. G., Frizzell, K. M., Gamble, M. J., Dumond, M. E., Krishnakumar, R., Yang, T., Sauve, A. A. & Kraus, W. L. 2009. Enzymes in the NAD^+ salvage pathway regulate SIRT1 activity at target gene promoters. *J Biol Chem,* 284**,** 20408-17.

Zhang, X., Tian, W., Cai, X., Wang, X., Dang, W., Tang, H., Cao, H., Wang, L. & Chen, T. 2013. Hydrazinocurcumin Encapsuled nanoparticles "re-educate" tumor-associated macrophages and exhibit anti-tumor effects on breast cancer following STAT3 suppression. *PLoS One,* 8**,** e65896.

Zhong, L., D'urso, A., Toiber, D., Sebastian, C., Henry, R. E., Vadysirisack, D. D., Guimaraes, A., Marinelli, B., Wikstrom, J. D., Nir, T., Clish, C. B., Vaitheesvaran, B., Iliopoulos, O., Kurland, I., Dor, Y., Weissleder, R., Shirihai, O. S., Ellisen, L. W., Espinosa, J. M. & Mostoslavsky, R. 2010. The histone deacetylase Sirt6 regulates glucose homeostasis via Hif1alpha. *Cell,* 140**,** 280-93.

Ziegler, M. 2000. New functions of a long-known molecule. Emerging roles of NAD^+ in cellular signaling. *Eur J Biochem,* 267**,** 1550-64.

Appendices

Biosci. Rep. (2016) / 36 / art:e00301 / doi 10.1042/BSR20150247

Original Paper

OPEN ACCESS

Intracellular NAD^+ levels are associated with LPS-induced TNF-α release in pro-inflammatory macrophages

Abbas Jawad Al-Shabany*, Alan John Moody*, Andrew David Foey† and Richard Andrew Billington*[1]

*School of Biological Sciences, University of Plymouth, Drake Circus, Plymouth, PL4 8AA, U.K.
†School of Biomedical and Healthcare Sciences, University of Plymouth, Drake Circus, Plymouth, PL4 8AA, U.K.

Synopsis

Metabolism and immune responses have been shown to be closely linked and as our understanding increases, so do the intricacies of the level of linkage. NAD^+ has previously been shown to regulate tumour necrosis factor-α (TNF-α) synthesis and TNF-α has been shown to regulate NAD^+ homoeostasis providing a link between a pro-inflammatory response and redox status. In the present study, we have used THP-1 differentiation into pro- (M1-like) and anti- (M2-like) inflammatory macrophage subset models to investigate this link further. Pro- and anti-inflammatory macrophages showed different resting NAD^+ levels and expression levels of NAD^+ homoeostasis enzymes. Challenge with bacterial lipopolysaccharide, a pro-inflammatory stimulus for macrophages, caused a large, biphasic and transient increase in NAD^+ levels in pro- but not anti-inflammatory macrophages that were correlated with TNF-α release and inhibition of certain NAD^+ synthesis pathways blocked TNF-α release. Lipopolysaccharide stimulation also caused changes in mRNA levels of some NAD^+ homoeostasis enzymes in M1-like cells. Surprisingly, despite M2-like cells not releasing TNF-α or changing NAD^+ levels in response to lipopolysaccharide, they showed similar mRNA changes compared with M1-like cells. These data further strengthen the link between pro-inflammatory responses in macrophages and NAD^+. The agonist-induced rise in NAD^+ shows striking parallels to well-known second messengers and raises the possibility that NAD^+ is acting in a similar manner in this model.

Key words: Immune responses, lipopolysaccharide (LPS), macrophages, pyridine nucleotides, second messenger, TNF-α.

Cite this article as: Bioscience Reports (2016) **36**, e00301, doi:10.1042/BSR20150247

INTRODUCTION

Previous work has revealed a fascinating link between metabolism and the ability of an organism to mount an immune response [1]. This link is bidirectional with examples of changes in metabolism being required in order to mount the appropriate response and with immune mediators being able to modulate metabolism [2]. Indeed, many diseases that were previously considered to be pure metabolic disorders now being reconsidered also as inflammatory diseases and *vice versa* [2]. Immunometabolism has been particularly well studied in macrophages, myeloid derived phagocytes with different phenotypes that can be involved in numerous innate immune functions from bacterial killing to wound healing [3]. In particular, classically activated, pro-inflammatory (M1) macrophages are predominantly glycolytic whereas alternatively activated; anti-inflammatory (M2) macrophages rely on oxidative metabolism [4]. Forcing M1s to become oxidative, or M2s to become glycolytic, leads to a switch in phenotype. A front-line response to bacterial infection needs to be short lived as the consequent production of large amounts of pro-inflammatory mediators such as tumour necrosis factor-α (TNF-α) can lead to a pro-inflammatory cascade resulting in potentially fatal cytokine storm [5].

Glycolysis can operate under anaerobic conditions (such as those that may be found at sites of infection) for short periods of time but is unsustainable in the long term due to lactate and ROS production, reflecting the role of M1s. On the other hand, M2s are involved in much longer term anti-inflammatory processes in which cytokine storm is not possible. Thus M2s are much more suited to aerobic oxidative metabolism of glucose and fatty acids which, while slower than glycolysis, produces more ATP per gram of substrate and can be sustained practically indefinitely. Given that NAD^+ is an absolute requirement for

Abbreviations: DPI, diphenyliodonium NAMPT, nicotinamide phosphoribosyl transferase; NMNAT, nicotinamide mononucleotide adenylyl transferase; qPCR, quantitative PCR; TLR4, Toll-like receptor 4; TNF-α, tumour necrosis factor-α.

[1] To whom correspondence should be addressed (email richard.billington@plymouth.ac.uk).

© 2016 Authors. This is an open access article published by Portland Press Limited and distributed under the Creative Commons Attribution Licence 3.0.

Modulation of NAD synthesis controls TNF-α responses in macrophage phenotype.

Abbas Al-Shabany, A. John Moody, Andrew D. Foey, Richard A. Billington
University of Plymouth, School of Biological Sciences, PL4 8 AA, UK.

Introduction

When LPS is recognised by TLR4 on macrophages, pro –inflammatory cytokines such as tumour necrosis factor-α (TNF-α; 1) are produced. The link between NAD^+ and TNF-α is well established. NAD^+-mediated sirtuin activity has been shown to modulate TNF-α production in pro-inflammatory macrophages (2) and TNF-α modulates the expression of NAD^+ homeostasis enzymes. Thus, this relationship provides a link between redox (and thus metabolic) status and the regulation of pro-inflammatory responses.

While the relationship between NAD^+ and TNF-α is well documented, the mechanism by which NAD^+ homeostasis is involved is not fully understood. Three major pathways are involved in NAD-biosynthesis. These pathways use three different precursors; nicotinamide/nicotinic acid, nicotinamide riboside and tryptophan (3, 4).

We have made use of the differentiation of THP-1 monocytes to generate cells with characteristics of pro-inflammatory (M1-like) macrophages by using PMA (phorbol-12-myristate-13-acetate) in order to investigate NAD^+ homeostasis and whether it can mediate macrophage responses.

Here we provide evidence that NAD^+ synthesis is also involved in the LPS-stimulated release of TNF-α and that NAD^+ may play a role in the termination of TNF-α responses, further strengthening the intimate relationship between TNF-α and NAD^+.

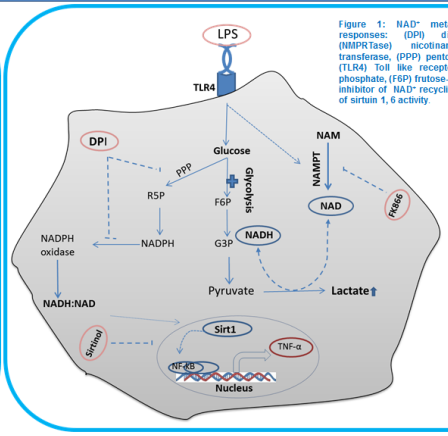

Figure 1: NAD^+ metabolism and immune responses; (DPI) diphenylene iodonium, (NMPRTase) nicotinamide phosphoribosyl transferase, (PPP) pentose phosphate pathway, (TLR4) Toll like receptor 4, (G6P) glucose-6-phosphate, (F6P) frutose-6-phosphate, (FK866) an inhibitor of NAD^+ recycling, (sirtinol) an inhibitor of sirtuin 1, 6 activity.

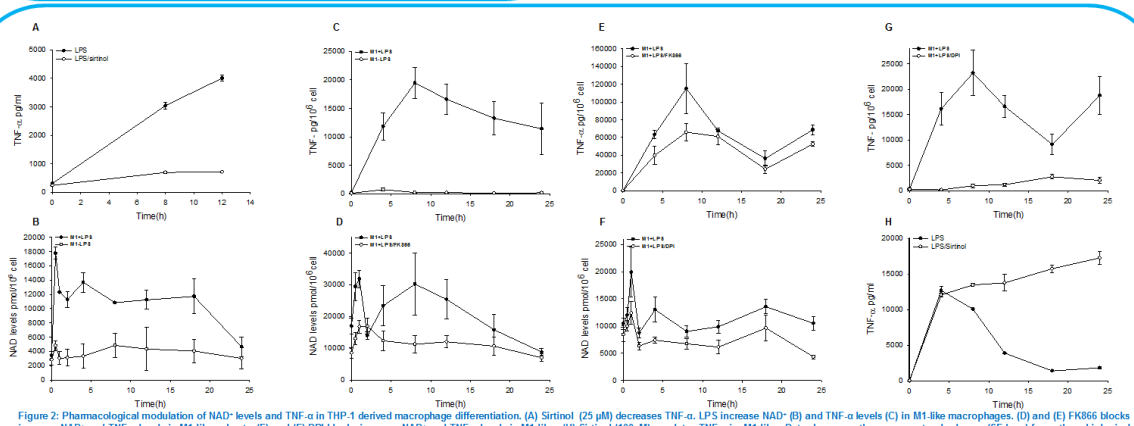

Figure 2: Pharmacological modulation of NAD^+ levels and TNF-α in THP-1 derived macrophage differentiation. (A) Sirtinol (25 μM) decreases TNF-α, LPS increase NAD^+ (B) and TNF-α levels (C) in M1-like macrophages. (D) and (E) FK866 blocks increase NAD^+ and TNF-α levels in M1-like subsets. (E) and (F) DPI blocks increase NAD^+ and TNF-α levels in M1-like . (H) Sirtinol (100μM) regulates TNF-α in M1-like . Data shown are the means ± standard error (SE bars) from three biological replications.

Method

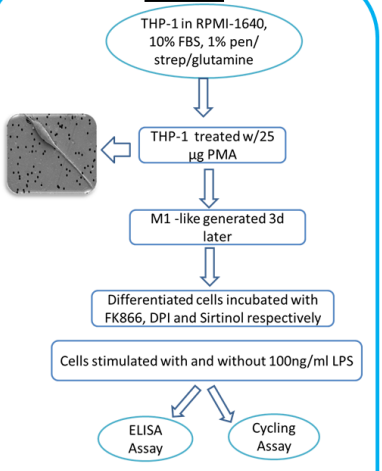

References

1-Takeuchi and Akira, (2010) *Cell*. (140) 805–820.
2-Van Gool *et al.*, (2009) *Nat. Med.* 15 (2) 206-210.
3-Cross, A. R. (1987) *Biochem. Pharmcol.* 33, 489-493.
4-Hou, *et al.*,(2007) *Cancer Res.* 792-801.

Results

NAD metabolism and innate immune responses.

Firstly, we confirmed the finding that NAD^+ levels are involved in TNF-α production by treating cells with sirtinol (a sirtuin inhibitor) for 24 h before treatment with LPS. Control cells showed a robust TNF-α release as expected while sirtinol treated cells released very little TNF-α. This only occurred after 24 h of pre-treatment as 1 h pre-treatment with sirtinol failed to reduce TNF-α release (data not shown) suggesting that the effect is at the level of transcription/translation rather than at the level of TNF-α release (Figure 2 A).

In order to investigate a possible link between LPS stimulation, TNF-α release and NAD^+, we stimulated cells with LPS and measured both NAD^+ levels and TNF-α release. LPS increased both NAD^+ levels and TNF-α release (Figure 2 B, C) with the NAD^+ increase showing a biphasic profile with a rapid initial spike followed by a longer rise while TNF-α levels peaked after 8 hours before slowly declining. To elucidate which of the NAD^+ synthesis pathways is responsible for the NAD^+ rise, we first tested the effect of FK866, a NAMPT (nicotinamide phosphoribosyl transferase; NAD^+ recycling) inhibitor.

Differentiated macrophages were incubated with 100nM FK866 for 1 hour prior to stimulation with 100 ng/ml LPS, versus control cells. FK866 causes NAD^+ levels to rise only a small amount in response to LPS (Figure 2 D) with the greatest effect on the longer term, sustained rise. TNF-α did still increase but FK866 reduced the amount released (Figure 2 E). DPI (100μM DPI for 0.5 h prior to exposure to LPS stimulation), an inhibitor of NAD(P)H oxidase, blocked the NAD^+ rise as expected and almost completely inhibited TNF-α increases (Figure 2 F, G).

When we performed LPS stimulation in the presence of sirtinol (100 μM, 1 h pre-treatment) there was no effect on the initial TNF-α release. However, we observed that sirtinol was able to completely block the second part of the TNF-α response where levels decayed back to unstimulated levels over 24 h. This suggests that sirtuins and thus NAD+ levels, are involved in the regulation this phase of the response (Figure 2 H).

Discussion

NAD^+ has previously been shown to have an intimate relationship with TNF-α at the transcriptional level. Here we show that this relationship may be more intimate than previously thought. LPS stimulation of M1-like macrophages causes significant changes in NAD^+ levels and induces TNF-α release.

The changes in NAD^+ levels can be blocked by inhibiting either NAD^+ synthesis through the NAD^+ recycling pathway or by blocking NADH oxidation by NAD(P)H oxidase. It is interesting to note that, while NAD(P)H oxidase inhibition almost completely knocks out TNF-α release, inhibition of NAD^+ recycling has a lesser effect. This would suggest that both NAD+ and perhaps the free radicals generated by NAD(P)H oxidase might be required for release. It is known that TNF-α release requires active glycolysis and thus, the LPS-induced increase in NAD^+ that we observe suggest that this may occur in order to provide NAD^+ for glycolysis.

Glycolysis is inhibited by high NADH levels as NAD^+ is absolutely required as a coenzyme. Indeed, lactic fermentation exists to oxidise NADH to NAD^+ under anaerobic conditions such that glycolysis may continue. These data provide a further link between metabolic status and immune regulation and to further strengthen the link between NAD^+ levels and TNF-α, this time at the level of release.

We also investigated the effect of sirtinol, a sirtuin inhibitor. Sirtuins require NAD^+ as an acetate acceptor in order to perform deacetylation reactions. We confirm previous data that showed that synthesis of TNF-α is sirtuin dependent. We also observed that sirtinol blocks the decay of TNF-α after LPS stimulation with TNF-α levels not decreasing in 24 h as in the control. This would suggest that NAD^+ levels (via sirtuins) mediate that decay phase. The second phase of the NAD^+ increase we observe under LPS stimulation is prolonged and covers the period of the TNF-α decay phase suggesting they may be correlated.

These experiments were performed *in vitro* and it is hard to predict how this may occur in an *in vivo* setting. However, these data again strengthen the link between NAD^+ levels and TNF-α and thus metabolism and pro-inflammatory responses.

NAD levels in ANTI- and PRO-inflammatory macrophages

Abbas Al-shabany, Andrew D. Foey , A. John Moody, Richard A. Billington
CRTB, School of Biomedical and Biological Sciences, University of Plymouth

Abstract

It is becoming clear that the intracellular levels of NAD are an important regulator of a number of fundamental cell signalling pathways. Among these, regulation of gene expression by the NAD-dependent Sirtuin enzymes has been shown to play a role in the modulation of cytokine expression and release particularly for the pro-inflammatory cytokine TNF-α. Here we have made use of the differentiation of THP-1 monocytes via different agents to generate cells with characteristics of pro-inflammatory (M1) or anti-inflammatory (M2) macrophages in order to investigate any potential roles of NAD homeostasis pathways in determining the phenotype of these cells. Of particular interest is the IDO pathway which feeds into NAD synthesis and has been shown to be associated with anti-inflammatory phenotypes. NAD levels differ markedly between M1 and M2 cells with M1s having much higher basal levels than M2s. Upon stimulation with LPS NAD levels change dynamically in M1s but not in M2s suggesting a fundamental role of NAD levels in the bacterial response. M1s release high levels of TNF-α and low levels of IL-6 while M2s do the opposite. Initial data suggests that M1s may have high NAD synthesis activity but low degradation activity while the opposite seems to be the case in M2s. These findings open the possibility of pharmacological modulation of NAD synthesis as a way of modulating immune responses.

Introduction

It is well established that NAD is required for a broad range of metabolic pathways. Beyond its role as a cofactor, NAD serves as a substrate for a number on enzymatic signalling pathways. In mammalian immune cells, for example, a key role has been shown for NAD and its metabolites in immune transcriptional regulation. In particular, the regulatory role of NAD-dependent sirtuin deacetylase activity in innate immune cells (1). Thus, by using NAD, Silent information regulator 2 (Sirt), can control the production and secretion of TNF-α within the cells (2).

Cellular NAD homeostasis is complex and a number of pathways exist to synthesise NAD. Beyond its salvage biosynthesis pathway, NAD can also be generated *de novo* from Tryptophan via the indoleamine 2, 3-dioxygenase (IDO) pathway. In this pathway, IDO is the rate limiting enzyme that converts Tryptophan, through series enzymatic reactions, into quinolinic acid which, in turn, is converted to NAD (3).

IDO activity is indeed required for control both the innate and the adaptive immunity. Two main mechanisms underlie the immune regulatory function of the IDO pathway: one is IDO mediated tryptophan depletion, resulting in starvation of the immune cell microenvironment (4). The other is that the activity of IDO is accompanied by production of series of cytotoxic catabolites which exert their effects on tissue microenvironments, suppressing cell proliferation and activation (5). In immune cells, such as dendritic cells, IDO plays a key role in mediating the flux between pathways that lead to pro- and anti- inflammatory cytokine production (6).

Given the apparent importance of NAD and NAD biosynthesis in immune regulation, we have looked at potential roles of NAD in determining the pro- or anti-inflammatory phenotype of macrophage subsets.

Methods

Cell culture and differentiation

Human monocytic leukaemia THP-1 cells were obtained from ECACC and maintained in RPMI-1640 with 10% FBS and 1% pen/strep. To induce differentiation, cells were treated with 25 ng/ml T PMA or 10nM vitamin D_3 for 3 and 7 days respectively. For cell stimulation, the cells were incubated with and without 100ng/ml LPS.

Intracellular NAD measurement

NAD was extracted and then measured by an enzymatic cycling assay (Leonardo et al., 1996).

Cytokine quantification

Supernatants from the cell culture were analysed for TNF-α and IL-6 using a commercial ELISA kit (3D pharmingen).

Results

Intracellular NAD levels and cytokines are regulated by LPS

After differentiation of THP-1 cells into M1/M2-like macrophages we measured intracellular NAD levels both with and without challenging with LPS. Upon stimulation with LPS, pro-inflammatory, M1-like cells showed a large increase in intracellular NAD levels that peaked after one hour and decayed back to almost unstimulated levels by 24 hours (Fig 1a). On the other hand, anti-inflammatory, M2-like cells showed no significant change in NAD levels when challenged with LPS (Fig 1b). The medium from the same cells was also assayed for the pro-inflammatory cytokine TNF-α and the and IL-6 (Fig 2). As expected, M1 cells released large amounts of TNF-α but little IL-6 while the opposite was true for M2 cells. These data fit nicely with the observation that M1s are pro-inflammatory while M2s are anti-inflammatory.

Results (cont)

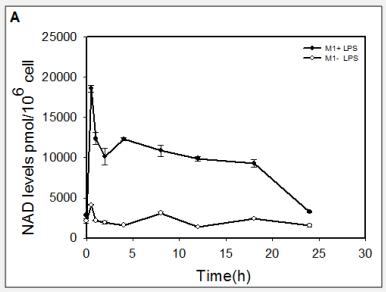

Figure 1: Intracellular NAD levels in (A) M1-like, and (B) M2-like cells under LPS stimulation. (n = 3)

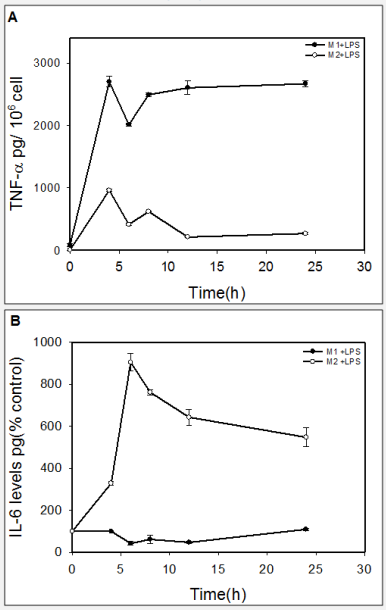

Figure 2: Cytokine release by M1- and M2-like cells under LPS stimulation; (A)TNF-α and (B) IL-6. (n = 3)

References

1- Lin et al., *Curr Opin Cell Biol*. 2003;15:241–246.
2- Van Gool F et al., *Nat Med*. 2009;15:206–10.
3- Magni et al., *Cell. Mol. Life Sci*. 2004; 61, 19–34.
4- Mellor AL. *Biochem Biophys Res Commun*. 2005; 338(1):20–24.
5- Frumento et al. J Exp Med. 2002; 196 (4):459–468.
6- Hill et al. *Eur. J. Immunol*. 2007; 37 :3054-3062.

Results (cont)

NAD homeostasis in M1 and M2 cells

Given the apparent differences between the two phenotypes, we investigated the relative NAD production and degradation capacity of the two cell types by treating them with FK866, an inhibitor of NAD synthesis (via inhibition of NMPRTase; Fig 3) or with nicotinamide, a dietary NAD precursor, or quinolate, an NAD precursor formed via the IDO pathway (Fig 4).

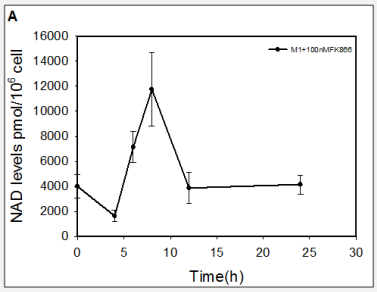

Fig. 3: Effect of 100nM FK866 on NAD levels in (A) M1-like, and (B) M2-like cells. (n = 3)

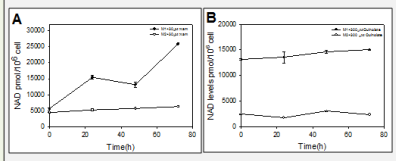

Figure 4: Intracellular NAD levels in M1- and M2- like cells treated with (A) nicotinamide and (B) quinolate for 1-3 days. (n = 3)

Disscusion

Our results suggest that pro-inflammatory M1-like cells are characterised by changes in NAD levels under LPS stimulation while M2-like cells (anti-inflammatory) are not. Previous work has shown that NAD is an important regulator of TNF-α synthesis and release and our findings confirm this relationship as M1-like cells released significant amounts of TNF-α concurrent with the NAD rise. M2-like cells on the other hand, released significant amounts of IL-6, an anti-inflammatory cytokine but intracellular NAD levels did not change under LPS challenge. FK866, caused a drop in NAD levels in M2-like cells but had little effect in M1-like cells. This suggests that the rate of NAD consumption is high in M2-like cells as FK866 blocks NAD recycling while the rate of NAD consumption in M1-like cells is low. These data also fit with the observation that M1-like cells are able to rapidly increase their NAD levels while M2-like cells are not. Coupled with this, NAD synthesis from the NAD precursor nicotinamide (but not quinolate) was high in M1-like cells but low in M2-like cells again supporting the rapid change in NAD levels in M1-like cells.

This might be of high importance in terms of characterization of these two phenotypes. Also, the rate of NAD synthesis/consumption might reflect the involvement of NAD in wide range of inflammatory signaling pathways.

Our findings might open the door to approach by which we would be able to regulate the function for both M1-like and M2-like cells.

Modulation of NAD+ homeostasis controls TNF-α secretion in differentiated macrophages

Abbas Al-Shabany, A. John Moody, *Andrew D. Foey, Richard A. Billington

School of Biological Sciences, *School of Biomedical and Healthcare Sciences,

University of Plymouth, Drake Circus, Plymouth, PL4 8AA, UK

Introduction

When LPS is recognised by TLR4 on macrophages, pro–inflammatory cytokines such as tumour necrosis factor-α (TNF-α; 1) are produced. The link between NAD^+ and TNF-α is well established. NAD^+-mediated sirtuin activity has been shown to modulate TNF-α production in pro-inflammatory macrophages (2) and TNF-α modulates the expression of NAD^+ homeostasis enzymes. Thus, this relationship provides a link between redox (and thus metabolic) status and the regulation of pro-inflammatory responses. While the relationship between NAD^+ and TNF-α is well documented, the mechanism by which NAD^+ homeostasis is involved is not fully understood. Three major pathways are involved in NAD-biosynthesis. These pathways use three different precursors; nicotinamide/nicotinic acid, nicotinamide riboside and tryptophan (3, 4).

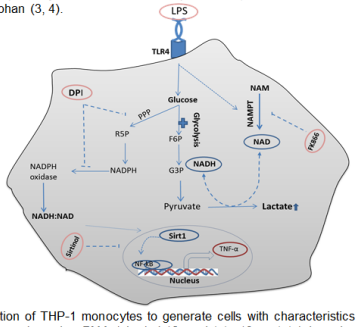

Figure 1: NAD^+ metabolism and TNF-α responses in macrophages: LPS increases glycolysis activity and lactate production and modulation of NAD^+ homeostasis regulates TNF-α secretion. (DPI) diphenylene iodonium, (NMPRTase), nicotinamide phosphoribosyl transferase, (PPP) pentose phosphate pathway, (TLR4) Toll like receptor 4, (G6P) glucose-6-phosphate, (F6P) frutose-6-phosphate, G3P, glyceraldehyde-3-phosphate, NAM, nicotinamide, (FK866) an inhibitor of NAD^+ recycling, (sirtinol) an inhibitor of sirtuin 1, 6 activity (NAD consuming enzyme).

We have made use of the differentiation of THP-1 monocytes to generate cells with characteristics of pro-inflammatory (M1-like) macrophages by using PMA (phorbol-12-myristate-13-acetate) in order to investigate NAD^+ homeostasis and whether it can mediate macrophage responses. Here we provide evidence that NAD^+ synthesis is also involved in the LPS-stimulated release of TNF-α and that NAD^+ may play a role in the termination of TNF-α responses, further strengthening the intimate relationship between TNF-α and NAD^+.

Methods

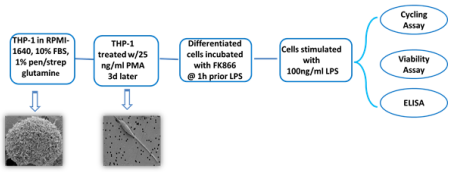

Results

NAD metabolism and innate immune responses

Firstly, we confirmed the finding that NAD^+ levels are involved in TNF-α production by treating cells with sirtinol (a sirtuin inhibitor) for 24 h before treatment with LPS. Control cells showed a robust TNF-α release as expected while sirtinol treated cells released very little TNF-α.This only occurred after 24 h of pre-treatment as 1 h pre-treatment with sirtinol failed to reduce TNF-α release (data shown in Figure, 4 A) suggesting that the effect is at the level of transcription/translation rather than at the level of TNF-α release (Figure 2 A). In order to investigate a possible link between LPS stimulation, TNF-α release and NAD^+, we stimulated cells with LPS and measured both NAD^+ levels and TNF-α release. LPS increased both NAD^+ levels and TNF-α release (Figure 2 B, C) with the NAD^+ increase showing a biphasic profile with a rapid initial spike followed by a longer rise while TNF-α levels peaked after 8 hours before slowly declining.

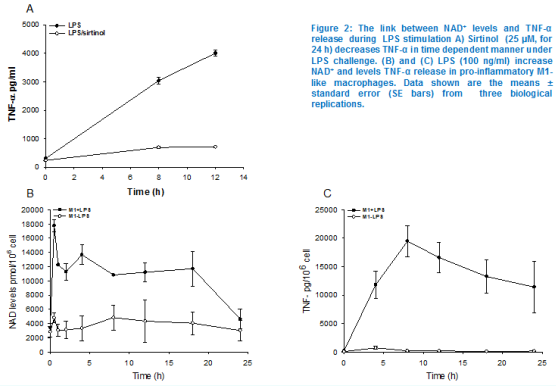

Figure 2: The link between NAD^+ levels and TNF-α release during LPS stimulation A) Sirtinol (25 μM, for 24 h) decreases TNF-α in time dependent manner under LPS challenge. (B) and (C) LPS (100 ng/ml) increase NAD^+ and levels TNF-α release in pro-inflammatory M1-like macrophages. Data shown are the means ± standard error (SE bars) from three biological replications.

Results (Cont.)

Pharmacological modulation of NAD metabolism

To elucidate which of the NAD^+ synthesis pathways is responsible for the NAD^+ rise, we first tested the effect of FK866, a NAMPT (nicotinamide phosphoribosyl transferase; NAD^+ recycling) inhibitor. Differentiated macrophages were incubated with 100nM FK866 for 1 hour prior to stimulation with 100 ng/ml LPS, versus control cells. FK866 causes NAD^+ levels to rise only a small amount in response to LPS (Figure 3 A) with the greatest effect on the longer term, sustained rise. TNF-α did still increase but FK866 reduced the amount released (Figure 3 B). DPI (100μM DPI for 0.5 h prior to exposure to LPS stimulation), an inhibitor of NAD(P)H oxidase, blocked the NAD^+ rise as expected and almost completely inhibited TNF-α increases (Figure 2 C, D).

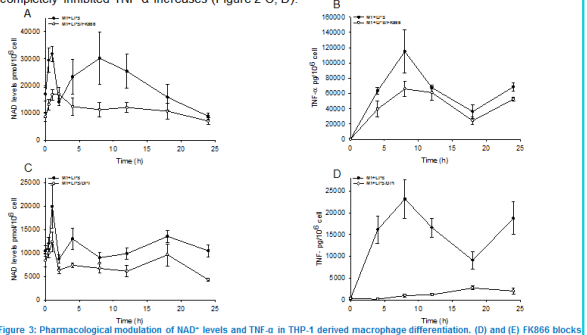

Figure 3: Pharmacological modulation of NAD^+ levels and TNF-α in THP-1 derived macrophage differentiation. (D) and (E) FK866 blocks increase NAD^+ and TNF-α levels in M1-like subsets. (E) and (F) DPI blocks increase NAD^+ and TNF-α levels in M1-like . Data shown are the means ± standard error (SE bars) from three biological replications.

Elevated NAD^+ levels are associated with TNF-α release

When we performed LPS stimulation in the presence of sirtinol (25 μM, 1 h pre-treatment) there was no effect on the initial TNF-α release. However, we observed that sirtinol was able to increase both NAD^+ and TNF-α levels. This suggests that sirtuins and thus NAD^+ levels, are involved in the regulation of TNF-α (Figure 4 A, B).

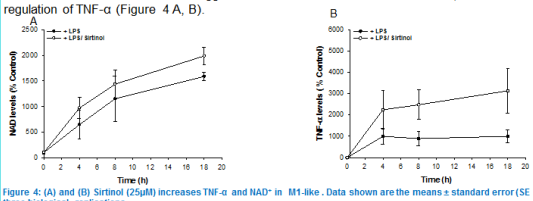

Figure 4: (A) and (B) Sirtinol (25μM) increases TNF-α and NAD^+ in M1-like . Data shown are the means ± standard error (SE bars) from three biological replications.

Discussion

NAD^+ has previously been shown to have an intimate relationship with TNF-α at the transcriptional level. Here we show that this relationship may be more intimate than previously thought. LPS stimulation of M1-like macrophages causes significant changes in NAD^+ levels and induces TNF-α release. The changes in NAD^+ levels can be blocked by inhibiting either NAD^+ synthesis through the NAD^+ recycling pathway or by blocking NADH oxidation by NAD(P)H oxidase. It is interesting to note that, while NAD(P)H oxidase inhibition almost completely knocks out TNF-α release, inhibition of NAD^+ recycling has a lesser effect. This would suggest that both NAD^+ and perhaps the free radicals generated by NAD(P)H oxidase might be required for release. It is known that TNF-α release requires active glycolysis and thus, the LPS-induced increase in NAD^+ that we observe suggest that this may occur in order to provide NAD^+ for glycolysis.

Glycolysis is inhibited by high NADH levels as NAD^+ is absolutely required as a coenzyme. Indeed, lactic fermentation exists to oxidise NADH to NAD^+ under anaerobic conditions such that glycolysis may continue. These data provide a further link between metabolic status and immune regulation and to further strengthen the link between NAD^+ levels and TNF-α, this time at the level of release. We also investigated the effect of sirtinol, a sirtuin inhibitor. Sirtuins require NAD^+ as an acetate acceptor in order to perform deacetylation reactions. We confirm previous data that showed that synthesis of TNF-α is sirtuin dependent. We also observed that sirtinol blocks the decay of TNF-α after LPS stimulation with TNF-α levels not decreasing in 24 h as in the control. This would suggest that NAD^+ levels (via sirtuins) mediate that decay phase. The second phase of the NAD^+ increase we observe under LPS stimulation is prolonged and covers the period of the TNF-α decay phase suggesting they may be correlated.

These experiments were performed in *vitro* and it is hard to predict how this may occur in an in vivo setting. However, these data again strengthen the link between NAD^+ levels and TNF-α and thus metabolism and pro-inflammatory responses.

References

1-Takeuchi and Akira, (2010) *Cell*. (140) 805–820.
2-Van Gool *et al*., (2009) *Nat. Med.* 15 (2) 206-210.
3-Cross, A. R. (1987) *Biochem. Pharmcol.* 33, 489-493.
4-Hou, *et al*., (2007) *Cancer Res.* 792-801.

Acknowledgement

We would like to thank Chemistry Department, College of Science, AL-Qadisiyah university, Ministry of Higher Education/Iraq for financial support. e-mail: abbas.al-shabany@plymouth.ac.uk

Differential expression of NAD⁺ homeostasis enzymes and immune response in pro- and anti-inflammatory macrophages

Abbas Al-Shabany, A. John Moody, Andrew D. Foey, Richard A. Billington, University of Plymouth,
School of Biological Sciences, PL4 8 AA, UK

Introduction

It is now appreciated that classically activated (M1) macrophages rely strongly on glycolysis and thus NAD⁺ for their immune function. NAD-mediated sirtuin activity has been shown to modulate TNF-α release and responses in pro-inflammatory macrophages [1]. While the relationship between NAD⁺ and TNF-α is well documented, the mechanism by which NAD⁺ homeostasis is involved is not fully understood. The intracellular NAD⁺ can be produced (Fig,1) from three different pathways using different precursors; nicotinamide/nicotinic acid (vitamin B3/niacin) via NAMPT (salvage pathway) [2] nicotinamide riboside via nicotinamide riboside kinase (NRK) [3] and tryptophan via the indole amine 2,3-dioxygenase (IDO) pathway (*de novo* pathway) [3] and it is thought that the nicotinamide/nicotinic acid (recycling) pathway is the most active. Recent interest in the pharmacological modulation of NAD⁺ homeostasis has led to a number of drugs entering clinical trials as chemotherapeutic agents for cancer. Given the link between NAD⁺ and TNF-α, it is also possible that such agents could be used to modulate pro-inflammatory responses. Indeed, FK866, an inhibitor of the NAD⁺ recycling pathway, decreased TNF-α secretion in THP-1 monocytes and human monocyte during LPS stimulation [4].

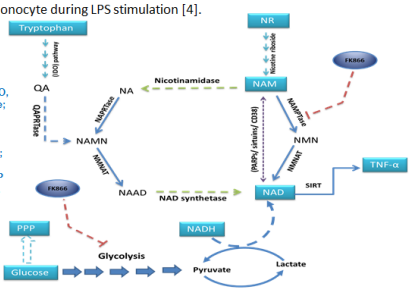

Figure,1: NAD metabolic pathways: IDO, indoleamine-2,3 dioxygenase; NA, nicotinic acid; NAAD, nicotinic acid adenine dinucleotide; NMN, Nicotinamide mononucleotide; NMNAT, NMN adenylyl transferase; NMPRTase, PPP pentose phosphate pathway.

We have made use of the differentiation of THP-1 monocytes to generate cells with characteristics of pro-inflammatory (M1-like) and anti-inflammatory using PMA (phorbol-12-myristate-13-acetate) and vitamin D_3, respectively, in order to investigate the pharmacological modulation of NAD⁺ metabolism and whether it can mediate macrophages immune responses.

Methods

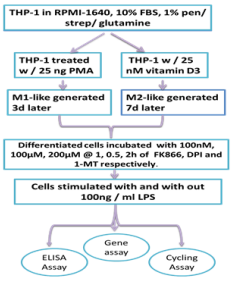

Results

NAD⁺ levels and TNF-α secretion in macrophages

The link between NAD⁺ metabolism and inflammatory responses is well established in macrophages. Briefly, NAD⁺ regulates production of TNF-α in [1] and TNF-α modulates the expression of a number of enzymes involved in NAD⁺ homeostasis [5]. In order to investigate a possible link between LPS stimulation, TNF-α release and NAD⁺, we stimulated cells with LPS and measured both NAD⁺ levels and TNF-α release. LPS increased both NAD⁺ levels and TNF-α release (Fig. 2 A, B) with the NAD⁺ increase showing a biphasic profile with a rapid initial spike followed by a longer rise while TNF-α levels peaked after 8 hours before slowly declining. On the other hand, anti-inflammatory M2-like cells showed no change in NAD⁺ levels but only secreted a relatively small amount of TNF-α which corresponded to less than 10% of that secreted by M1-like cells when challenged with LPS (Fig. 2 C, D).

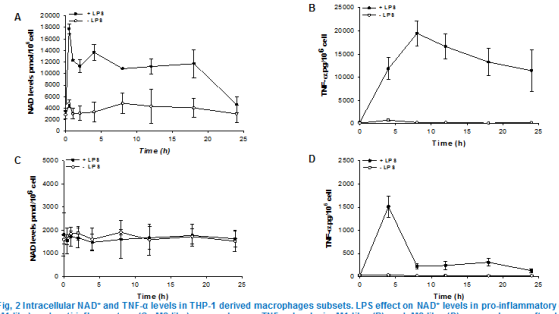

Fig, 2 Intracellular NAD⁺ and TNF-α levels in THP-1 derived macrophages subsets. LPS effect on NAD⁺ levels in pro-inflammatory (A; M1-like) and anti-inflammatory (C; M2-like) macrophages. TNF-α levels in M1-like (B) and M2-like (D) macrophages after LPS challenge. Data shown are mean ± SEM of three separate experiments (n = 3).

Results (cont.)

Gene profile of NAD⁺ homeostasis enzymes in macrophages

Given the apparent differences in NAD⁺ levels between the two phenotypes, the gene expression of NAD⁺ homeostasis have been investigated. Both phenotypes showed increased of IDO compared to THP-1. CD38 and NAMPT was upregulated in M1-like and down-regulated in M2-like cells while the opposite was true for CD157 (Fig, 3 A). LPS caused a significant increase in IDO with smaller increases in CD38, CD157 and NAMPT expression while NMNAT expression was unaffected (Fig, 3 B).

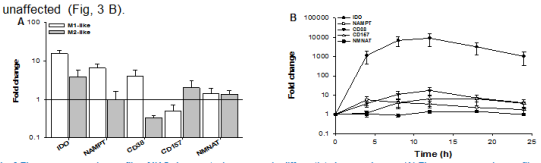

Fig, 3 The gene expression profile of NAD⁺ homeostasis enzymes in differentiated macrophages. (A) The gene expression profile of NAD⁺ homeostasis enzymes in rested M1- and M2-like macrophages . Gene expression was expressed as a fold change relative to THP-1 monocyte cell (undifferentiated), (B) The gene expression profile of NAD⁺ homeostasis enzymes in M1-like macrophages with LPS challenge. Data shown are mean ± SEM of three separate experiments (n = 3).

NAD⁺ levels, Glycolysis and TNF-α secretion in macrophages

Given the increase in NAD⁺ levels, we suspected that LPS stimulation might lead to distinct glycolytic activity in M1-like. The results confirm these assumptions as glycolysis capacity and lactate production increased while respiration was not affected in response to LPS challenge (Fig, 4 A, B, C). The link between NAD⁺ ,TNF-α and glycolysis was investigated by FK866. The FK866 treatment inhibited NAD⁺ , TNF-α levels and glycolysis while respiration was not affected (Fig, 4 D, E, F).

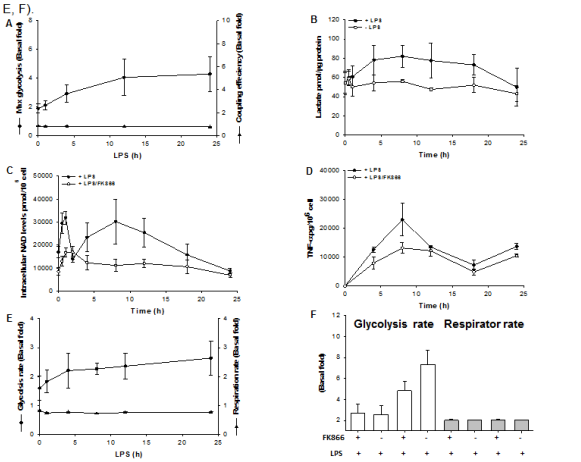

Fig, 4 The effect of FK866 treatment on NAD⁺ and TNF-α levels and Glycolytic metabolism under LPS challenge in pro-inflammatory macrophages. LPS increase glycolytic capacity (A), lactate production (B) and glycolysis (E) in M1-like. FK866 treatment inhibit NAD⁺ levels , (C), TNF-α levels (D) and glycolysis (F). Data shown are mean ± SEM of three separate experiments (n = 3).

Conclusions

It is becoming clear that cellular metabolic status is intrinsically linked to immune system function, particularly in macrophages. One of the best studied links is that between NAD⁺/NADH and TNF-α with NAD(H) levels known to regulate TNF-α synthesis [1], and TNF-α levels known to regulate expression of NAD(H) homeostasis enzymes [5]. Here we have further extended the knowledge on this link by showing that TNF-α release is also correlated to metabolism and NAD⁺ levels in a pro-inflammatory (M1-like) macrophage model. Our data have shown that LPS stimulation of M1-like macrophages causes significant changes in NAD⁺ levels suggesting that pro-inflammatory M1-like cells are characterized by changes in NAD⁺ while M2-like cells (anti-inflammatory) are not. NAD⁺ levels also appear to be correlated with secretion of TNF-α in M1-like cells and not in M2-like confirming the existing link between NAD⁺ and pro-inflammatory TNF-α response. The two phenotypes differed in their relative levels of expression of NAD⁺ homeostasis enzymes and in their resting levels of NAD⁺. Also, LPS increased the expression of same enzymes (CD38 and CD157) with Large effect on NAMPT in M1 might suggest that the cells are priming themselves for NAD⁺ production as this is the rate limiting enzyme of the recycling pathway. It is likely that the TNF-α released during the experiment is partially responsible for the expression observed with previous results have shown that TNF-α application to macrophages increased the expression of the same enzymes [4]. Collectively, our data suggest that the two different phenotypes appear to have quite different mechanisms and levels of machinery for NAD⁺ homeostasis, raising the exciting possibility that NAD⁺ homeostasis may be phenotype-specific and even an underlying cause of phenotypic differences. It is known that TNF-α release requires active glycolysis and thus, the LPS-induced the observed increase in NAD⁺, we suggest that this may occur in order to provide NAD⁺ for glycolysis. To investigate this link, we used FK866 as inhibitor for the NAMPT, the main source for NAD production. Indeed, the results show that the inhibition of NAD⁺ led to inhibit glycolysis and TNF-α secretion. These data again strengthen the link between NAD⁺ levels, TNF-α and thus glycolysis and pro-inflammatory responses.

References

[1] Van Gool *et al. Nat. Med.* 2009 15, 206-210
[2] MacIver *et al.*, 2008. *J.Leukoc.Biol.* 84, 949-957
[3] Magni *et al.*, 1999 *Adv. Enzymol. Relat. Areas Mol. Biol.* 73, 135-182
[4] Schilling et al., 2012. Innate immun. 18, 518-530
[5] Iqbal and Zaidi, 2006 *Biochem. Biophys. Res. Commun.* 342, 1312-1318

Acknowledgement

We would like to thank Chemistry Department, College of Science, AL-Qadisiyah university, ministry of higher education for financial support. e-mail: **abbas.al-shabany@plymouth.ac.uk**

Pharmacological Modulation of NAD alters TNF-α responses in macrophage subsets

Abbas Al-Shabany, A. John Moody, Andrew D. Foey, Richard A. Billington
University of Plymouth, School of Biological Sciences, PL8 AA, UK.

Introduction

The link between NAD^+ metabolism and inflammatory responses is well established. Three major pathways are involved in NAD-biosynthesis. These pathways use three different precursors; nicotinamide/nicotinic acid, nicotinamide riboside and tryptophan. The latter is the least frequent precursor for NAD^+ generation and is metabolised to nicotinic acid via the well known IDO pathway (Figure 1; Cory, 1992).

Despite the well-established link between NAD^+ metabolism and immune responses, there is still need to elucidate the mechanisms that mediate how NAD^+ modulates macrophage inflammatory responses such that future work can be directed at targeting these pathways for immune modulation.

Our previous work has confirmed the involvement of NAD^+ in pro-inflammatory cytokine production and release in response to LPS. Therefore, a pharmacological approach has been taken in the this study to understand which NAD^+ biosynthesis pathways modulate these responses.

Three inhibitors have been used in our study: DPI (diphenylene iodonium), which is widely used as a competitive inhibitor for NADPH oxidase (Cross, 1987); 1-methyl tryptophan, a competitive inhibitor, of the IDO pathway inhibition; FK866, which is a NAD^+ salvage pathway inhibitor that blocks NAMPT (Grant and Kapoor, 2003; Hue *et al.*, 2007).

We have made use of the differentiation of THP-1 monocytes to generate cells with characteristics of pro-inflammatory (M1-like) using PMA (phorbol-12-myristate-13-acetate) in order to investigate the pharmacological modulation of NAD^+ metabolism and whether it can mediate macrophages immune responses.

Method

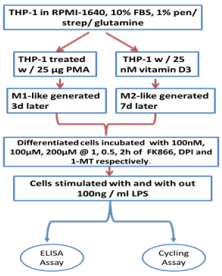

Results

NAD metabolism modulation and innate immune responses.

LPS increases both NAD^+ and TNF-α levels in pro-inflammatory macrophages (M1-like; Figure 2 A, B). The NAD^+ increase shows a biphasic profile with a rapid initial spike followed by a longer rise after LPS stimulation while the TNF-α levels peak after 8 hours before slowly declining. The relationship between NAD^+ and TNF-α levels is sirtuin dependent (data not shown). In order to elucidate which of the NAD^+ synthesis pathways is responsible for the NAD^+ rises, we first tested the effect of FK866 on intracellular NAD^+ levels in THP-1 derived macrophages. Differentiated macrophages were incubated with 100nM FK866 for 1 hour prior to stimulation with 100 ng/ml LPS, versus control cells. FK866 causes NAD^+ levels not to increase in response to LPS in M1-like macrophages (Fig 2 C) with the greatest effect on the longer term, sustained rise. TNF-α does still increase but that increase is lower than in the absence of FK866 (Fig 2 D). DPI blocked NAD^+ as well as TNF-α increases (Fig 3 A, B). In contrast, while 1-MT was able to decrease the intracellular NAD^+ levels slightly, it did not affect TNF-α responses (Fig 3 C, D).

Results

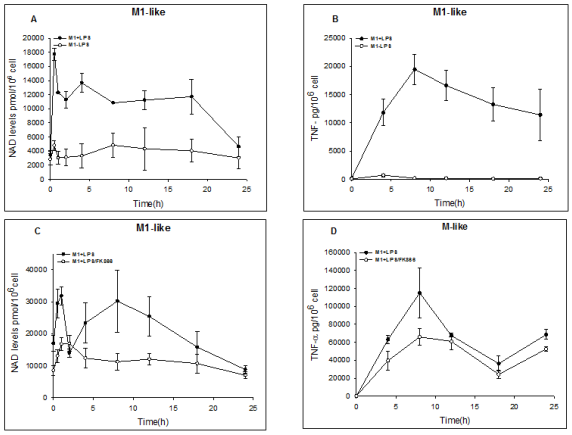

Figure (2): Pharmacological modulation of NAD^+ levels and TNF-α using (100nM) FK866 in THP-1 derived macrophage differentiation. (A) and (B), LPS increase NAD^+ and TNF-α levels in M1-like macrophages. (C) and (D) FK866 blocks increase NAD^+ and TNF-α levels in M1-like subsets. Data shown are the means ± standard error (SE bars) from three biological replications.

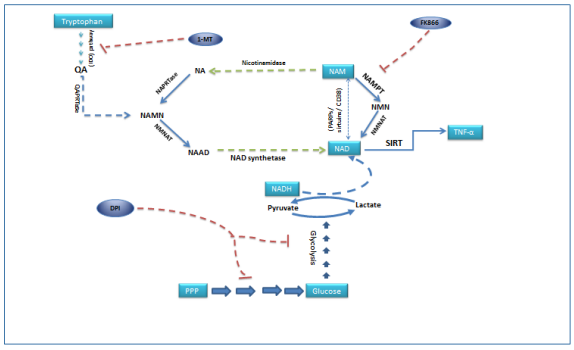

Figure (1): NAD metabolic pathways: IDO, indoleamine-2,3-dioxygenase; NA, nicotinic acid; NAAD, nicotinic acid adenine dinucleotide; NMN, nicotinamide mononucleotide; NMNAT, NMN adenylyl transferase; NMPRTase, PPP pentose phosphate pathway.

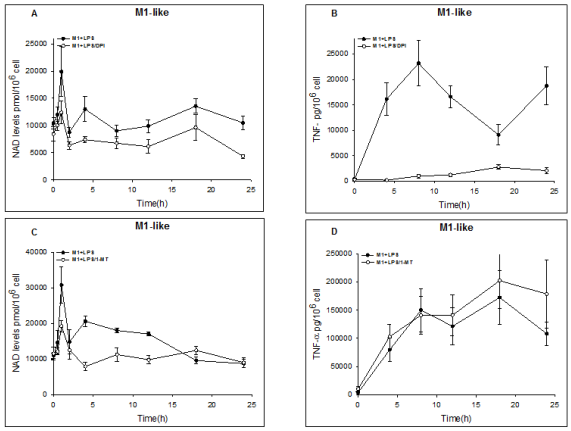

Figure (3): (A) and (B) DPI blocks increase NAD^+ levels and not TNF-α release in M1-like . (C) and (D) 1-MT affects NAD^+ levels but not TNF-α levels in M1-like.Data shown are the means ± standard error (SE bars) from three biological replications.

Discussion

It is clear that LPS stimulation of M1-like macrophages causes significant changes in NAD^+ levels. Such changes in NAD^+ levels are unusual in cells and it is thus important to discover the mechanism responsible. As those increases are linked to TNF-α synthesis and release, the pathways responsible may offer interesting pharmacological targets for the modulation of pro-inflammatory responses by macrophages.

FK866 blocks the NAD^+ recycling pathway and was able to attenuate NAD^+ rises particularly in the second phase of the response although a small initial spike remained. These data suggest that NAD^+ recycling may play a significant role, at least in the sustained NAD^+ rise. The effect of FK866 on TNF-α levels was not striking although it was able to decrease TNF-α release.

DPI blocks the conversion of NADH to NAD^+ via NAD(P)H oxidases in the respiratory burst. DPI was able to largely inhibit both NAD^+ and TNF-α level rises suggesting that the source of the NAD+ may be partly through the oxidation of NADH as might be expected upon bacterial challenge.

1-MT showed some effects on NAD^+ levels under LPS challenge but was unable to block the TNF-α level rise, suggesting that the IDO pathway plays an insignificant role in LPS-induced TNF-α production.

NAD^+ homeostasis pathways are an attractive target for immune modulation particularly with respect to attenuating pro-inflammatory responses given the well-known links between NAD^+ and TNF-α levels. It appears that the mechanisms that lead to the rise in NAD^+ levels in response to LPS in M1-like cells is complex and may be regulated via a combination of pathways.

Furthermore, our results suggest that simply blocking the LPS-induced NAD^+ increase is not, alone, sufficient to block TNF-α production/release as evidenced by the different effects on TNF-α levels of FK866 and DPI when their effects on the NAD^+ levels were very similar.

We suggest also that the IDO pathway plays little or no role in TNF-α release despite playing a role in NAD^+ production.

Further clarification of the exact mechanisms involved will be required before precisely targeted pharmacological approaches can be tested for immunomodulatory effects.

References

1-Cory, J. Purine and pyrimidine nucleotide metabolism. In: T. Devlin (ed.), Textbook of Biochemistry with Clinical Correlations, Ed. 3, pp. 529–574. Brisbane, Australia: Wiley, 1992.

2-Cross, A. R. (1987) Biochem. Pharmcol. 33,489-493'

3-Grant and Kapoor, (2003), Biochem. J, 1033-1063.

4-Hou, *et al.*,(2007), Cancer Res,792-801.

Acknowledgments

We would like to thank Chemistry Department, College of Science, AL-Qadisiyah university, Ministry of Higher Education for financial support.

e-mail: abbas.al-shabany@plymouth.ac.uk